PREDICTING STORAGE VESSEL GEOMETRY REQUIREMENTS FOR DISCHARGE OF EXTREME SHAPE MATERIALS.

AMINU OWONIKOKO

A thesis submitted in partial fulfilment of the requirements of the University of Greenwich for the Degree of Master of Philosophy.

2012

DECLARATION

I certify that this project has not been accepted in substance for any degree, and is not concurrently being submitted for any degree other than that of Master of Philosophy (MPhil) being studied at The University of Greenwich, United Kingdom. I also declare that this work is the result of my own investigations except where otherwise identified by references and that I have not plagiarised the work of others.

Aminu Owonikoko

MPhil Student

Supported by:

Dr. Rob Berry
First Supervisor

Professor Mike Bradley
Second Supervisor

DEDICATION

I dedicate this project to my loving and adorable late parents: Alhaji Ashrudeen Akano Owonikoko and Alhaja Munirat Akanke Owonikoko who gave me the privilege to acquire solid educational foundations (both Western and Arabic education) which have helped me to acquire further world renowned education in United Kingdom. I beseech Almighty God to grant them al-janah firdaus.

MOTIVATIONAL QUOTE

'Whenever you are asked if you can do a job, tell them "certainly I can". Then get busy and find out how to do it'

--------- Theodore Roosevelt (26th President of the USA)

ACKNOWLEDGEMENTS

All thanks go to my caring supervisors: Dr. Rob Berry and Professor Mike Bradley. I am deeply indebted to them for their assistance both in academia world and outside academia. Without them this project will not be achieved. I pray that God Almighty bless them and their families in this world and hereafter.

I am really grateful to The Wolfson Centre for providing financial assistance which has served as one of the key enablers for me to complete this research work. Also, I am very grateful to the entire member of The Wolfson Centre staff and colleagues who have provided conducive environment to carry out my research particularly Mrs Caroline Chapman. Also many thanks to John Larkin and Trevor Mortley for their assistance in constructing my test rigs.

I am also grateful to my lovely siblings (Belawu, Afeez, Khadijat and Aminat) for their moral and spiritual assistance ever since I have been in the United Kingdom. My special thanks to The Wolfson Centre, Ms Grace Ugbah, Mummy Sokoya, Odueke's Family, Ms Bukola Akinware, Mr Ibrahim Pakoto, Nasfat Jammah Branch at London South Bank University, Mr Muritala Mohammed, Mr Mutari Abubakari (NRI Greenwich former student), Ms Omolara Olorunoje, Mr and Mrs Sikiru Owonikoko for their consummate assistance when I was sick during my research programme.

Special recognition is due to my dear brother: Mr Afeez Adeniyi Owonikoko, my cousins: Barrister Ahmed Adeniyi Raji (SAN) and Dr Abubakar Olusola Saraki. Also my good friend Ade Otegbeye who welcomed me into Great Britain with open hands. They have been a source of help and motivation to me. I love you all so much!

ABSTRACT

The rush to sustainable/renewable energy to mitigate the global warming or green-house gas emissions is global and is increasing everyday especially on bioenergy/biofuels. Clean Development Mechanism was developed in the Kyoto Protocol to ensure the mitigation of global warming is achieved in developing countries and developed (industrialised) countries. To achieve these important goals, the right equipment to handle and process biomass materials is required in order to produce the carbon-neutral energy (renewable energy).

In order to specify the right equipment and to evaluate the existing process technologies which are not meeting the expectations of the industry, the bulk mechanical/flow properties that make up the feedstock (raw materials) used to generate the biofuels needs to be characterised. The particles that make up biofuels materials (i.e. biomass and waste materials) are extreme/irregular in shape. They are classified as extreme shape materials (ESM) "Class 3" by The Wolfson Centre for Bulk Solids Handling Technology based on their many years of research into these materials. They are elastic, fibrous, flaky, and stringy in nature and have a tendency to nest or interlace (Bradley and Farnish, 2004; FEM 2581/2582, 1991; Mattsson, J.E 1990; Bell T.A. 1999; Johanson J.R., 1989; McGee Eddie, 2009). Examples of ESM are woodchips, miscanthus (elephant grass), shredded paper, municipal solid wastes, industrial and commercial wastes, corn stover, straw, lawn grass, chicken/poultry litter, etc.

Most conversion (process) technologies like pyrolysis, gasification, combustion, trans-esterification, anaerobic digestion, fermentation under-perform because biomass and waste materials are resistant to flow in the feeder (silo/hopper) which supplies feedstock into the conversion chambers. Research outputs have shown that the resistance to flow of extreme shape biomass is due to their high aspect ratio, inherent low bulk density, inherent high moisture content and their stress phobic nature (Owonikoko et al, 2010; Johanson J.R., 1989; Bundalli N., 1986; The Roger et al, 1994; Bradley and Farnish, 2004) which contributes significantly to their nesting/entanglement behaviour. In order to de-nest class 3 materials (Extreme Shape Materials), the flow (mechanical) properties of the materials have been researched.

The techniques developed and adopted have provided a framework to produce a design procedure to determine the hopper geometry, wall angle, outlet size and internal finish required to ensure a given biomass and waste materials discharge reliably from the vessel.

Table of contents

Declaration 2
Dedication 3
Acknowledgement 4
Abstract 5

Chapter 1: Introduction and Pre-literature Review……18

1.0 Introduction 18
1.1 Non-renewable Energy 18
1.2 Sustainable/Renewable Energy 18
1.2.1 Biofuels/Bioenergy 19
1.3 Industry Context: the need for characterisation of flowability and design of storage facilities 21
1.4 Characterisation of Particle Shape 24
1.5 Storage Vessel Geometry 25
1.5.1 Current Practice for Conventional Powders 26
1.5.2 Flow Obstructions 27
1.5.3 Comparison of Storage Vessel Geometry 32
1.6 Research Objectives 33
1.7 Preview of the Research Work 34

Chapter 2: Literature Review…….35

2.0 Introduction 35
2.1 Trend in Bioenergy/Biofuels Industry 35
2.2 Biomass 36
2.3 Industrial Best Practise for Storage and Handling of Biomass 37
2.3.1 Current Biomass Handling Technology for Discharge from Storage 37
2.3.1.1 Full live bottom dischargers 37
2.3.1.2 Moving Hole Feeder 39
2.3.2 Evaluation/auditing of existing bioenergy plants 39
2.4 Biomass Conversion Processes 40
2.4.1 Influence of Biomass Characterisation on the Conversion Processes 41
2.5 Biomass Bulk Flow Property Characterisation Tests 42
2.5.1 Uniaxial Tester 42
2.5.1.1 Models for the behaviour of biomass 45

2.5.2 Shear Testers 46
2.5.3 Tensile Tester 48
2.6 Silo Discharge Tests 49
2.6.1 Wolfson Centre Hopper Test 49
2.6.2 Jan Erik Mattsson's Silo Test 50
2.6.3 Aperture Tester by Bundalli 50
2.7 Summary 51

Chapter 3: Test Materials and Preliminary Results……52

3.0 Introduction 52
3.1 Selection of test materials: Extreme Shape Materials 52
3.2 Characterisation of the particle size and shape 53
3.2.1 Description of particle dimensions distribution 58
3.2.1.1 Hammer milled wood/miscanthus 58
3.2.1.2 Wood shavings 60
3.2.1.3 Oat flakes 62
3.2.1.4 Straw 63
3.2.1.5 Reed canary grass 65
3.2.1.6 Grass A 66
3.2.1.7 Grass B 67
3.3 Relationship between the particle size and test cell / silo geometry 68
3.4 Column Test 69
3.4.1 Test setup 71
3.5 Tensile Tester 72
3.5.1 Tensile Tester Description 72
3.5.2 Test Procedure 73
3.6 Core Flow Test 74
3.6.1 Description of the core flow test rig 74
3.6.2 Mode of Operation of the Core Flow Test 75
3.6.3 Modifications to the Core-flow test rig 76
3.7 Mass Flow Test 76

3.7.1 Mode of Operation of the Rig 78

3.8 Shear Tester 80

3.8.1 Wolfson-Brookfield Powder Flow Tester 80

3.8.2 Standard Flow Function Test 81

3.8.3 Powder Flow Tester Procedure 81

Chapter 4: Results Summary and Discussion (Exploratory Work)……....83

4.0 Introduction 83

4.1 Column Test 83

4.2 Tensile Tester 84

4.2.1 Mechanism of Failure/Flow 85

4.3 Core Flow Test 87

4.4 Mass Flow Test 91

4.5 Shear Tester 94

Chapter 5: Results and Discussion of Arching Experiments

(in a modified mass-flow silo)……..98

5.0 Introduction 98

5.1 Features of the novel silo 98

5.2 Silo Discharge Behaviour of Biomass Materials 101

5.2.1 Chopped Miscanthus Behaviour at 41 degree wall angle 102

5.2.2 Chopped Miscanthus Behaviour at 23° wall angle 103

5.2.3 Wood Shavings Behaviour at 41° wall angle 104

5.2.4 Wood Shavings Behaviour at 23° wall angle 105

5.2.5 Straw Behaviour at 41° wall angle 106

5.2.6 Straw Behaviour at 23° wall angle 107

5.2.7 Oat flakes Behaviour at 41° wall angle 108

5.2.8 Oat flakes Behaviour at 23° wall angle 109

5.2.9 Reed Canary Grass Behaviour at 41° wall angle 110

5.2.10 Reed Canary Grass Behaviour at 23° wall angle 111

5.3 Conclusion 112

Chapter 6: Development and Evaluation of a Critical Arch Model……...113

6.0 Introduction 113

6.1 Arching Dimension Measurements 114

6.1.1 Oat flakes 116

6.1.2 Chopped Miscanthus 116

6.1.3 Wood Shavings 116

6.1.4 Straw 117

6.1.5 Reed Canary Grass 117

6.1.6 Conclusion 117

6.2 Improving the Arching Model 118

6.3 Stress Distribution in Extreme Shape Materials Vessel 121

6.4 Arching Model 123

6.4.1 Arching Dimension versus Bed Head (Experimental and predicted results) 126

6.5 Conclusion 129

Chapter 7: Conclusions and Recommendations for further work……..131

7.0 Introduction 131

7.1 Silo Discharge Tests 131

7.2 Characterisation Tests 132

7.3 Modelling and Predicting Arching Dimension 134

7.4 Further Work Suggestions 135

References 138

APPENDICIES

Appendix A: Results and Discussion of Biomass Characterisation Tests 145

Table Appendix (A): Core Flow Test 172

Table Appendix (B): Mass Flow Test 189

Photographic Appendix (A): Core Flow Test 201

Photographic Appendix (B): Mass Flow Test 205

Photographic Appendix (C): Column Test 209

Photographic Appendix (D): Core and Mass Flow Test at the Initial Stage 211

Photographic Appendix (E): Uniaxial Failure Test on Extreme Shape Materials 213

Appendix B (i): Bulk Density Measurements Results 214

Appendix B (ii): Tensile Strength Measurements with Extrapolated Data 219

Appendix C: Calculated Stress Distribution and Arching Dimensions 222

Appendix (F): Paper

LIST OF FIGURES

Figure 1: Woodchips: an example of biomass 21
Figure 2: Industrial start up time for different feedstocks 22
Figure 3: Current Vessel Geometry employ in the industry 23
Figure 4: Characterisation of particle shape 25
Figure 5: (A) Conical-shaped hopper, (B) Wedge-shaped hopper
(C) Flat-bottomed cylinder hopper 26
Figure 6: Mass flow silo 27
Figure 7: Core flow silo 27
Figure 8: Mechanical Arching 28
Figure 9: Cohesive Arching 29
Figure 10: Rat holing 30
Figure 11: International Energy Agency World Energy Outlook 2008 36
Figure 12: Sliding-frame type discharger 38
Figure 13: Planetary/Multiple Screw Feeder 38
Figure 14: Moving Hole Feeder Concept 39
Figure 15: Illustration of conversion processes, products and markets 41
Figure 16: Uniaxial Unconfined Failure Test on Cohesive Bulk Solids 43
Figure 17: Element of powder in a cohesive arch over the outlet of a silo 43
Figure 18: Flow function of a powder 44
Figure 19: Uniaxial Test on chicken/poultry litter 45
Figure 20a: Behavioural traits of ordinary bulk solids under loads 46
Figure 20b: Behavioural traits of Extreme Shape Materials under loads 46
Figure 21: Large Wolfson Annular Shear Tester 48
Figure 22: Wolfson Centre Hopper Test Rig 49
Figure 23: Mattsson's Silo Discharge Test Concept 50
Figure 24: Aperture Tester by Bundalli 51
Figure 25: Extreme Shape Materials showing combination of
acicular fibre & flake 52
Figure 26: Illustration of rigid and elastic extreme shape materials 53

Figure 27: Micrograph of particle size and shapes a) Hammer milled wood, b) Miscanthus, c) shredded paper & d) Lawn grass A 56

Figure 28: Micrograph of particle size and shapes a) Lawn Grass B, b) wood shaving, c) match sticks & d) Straw 57

Figure 29: Micrograph of particle size and shapes for (e) Oat flakes and (f) Reed canary Grass 58

Figure 30: Particle size distribution of long length for hammer milled wood/miscanthus 59

Figure 31: Particle size distribution of intermediate length for hammer milled wood/miscanthus 59

Figure 32: Particle size distribution of short length for hammer milled wood/miscanthus 60

Figure 33: Particle size distribution of long length for wood shavings 61

Figure 34: Particle size distribution of intermediate length for wood shavings 61

Figure 35: Particle size distribution of short length for wood shavings 62

Figure 36: Particle size distribution of long length for oat flakes 62

Figure 37: Particle size distribution of intermediate length for oat flakes 63

Figure 38: Particle size distribution of short length for oat flakes 63

Figure 39: Particle size distribution of long length for straw 64

Figure 40: Particle size distribution of intermediate length for straw 64

Figure 41: Particle size distribution of short length for straw 65

Figure 42: Particle size distribution of long length for reed canary grass 65

Figure 43: Particle size distribution of intermediate length for reed canary grass 66

Figure 44: Particle size distribution of short length for reed canary grass 66

Figure 45: Particle size distribution of long length for Grass A 67

Figure 46: Particle size distribution of long length for Grass B 67

Figure 47: Schematic illustration of the concept of the column test, a) column filling b) failure or flow of free flowing biomass material & c) stability or non-flow of extreme shape biomass materials 70

Figure 48: Column Test Technique for the flow properties of biomass particles (Column Stability) 71

Figure 49: Buckling failure mode of chopped miscanthus 72

Figure 50: Illustration of Tensile Tester 73

Figure 51: Arrangement of the rings inside the silo
(the rings are made out of cast nylon) 75

Figure 52: Core flow test rig 75

Figure 53: Second ring arrangement inside the “silo” (barrel) 76

Figure 54: Schematic diagram of variable geometry silo 77

Figure 55: Biomass test material (hammer milled wood) sitting inside the
adjustable plane flow hopper 78

Figure 56: Chopped Miscanthus Rat-hole (view from the top of the particle bed) 79

Figure 57: Chopped Miscanthus mechanical arch (bottom view of the hopper) 79

Figure 58: Variable geometry silo internal surface and Gravity
flow of hammer milled wood 80

Figure 59: Wolfson-Brookfield Powder Flow Tester with accessories 81

Figure 60: Powder Flow Tester with Powder Flow Pro Software with USB
cable displaying particles at pre-shearing stage and other accessories set-up 82

Figure 61: Nesting characteristics of different matchsticks length inside
different tube diameters 84

Figure 62: Tensile test results for biomass materials
“lawn grass and shredded paper” 85

Figure 63: Tensile Strength Measurement of Extreme shape materials 86

Figure 64: Comparisons of the mechanical arches formed by different materials
in the core-flow test a) hammer milled wood b) shredded paper c) grass A &
d) grass B 88

Figure 65: Rat holes formed by hammer milled wood (a& c)
and miscanthus (b&d) 89

Figure 66a: Effects of bed height on the size of rat-hole formed in

the core flow bin for hammer milled wood (small initial outlet) 89
Figure 66b: Effects of bed height on the size of rat-hole formed in
the core flow bin for chopped miscanthus (small initial outlet) 90
Figure 67a: Effects of bed height on the size of rat-hole formed in
the core flow bin for hammer milled wood (large initial outlet) 90
Figure 67b: Effects of bed height on the size of rat-hole formed in
the core flow bin for chopped miscanthus (large initial outlet) 91
Figure 68a: Effect of the head height on the arching dimension
of hammer milled wood 92
Figure 68b: Effect of the head height on the arching dimension
of chopped miscanthus 93
Figure 69: Obstructions form in the mass-flow silo, a) hammer milled wood arch
over a 200mm span, b) Shredded paper arch over a 200mm span,
c) Rat-hole formed for hammer milled wood,
d) Asymmetric discharge of miscanthus 94
Figure 70a: Flow Function 96
Figure 70b: Internal friction function 96
Figure 70c: Bulk density function 97
Figure 71: New Wedge shape silo showing front and side views 99
Figure 72: New Adjustable (Wedge-shaped) Hopper (Internal Surface) 99
Figure 73: New Adjustable (Wedge-shaped) Hopper Picture (Whole Vessel) 100
Figure 74: Silo discharge characteristics of chopped miscanthus at
41° wall angle 102
Figure 75: Silo discharge characteristics of chopped miscanthus at
23° wall angle 103
Figure 76: Silo discharge characteristics of wood shavings at
41° wall angle 104
Figure 77: Silo discharge characteristics of wood shavings at

23° wall angle 105
Figure 78: Silo discharge characteristics of straw at 41° wall angle 106
Figure 79: Silo discharge characteristics of straw at 23° wall angle 107
Figure 80: Silo discharge characteristics of oat flakes at 41° wall angle 108
Figure 81: Silo discharge characteristics of oat flakes at 23° wall angle 109

Figure 82: Silo discharge characteristics of reed canary grass at
41° wall angle 110
Figure 83: Silo discharge characteristics of reed canary grass at
23° wall angle 111

Figure 84: Tensile tester features 115

Figure 85: Arching Dimensions Comparison for Extreme Shape Materials (A) 116

Figure 86: Bulk density functions for extreme shape materials 119

Figure 87: Tensile strength functions for extreme shape materials without straw 120

Figure 88: Tensile strength functions for extreme shape materials with
straw included 121

Figure 89: Assummed Vertical Stress Distributions in the plane flow silo for various extreme shape materials 123

Figure 90: Arching Dimensions Comparison for Extreme Shape Materials
without straw (B) 124

Figure 91: Arching Dimensions Comparison for Extreme Shape Materials
with Straw included (B) 125

Figure 92: Actual arching dimensions versus bed head at 23° wall angle 127

Figure 93: Actual arching dimensions versus bed head at 41° wall angle 127

Figure 94: Correlation between particle length and actual arching dimension 128

Figure 95: Predicted arching dimensions versus bed head 128

Figure 96: Predicted arching dimensions versus bed head with Straw included 129

LIST OF TABLES

Table 1: Comparison of the particle properties and bulk densities
of the different extreme shape materials tested 55
Table 2: Comparison of assumed mean particle dimensions and the minimum
test cell/ silo dimension to prevent the influence of particle size on the results 69

Chapter 1: Introduction and Pre-literature Review

1.0 Introduction

The world we live in today cannot be sustained without the use of energy but the source of the energy is very pertinent if we are to live a life that is free of hazards. The common sources of energy are non-renewable. The renewable sources tap their energy from the sun while non-renewable energy are fossils and they are depleting fast. Examples of renewable energy are: geothermal, hydro, solar, wave, wind, tidal and biofuels/bioenergy (biomass). They are all relatively clean compared to fossil fuel, safe unlike nuclear energy and they will not run out (deplete) unlike fossil oil, gas and coal. Examples of non-renewable energy are: coal, petroleum and nuclear.

1.1 Non-renewable Energy

The World Energy Council opined that the world would be reliant on non-sustainable energy for decades to come (Goldemberg Jose, 2000). Both developed and developing countries are certain to expand their use of non-sustainable energy (fossil fuels). Yet, there will be strong resistance to this expansion if the non-sustainable energy community cannot demonstrate that it can be accomplished in a manner that reduces environmental degradation.

1.2 Sustainable/Renewable Energy

Sustainable energy sources have been pertinent for humans since the inception of civilization. Sustainable energy technologies use facilities that are not conventionally subject to erosion. The energy that reached the earth's surface from the solar radiation is about 1000 times more than all the world's energy requirements. The potential of available sustainable energy is enormous to the extent that their sources can meet many times the current world energy needs. Sustainable energy can make the provision of long-term renewable energy supplies; minimize global and local environmental pollution. Sustainable energy also known as renewable energy provide chances for local production of equipment, possibilities of providing commercially appealing options to satisfy specific wants in rural areas and developing countries for their energy services and facilities (Turkenburg Wim C., 2000).

1.2.1 Biofuels/Bioenergy

Bioenergy is the energy produced from biomass or waste materials. Biomass is all plant and animal matter that has not been fossilised. Many biomass streams are effectively waste materials (Bradley, 2010). Waste materials are often classified as biomass because they are organic and biofuels can be generated from them. In this project both biomass and waste materials are extreme in shape and they will be used interchangeably. Rationally, wastes are left over generated from various households (domestic wastes) and industries. Biomass can be used to generate power. Energy may be generated from biomass in different ways such as liquid fuels, heat or electricity. Examples of biomass and waste materials are animal dung, crop wastes like corn stover, wood wastes like woodchips, trees, municipal solid wastes, shredded paper, industrial and commercial wastes and the crop itself. They are generally referred to as biomass. There is a vast resource that is largely untapped. This brings about the discovery of energy crops (crops that are intentionally grown for the purpose of energy generation) like broomcorn, jatropha, poplars, miscanthus, short rotation coppice, corn etc.

The energy content in biomass is basically from solar energy (directly from the sun) and is kept in the biomass in the nature of energy from chemical (i.e. chemical energy). The chemical energy that is stored in the biomass can be converted into useful form of energy by a number of relatively simple processes like combustion, gasification, pyrolysis, fermentation, anaerobic digestion and fermentation.

The idea of manufacturing chemicals and fuels from biomass is not a new one. Since the 1800's chemicals like ethanol, cellulose, methanol, vegetable oils and others have been extracted from biomass to produce different end products which serve as raw materials for another industry or as a final product for consumers. Typical examples of these products are adhesives, solvents, paints and synthetic cloths. Biomass products were phased out after the introduction of petrochemicals from 1930.(http://www.energy.iastate.edu/renewable/biomass/ accessed on December 27 2010).

This project is focused on predicting the storage vessel geometry requirements for reliable discharge of biomass and waste materials so that they can be used for

combustion or processed for the production of biofuels for automobiles and other bio based chemical applications. Figure 1 below shows woodchips as an example of biomass materials. At present previous research at The Wolfson Centre has shown that Biomass and waste materials can be categorised into 3 classes (Bradley and Farnish, 2004; Bradley 2009).

Class 1 are free flowing without extreme particle shape. They are rounded particles or pellets but not cohesive. Their behaviour is similar to dry sand. They could be coarse or medium crushed materials. Examples of this type of materials are: wheat feed pellets (a cereal co-product), pelleted wood and sewage sludge pellets in a dry condition.

Class 2 are cohesive without extreme particle shape. They are also rounded but similar to wet sand in behaviour. They could be milled materials, wet powders and fine powders. An example of this material is milled nuts.

One of the significant unsolved challenges for handling biomass materials is the problem of nesting "entangling" that occurs when biomass particles are extreme in shape e.g. fibrous such as grasses, or flaky such as wood shavings. These materials are known as Class 3.

Figure 1: Woodchips: an example of biomass (source: http://newcarfuels.com/wp-content/uploads/2008/10/wood-chips.jpg). Accessed on December 27, 2010.

1.3 Industry Context: the need for characterisation of flowability and design of storage facilities

Currently, there are 18 coal-fired power plants that handle biomass (as classified by Department of Business Enterprise and Regulatory Reform) in the United Kingdom (Bradley et al, 2011). Other energy industry in the United Kingdom, United States of America and other parts of the world are switching from fossil fuel generation to renewable (biofuel) generation due to new government legislation and customers perception about the need for green energy. These power generators were initially co-firing biomass with coal either directly or indirectly but now they are looking to convert to 100% biomass. This change has warranted that industry modify their existing handling equipment like storage vessels or procure new handling equipment because of the incompatibility between the flow properties of the new biomass materials and the existing handling equipment. The current approach that most energy industries and equipment manufacturers use to design and redesign or retrofit the handling equipment is a trial and error approach or throughput based approach (ton/hr or ton/year based decision). These approaches are awkward and cause the industry production downtime and sometimes it causes the industry to shut-down, due to material flow problems. The Rand Report (Merrow Edward W., 1986) compared the start-up of 40 new processing plants in the USA. These were characterised by

feedstock type: liquid-gas, refined solids (bulk solids that has been processed) and raw solids (bulk solids freshly mined from the ground). However, based on the report (see figure 2 below), it demonstrated that liquid-gas plants can be design adequately but for refined and raw solids, there is a severe lack of design guidance. Raw solids take longer time to start-up as compared to planned start-up time. Biomass materials are more troublesome and difficult to handle than the raw solids displayed in the figure 2, so the actual start-up time for biomass might be longer if proper mechanical characterisation approach is not dully performed.

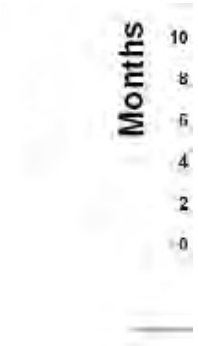

Figure 2: Industrial start up time for different feedstocks (Merrow Edward, 1986)

Often, a typical biomass processing plant has more storage and conveyor systems than the actual conversion processes like combustion, gasification and pyrolysis (Bradley, 2010). Over the years the handling equipment manufacturers and biofuels industry have displayed a lack of materials characterisation (flow properties of the materials). This lack of knowledge has been costing the industry a lot of money every year. The incompatibility between the current handling equipment and flow properties of the materials results in storage vessels that do not discharge. The no-flow characteristics of the materials affect the whole industrial process up and down stream of a problem. Some biomass handling solutions are currently available like full live bottom dischargers (e.g. planetary screw discharger) (Bradley and Farnish, 2004) but these are very expensive, making it difficult for entrepreneurs to enter the renewable energy business and making it difficult for biofuels to compete with fossil fuels at the world market.

Another practise in the industry is the misconception that the vessel wall must be negatively sloped to prevent mechanical arch and rat-holing (Bundalli, 1986). Example of this is shown in the figure 3 below. As a result of this misconception, numerous biomass handling systems are currently using vessels with large outlet areas which require enormous and exorbitantly expensive feeders.

Figure 3: Current Vessel Geometry employ in the industry (Bundalli, 1986).

In order to solve the handling problems and dispel this misconception, the need for characterisation of renewable energy feedstock/raw materials is very pertinent. This will help to identify whether a specific feedstock will be troublesome or well-behaved during handling. Also, the flow properties measurements will help to guide the handling equipment manufacturers in their design stage and help the industry at large to evaluate the existing plants. This project has been carried out in order to provide this guide and provide numerical data that would help to solve the handling issues in the renewable energy industry.

Currently, there are established standard characterisation techniques like shear tester e.g. Jenike Shear tester (Jenike, 1961), Brookfield powder flow tester (Berry et al, 2010), Schulze Ring shear tester (Schulze, 1996) for traditional powders used in other industries like food industry, pharmaceutical industry, coal industry, chemical

industry as will be explained later in chapter 3 (section 3.8). All these shearing techniques are unsuitable for extreme shape materials (biomass) because they nest together and do not shear. This will be explained later in chapter 3 where Brookfield powder flow tester was used as a standard shear tester to conduct the comparative test between regular and irregular shape materials. Therefore, the need to develop and prove a new characterisation technique has been established.

The project has evolved to produce reasonable results to guide the biomass industry. The research has revealed the key problems behind the difficulty of handling biomass materials. The problems are variables like particle shape, low bulk density and high aspect ratio of the particles. Experimental investigations were carried out on different industrial biomass materials like hammer milled wood, miscanthus, straw, wood shavings and reed canary grass, etc. The results obtained from the experimental investigations were compared with predicted values which were calculated from a novel mathematical model. The techniques employed to carry out the experimental investigations and methods used to formulate the mathematical models are presented in chapter 4 and 5.

1.4 Characterisation of Particle Shape

In order to know whether a given material is going to flow reliably in a storage vessel and whether the material is going to be compatible with the storage vessel the need for characterisation of the materials is very important. This also serves as a guide in predicting the storage vessel geometry for the extreme shape materials. A review of the literature has shown that the recognised approach for characterising particle shape is to draw a cuboid around the particle and define the lengths of the longest L, intermediate I and shortest S dimensions (Blott Simon and Pye Kenneth, 2008). The shape can then be defined on the diagram shown below in fig 4, which gives three extremes of particle shape:

- Equant where all 3 dimension are equal so particle is a cube or sphere,
- Platy where the longest and intermediate dimensions are equal and are very much larger than the shortest dimension e.g. a flake.
- Elongate where the shortest and intermediate dimensions are equal and are very much smaller than the longest dimension e.g. a fibre.

This characterisation approach has been used to determine the longest, intermediate and short dimensions for the extreme shape materials used in this project. The data obtained from this measurement have been used to calculate the aspect ratio of each material. The results are presented in table 1 in chapter 3. The problem with this characterisation approach however, is that it can give misleading information if applied to particles which are curved, split. E.g. a "Y" shape fibre would be interpreted as "platy" when strictly it is "elongate".

Figure 4: Characterisation of particle shape (Blott and Pye, 2008)

1.5 Storage Vessel Geometry

Conventional theory is that extreme shape materials will not discharge from a convergent hopper under gravity; hence full live bottom vessels are used. In order to dispel this misconception, the need to design a storage vessel that discharges extreme shape materials reliably under gravity is very important to the bio refinery industry.

Three major types of storage vessels that are commonly used in the industry are conical-shaped hopper, wedge-shaped hopper and flat-bottomed hopper (figure 5 below).

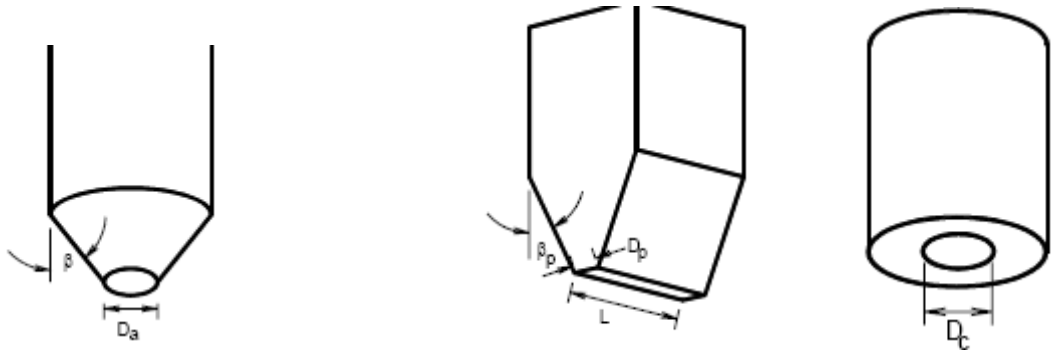

(A) (B) (C)

Figure 5: (A) Conical-shaped hopper, (B) Wedge-shaped hopper (C) Flat-bottomed cylinder hopper.

1.5.1 Current Practice for Conventional Powders

The current practice for storage and discharge of conventional powders is mass flow and core flow silo storage.

- **Mass flow silo:** It is a flow pattern illustrated in figure 6 whereby the first material that enters the storage comes out first and last material that enters the storage comes out last (First in, first out). During discharge, all the material is moving. The entire capacity of the storage is live. There is no dead zone inside the storage. The materials slide on the wall especially at the converging zone of the silo (see figure 6 below). The angle of convergence is governed by the magnitude of the friction between the material and the wall. The higher the wall friction angle the steeper the wall convergence.
- **Core flow silo:** Is a flow pattern illustrated in figure 7 whereby the material that enters the silo first is discharged last. During discharge material flows through a central core above the outlet. Material is fed into the core from the top free surface and the material around the wall remains static until the level drops to the point where it becomes the top surface. The converging wall angle is shallow compared to mass flow. Many industrial storage facilities discharge in core flow (shown in Figure 7) and most biomass particles meet the requirement usually specified for acceptability of core flow requirements

which are: free flowing, non-degrading, coarse especially when dried, segregation is not a barrier (Marinelli J and Carson J.W., 1992). However experience has shown that even though many biomass materials fulfil these criteria of acceptability for core flow discharge, a large proportion of them will not flow reliably (or at all) in this mode.

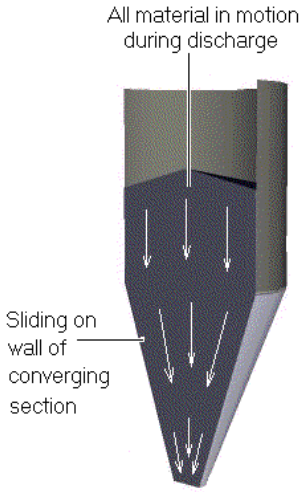

Figure 6: Mass flow silo

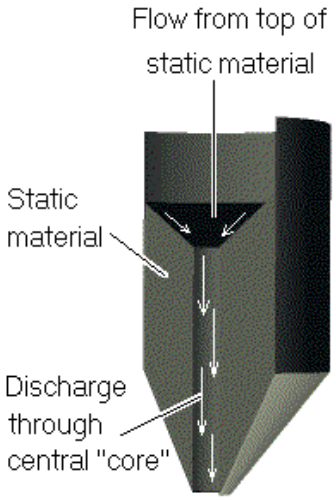

Figure 7: Core flow silo

(Source: http://www.gre.ac.uk/wolfsoncentre/consultancy/hoppersandsilos)

1.5.2 Flow Obstructions

When particles are stored/charged inside the vessel they may experience flow obstructions when they are to be discharged from the vessel especially when the flow properties of the particles are not taken into account when the vessel is designed and constructed. The most common flow obstructions are mechanical arching, cohesive arching and rat holing. The flow obstructions depend on the nature of the particles especially particle size and shape and bulk cohesiveness. The flow obstructions that are peculiar to biomass are mechanical arching and rat-holing based on experimental investigations carried out in this project. The 3 common flow obstructions and critical outlet dimension required for the particles to discharge reliably from the vessel are briefly discussed below.

- **Mechanical Arching**

Mechanical arching is the flow obstruction in a mass flow or core flow vessel where large particles (e.g. coarse or extreme shape materials) are competing for the small outlet as a result they form a stable particle arch/bridge across the outlet which prevents the discharge of the particles from the vessel. This is reflected in the figure 8 below. The general rule in the literature (Marinelli Joseph, 2011) is that if the outlet of storage vessel (particularly cones) is less than 6 to 8 times greater than the maximum particle size there is a possibility of the materials jamming and producing a mechanical arch over the outlet.

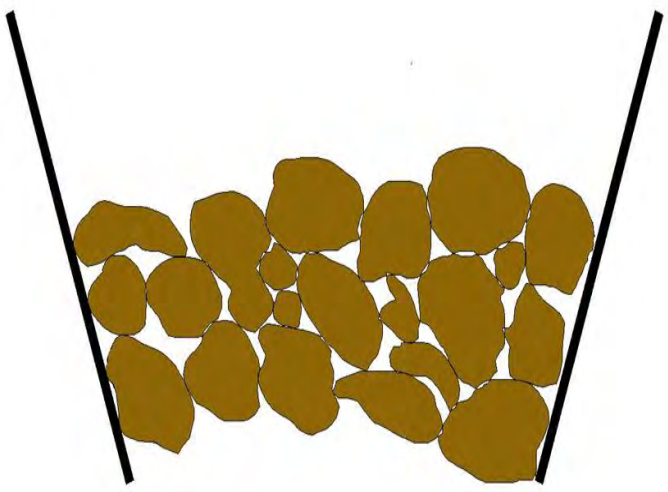

Figure 8: Mechanical Arching (Courtesy of Dr. Berry)

- **Cohesive Arching**

Cohesive arching is the flow limiting obstruction that takes place inside a mass flow vessel and it is particularly associated with fine powders. It occurs when a stable arch forms across the outlet of the vessel thus preventing flow of the powder from the vessel. If the outlet of silo were increased eventually the self-weight would exceed strength of the powder and arch will collapse. This is shown in figure 9 below. It should be noted that arching can occur in a core flow vessel but once the arch collapses rat-holing will occur.

Figure 9: Cohesive Arching (Source: Wolfson Centre short course CD)

- **Rat-holing**

Rat-holing (also known as piping) is the flow limiting condition in a core flow vessel. This is where the powder above the outlet discharges but the material at the top surface does not flow leaving a stable core. This is shown in figure 10 below. If the outlet diameter of the silo is increased the hoop stress in the core will increase and eventually will overcome the strength of the powder and cause flow.

Figure 10: Rat-holing (Source: The Wolfson Centre short course CD)

- **Critical Arching and Rat-hole Dimension**

Critical arching dimension is the minimum recommended outlet dimension for vessel geometry for the given material/particle to discharge reliably. The state of art in this theory is the work of Jenike 1964. He formulated two mathematical models (presented below) used in estimating arching dimension for conical and plane (wedge) vessel and rat-hole dimension. He developed the numerical 2D radial stress field model to predict the stress in mass-flow hoppers. The two models have been successfully used for traditional powders such as coal, flour, cement, granulated sugar. It has also been used as a fundamental base in designing and constructing new shear testers such as Brookfield powder flow tester (Berry et al, 2010), Schulze Ring shear tester (Schulze, 1996).

The premise of the formulae is that gravity flow will take place inside the vessel (either plane or conical) provided the strength developed by the material at the outlet is not strong enough to support the weight of the material above it. It means the arch will crush and the materials tend to flow reliably.

Furthermore, the critical arching dimension is directly proportional to the cohesive strength developed by the material and inversely proportional to the bulk density and acceleration due to gravity. The same theory is applicable to the rat-hole diameter except the shape factors [G(Θ) and H(Θ)] which are different from each other based on the difference between arching dimension which represents the outlet and rat-hole dimension.

Conical/Wedge vessel formula: $D_{p,c} = \sigma_c H(\Theta) / \rho_b g$ Equation 1

Where $H(\Theta) \approx 2$ for Conical Vessel and ≈ 1 for Wedge/Plane vessel

Rat-hole diameter formula: $D_{rh} = \sigma_c G(\Theta) / \rho_b g$ Equation 2

Where $G(\Theta)$ is between$\approx$ 2-10 regardless of the vessel type

σ_c = Cohesive strength of the bulk solid

ρ_b = Bulk density/self-weight of the bulk solid

g = Acceleration due to gravity 9.81m/s^2

$D_{p,c}$ = Critical arching dimension for conical and plane vessels

D_{rh} = Rat-hole dimension for both conical and plane vessel

These two prominent mathematical models have been used over the years to predict arching dimension for cohesive materials. This project is particularly focused on extreme shape materials which are not cohesive but the concept of the models have been used in this project especially for the plane (wedge) shape vessel based on the reasons explained in chapter 1 (section 1.5). The mathematical model for the plane vessel above was modified for this project by replacing the cohesive strength with tensile strength to reflect the behaviour of extreme shape materials when under stress/pressure. They only exhibit tensile strength because of their irregular shape and texture. The modified mathematical model has been used in estimating predicted arching dimensions for different extreme shape materials which are presented in chapter 6. The predicted data have been compared with the experimental (actual) data in chapter 6.

1.5.3 Comparison of Storage Vessel Geometry

Conical and flat-bottomed cylindrical hoppers shown in figure 5 above are not appropriate for extreme shape materials because they generate a core flow profile inside storage which is undesirable in the bioenergy industry, though they are easy to fabricate (Bates Lyn, 2003). They are undesirable in the bioenergy industry because materials can be static (dead) inside the storage without moving for long periods of time which could lead to unintended fermentation and formation of moulds which can cause "farmers lung" disease also self-heating and fire. Wedge-shape hoppers shown in figure 5 above are more flexible and robust than conical and flat-bottomed cylinder hopper (Marinelli Joseph, 2012; John and Jianjun, 2011) this is because vessel converges in one direction only and mass flow can be achieved at shallower convergence. They can handle a wide range of different materials like extreme shape materials. They are also favourable for experimental investigation because a mechanism to change wall angle and the outlet size can be devised in order to experimentally determine the minimum outlet size for flow of different materials. This research project has chosen wedge shape hopper (plane flow hopper) as the main focus over other hopper type because of the aforementioned reasons.

Practically, both wedge shape and flat bottom cylinder hoppers have been used in this project to carry out the experimental investigations on various biomass materials like woodchips, miscanthus, wood shavings, straw, lawn grass, shredded paper, oat flakes and reed canary grass. Experience proves that mass flow can be achieved in wedge shape hopper provided the outlet size is wide enough. The problem is predicting what the outlet size should be, without having to resort to measuring it. The flat bottom cylinder used generated core flow with very poor discharge performance for the extreme shape materials. Based on the test conducted the outlet size for core flow must approximately equal to bin size e.g. full live bottom before material discharges reliably.

In this project both experimental results obtained from the test rigs and predictive results obtained from the constitutive mathematical models will be related to wedge shape/plane flow hopper except where it is otherwise stated as for flat bottom silo which was used at the initial stage of the project. It was used for comparative studies

between wedge shape and flat bottom silos which were used as a decision making tool to choose wedge shape hopper for the proper process test for other industrial biomass materials.

Two wedge shape hoppers have been used in this project to conduct the experimental investigations. The rationale behind this is because the first existing wedge shape hopper was delivered out of a PhD project that looked into the measurement of cohesive arching of non-extreme shape materials. The two hoppers were constructed from stainless 2B material. The maximum width of this hopper (first wedge shape hopper) was 200mm, length was 600mm and wall angle was 20° to the vertical axis. During the experimental investigations that were carried out on the first rig most biomass materials tested on this rig would not flow reliably at a 200mm slot width. They formed stable mechanical arches and rat-holed often. Thus, a second test rig was required. The second test rig was designed and constructed to accommodate more materials in order to see the impact of bed head on the flowability and increase the width of the slot to maximum of 500mm while the length was still the same at 600mm. In addition, the wall angle was more flexible. Two prominent wall angles were used 23 & 41°. The rationale behind this is to know the influence of wall angle on the flowability of extreme shape materials. Results showed that materials tend to flow more reliably at 23° wall angle (to the vertical) than at the 41° particularly at wide outlet sizes (from 300 to 500mm). It also depends on the characteristics of the materials. For example, oat flakes behave better even at the smallest outlet size like 15 mm while straw is very troublesome and only flows reliably at biggest outlet size of 500mm. Both empirical and predictive results are given in chapter 4, 5, 6 and the appendices. It should be noted that all tests were for uncontrolled gravity discharge for the biomass. The use of feeders to control flow was not considered because we were interested primarily in the magnitude of the outlet size required for gravity flow and the presence of the former would affect the flow pattern and effective outlet area if the geometry of the feeder interface did not give an even draw over the outlet area.

1.6 Research Objectives

This project is focused on class 3 materials (Bradley and Farnish, 2004), extreme shape materials from handling perspective. Class 3 are non-cohesive (free-flowing at very low stresses) extreme shape materials, e.g. either fibres (elongate) or flakes

(platy) as defined previously in section 1.4. They are the most difficult to handle and difficult to characterise due to their high aspect ratio, low bulk density, variable moisture content, elasticity and their stress phobic nature. Examples of extreme shape materials are: chopped straw and grass, corn stover, sawdust, wood shavings, chicken/poultry litter, shredded paper/plastic, many wastes from sheet material, herbaceous materials etc.

Traditionally the flow properties of bulk solids are characterised using shear cells that have a limited shear strain or shear displacement. Class 3 materials do not shear in the conventional sense because they are extremely elastic and tend to tangle together, so are unsuited to these techniques. Therefore little work has been done to characterise them. As a result of this, the objectives of this project were:

- Characterisation of the flow properties of the extreme shape materials- e.g. fibrous and springy solids like woodchips, grass, paper shreds etc.
- Development of constitutive model for flow of extreme shape materials.
- Production of holistic silo design guidelines for reliable flow of extreme shape materials.

1.7 Preview of the Research Work

This thesis is structured as presented below:

- Chapter 2 reviews bodies of literature relevant to the project work.
- Chapter 3 discusses the biomass test materials employed in this project and the particle size/shape characterisation is documented. Preliminary results are provided.
- Chapter 4 discusses further results (both experimental and predictive results)
- Chapter 5 presents analysis and modelling development and testing of arching model.
- Chapter 6 discusses the development and evaluation of a critical arch model.
- Chapter 7 provides conclusions of the work and recommendations for further work.

Chapter 2: Literature Review

2.0 Introduction

Part of the methodologies employed to tackle this project was to review the literature relating to biomass handling in order to identify gaps and further knowledge of the research area. Some aspects of the literature have been reviewed in the introduction (Chapter 1) of this thesis. The structure of the literature review is as follows. Section 2.1 describes political trends for bio energy production, while section 2.2 describes the different types of biomass material currently being handled. The current best practice for storage vessel design is presented in section 2.3. Various biomass conversion processes are presented in section 2.4. The current techniques for characterising the flow properties of bulk solids and their suitability to extreme shape biomass is presented in section 2.5, while techniques for particle characterisation are presented in section 2.6. A summary of the literature is given in section 2.7.

2.1 Trend in Bioenergy/Biofuels Industry

The Department of Energy and Climate Change are struggling, in order to meet future European Union targets to produce 15% of the United Kingdom's energy from sustainable sources by 2020 (Department of Energy and Climate Change,2011). Also, in ten years' time, the higher education sector is required to minimise their greenhouse gas emissions by 34% according to the Climate Change Act 2008. In other parts of the world, 17% of total energy used in Canada comes from sustainable sources while in United States of America, 7% of total energy is from sustainable sources (Fasina Oladiran, 2006). In Sweden, 49% of total energy is from sustainable sources. The percentage is very small compared to their targets. Apart from the global warming issues, their dependency on foreign oil is a factor for their willingness to generate more energy from sustainable sources especially United States of America.

In addition by 2020 renewable energy is expected to provide a minimum of 10% of the total gasoline and diesel consumed in transport by member states of the European Union under the renewable energy directive of the European Commission (2009/28/EC). Most of these biofuels will come from second generation non-food

grade feedstock, which are extreme in shape and difficult to handle will not compete with food crops. In order to meet the highlighted targets, appropriate equipment needs to be specified and put in the right place, at the right time.

The World Energy Outlook by International Energy Agency is given below (figure 11) where biomass contributes a major quota, 1000-2000Mtoe (Million tonnes of oil equivalent) per annum. Despite the major contribution of biomass little work has been done to characterise their behaviour properties which is a requirement if we want to achieve efficient handling and conversion processes in order to meet the world energy forecast demands.

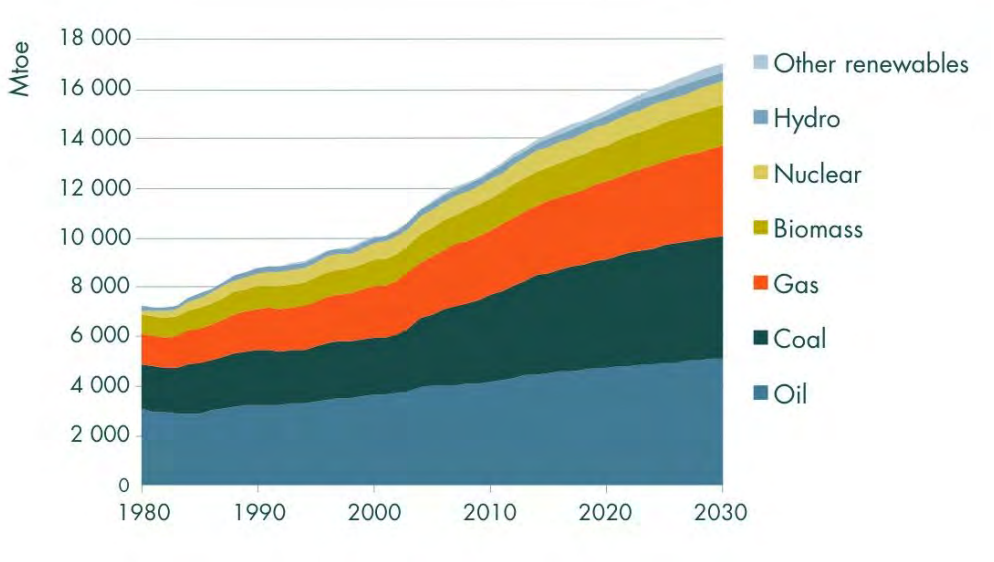

Figure 11: International Energy Agency World Energy Outlook 2008 (source: http://www.iosa.ca/the_issues/energy_supply/) Re-accessed on July 12, 2012.

2.2 Biomass

Various definitions have been given to biomass by different researchers but in simple terms biomass is all plant and animal matter that has not been fossilised as previously defined in chapter 1. Biomass has been classified as first generation and second generation. First generation biomass materials are food grade crops like corn, sugarcane, wheat, sorghum, vegetable oil. However, because of global pressures on food grade biomass, to control food prices in both developing and developed countries, the need for second generation biomass arises. United States of America

has opined to generate 60 billion litres of bioenergy/biofuels from second generation biomass by 2022 (Eisentraut Anselm, 2010). Second generation biomass materials are all non- food grade biomass materials, these are a mix of waste materials and energy crops. An energy crop is a plant that has been grown for purpose of harvesting and burning as a fuel. Examples of waste materials include: shredded paper, dried distillers grain, meat and bone meal, dried sewage sludge. Examples of energy crops might include: woodchips, miscanthus, grass, straw, oil seed rape, coppiced willow, coppiced poplar, jatropha, broomcorn, switch grass etc.

Most second generation biomass particles are extreme in shape and they are handled in bulk form. This project is focused on extreme shape biomass material handling.

2.3 Industrial Best Practise for Storage and Handling of Biomass

The current method for equipment design for biomass and waste materials handling is based on "trial and error" which often results in over design and under design of the equipment. This results in production down time because of incompatibility between the biomass materials and the equipment causing poor or unreliable flow of the fuel.

2.3.1 Current Biomass Handling Technology for Discharge from Storage

The current biomass handling methods are briefly discussed in this section. Conventional theory is that extreme shape materials will not discharge from a convergent hopper under gravity; hence full live bottom vessels are used. The two current methods are full live bottom dischargers and moving-hole feeder by Kamengo in Canada.

2.3.1.1 Full live bottom dischargers

The current popular handling technology for biomass and waste is full-live-bottom discharger (Bradley and Farnish, 2004; Bradley 2009). Examples of full-live-bottom discharger are: planetary screw discharger, push floor (sliding frame) discharger and walking floor discharger.

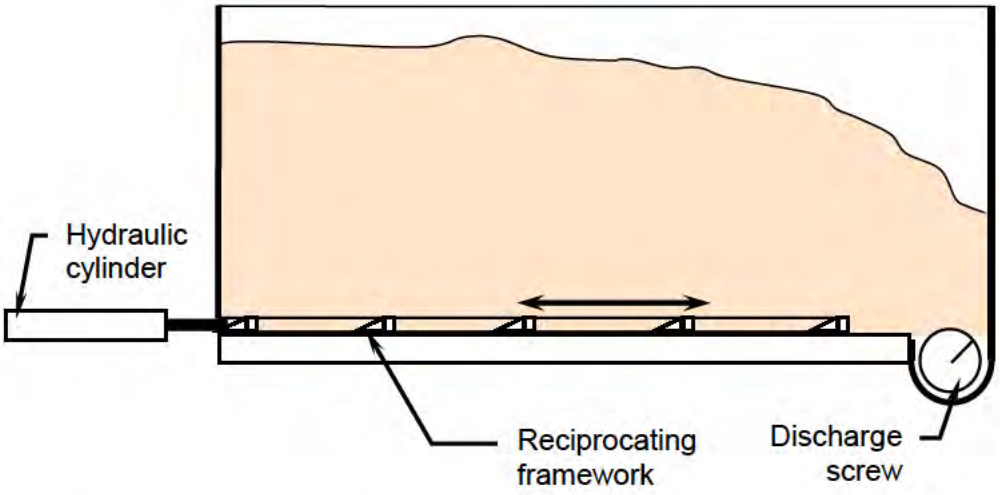

Figure 12: Sliding-frame type discharger (Bradley and Farnish, 2004)

One problem associated with these types of dischargers is that they generate high stresses in the transport mechanism required to overcome the strength generated by the materials. As a result of this and the large area they must cover, they are very expensive compared to that required for a conventional hopper. They need wide shallow bunker/vessels to minimise stresses due to self-weight especially in sliding frame type machine. They can suffer severe wear and screw breakage especially in planetary or multiple screw machine (Bradley and Farnish, 2004; Bradley 2009). Photograph of planetary or multiple screw feeder is given in figure 13 below.

Figure 13: Planetary/Multiple Screw Feeder
(http://www.continentalscrew.com/products/multiscrew.html accessed May 17, 2012)

2.3.1.2 Moving Hole Feeder

This is another biomass handling technology developed by Kamengo Technology in Canada. It is a non-consolidating feeder. The feeder avoids shearing the material inside the vessel, which in the case of extreme shape materials causes them to consolidate and resist movement. The moving-hole-feeder is not a full live bottom but it fits on the bottom of a wedge-shaped hopper. Material discharges as arch above feeder slot collapses/breaks as figure 14 below (Bundali 2000). However, the concept does not totally solve mechanical arch in the silo/vessel which are common to biomass and waste materials. If the mechanical arch (particles entanglement) in the hopper above fails to collapse/break, the moving-hole feeder will not be effective. I.e. the span of the moving hole must be larger than the critical arching dimension of the biomass.

Figure 14: Moving-Hole Feeder Concept (Bundali, 2000)

2.3.2 Evaluation/auditing of existing bioenergy plants

A bioenergy plant survey was carried out with the use of a questionnaire. The questionnaire was designed in a simple format so that the respondent can answer the questions as quickly as possible. The aim of the survey was to gain knowledge of the kind of biomass handling issues the industry is facing. 354 organisations were contacted and 24 organisations responded. The following lessons were learnt and various observations were made:

- A wide range of biomass and waste materials are currently being handled in the bioenergy industry such as wood chips (hardwoods and softwoods),

pellets & briquettes, straw, municipal solid wastes, chicken litter, silage, apple pomace, slurry, whole crop, wheat, palm residue, bagasse, sawdust, bark shavings, forest residue, recycled pallets, charcoal, shredded waste, refuse derived fuel, and sludge.

- Various particle grades (shape and size), moisture content, wood pellets dimension, wood briquette dimension were noted.
- Various types of conveying and feeding systems: walking floor, conveyors (screw, belt, drag link, scraper etc), augers, bucket elevators, silos, etc were noted.
- The key handling issues were: awkward storage and flow properties, difficulty in characterising materials, conveyors jamming due to the incorrect specification of wood being used, materials flooding, heaping and blockages.
- Material specification is based on a wide variety of reasons. Some chose their material based on: energy output; requirements of the combustion equipment; availability and cost; defined by the customers; shape and size determine by machine; avoid blockage of machine and corrosion, etc.

Most respondents have biomass and waste material handling problems. They agreed that there will be no bioenergy business without adequate handling of the feedstock. Getting the feedstock to behave well inside the storage/vessels requires the study of flow/mechanical properties of the feedstock because different bioenergy industries employ different feedstocks.

2.4 Biomass Conversion Processes

Biomass can be converted into energy in the form of transport (liquid) fuel, heat or power generation. The main objective of biomass processing before its use is to improve the characteristics of the material as fuel. The conversion processes usually involve the minimization of the water content of the material, resulting in the simultaneous increase in its thermal value and ensure its preservation and adding value to the handling characteristics of the material, like processing it into fluid, this may be gas or liquid (Charles and Essel, 1996).

Energy can be produced from biomass using various transformation processes. Figure 15 depicts the best transformation ways that are employed, products and their various markets are also reflected. The conversion is typically done in two stages: primary

and secondary stages. There are three main types of primary stage processes that convert biomass into intermediate end products. They are:

- Thermal processes which include gasification, pyrolysis and combustion
- Biological processes which include anaerobic digestion, hydrolysis and fermentation.
- Chemical processes which include trans-esterification.

The products of all these processes serve as feedstocks (raw materials) for the secondary stage, in which the intermediate products are converted to energy.

Figure 15: Illustration of conversion processes, products and markets (Bridgwater Tony, 2002)

2.4.1 Influence of Biomass Characterisation on the Conversion Processes

All the conversion processes stated above can only perform well if the process equipment such as the silo/storage vessel and feeder are designed in line with flow (mechanical) properties of the feedstock (biomass). Most biomass materials do not deform under shear stress (that is, they do not slide) especially the so-called "class 3" materials (materials with extreme shape) (Bradley and Farnish, 2004; Basu Prabir,

2010). Instead, they form nesting bond (entanglement) which cause their resistance to flow. As a result of this, they form large arch span across the outlet of the vessel and fail to flow (discharge). When this happens, the upstream process will not be able to feed the downstream process and this can lead to production downtime or even the shutdown of the plant. These kind of troublesome characteristics pose a great challenge to the equipment designer and process engineer. This is where this research project is focused.

2.5 Biomass Bulk Flow Property Characterisation Tests

The global shift to alternative energy is increasing daily. This is driving demand for energy from renewable biomass fuels. In order to meet the demand with cost effective operations, there is a need for novel technology that will enable equipment to be designed for reliable flow of the feedstock.

Feedstocks like chicken litter, corn stover, wood chips, miscanthus, switchgrass, municipal solid waste etc for the renewable energy industry are difficult to handle because of their extreme (irregular) particle shape and size; unlike ordinary powder or granular materials, they form "nests", blocking flow channels. The equipment providers/designers to the bioenergy industry currently encounter problems of putting values to the mechanical/flow properties of the material to characterise them. The flowability measurement which works well with ordinary powder and granule particles totally breaks down, when employed on fibrous, irregular shaped biomass materials (Bradley and Farnish, 2004).

2.5.1 Uniaxial Tester

Uniaxial Test Technique is a traditional method of determining the amount of stress (axial strength) a bulk particulate can withstand before it can flow or collapse. The process of conducting the test is very simple: a sample of particulate material is filled into a cylindrical mould and compressed axially with a controlled load. Thereafter, the load and mould are removed so that the particulate material is unconfined (i.e. the stress on the sides of the column are zero). An increasing vertical load is then placed onto the top of the compact until it fails (Bradley and Farnish, 2004). Often the bulk

particulate fails diagonally during the test (see figure 16). The unconfined failure test is useful because it directly replicates the stress conditions that a bulk particulate experiences during arching in a hopper as shown in figure 17. The test is repeated for a number of increasing consolidation loads and the results are used to construct the flow function. The flow function shown in figure 18 describes the flowability of a bulk solid. The horizontal axis is stress to which the bulk solid is compacted to during consolidation. The vertical axis presents the corresponding peak unconfined failure strengths that the columns could support prior to failure.

Figure 16: Uniaxial Unconfined Failure Test on Cohesive Bulk Solids (Courtesy of Dr. Rob Berry)

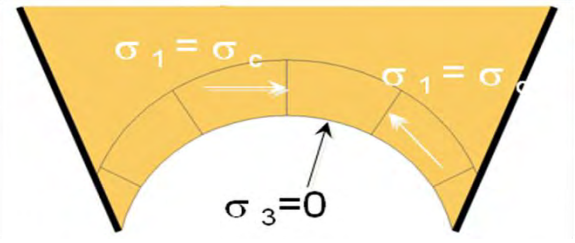

Figure 17: Element of powder in a cohesive arch over the outlet of a silo (Courtesy of Dr. Rob Berry).

From figure 17 above, it is clearly shown that all stresses in the cohesive arch are compressive because of the equant shape of the powder. The relevance of tensile

strength here is that mechanical arch that forms at the vessel outlet when extreme shape materials are in the vessel can be untangled provided the outlet is large enough. The outlet size corresponds to the tensile strength in the sense that when the outlet gate is open often extreme shape materials forms mechanical arch under the vertical stress (normal stress) because extreme shape materials do not shear under their own weight. Therefore, tensile force is required to pull the entangled materials apart for the material to flow. That is why the outlet has to be increased gradually until the materials untangle totally thereby generating flow.

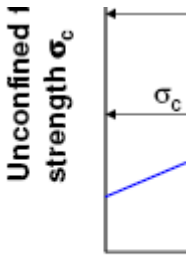

Figure 18: Flow function of a powder (Courtesy of Dr. Rob Berry)

However, the problem with this technique (uniaxial tester) is that when it is used for extreme shape materials, the sample does not fail and collapse. Instead the sample compresses but remains stable even when the applied load is much larger than the consolidation load. Thus the test cannot characterise the strength of these materials. Experimentally, this technique was adopted on extreme shape materials for further research investigations on extreme shape material characterisation. The test was conducted on hammer milled wood/woodchips, chopped miscanthus, shredded paper, lawn grass, chicken litter and sawdust. Overall, it was observed that, irrespective of the amount of load used for compaction and failure, the extreme shape materials will not collapse/fail diagonally as in cohesive powders but it will crush, entangle (nest) and form a great intense mass under the stress of the material that overlaid (Bradley and Farnish,2004;Bates Lyn, 2006). As a result of this, the uniaxially compacted material eventually failed by buckling (figure 19 below)

Figure 19: Uniaxial Test on chicken/poultry litter (Courtesy from Dr. Rob Berry: Wolfson Centre).

2.5.1.1 Models for the behaviour of biomass

When a column of granular material or powder that has particles that are approximately rounded, or equant is compressed in a confined cylinder the particle contacts tend to rotate somewhat so that some of the applied load is transmitted horizontally. This is the stress ratio of the material K and the concept of this is illustrated in figure 20a below. If this experiment is repeated with extreme shape biomass materials very different behaviour is observed.

If the extreme shape material is made up of particles that are very elastic, when the columns of particles are compressed in a vertical direction, the particles deform elastically in such a way that the particles flatten and the interparticle load remains vertical and there is no lateral transmission of the load. This concept is illustrated in (Bradley and Farnish, 2004) figure 20 b below. If the particles of the extreme shape material are rigid, the vertical deformation is reduced but the ability of the particles to rotate is prevented by the many contacts over the length so the load transmission remains vertical and there is no lateral transmission of the load. Hence the material does not spread laterally and fail as a powder would.

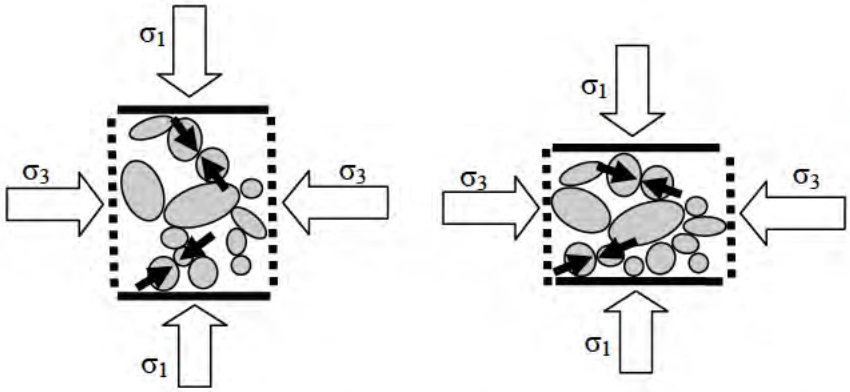

Figure 20a: Behavioural traits of ordinary bulk solids under loads (Bradley and Farnish, 2004)

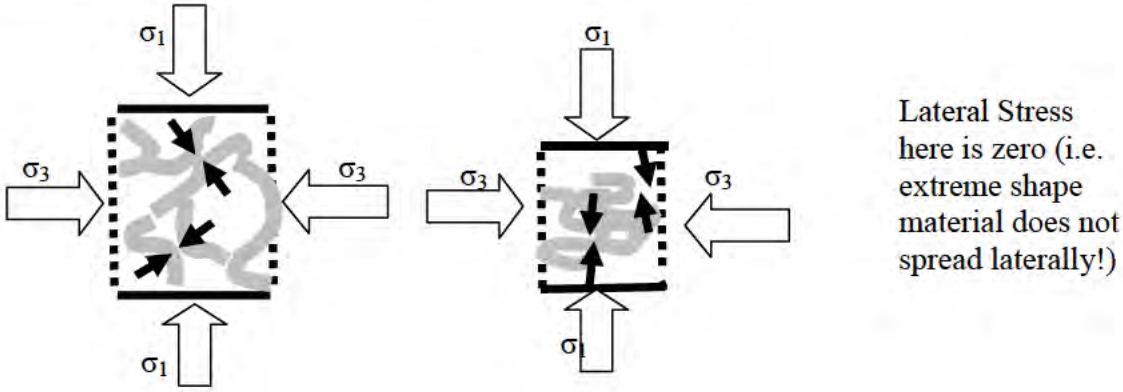

Figure 20b: Behavioural traits of Extreme Shape Materials under loads (Bradley and Farnish, 2004)

2.5.2 Shear Testers

The Jenike shear tester was the accepted standard test for measuring powder flow properties. This device is limited by its relatively small dimensions 95mm diameter (20mm depth), absolute maximum particle size is 5mm (Jenike, 1961 & 1964; Marinelli Joseph, 2000; Chevanan Nehru et al., 2009). More importantly for biomass materials (extreme shape materials) it is the limited shear strain capability of the machine which means with elastic biomass materials there is not enough shear displacement to cause failure. More recent torsional shear cells such as the Schulze and Brookfield powder flow tester have unlimited shear displacement so the sample can be failed. However, the dimensions of the shear cells are 150mm diameter

annulus, 25mm width. This gives very small particle top size 2mm (Berry, R.J. 2010 et al).

The only alternative is the large Wolfson Annular tester (figure 21), 1m diameter, which has a recommended particle top size of around 25mm (Khan Naushad, 2008). On top of all this, we know from experience of the uniaxial tester that these materials do not shear during failure, so the rotational displacement of the cell causes the material to ball up at the back of each pocket, resulting in an increase in the sample height and localised tilting of the lid. Thus this test is inappropriate because the assumption that shear forces are uniform over the cross sectional area of the cell are in error, and actually measures the torque or shear stress required to redistribute the material around the trough.

In addition, a full range of existing testers have been reviewed by Berry R.J (2004), Carson J.W (2006) and Schwedes J (1999). Again the reviewed testers are only suitable for ordinary powders and granular particles. Thus, the need for predicting storage vessel requirements for reliable discharge of biomass/waste particles (extreme shape materials) is established and essential.

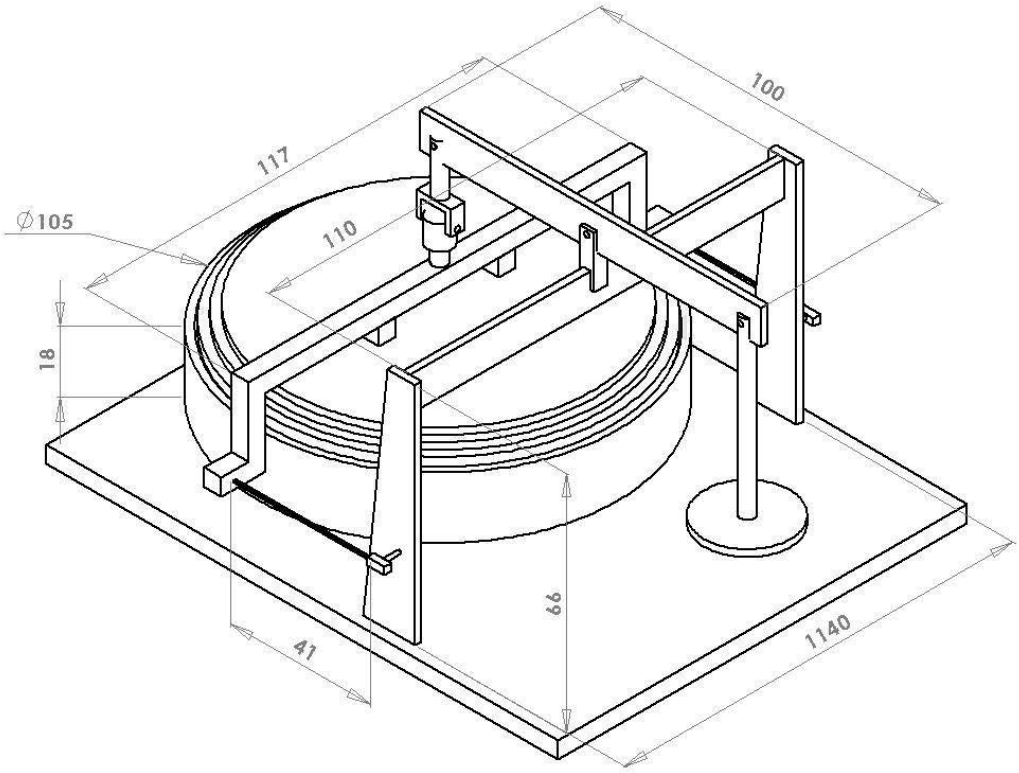

Figure 21: Large Wolfson Annular Shear Tester (Courtesy of Dr. Rob Berry)

2.5.3 Tensile Tester

Khan Naushad (2008) and Chevanan Nehru et al (2009) constructed different large version of shear cell to measure the flowability data of some biomass materials (such as chopped switchgrass, wheat straw and corn stover) which are extreme in shape but in reality biomass materials with extreme shape particles do not shear (slide) under their own weight. The flow data from Nehru's shear cell cannot replicate what designers will experience in real life (i.e. it cannot be used to design biomass handling equipments). As a result of this limitation, a new biaxial tester was conceived at The Wolfson Centre for Bulk Solids Handling Technology, named Tensile Tester. The tensile tester was designed and constructed to study the effect of strip length on flow of shredded sheet material (Idagbon Nicholas, 2009). It can also be employed to measure the tensile strength of other biomass materials especially "class 3" biomass. It would benefit from further reengineering in this project with a load cell to allow measurement of wide varieties of biomass and waste materials but it was used

successfully in this project. The mechanism of the tester and detailed illustration are given in chapter 3.

2.6 Silo Discharge Tests

Due to the failure of the traditional shear testers to measure the flowability parameters of extreme shape materials, silo(hopper) test methods have been developed over the years by The Wolfson Centre for Bulk Solids Handling Technology (Bradley and Farnish, 2004);Mattsson (1990);Mattsson (1997);Mattsson and Kofman (2002); Mattsson et al, 2004, Bundalli, N. (1989), Eckhoff and Leversen (1974), Wright (1970).

2.6.1 Wolfson Centre Hopper Test

The hopper test rig is a wedge shape hopper. The principal is the same with Eckhoff & Leversen (1974) and Wright (1970). It is designed in such a way that the geometry can be changed in order to facilitate increase in the outlet size until the material discharges reliably. Also, the required wall slope to achieve mass flow can be obtained. Figure 22 below shows chopped plastic flakes inside the hopper test rig.

Figure 22: Wolfson Centre Hopper Test Rig (Courtesy from Dr. Rob Berry)

2.6.2 Jan Erik Mattsson's Silo Test

The concept is similar to Wolfson's hopper test rig because it also adopts the idea of increasing the outlet size until the mechanical arch collapse/break and materials start discharging/flowing. However instead of using a converging hopper it uses a flat bottomed vessel. The critical outlet at which the materials (Extreme Shape Materials: such as reed canary grass, wheat straw, salix shoots chunks, birch stemwood chunks, saw dust, wood powder, wood pellets, salix shoots chips, birch stemwood chips, wood briquettes, birch stemwood chunks, logging residues chips) start flowing reliably is measured as the reliable outlet size for the particular materials. The limitation to this kind of technique is that it does not give wall slope required to achieve mass flow pattern inside the storage which is desired in industry. Figure 23 illustrate the concept. In addition, Mattsson's approach was solely based on experimental investigations in determining the critical outlet dimension for the biomass materials. No mathematical model has been done to calculate the critical outlet dimension for the biomass materials based on the available literatures.

Figure 23: Mattsson's Silo Discharge Test Concept: Outlet size continuous increment (Mattsson and Kofman 2002)

2.6.3 Aperture Tester by Bundalli

The concept of aperture tester was used to further develop the moving hole feeder commercialised by Kamengo Technology in Canada as described in the previous chapter. The aperture tester is made of a box that is rectangular in shape with clear sides made of plastic (figure 24). The box bottom is formed by dual stainless steel slides that are polished. The slides converge in the middle of the box (The Roger et al, 1994). Retracting the slides generates an outlet size beneath the box which is similar but not exact to Wolfson's hopper test and Mattsson's silo test. Also, this tester does not indicate wall slope required to achieve mass flow (first in, first out) pattern inside the storage/vessel.

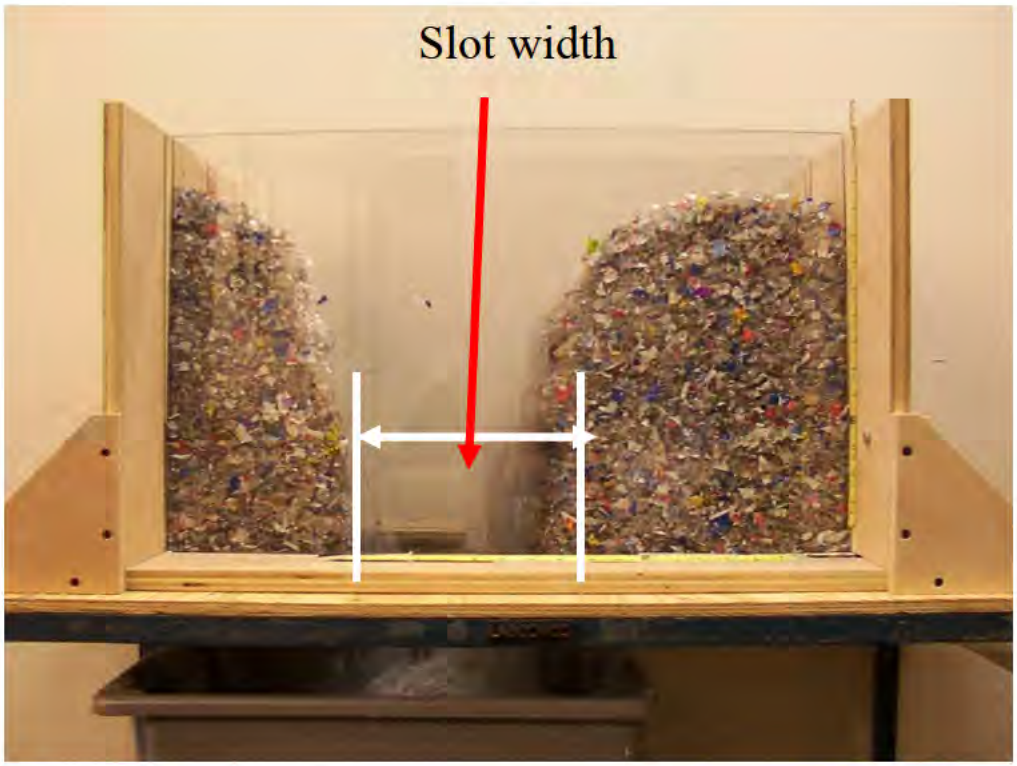

Figure 24: Aperture Tester by Bundalli (Courtesy from Timothy Bell- DuPont, USA)

2.7 Summary

Biomass and waste materials which are extreme in shape and size are currently in demand as one important alternative feedstock to generate biofuels which could mitigate the global warming. These materials can only be used productively if their flow properties are well understood. Various shear testers and uniaxial tester have been reviewed in order to understand the existing characterisation practise for traditional powder and granules and why this characterisation test approach fails completely on extreme shape materials. Results from the literature and practical experience have shown that extreme shape materials do not shear during failure. Current silo discharge tests for extreme shape materials were also reviewed. Most current silo discharge tests reviewed are core flow discharge which are undesirable for biomass and waste materials because not all the materials will be able to discharge reliably as expected in the bioenergy industry, except The Wolfson Centre hopper which was designed as mass flow discharge but it cannot accommodate wide variety of extreme shape materials because of its small outlet size.

Chapter 3: Test Materials and Preliminary Results

3.0 Introduction

The test materials were selected for their extreme particle shape because they are examples of those being currently handled in industry as outlined in section 3.2. The preliminary experimental investigations included:

- characterisation of the particles (section 3.2)
- novel characterisation of the flow properties (section 3.4) using a column test and (section 3.5) using a tensile tester
- measurement of the critical outlet dimension for reliable gravity flow in core-flow (section 3.6) and mass-flow (section 3.7),
- characterisation of the flow properties (section 3.8) using standard shear testers

3.1 Selection of test materials: Extreme Shape Materials

Extreme shape materials are fibrous materials that are irregular in shape and size. In particular, they have different measurements in the three dimensions (length, thickness and width) unlike traditional particles like lactose where all the 3 dimensions are approximately equal. They (extreme shape materials) have either 1 dimension that is very much larger than the other two, e.g. a fibre (elongate materials), or two dimensions very much larger than the third e.g. a flake (platy materials). See figure 25 below.

Elongate

Platy

Figure 25: Extreme Shape Materials showing combination of acicular fibre & flake

The other aspect is the elasticity (spring-back effect) of the material. Some of the materials have rigid flakes or fibres while others are elastic. When the rigid materials

like matchsticks are subjected to consolidation load (σ_1), after taking the mould off and consolidation load, there is no spring-back effect; they remain stagnant unlike flexible (elastic) materials which most biomass are, they spring-back after taking off the mould and the consolidation load (See figure 26 below) thus sample loses strength prior to failure measurement.

Figure 26: Illustration of rigid and elastic extreme shape materials

Thus extreme shape biomass materials have high aspect ratio, they have low bulk density, so, gravity exerts small force on them. When they are under stress, they mat /knit (entangle/nest) together. The first selected material was matchsticks because some extreme shape materials are shaped like acicular particles (needle-like particles e.g. matchsticks) (Klein Ileleji, 2010) causing them to nest (entangle) and resist flow inside vessel which is the common trait among biomass and waste materials. The matchsticks were used to develop experimental investigation into the behavioural traits of other extreme shape materials. Other industrial grade materials were employed namely: hammer milled wood, chopped miscanthus, shredded paper, lawn grass, wood shavings, straw and oat flakes.

3.2 Characterisation of the particle size and shape

The traditional techniques for characterising the particle size of bulk solid are primarily sieving and laser diffraction. Both these techniques assume that the particle dimensions are approximately equal in all directions (equant) to describe the particle size. This however presents a significant problem when trying to characterise extreme shape materials, i.e. flakes or platy particle will only pass through a mesh that

is slightly larger than the longest and intermediate dimensions of the particle (but giving no information about the shortest dimension. Conversely a "fibrous" or elongate particle could pass through a mesh just larger than the intermediate and shortest dimension, giving no information about the longest dimension. However in practice it will not sieve and will bridge on the screen.

Therefore the only realistic option for determining the size and shape is to use digital imaging analysis as is presented in the following sections. Still there are significant limitations with this approach. Firstly it is only possible to view a small sample of particles, so this may not represent accurately the full distribution of sizes and shapes of the material. Secondly the image is 2D so the third dimension is unknown. Finally while an automated system for scanning and recording the dimensions of the particles could be devised, no such machine is commercially available to deal with the large particle sizes prevalent in biomass (they are made for smaller particles), so each particle must be measured individually from a scan which is extremely time consuming, severely limiting the quantity of particle measurements that can realistically be obtained.

Presented below are the average dimensions taken from a sample of 20 particles off the scans. These are the lengths and the widths only. The 3rd dimension, i.e. the shortest dimension of platy materials ("flakes") and the shortest and intermediate dimensions of elongate materials ("fibres") were measured using a digital micrometer. A shape factor was determined for each material by dividing the longest dimension by the intermediate dimension. This is the standard for measuring aspect ratio or shape factor of any materials.

Regarding the bulk densities of the materials these were determined from the weight of material filled into the known volume of the test cell of 300mm diameter and 100mm depth under 14KPa applied stress (normal stress). Thus these are the equivalent to the consolidated bulk densities of the materials.

Table 1 Comparison of the particle properties and bulk densities of the different extreme shape materials tested

Material	Mean Particle dimensions				Bulk density [kg/m^3]	Moisture content [%]	Flowability:free flowing Yes/No
	Long [mm]	Intermediate [mm]	Short [mm]	Aspect ratio			
Hammer milled wood	6	1	0.4	6	152	8	Y
Miscanthus	6	1	0.4	6	167	3	Y
Paper	297	5	0.1	59	212	-	Y
Grass A	240	1	0.4	240	36	-	Y
Grass B	200	0.5	0.1	400	35	-	Y
Wood shavings	16	6	0.5	3	85	-	Y
Match sticks	40	2	2	20	104	-	Y
Oat flakes	4	2	0.6	2	436	-	Y
Straw	140	4	0.7	35	35	-	Y
Reed Canary Grass	42	2	0.5	21	128	-	Y

Note: The standard deviation for the particle dimensions are given in Appendix C.

a)

b)

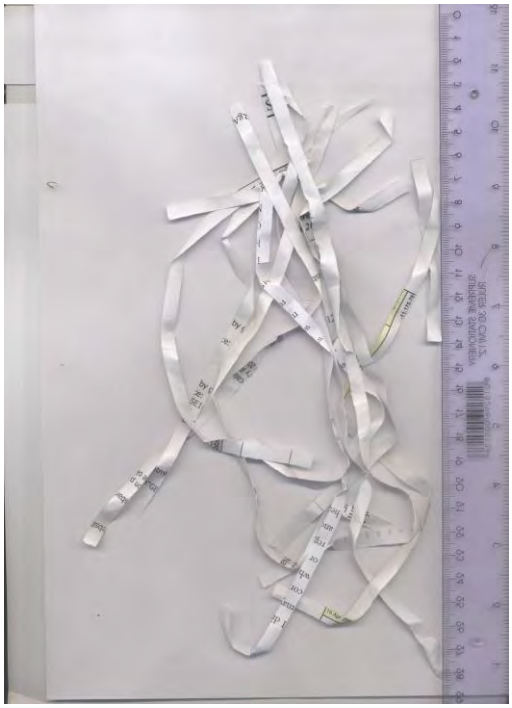

c)

d)

Figure 27: Micrograph of particle size and shapes a) Hammer milled wood, b) Miscanthus, c) shredded paper & d) Lawn grass A

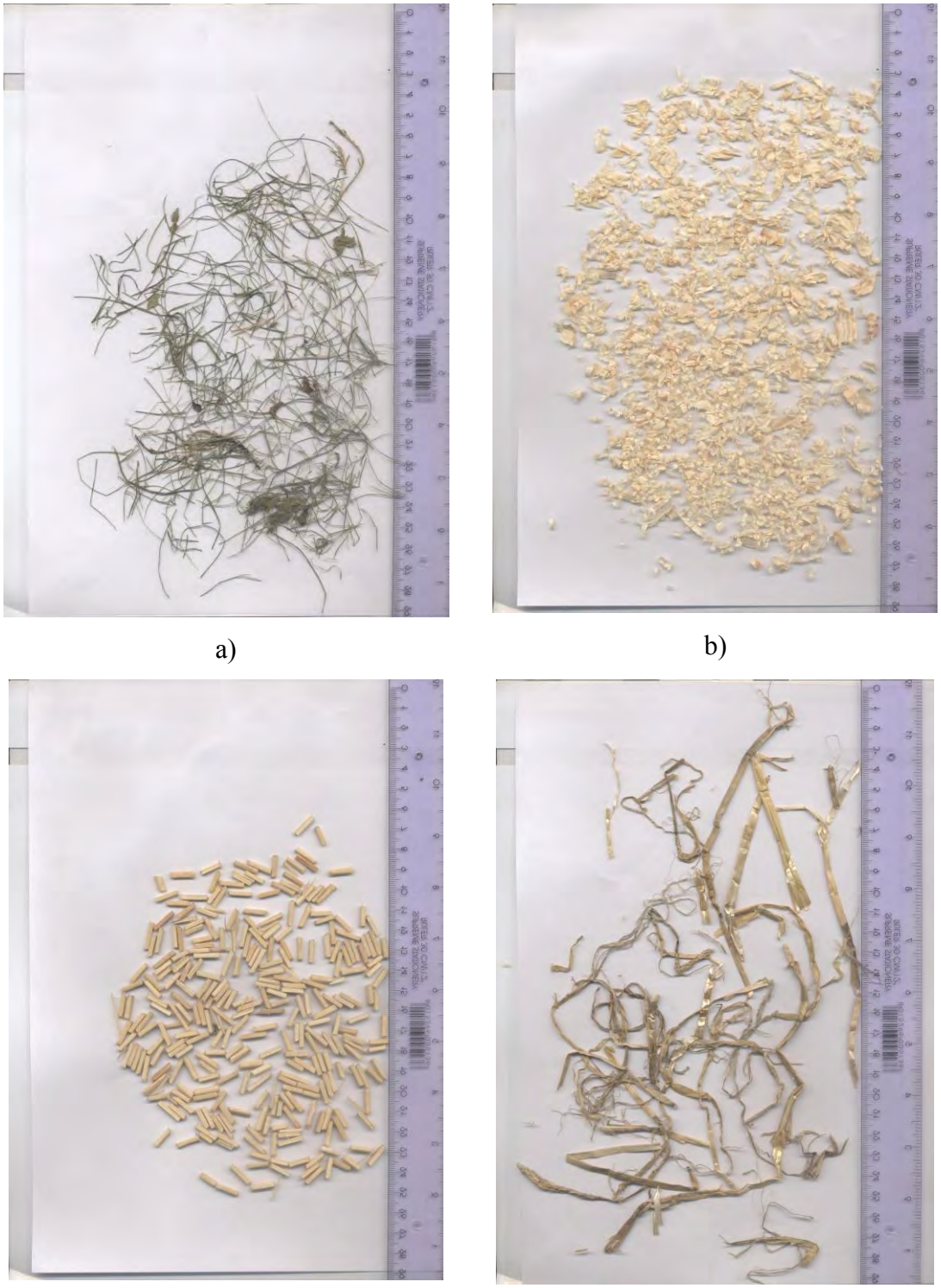

a) b)

c) d)

Figure 28: Micrograph of particle size and shapes a) Lawn Grass B, b) wood shaving, c) match sticks & d) Straw

e)

f)

Figure 29: Micrograph of particle size and shapes for (e) Oat flakes and (f) Reed canary Grass

3.2.1 Description of Particle Dimensions Distribution

The particle size distribution analysis was done on the above shown materials except shredded paper and matchsticks. Shredded paper and matchsticks approximately have the same lengths in the 3 dimensions (i.e. the long length is constant, intermediate length is constant and short length is constant). The intermediate length represents the width of the material while short length represents the thickness of the material.

3.2.1.1 Hammer Milled Wood/Miscanthus

Both hammer milled wood and miscanthus has the same characteristics. For the long length distribution, most of the particles are in the range of 5mm to 6mm. Very few particles are in the range 6mm to 8mm. This is reflected in the figure 30 below. The intermediate length distribution shown in figure 31 below shows that majority of the particles fall into 1mm width. Other particles are in between 1 to 1.4. For the short length distribution which represents the thickness of the particles, majority of the particles are 0.4mm thick. Very few particles are in between 0.4mm to 0.9mm. This is reflected in figure 32 below.

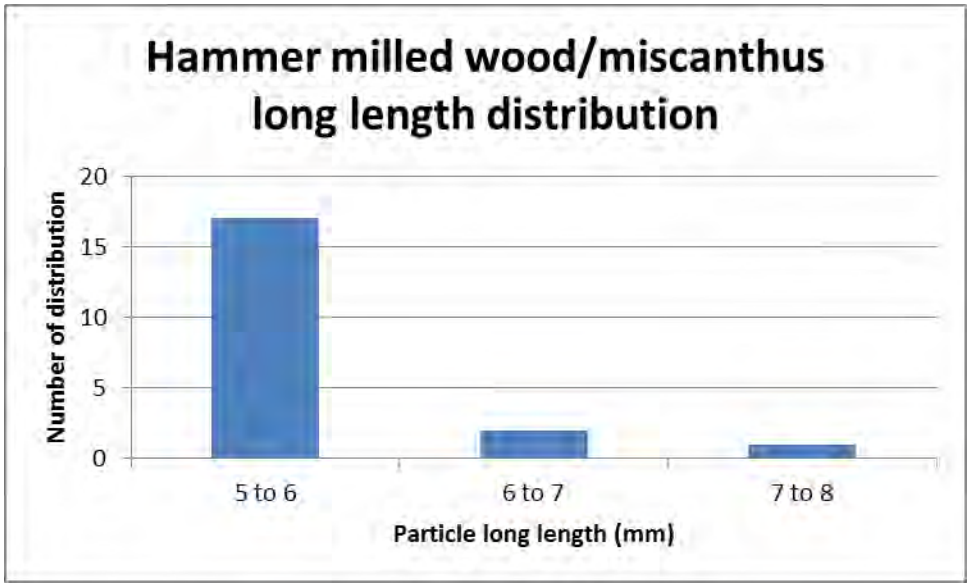

Figure 30: Particle size distribution of long length for hammer milled wood/miscanthus.

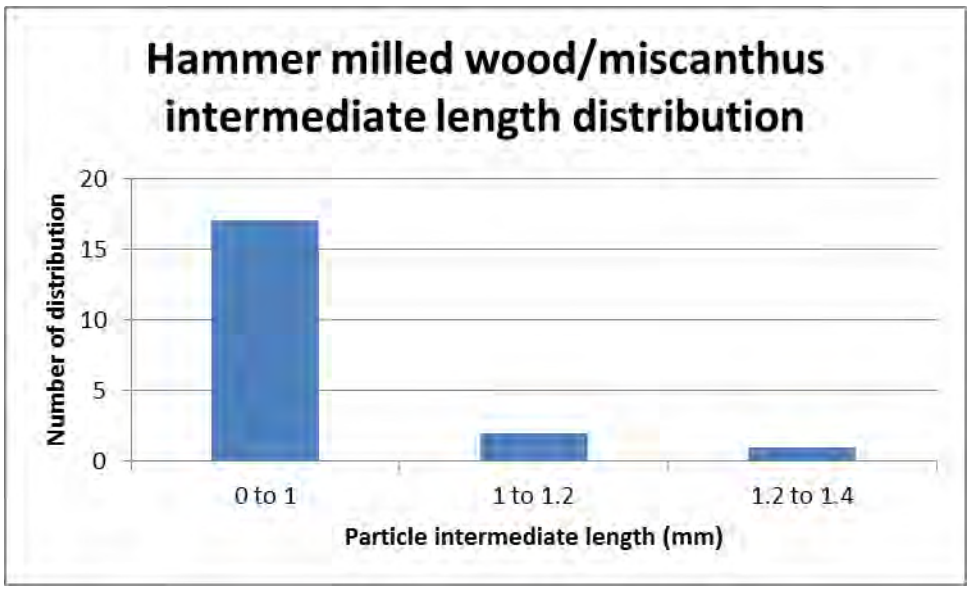

Figure 31: Particle size distribution of intermediate length for hammer milled wood/miscanthus.

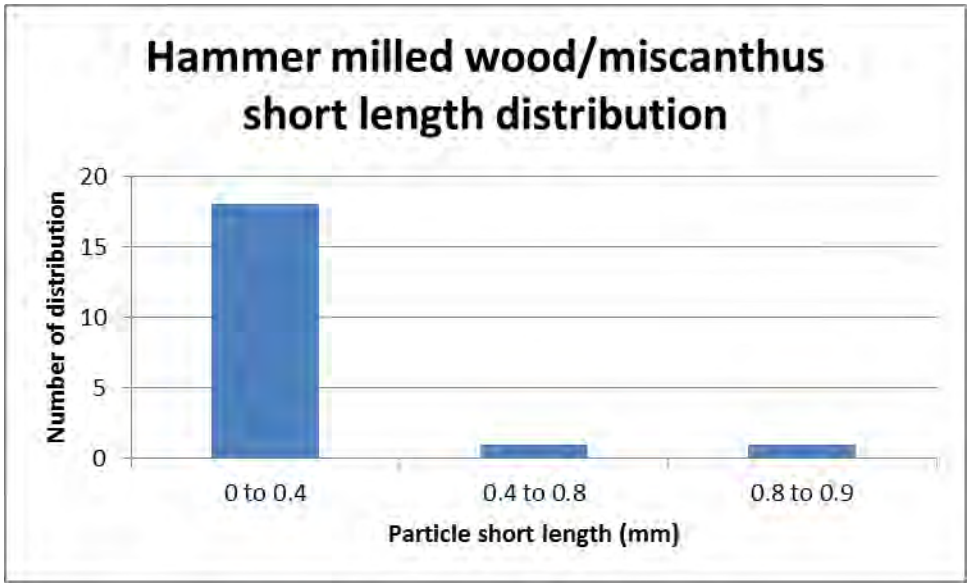

Figure 32: Particle size distribution of short length for hammer milled wood/miscanthus.

3.2.1.2 Wood Shavings

The distributions of particles dimensions (long, intermediate, short lengths) are wide. This is reflected in the figure 33, 34 and 35 below. For the long length distribution, the particles are widely distributed between 5mm to 23mm. Particles of length 8mm to 11mm are the majority follow by 11mm to 14 and 17mm to 20mm. For the intermediate length distribution, majority of the particles fall into category of 3mm to 7mm. For the short length distribution, majority of the particles are in the category of 0.2mm to 0.4mm.

Figure 33: Particle size distribution of long length for wood shavings

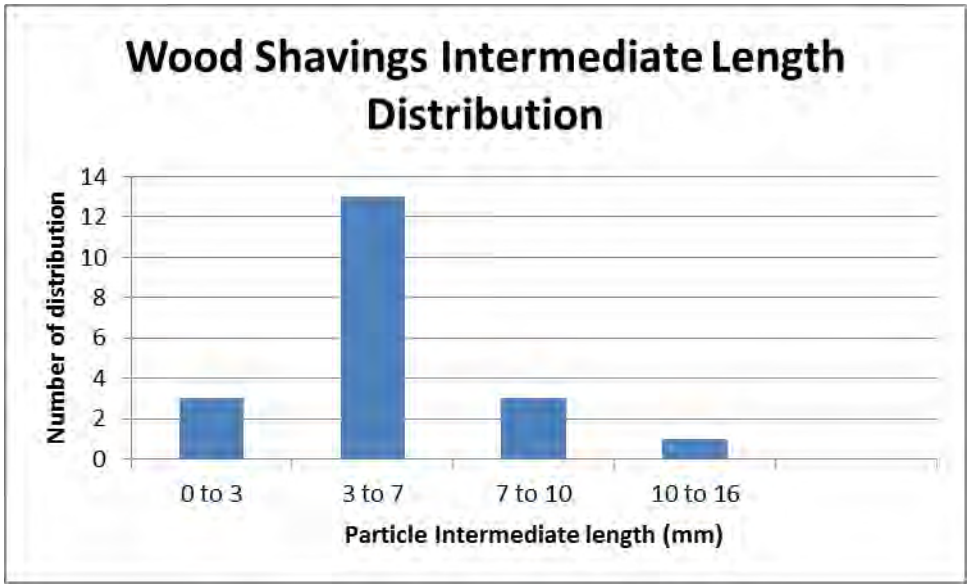

Figure 34: Particle size distribution of intermediate length for wood shavings

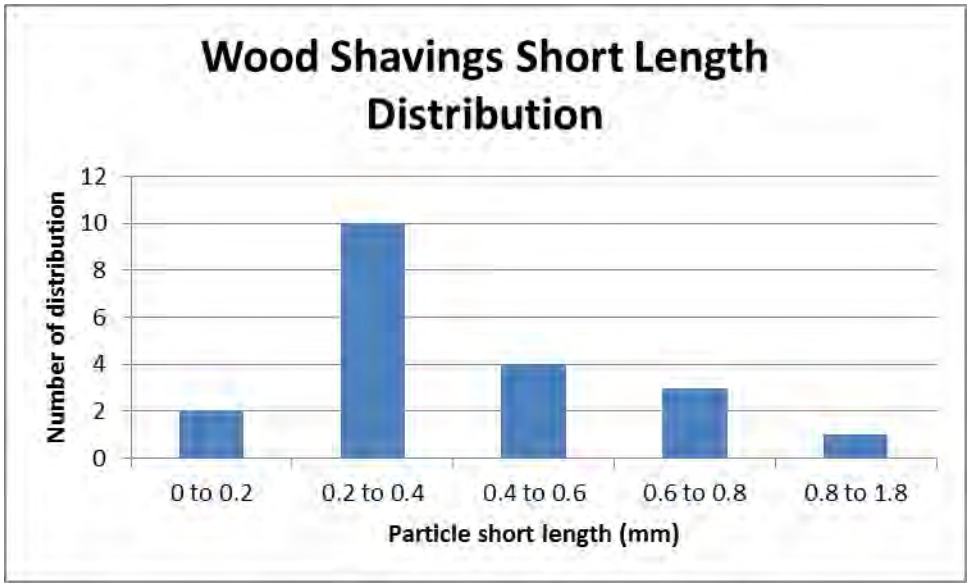

Figure 35: Particle size distribution of short length for wood shavings

3.2.1.3 Oat flakes

For the long length distribution which is shown in figure 36 below, out of the six categories of the particles, particles which have length between 3.5mm to 4mm are the majority follow by particles between 2.5mm to 3.5mm. For the intermediate length distribution, majority of the particles fall into category of 1.5mm to 2mm as shown in figure 37 below. For the short length distribution shown in figure 38 below, majority of the particles are in the category of 0.4mm to 0.6mm. Other categories are 0.2mm to 0.4mm and 0.6mm to 0.8mm.

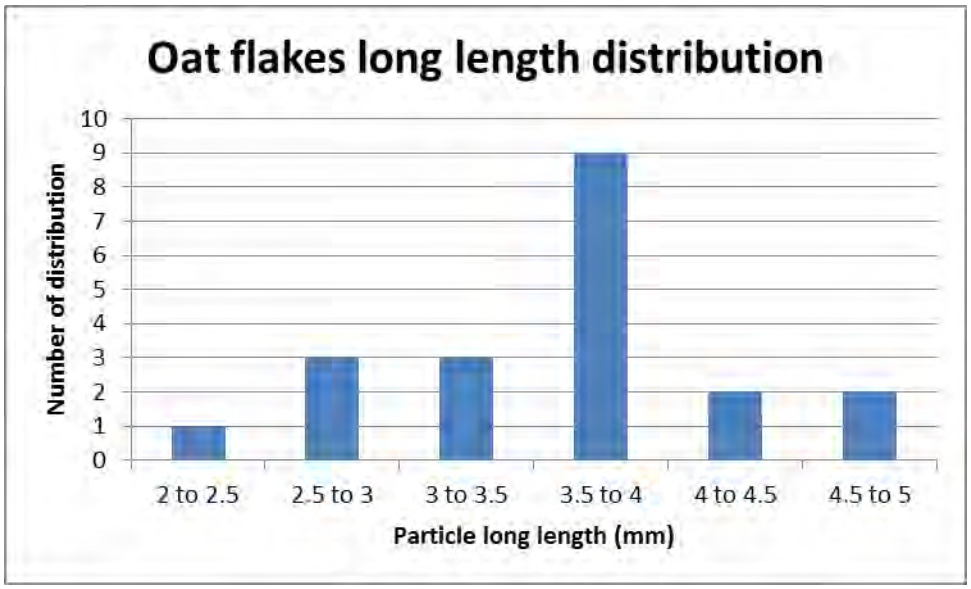

Figure 36: Particle size distribution of long length for oat flakes

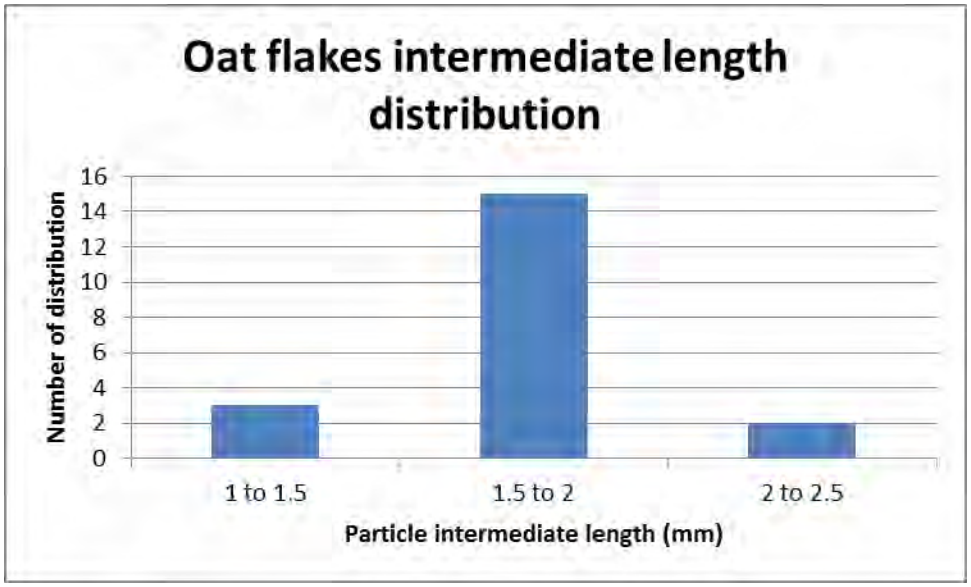

Figure 37: Particle size distribution of intermediate length for oat flakes

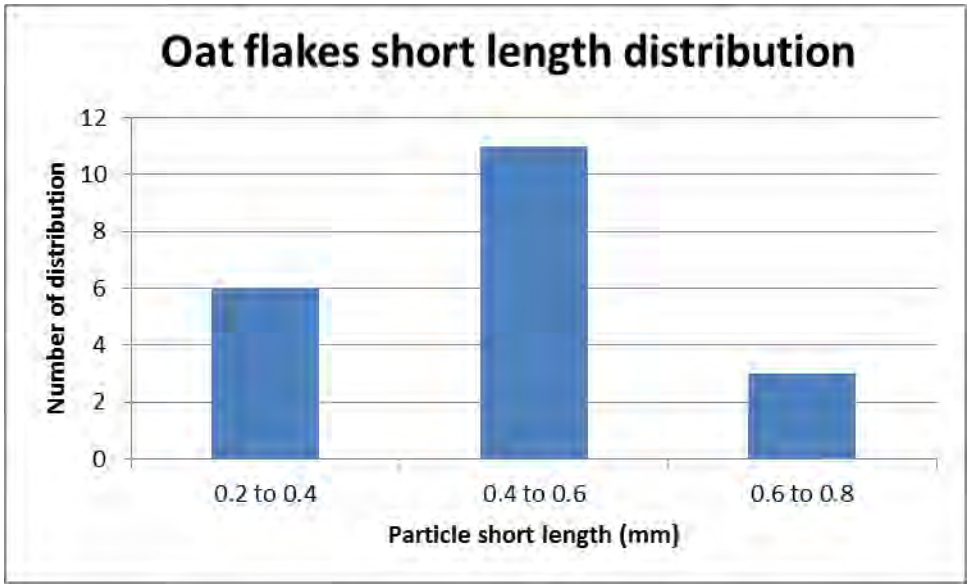

Figure 38: Particle size distribution of short length for oat flakes

3.2.1.4 Straw

The long length distribution is wider compare to other 2 lengths (intermediate and short). This is reflected in figure 39, 40 and 41 below. For the long length distribution, majority of the particles are in the category of 140mm to 160mm follow by 80mm to 100mm. For the intermediate length distribution, majority of the particles are in the category of 4mm to 5mm follow by 3mm to 3.5mm. For the short length distribution, majority of the particles are in the category of 0.3mm to 0.5mm follow by 0.5mm to 0.7mm.

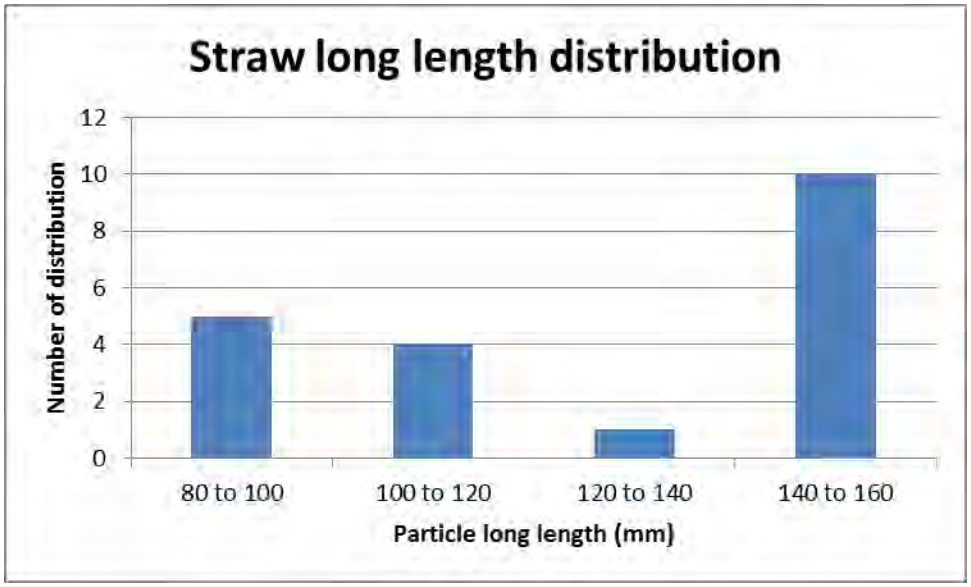

Figure 39: Particle size distribution of long length for straw

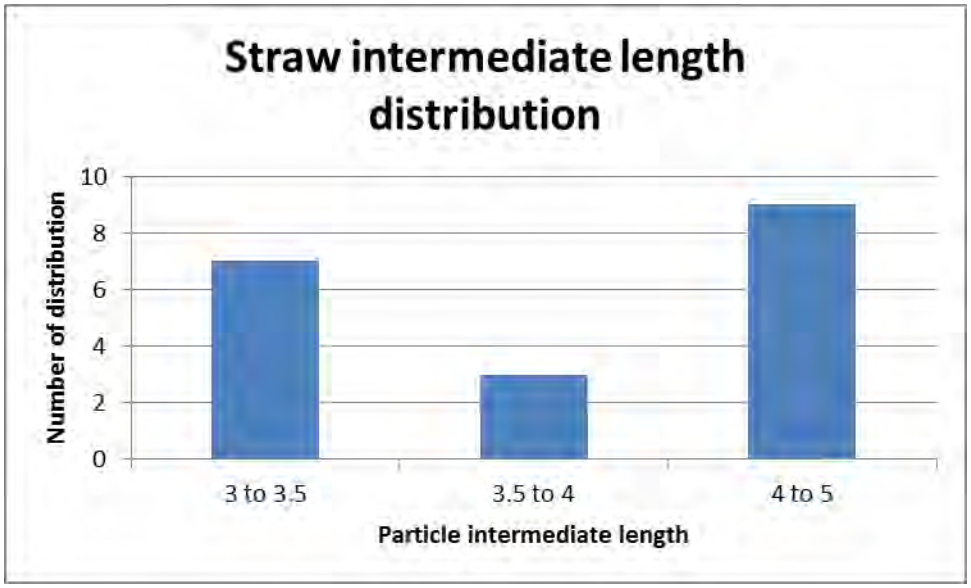

Figure 40: Particle size distribution of intermediate length for straw

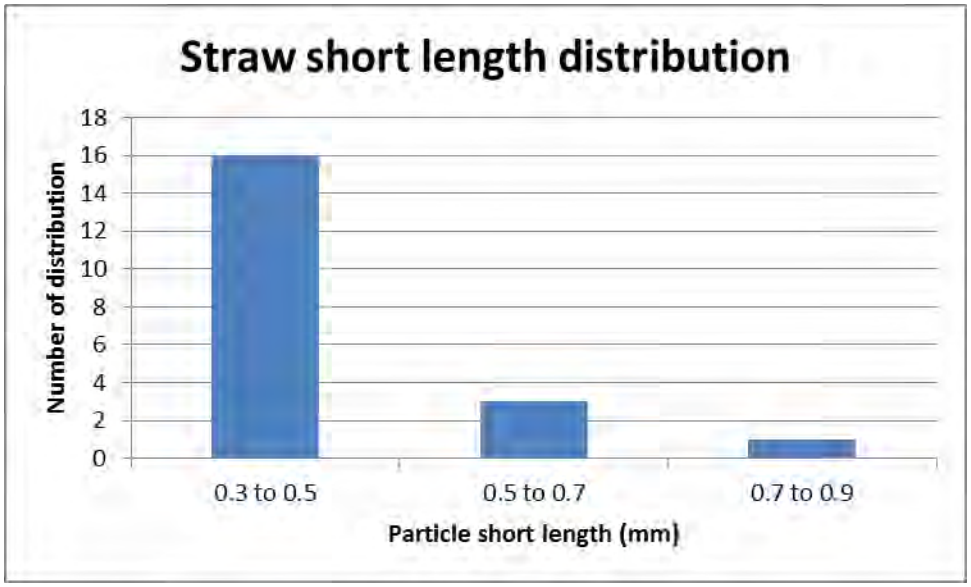

Figure 41: Particle size distribution of short length for straw

3.2.1.5 Reed Canary Grass

The lengths (long, intermediate and short) distribution of reed canary grass consistently fall into 3 categories as shown in figure 42, 43 and 44 below. For the long length distribution, majority of the particles fall into the category of 40mm to 45mm. The next category is 35mm to 40mm follow by 30mm to 35mm. For the intermediate length distribution, majority of the particles are in the category of 1.5mm to 2mm. Other categories are 2mm to 2.5mm and 2.5mm to 3mm. For the short length distribution, majority of the particles are in the category of 0.4mm to 0.6mm. Other categories in the distribution are 0.2mm to 0.4mm and 0.6mm to 0.8mm.

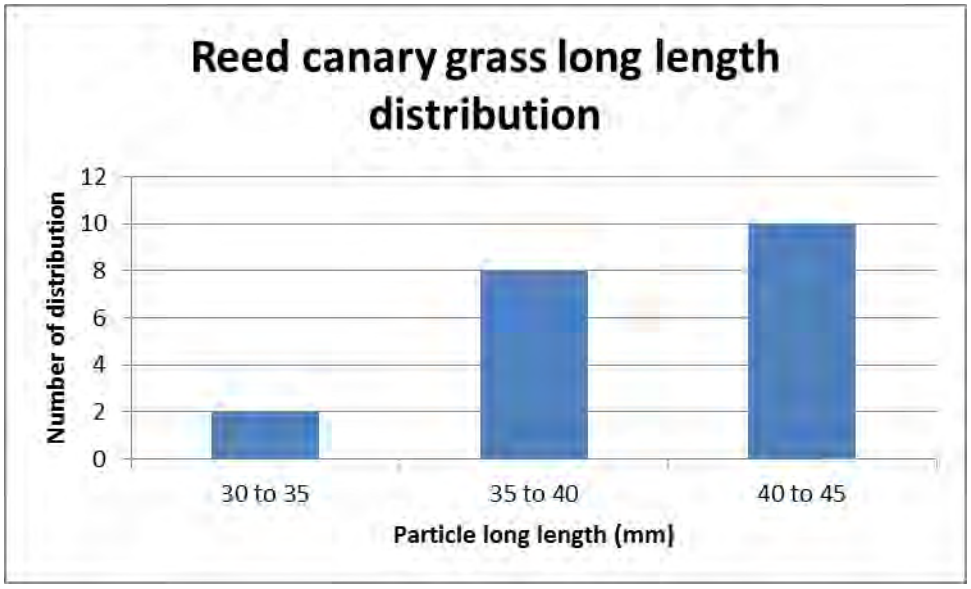

Figure 42: Particle size distribution of long length for reed canary grass

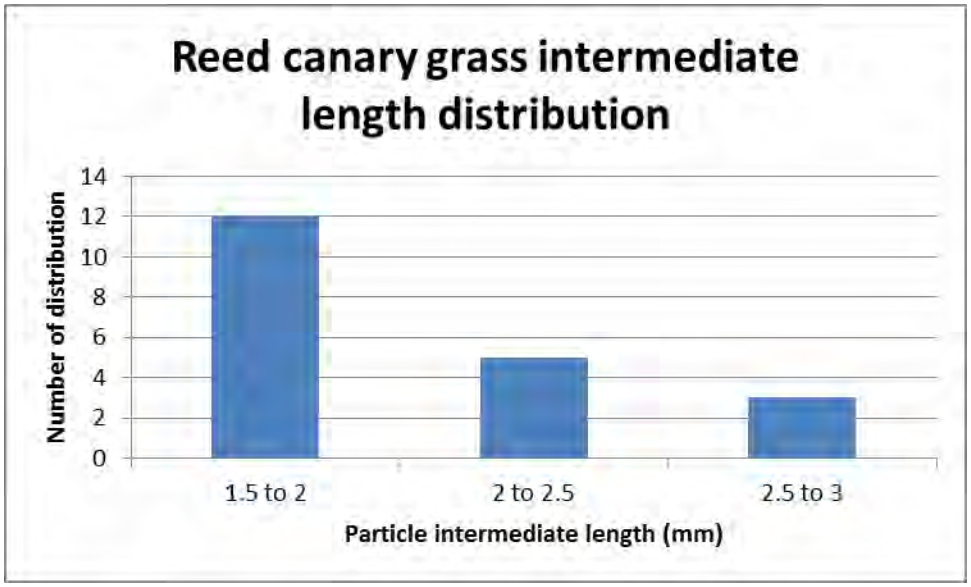

Figure 43: Particle size distribution of intermediate length for reed canary grass

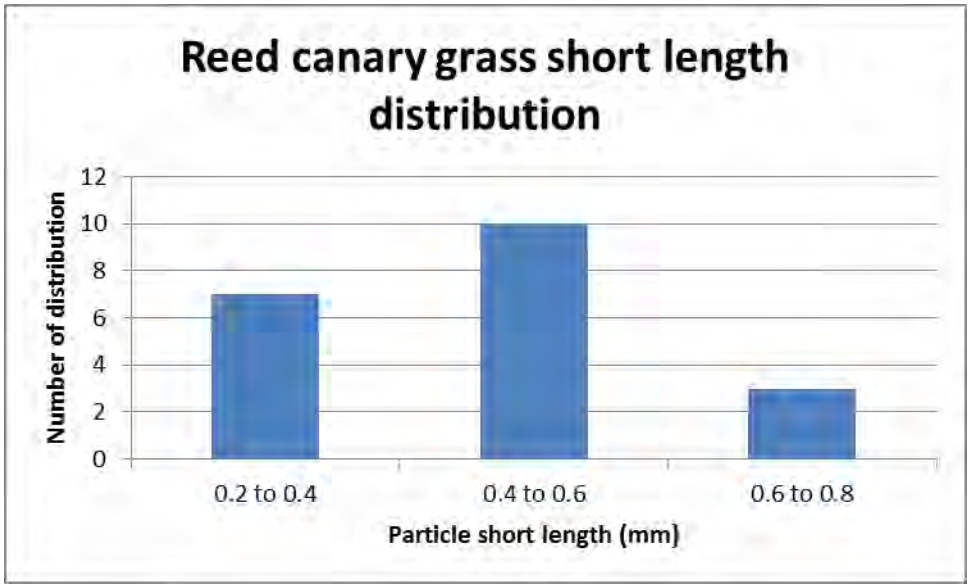

Figure 44: Particle size distribution of short length for reed canary grass

3.2.1.6 Grass A

The intermediate length for the grass A is constant. Also, the short length is constant. They do not change. The long length is distributed over 3 categories. The highest category is particles between 200mm to 250mm. Other categories are very small and they are 150mm to 200mm and 250mm to 300mm. This is reflected in figure 45 below.

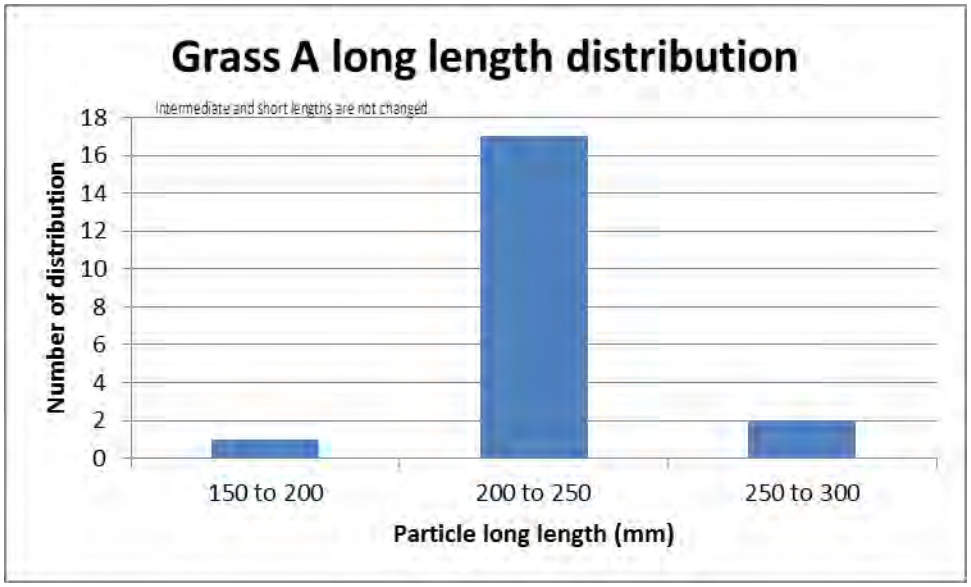

Figure 45: Particle size distribution of long length for Grass A

3.2.1.7 Grass B

The intermediate length for the grass B is constant. Also, the short length is constant. They do not change. The long length is distributed over 4 categories. The highest category is particles between 195mm to 205mm. Other categories are very small and they are 175mm to 185mm, 185mm to 195mm and 205mm to 215mm. This is reflected in figure 46 below.

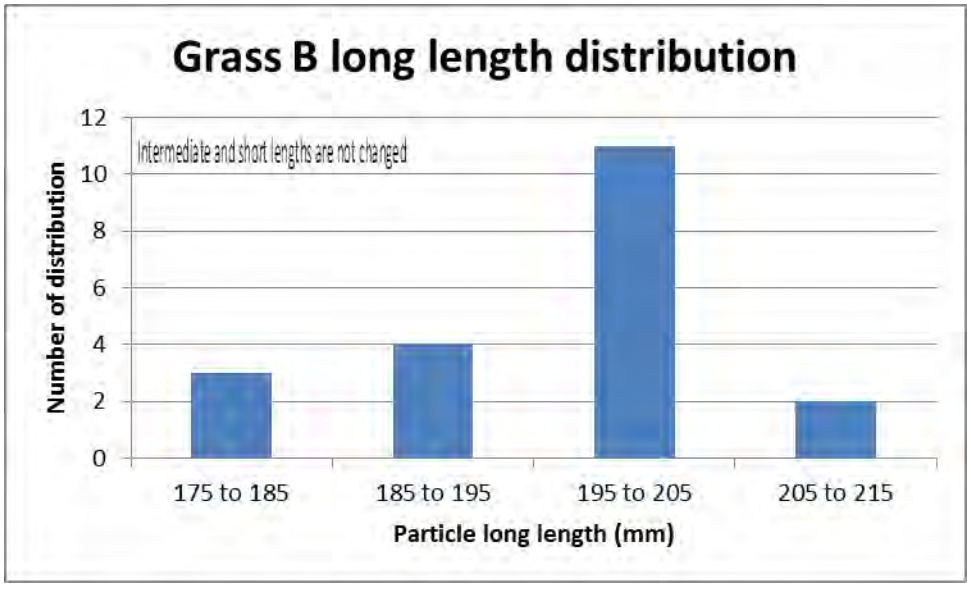

Figure 46: Particle size distribution of long length for Grass B

3.3 Relationship between the particle size and test cell / silo geometry

When undertaking flow property measurements of bulk solids it is necessary to ensure that the particle dimensions are small relative to those of the test cell /silo to ensure that we are measuring bulk properties rather than the strength of individual particles, which have interlocked across the geometry of the equipment. The general rule in the literature (Marinelli Joseph, 2011) is that if the outlet of storage vessel (cones) is less than 6 to 8 times greater than the maximum particle size there is a possibility of the materials jamming and producing a mechanical arch over the outlet. Similar rule goes for wedge shape hopper: if the slotted outlet size is less than 3 to 4 times the largest particle size there can be mechanical arch over the outlet. This rule applies to approximately equant particles (traditional powder like flour, sand, coal, etc) so the question is for platy "flaky" or elongate "fibrous" materials, which particle dimension should be used for determining the minimum dimension of test cells or silo to prevent mechanical arch? If we assume a mean dimension should be taken then the equivalent diameters of the test materials and minimum dimensions of equipment are given in table 2 below. The mean dimensions are calculated based on wedge shape hopper assumption as applied to non-extreme shape materials stated above. The mean particle dimension is calculated for each material by adding the long and intermediate lengths shown in Table 1 and dividing by 2. Minimum geometric length is calculated by multiplying mean particle dimension by 4. The results shown below (Table 2) are not consistent with what was experienced in the experimental investigations particularly in the plane flow (wedge shape flow) discharge tests. This approach proves further those techniques which apply to non-extreme shape materials are not suitable for extreme shape materials.

Table 2: Comparison of assumed mean particle dimensions and the minimum test cell/ silo dimension to prevent the influence of particle size on the results

Material	Mean particle dimension (mm)	Minimum geometric length (mm)
Hammer milled wood	3.5	14
Miscanthus	3.5	14
Oat flakes	3	12
Straw	72	288
Wood shavings	11	44
Matchsticks	21	84
Grass A	121	484
Grass B	100	400
Shredded paper	151	604

3.4 Column Test

The column test technique is a form of uniaxial test technique which was devised through discussion with my supervisors as a quick test for identifying whether a material exhibits nesting behaviour or not, prior to undertaking further characterisation work for equipment e.g. silo design. In essence the column test uses a length of hollow tube as shown in figure 47a, which is filled with bulk solid. The tube is lifted vertically in a smooth and controlled manner (whilst monitoring the tube height) while the behaviour of the bulk solid is observed. If the material is free flowing it will discharge and form a conical heap as the tube is elevated (see figure 47b). If the bulk solid exhibits nesting behaviour (is a class 3 biomass) it will form an unconfined vertical column as the tube is elevated (figure 47c). Because the results of the test will be influenced by the relative dimensions of the tube and the particles, this column test has been evaluated for a range of different biomass materials and tube dimensions as outlined below.

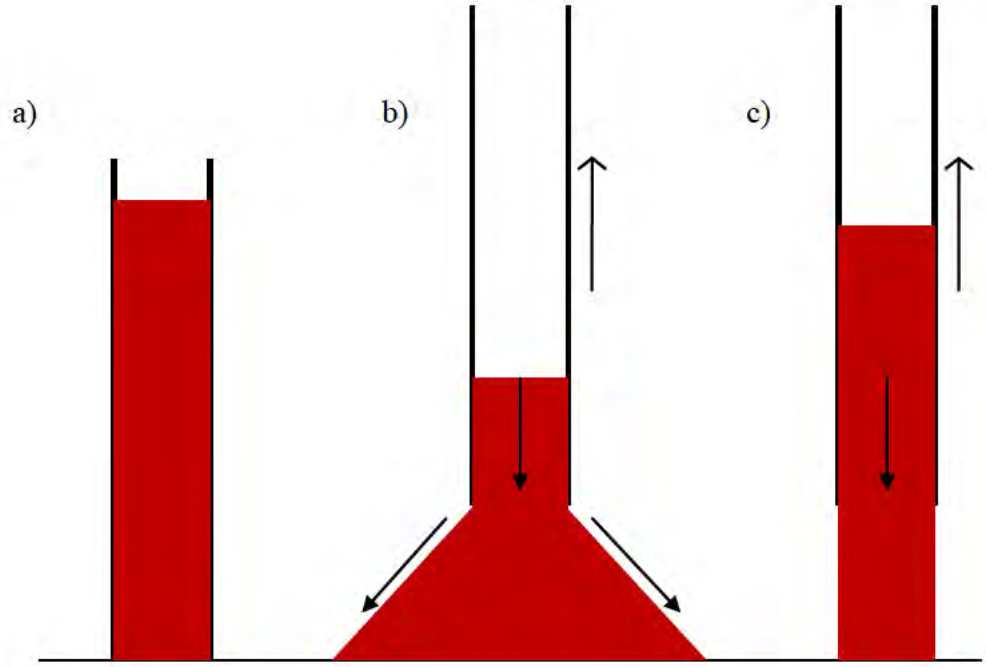

Figure 47: Schematic illustration of the concept of the column test, a) column filling b) failure or flow of free flowing biomass material & c) stability or non flow of extreme shape biomass materials

The column technique was employed to study the flow characteristics of 4 biomass materials supplied by Alstom and matchsticks in tubes of 64, 103 and 150mm diameters namely:

- Chopped miscanthus
- Dry hammer milled wood
- Wet hammer milled wood
- Ground Palm Kernel Nut: this material has not been previously referenced/mentioned because it did not form any stable column due to its spherical shape and size. They do not nest/entangle. This kind of material can be characterised using standard shear tester such as Brookfield Powder Flow Tester and Jenike Shear Tester.

3.4.1 Test setup

To facilitate the smooth controlled vertical motion of the column it was attached to a forklift truck via a horizontal plywood support platform. To undertake a test the tube was filled to the top with biomass and levelled. A steel rule was then used to regularly check the height of the tube outlet above the floor, while forklift was pumped in a slow, smooth controlled manner. If a column was formed as the tube was lifted, the height of the column when collapsed was recorded.

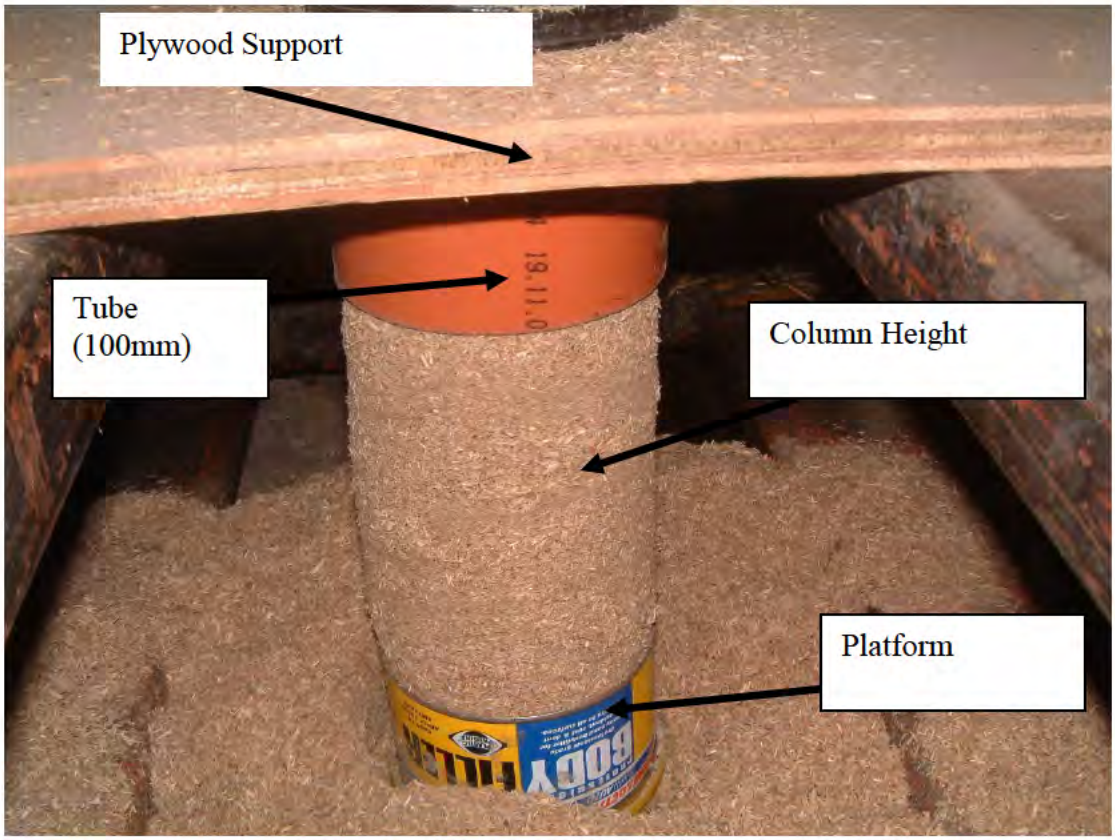

Figure 48: Column Test Technique for the flow properties of biomass particles (Column Stability of hammer milled wood).

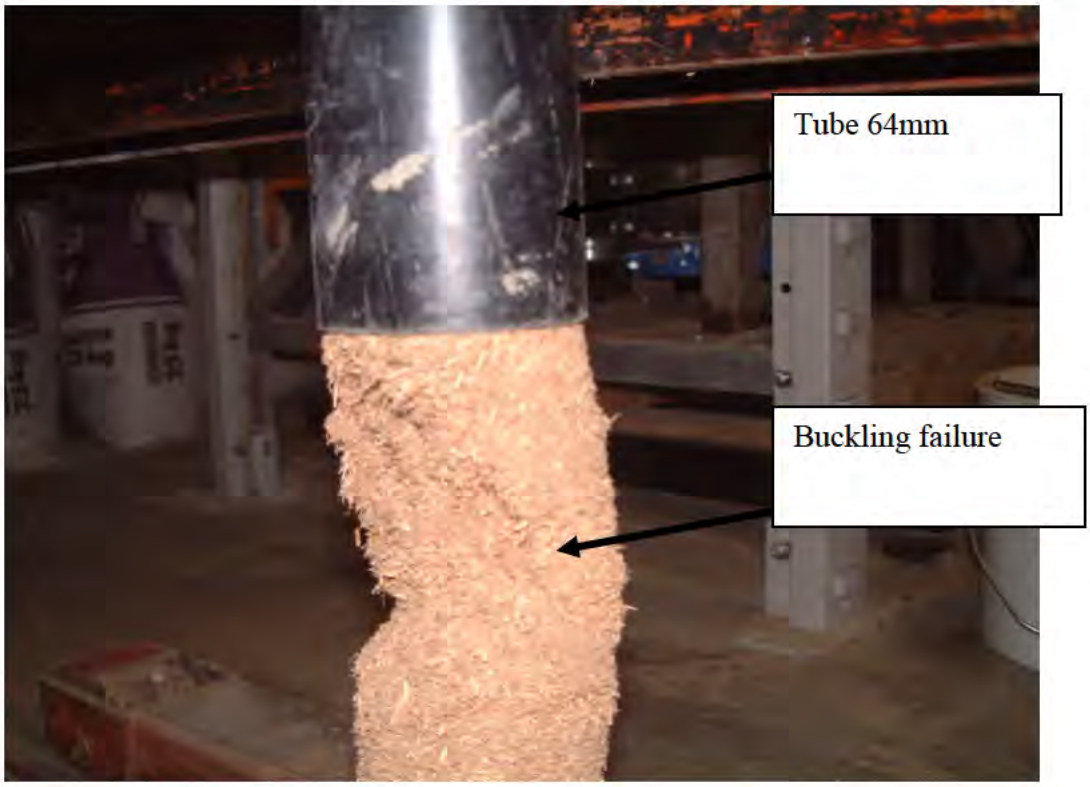

Figure 49: Buckling failure mode of chopped miscanthus

3.5 Tensile Tester

From the study of extreme shape biomass materials' response to compressive stress in the uniaxial unconfined and column tests, the materials become stronger, because the fibre rotate and orientate horizontally to support the vertical stress (as discussed in the mental model in section 2.5.1.1). To get an extreme shape biomass material to failure or flow a tensile stress must be applied perpendicular to the direction of the compressive load. This also correlates with what must also occur in mass-flow silo, as illustrated photographically in figure 22 (Chapter 2: section 2.6.1). To test this, a tensile tester was utilised.

3.5.1 Tensile Tester Description

The tester was delivered from an MSc Project (Idagbon Nicholas, 2009). It consists of two separate half cells with lids made from plywood. One of the cell halves is fixed and static while the other is dynamic. The fixed cell half is rigidly attached to a rectangular steel frame. The dynamic half-cell is suspended from the rigid steel frame via four steel wires arranged as a parallelogram linkage. A pulley system attached to

the rigid support frame opposite to the dynamic cell, applies a horizontal tensile force to the dynamic cell via a rope and pulley connected to a vertical load.

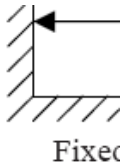

Figure 50: Illustration of Tensile Tester

3.5.2 Test Procedure

The two cells must be clamped in contact to avoid failure during the filling of the cells. Desired materials were filled inside the cells until it reaches the desired bed height (at least it must be more than half of the cells depth to have good measurements) and covered with the lids. Filling could be dump filling or random-spread filling. Materials were compacted with equal axial loads on both half cells. The axial (normal) loads used were; 2, 3, 4,5,6,7 kg (over both half-cell). The tensile force required to fail the biomass sample was measured. This was achieved by suspending a bucket over the pulley and gradually filling it with sand until the dynamic cell pulled away from the static cell. The amount of tensile load that separates the two cells was measured and recorded. This procedure was repeated on different extreme shape materials like hammer milled wood, shredded paper, miscanthus, straw, oat flakes, lawn grass A&B, woodshavings, matchsticks. On each material, the test was repeated five times.

3.6 Core Flow Test

The concept of the technique "core flow approach" emanated from the core flow test where acicular particles (matchsticks) were employed for the practical model (simulation). The core flow test rig was developed to measure the critical outlet dimensions for flow of a range of extreme shape materials, namely:

- Dry hammer milled wood
- Chopped Miscanthus
- Shredded paper
- Lawn grass "Class A"
- Lawn grass "Class B"

3.6.1 Description of the core flow test rig

The core flow test rig consists of a flat bottomed cylindrical silo with an incrementally adjustable outlet diameter (concentric rings): 100mm, 150mm, 200mm, 250mm, 300mm, 350mm, 400mm, and 450mm as shown in figure 30. The rings are made out of cast nylon. They are removed sequentially from smallest to largest in order to determine outlet diameter where the materials discharge under gravity. The concentric rings were placed on retractable dual metal bars (slide bars) to support and hold the rings firmly at both ends. The rings were positioned inside a rectangular plywood base with a circular hole drilled around the plywood. This allows step increases in the outlet diameter without imparting shear stress to the ensiled material.

The plywood was placed on the metal support with four legs. Big bag was placed beneath the outlet (rings) for the collection of the material after discharge. A detachable barrel/cylinder which was used to simulate a silo/bin was placed on the rings for the containment of the particles/materials as shown in figure 52.

3.6.2 Mode of Operation of the Core Flow Test

The test material was filled into the silo (manually loading material using a 10 litre drum and step ladder) to the desired bed height.

Thereafter, the retractable dual metal bars (slide bars) which were positioned at both ends of the rings were pulled gradually (enabling the rings to drop out one by one), incrementally increasing the outlet dimension until a reliable discharge (the point at which the fibres start to flow without any particles hang-up in the bin) was achieved. The ring diameter where reliable discharge was achieved was recorded as the critical outlet dimension.

Figure 51: Arrangement of the rings inside the silo (the rings are made out of cast nylon)

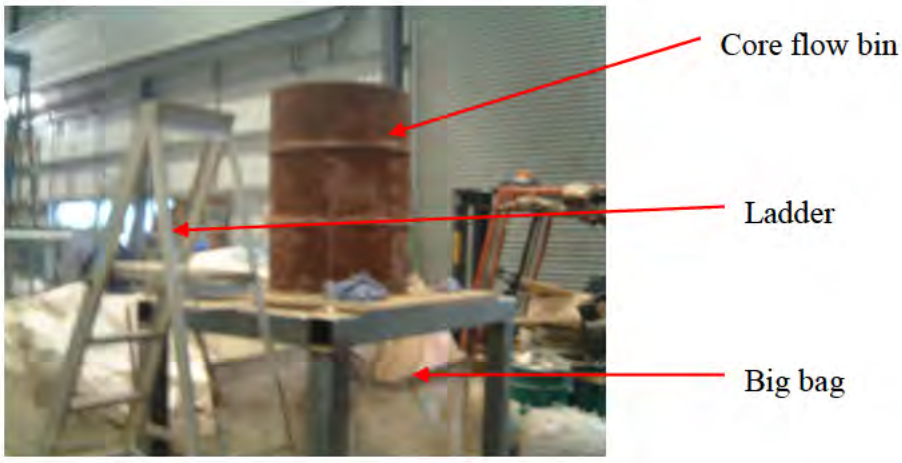

Figure 52: Core flow test rig

3.6.3 Modifications to the Core-flow test rig

Due to the time taken to fill the silo and then incrementally increase the outlet diameter to the point of flow, it was possible that time of storage at rest might be increasing the strength of the material. To investigate this possibility a second set of concentric rings were cut with the minimum outlet dimension consistent with values at which flow was found to occur for the range of materials tested. Thus second set of rings shown in figure 53 below gave three outlet dimensions of 400mm and 500mm respectively.

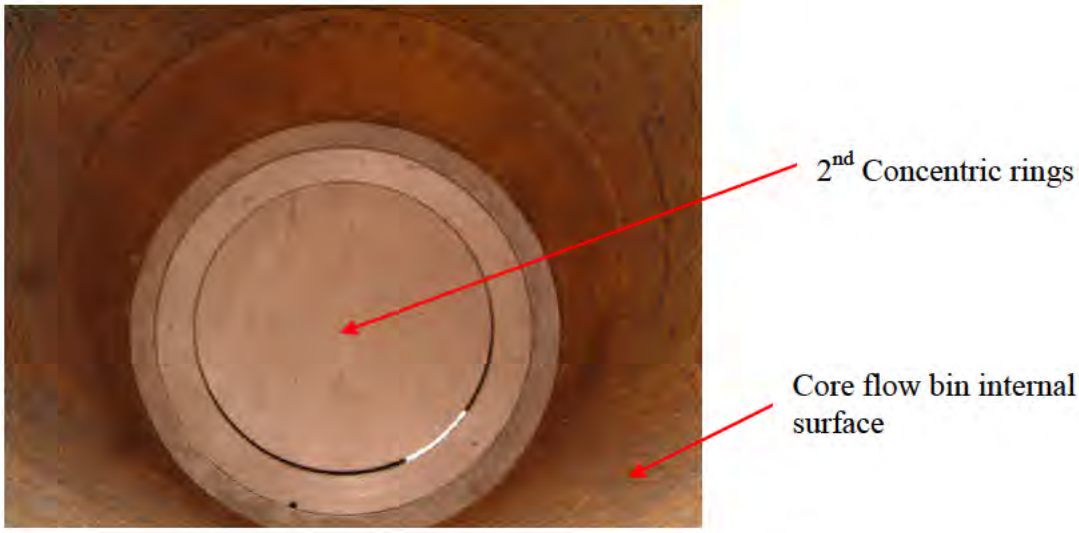

Figure 53: Second ring arrangement inside the "silo" (barrel)

3.7 Mass Flow Test

The test was conducted on the Wolfson Adjustable Plane Flow Hopper Rig. The hopper was delivered out of previous PhD research project which looked into conventional cohesive arch materials characterisation (Berry Rob, 2003). The hopper is wedge-shaped and made out of stainless steel in slot form (rectangular/oblong form) at the outlet. The width (breadth) of the outlet and the steep (wall) angle are adjustable while the length of the slot is constant. It was employed and incorporated into the current PhD research project because it was adjustable (at slot outlet and at angle). The flexibility of the hopper enabled easy measurement and determination of the outlet dimension and wall angle where the extreme shape materials discharge reliably and unreliably. The hopper is supported with four metal bars welded together to form a cube where the hopper is placed. A staircase was placed beside the rig for

easy manual filling of the hopper. The schematic diagram of the wedge shape vessel is shown in figure 54 below.

Figure 54: Schematic diagram of variable geometry silo (Courtesy of Dr. Rob Berry)

- A $1m^3$ big bag was placed at the bottom (outlet) of the hopper to collect the material after discharge. Hooper gate was constructed from plywood to activate and deactivate the particles inside the hopper. The adjustable hopper is operator-friendly (i.e. easy to use and handle).
- Each test was carried out five times to measure and validate the outlet dimension where materials/particles discharge under gravity and reliably.

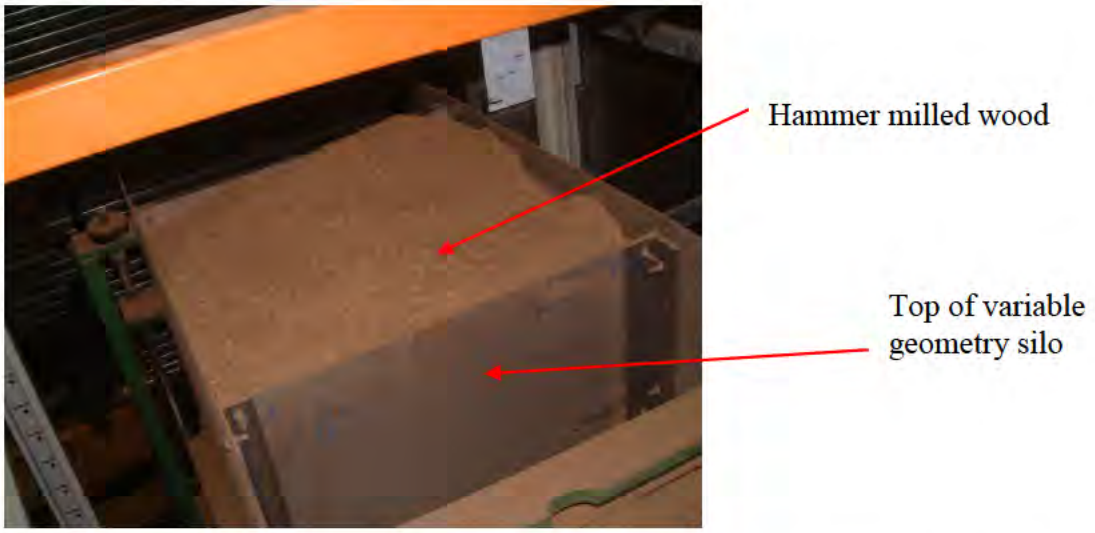

Figure 55: Biomass test material (hammer milled wood) sitting inside the adjustable plane flow hopper.

3.7.1 Mode of Operation of the Rig

The hopper filling was done by a mixture of "dump-filled" and "dump-filled and levelling" methods. The material was filled in a small barrel (fibre drum) and transferred to the hopper top via the staircase-ladder.

The hopper outlet diameter is adjusted to the datum (first) dimension and the gate was closed. Filling was continuous until the hopper is filled to the top surface or to the desired bed head (height) as shown in figure 55 above. After filling to the desired level based on the research need, the gate was opened and materials/particles start to discharge/flow until the hopper is empty.

The point at which there was reliable discharge/flow was measured and recorded inside the data-template created for the purpose of this research. This point was taken as the minimum outlet dimension.

Figure 56: Chopped Miscanthus Rathole (view from the top of the particle bed)

Figure 57: Chopped Miscanthus mechanical arch (bottom view of the hopper)

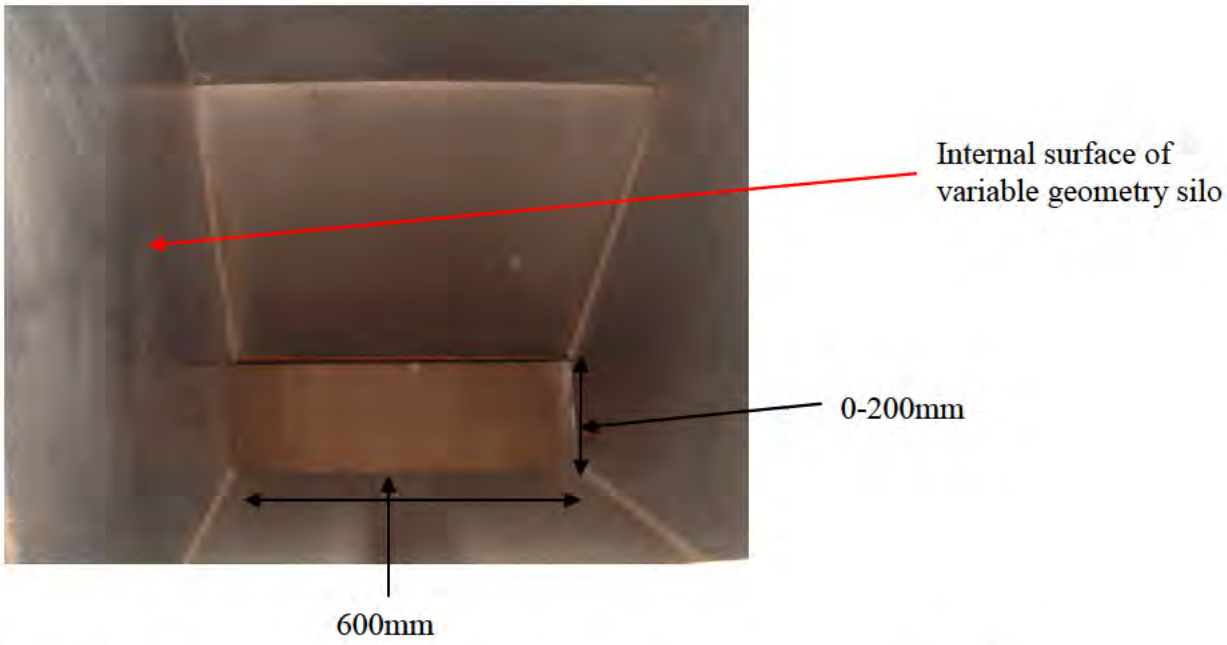

Figure 58: Variable geometry silo internal surface and Gravity flow of woodchips.

3.8 Shear Tester

The pitfalls of using shear tester to characterise extreme shape materials have been given in the chapter 2 but part of the methodologies set-up to achieve the aims and objectives of this research project was to spend some time on existing tester for conventional powders to understand the difference and the reasons why these methods break down totally for measuring extreme shape materials. In order to achieve this, Wolfson-Brookfield Powder Flow Tester was employed as a standard shear tester to conduct the comparative test. Two powders and two extreme (irregular) shape materials were employed.

3.8.1 Wolfson-Brookfield Powder Flow Tester

The Brookfield Powder Flow Tester was developed by The Wolfson Centre in conjunction with Brookfield Engineering (USA) in 2009. The powder flow tester can only measure the flow function of materials whose particles resist flow due to interparticle attractive forces (like surface tension, van der Waals forces, capillary forces) which cause cohesion because it uses a direct shear cell. The Powder Flow Tester is inadequate for measuring the flow properties of extreme shape materials particles because the particles of extreme shape materials are resistant to shear due to

entanglement of the particles and friction under compaction of the inter-particle forces which cause long span mechanical arch inside the bin. The picture of the Powder Flow Tester and accessories is shown in figure 59 below.

Figure 59: Wolfson-Brookfield Powder Flow Tester with accessories (Courtesy of Dr Rob Berry).

3.8.2 Standard Flow Function Test

Powder Flow Tester was used to measure the standard flow function of conventional powders and extreme shape materials particles. Standard flow function test is the major important test for measuring the flowability of bulk solids because it quantifies the material strength at a stress-free surface following consolidation to a given stress level and later compressive strength (σ_c) of the unconfined (unsupported) material. It also provides information on bulk density, effective angle of internal friction, flow index, flow intercept, critical arching values and critical rat-hole values.

3.8.3 Powder Flow Tester Procedure

After setting up the PFT, the laptop running the control software was connected to the Powder Flow Tester via USB cable. The first step in conducting the test was to measure the quantity of particles that will go into the trough. This was done by measuring the weight of trough before filling and after filling with particles. The weights were subtracted from each other and the weight of the particles was input into the software (Powder Flow Pro Software) in the laptop. The trough was filled to the top surface with the desired particles. Trough filling tools (outer catch tray, inner

catch tray and reversible scraper tool) were used to level and trim the surface of the particles inside the trough and to make sure the particles are well placed into the trough. Flow function lid (vane lid) was connected to the dynamic neck of the Powder Flow Tester. The flow function lid has vanes with pockets in between the vanes that perform the torsional shear on the particles directly. The filled trough was inserted inside the Powder Flow Tester in a position that was facing the flow function vane lid directly. Thereafter, the Powder Flow Tester was switched on from the laptop by clicking the appropriate button on the software template. The flow function vane lid protrudes gradually until it had contact with the material in the trough at the bottom so that both torsional and axial loads can compact and shear the particles. Thereafter, the test starts running automatically (figure 60). The test ran for about 30 minutes for each test material. Four different materials were tested, tests were limited by maximum particle size limit of the machine (2mm).

Figure 60: Powder Flow Tester with Powder Flow Pro Software with USB cable displaying particles at pre-shearing stage and other accessories set-up (source: www.brookfieldengineering.com) Accessed on 29/03/2010.

Chapter 4: Results Summary and Discussion (Exploratory Work)

4.0 Introduction

Results summary and discussion of column test, tensile tester, core flow test, mass flow test, and shear tester are provided in this chapter. Further information is provided in the appendix.

4.1 Column Test

The test was first evaluated using matchsticks. Tests were undertaken with tubes of different diameter, to evaluate the effect of the relationship between particle length and tube diameter. The issue being that as the particle length approaches the diameter of the tube, they must orientate vertically thus reducing the strength of the column formed. The matchsticks were cut into different length ranging from 5mm, 10mm, 20mm, 30mm and 40mm. The longer the matchstick length, the higher the column formed (see figure 61 below). When the particles are at 40mm, they interlock more providing a wider base for the column to stand on. This means that the higher the particles column height, the more difficult for the materials to discharge/flow inside the storage during handling.

All the extreme shape materials used for core-flow and mass-flow silo tests were put through the column test and showed consistent behaviour. The material that exhibited the worst behaviour was the shredded paper which arched in the tube and did not flow out. This was due to the physical properties of the materials: very low bulk density, elastic, the surface texture is smooth and also a mixture of different strip lengths. This material formed large mechanical arches in the silo tests. In the middle were the fibrous chopped miscanthus, dry hammer milled wood and wet hammer milled wood which are not cohesive/ sticky but still they formed high column heights and were capable of forming mechanical rat-holes and arches in the core and mass-flow tests. The most free-flowing material was the oat flakes which did not nest and as a result no column was formed. This material discharged reliably from small outlets in the silo discharge tests.

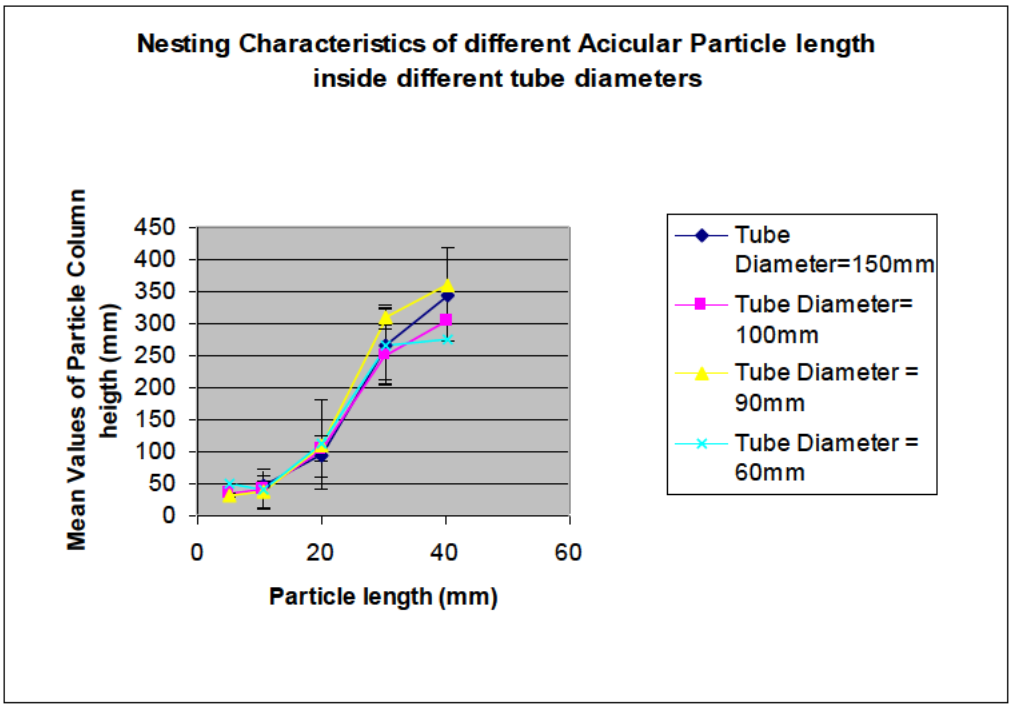

Figure 61: Nesting characteristics of different matchsticks length inside different tube diameters.

4.2 Tensile Tester

The test results from the tensile test rig were in line with the results obtained from the column test rig. The longer the particles length, the higher the tensile strength required to pull the materials apart especially unchopped (unmilled) lawn grass and unchopped shredded paper. These two materials also failed to discharge and rat-holed when they were tested at mass and core flow test rigs respectively. Matchsticks at longer length 40mm require high tensile stress to de-nest/untangle the particles and the smallest lengths 10 and 20mm had very small tensile strength. Chopped miscanthus, wet and dry hammer milled wood behave differently. Wet hammer milled wood required high tensile stresses to de-nest the particles while dry hammer milled wood (that is, small woodchips) and chopped miscanthus required less tensile stress. This could be attributed to the moisture content that binds the particles together, thus, increasing their bulk density. The moisture content increases the bulk density because particles swell and fill the voids in the bulk material. Due to the fine nature of the three particles, they rat-holed and formed various form of cliffs/hang-ups during storage in both mass and core flow silos. They also formed mechanical arches

and sometimes they discharge reliably depending on the bed head especially in the mass flow test rig. The results for the extreme shape materials are given in figure 62 below.

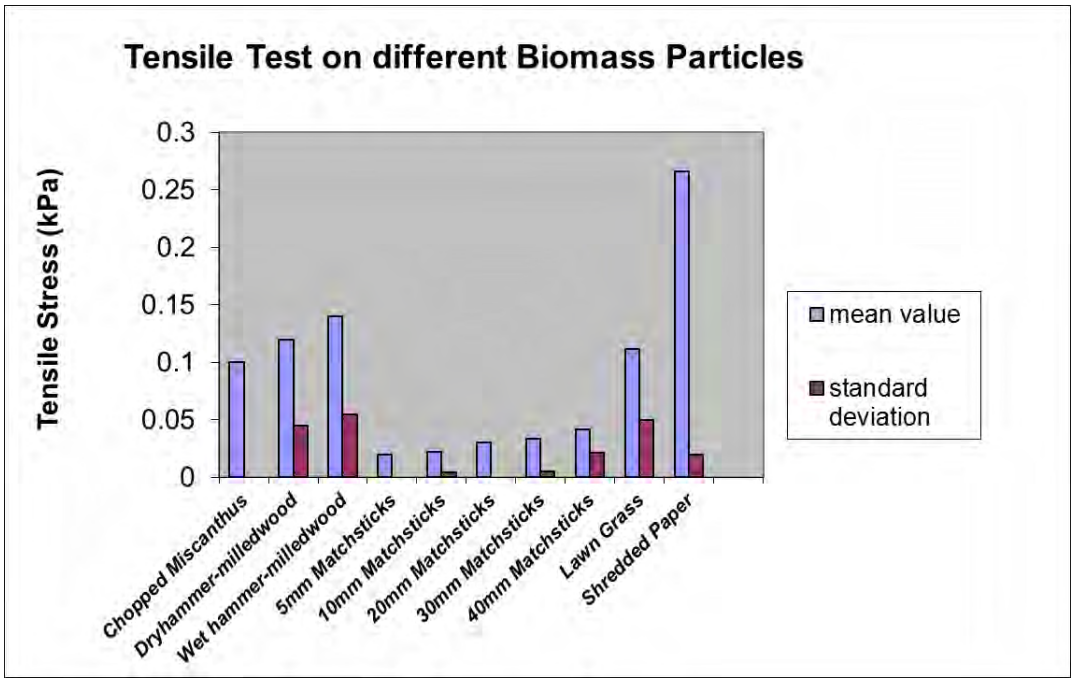

Figure 62: Tensile test results for biomass materials.

4.2.1 Mechanism of Failure/Flow

As the extreme shape material is compacted inside the tensile tester, which simulates the situation where the biomass fills up a vessel, settling takes place due to the biomass self-weight. Their self-weight is very low that is why gravity exerts small force on them to flow.

When the fibrous extreme shape particles are compacted, their length and number of contacts prevents them rotating independently, however because they are very elastic they can remain entangled but fold and orientate horizontally against one-another - increasing the number of contacts and the contact areas. Thus when the material is subjected to a tensile load for failure to occur either the friction at these multiple contacts or tensile strength of the multiple fibres must be overcome.

During compaction, the bulk density increases as a function of increasing normal/consolidation stress. Increase in normal stress determines how the material will entangle/knit to each other. Tensile stress is applied to the movable cell in order

to pull the two cells apart. As the movable cell keeps moving gradually while applying tensile stress, the entangled materials start to untangle until the material moves apart completely. This reflects the situation where the vessel outlet gate is open after the material has been filled into the vessel. The untangle region in the tensile tester reflects how the material discharge from the storage. The higher the tensile strength value, the higher the possibility that the material will require wide outlet size and steeper angle for the material to discharge under gravity. This has been experienced in the silo discharge test and tensile test on materials like straw.

At the later stage of the project, 5 materials (wood shavings, straw, oat flakes, reed canary grass, miscanthus) were tested on the tensile tester and on the novel silo discharge test. The results of the materials are given below in figure 63. Investigation shows that the straw material exhibits high tensile strength among the 5 materials. It is also most troublesome during the silo discharge test. It does not flow at small outlet dimensions regardless of the bed heads unlike oat flakes, reed canary grass, wood shavings and miscanthus which flow under gravity at small outlet dimensions.

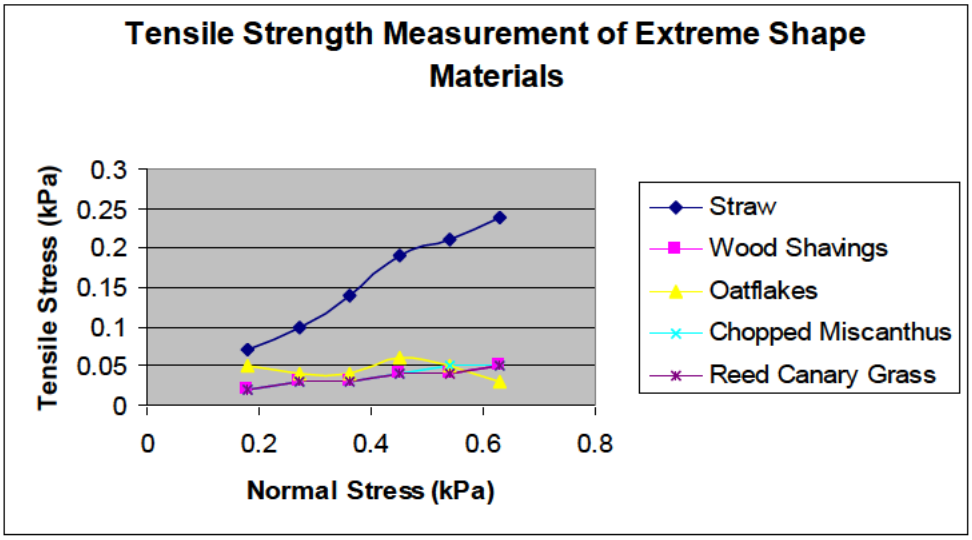

Figure 63: Tensile Strength Measurement of Extreme shape materials

4.3 Core Flow Test

The core flow test was developed to further prove the concept of column test and tensile tester. The investigation was done at three different bed heights (200mm, 400mm and 800mm). As the outlet dimension was incrementally increased, the arch collapse broke through to the top surface of the material to form a rat-hole. As the outlet dimension was increased further rat-holing persisted until the outlet dimension approached the diameter of the bin (e.g. 500mm outlet dimension in a 600mm diameter bin). This effect is illustrated in fig 66a &b and fig 67a & b for hammer milled wood and chopped miscanthus respectively, where the measured rat-hole dimension has been plotted as a function of the actual bin outlet diameter. In the figures each data point represents an average of five repeat tests. Note that the chopped miscanthus formed larger arches than the hammer milled wood.

The implication of this is that the extreme shape materials always arch in a core flow bin. Then, when the outlet is large enough to prevent arching, they rat-hole and the rat-hole persists until the outlet is virtually the full diameter of the bin. This occurs for every extreme shape material no matter what depth of material in the bin. Clearly there are practical limits of going significantly larger than the 0.6m tested due to the volumes of material required and the potential structural loads on the silo.

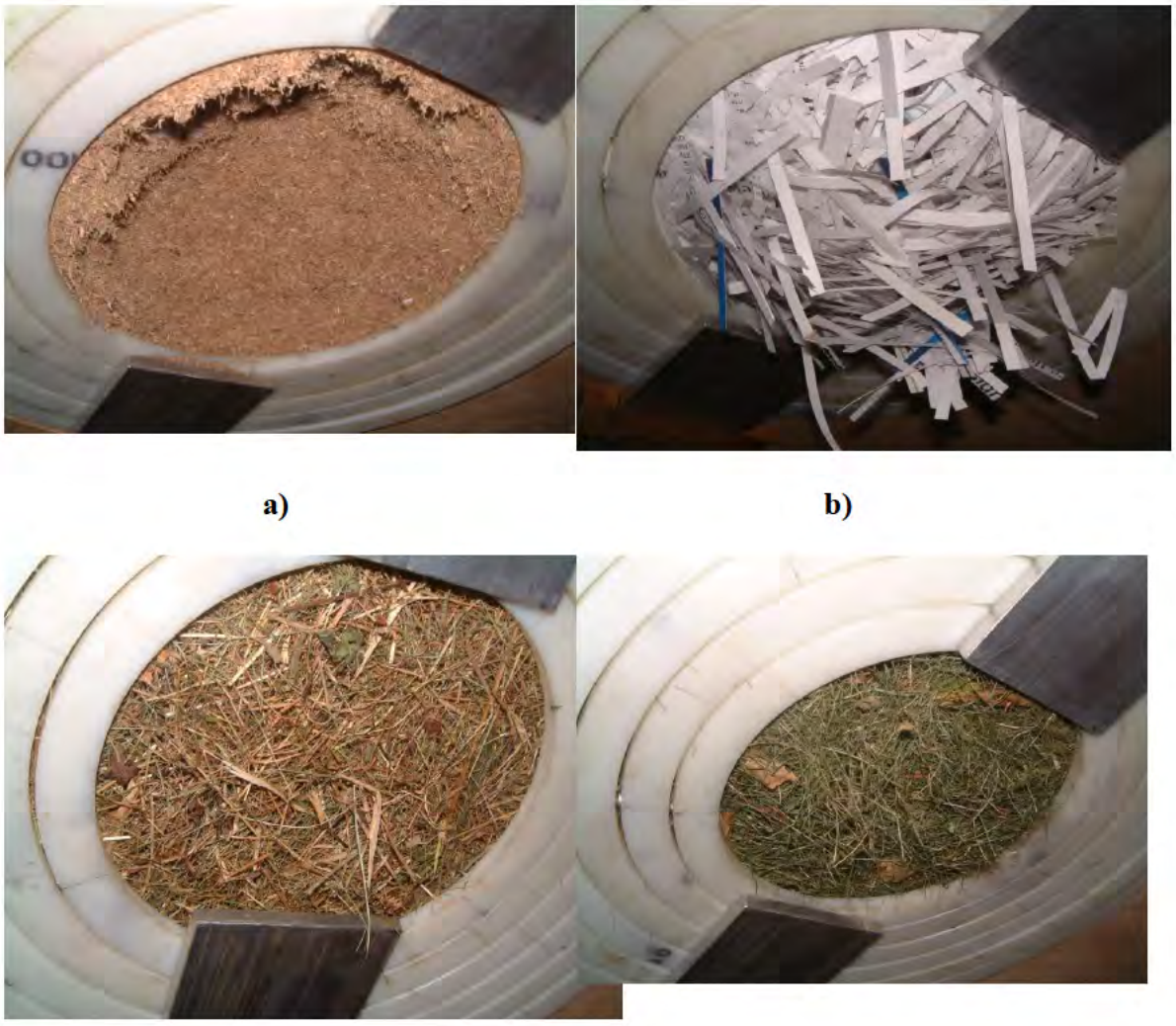

Figure 64: Comparisons of the mechanical arches formed by different materials in the core-flow test a) hammer milled wood b) shredded paper c) grass A & d) grass B

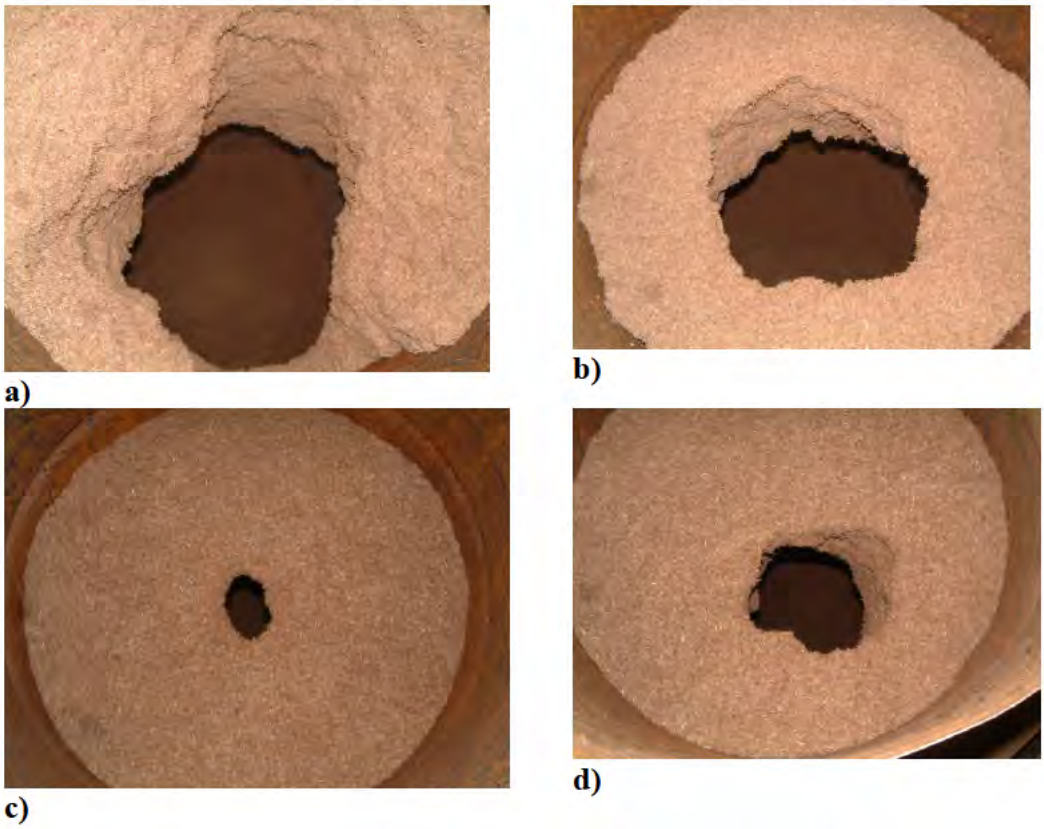

Figure 65: Rat holes formed by hammer milled wood (a& c) and miscanthus (b&d)

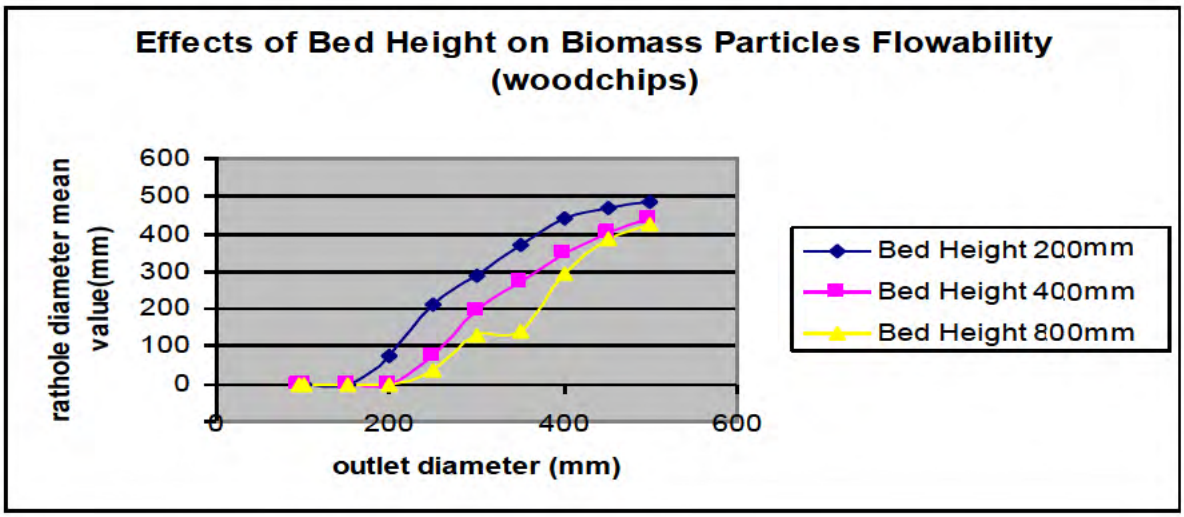

Figure 66a: Effects of bed height on the size of rat-hole formed in the core flow bin for woodchips/hammer milled wood (small initial outlet)

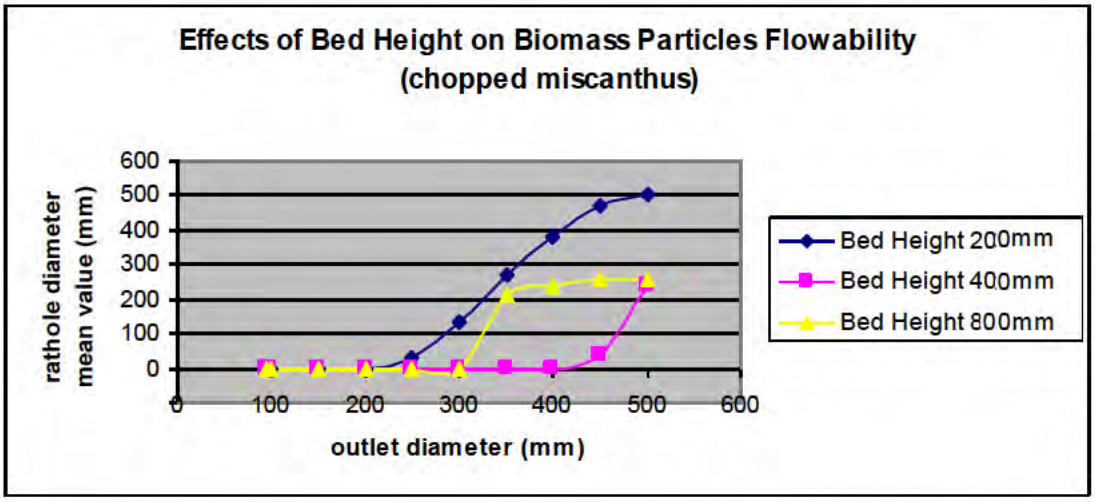

Figure 66b: Effects of bed height on the size of rat-hole formed in the core flow bin for chopped miscanthus (small initial outlet)

Note:

Based on the results in figure 66, the maximum size of arch supported by the material increased as the bed height increased. Also, the size of the rat-hole tended to get smaller as the bed height increased.

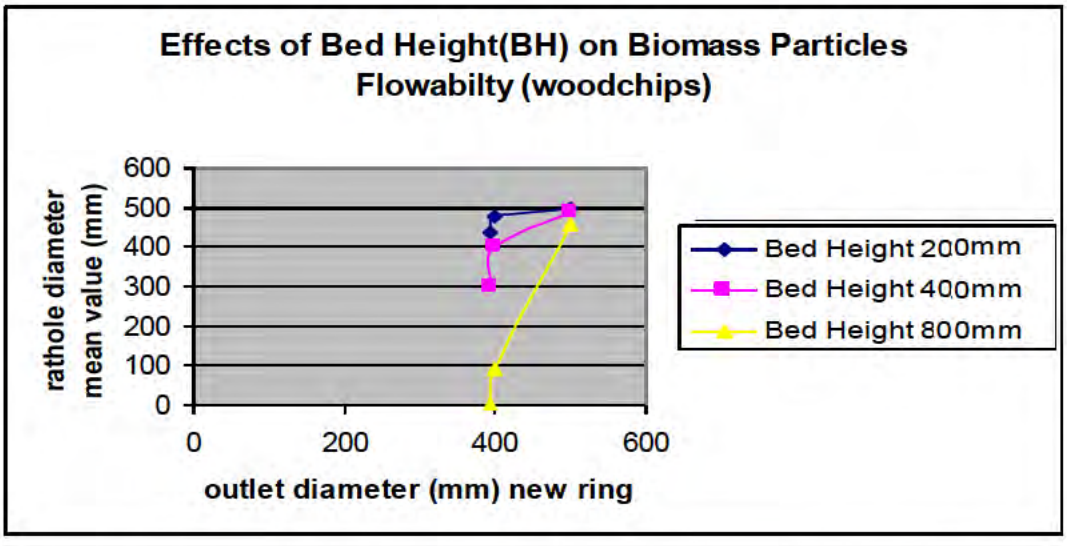

Figure 67a: Effects of bed height on the size of rat-hole formed in the core flow bin for woodchips/hammer milled wood (large initial outlet)

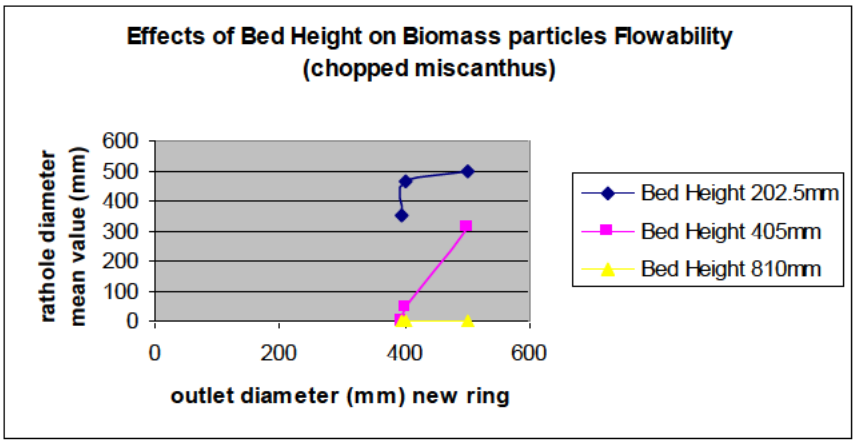

Figure 67b: Effects of bed height on the size of rat-hole formed in the core flow bin for chopped miscanthus (large initial outlet)

Note:

It was clear from all these results that core flow is fundamentally unsuitable discharge pattern for extreme shape materials.

4.4 Mass Flow Test

The mass flow tests were undertaken at four different bed heights (400mm, 600mm, 800mm and 1200mm) to investigate effect of consolidation stress level. For the mass-flow tests, as the outlet was increased the behaviour was as follows. Initially arching was observed (see figure 69a&b). As the outlet was increased at values close to the flow limiting value, complete discharge, i.e. mass-flow did not always occur, e.g. rat-holing see figure 69c and asymmetric discharge (see figure 69d). To quantify this behaviour, the discharge behaviour is presented in figure 68a for woodchips/hammer milled wood and figure 68b for chopped miscanthus, where the percentage of tests that discharge completely following five repeat tests are presented as a function of the hopper slot width, for different silo fill heights. Inspection of figure 68a shows that at the maximum 1200mm fill height, no discharge of woodchips occurs at the 100mm slot width. At a 150mm slot width 60% of tests fully discharge and at 200mm slot widths all tests discharged completely. For the more difficult flowing chopped miscanthus see figure 68b, at the 1200mm fill height no discharge occurred at 200mm maximum slot width of the silo test rig.

This suggests that, the higher the bed head, the more stress generated at the bottom (outlet) of silo which is in contrary to Jenike radial stress field principle to ordinary/traditional bulk solids which says that the stress particles generate at the bottom of the silo is not a function of the bed head. This is consistent with observations of the results of uniaxial tests on these extreme shape materials, i.e. the stress is transmitted vertically down through the material, but there is no lateral expansion and therefore minimal shear stress against the wall due to wall friction to support the weight of material. Too much stress on extreme shape materials make them to be difficult to handle. The photographs of the flow patterns of material retained in the vessel also indicate that mass-flow was not always occurring as demonstrated by the rat-hole formed (see figure 69c) with the wood chip in the supposedly "mass-flow" geometry vessel.

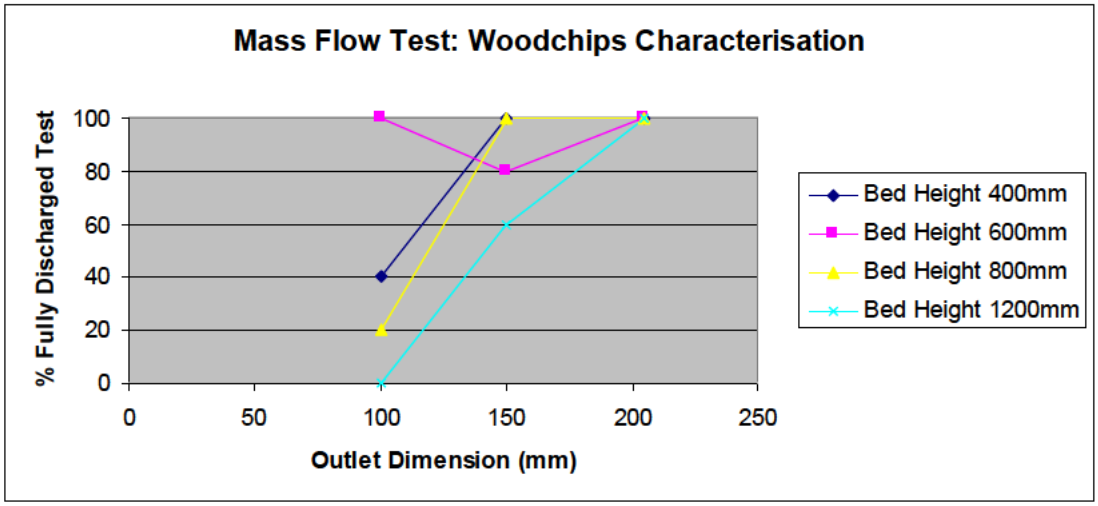

Figure 68a: Effect of the head height on the arching dimension of wood chips/hammer milled wood

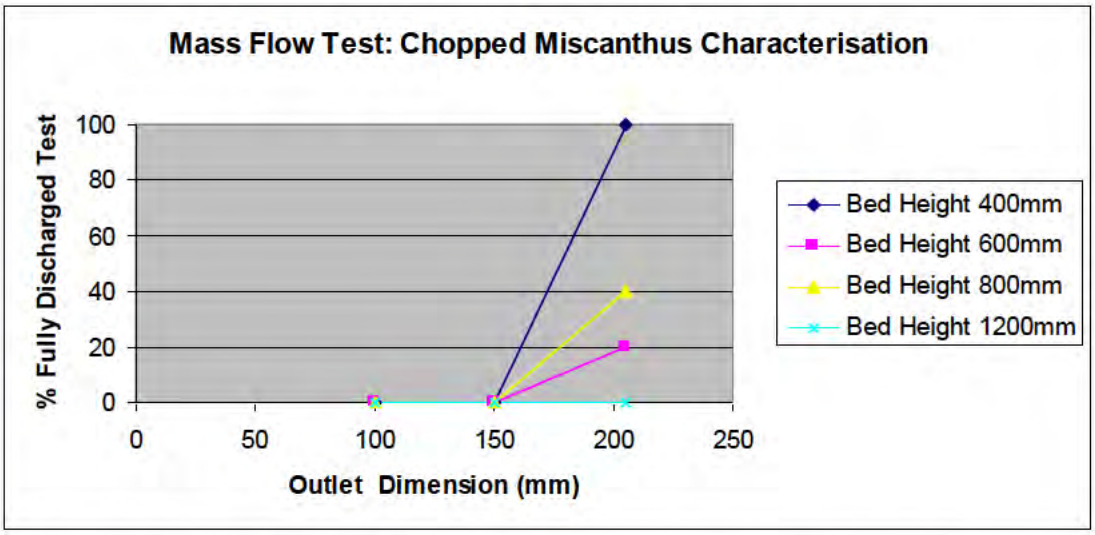

Figure 68b: Effect of the head height on the arching dimension of chopped miscanthus

This first set of tests was severely limited by the fact that most extreme shape materials arched over the 200mm maximum slot width of the silo. To over-come this, the silo was modified to enable the outlet dimension to be increased to approximately 0.5m width. The results of tests in the larger outlet silo are discussed later in Chapter 5.

a) hammer milled wood arch over a 200mm span

b) Shredded paper arch over a 200mm span

c) Rat-hole formed for hammer milled wood

d) Asymmetric discharge of miscanthus

Figure 69: Obstructions form in the mass-flow silo, a) hammer milled wood arch over a 200mm span, b) Shredded paper arch over a 200mm span, c) Rat-hole formed for wood chips, d) Asymmetric discharge of miscanthus

4.5 Shear Tester

Standard shear tester was employed to conduct the comparative test between ordinary powders and extreme shape materials. Both chopped miscanthus and woodchips/hammer milled wood were tested on standard shear tester as potential candidates for extreme shape materials.

These two materials were selected specifically because their relatively small particle dimensions (see chapter 3, table 1) which allow them to fit in the standard 150mm diameter (approx. 2mm particle top size) shear cell. Granulated sugar 800microns d50 was used as example of a free flowing material and sodium carbonate 100micron d50 was used as an example of an easy flowing material.

The flow properties of the four materials that were measured with the Brookfield Powder Flow Tester are presented below in fig 70a, b & c as a flow function, internal friction function and bulk density function respectively. Inspection of the bulk density functions figure 70c shows that the extreme shape materials have significantly lower bulk densities than the granular solids. Inspection of the flow functions, figure 70a shows that while the granulated sugar is free flowing and sodium carbonate easy flowing as expected, the extreme shape materials are in the cohesive/very cohesive region of the flow function. This seems incompatible with their physical handling properties in that they do not retain cohesive strength, e.g. if you compress them in your hand and release the stress, they expand and lose their strength. Also it was noted during the shear test that the lid on Powder Flow Tester was tilting because the fibres were being redistributed around the trough (balling-up) rather than shearing as expected. Thus the assumption that the forces are uniformly distributed around the trough is invalidated and the actual mechanism of failure in the cell does not match that which is assumed in the flow theory and the data interpretation algorithm.

Note that in order to test samples of the other extreme shape materials with their larger particle sizes (see chapter 3 table 1), the Wolfson Large Annular Shear Cell with its 25mm top size would have been required. However due to manual nature of the test it would have been extremely time consuming and not considered worthwhile due to the suspect nature of the results generated in the small cell.

Additionally, in order to increase the bulk density of the extreme shape materials communition (i.e. intended size reduction) can be employed to densify the bulk materials. Adequate care needs to be taken when selecting communition because it might upset the stress within particles which is not good for the extreme shape

materials because of their stress phobic (i.e. extreme shape materials does not like and tolerate stress) nature and other associated costs like procurement of communition equipment.

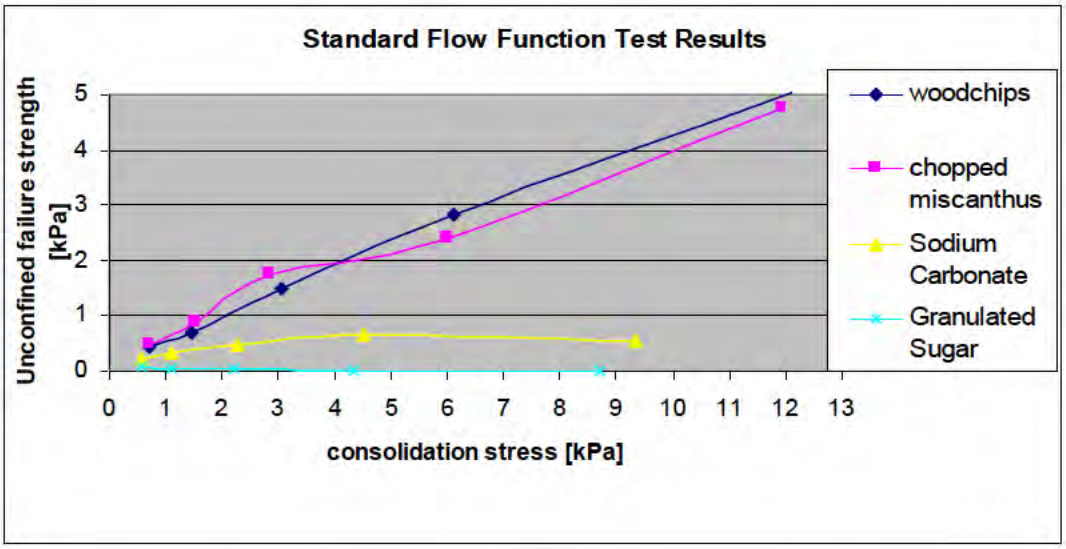

Figure 70a: Flow Function

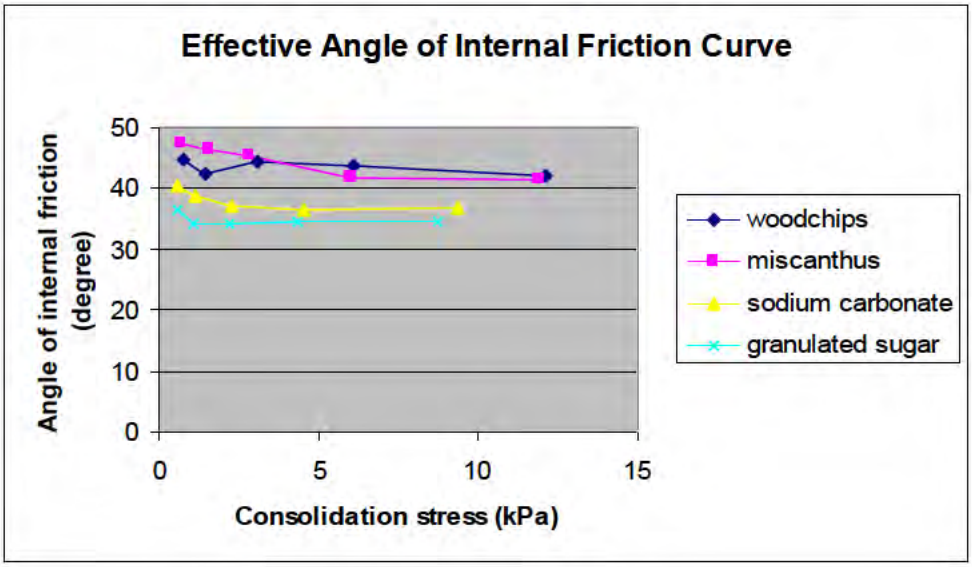

Figure 70b: Internal friction function

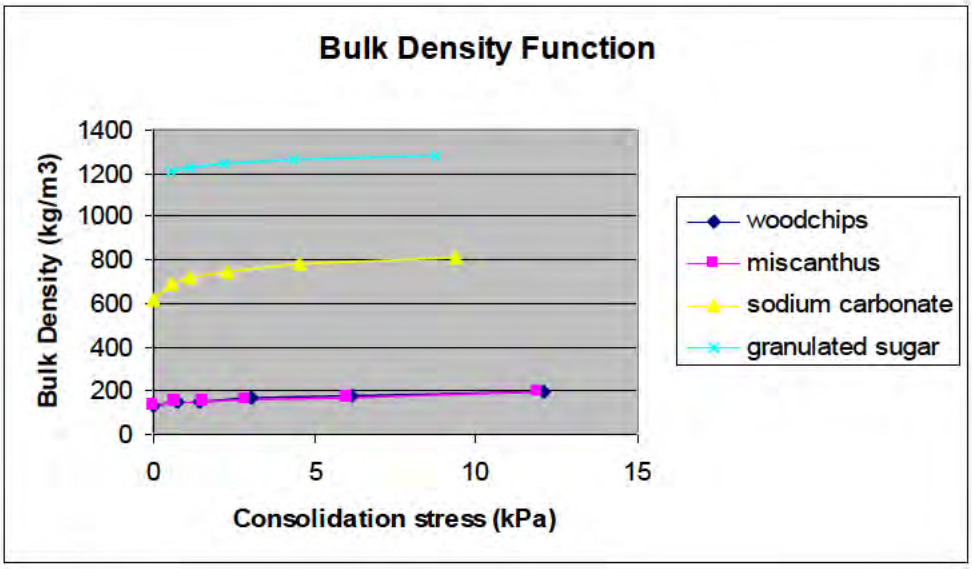

Figure 70c: Bulk density function

Chapter 5: Results and Discussion of Arching Experiments (in a modified mass-flow silo)

5.0 Introduction

This chapter outlines the design of modified mass-flow silo with a larger maximum slot width 500mm. The silo was constructed in order to experimentally measure the arching dimensions of the extreme shape biomass materials. A new planar (wedge) shape silo was designed and constructed as previously stated. The new silo is flexible enough to allow change of its wall angle and outlet slot width. The previous silo which was delivered from a PhD project had been used to study discharge characteristics of woodchips/hammer milled wood, chopped miscanthus, shredded paper, lawn grass A and B. The pitfalls with the previous silo were that: it was not flexible enough to achieve reliable flow under gravity. The maximum outlet slot was 200mm (width) and the maximum wall angle was 20°. The design was unable to accommodate any engineering modifications, as a result of this a new silo was designed and constructed.

5.1 Features of the novel silo

The novel silo was constructed using stainless steel 2B material. The stainless steel material was chosen because it is not prone to corrosion and also it has a smooth surface especially the internal surface which is most the important part to enable the materials to flow reliably without sticking to the wall of the silo and to avoid change in wall friction. The maximum slot dimension is 500mm width by 600mm length. The maximum hopper half angle is 41˚ to the vertical and the minimum is 23˚ to the vertical. The maximum height of the silo is 1250mm. The geometry changes of the vessel is achieved by moving dynamic wall of the vessel back and forth at the same time adjusting the flaps at the hopper region of the vessel to change the wall angle and the outlet (slot) dimension to the required level (see figure 72 and 73).

Figure 71: New Wedge shape silo showing front and side views

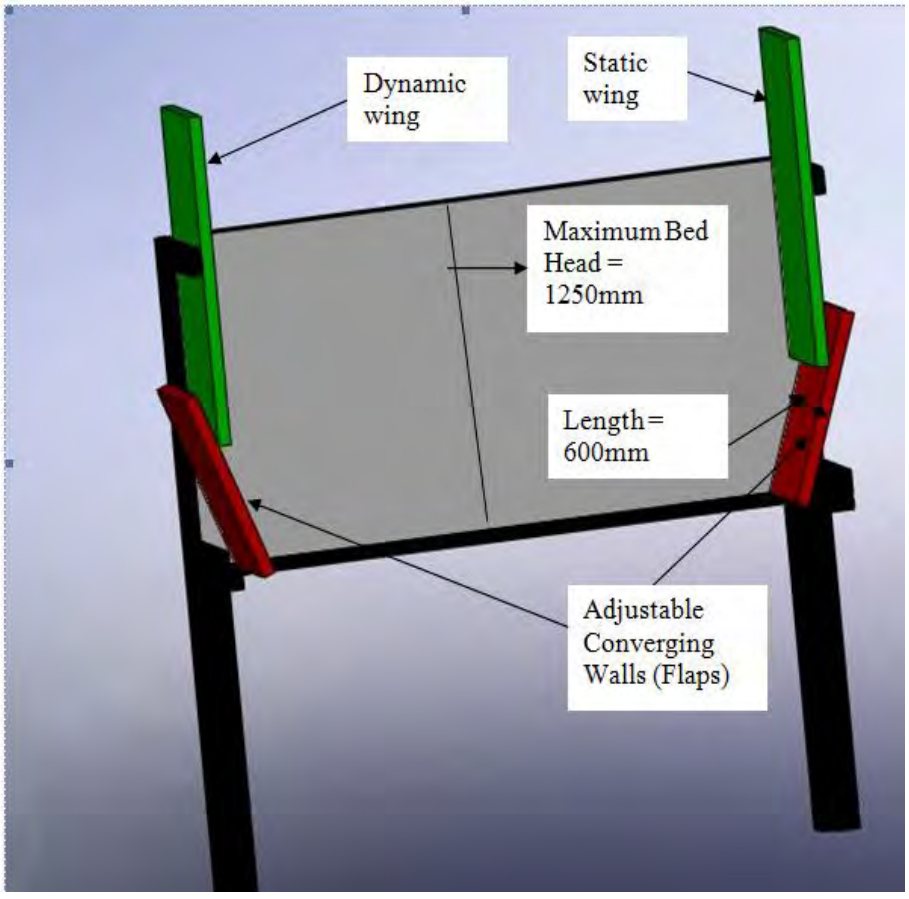

Figure 72: New Adjustable (Wedge-shaped) Hopper (Internal Surface)

Figure 73: New Adjustable (Wedge-shaped) Hopper Picture (Whole Vessel) (Courtesy of Oscar Angulo – Research Student at The Wolfson Centre)

5.2 Silo Discharge Behaviour of Biomass Materials

Five materials (reed canary grass, chopped miscanthus, straw, oat flakes and wood shavings) were tested at this phase of the research project. The silo discharge characteristics test is a proper process test in the sense that it proved both column test and tensile tester concept further especially the tensile tester which is capable of discriminating different biomass materials. The test was conducted at hopper half angles of 23 and 41˚ (to the vertical axis) to determine if this is significant factor in flow behaviour. Then in the following sections the results of the arching tests are presented on axes of outlet size as a function of silo fill (bed) height. In the graph three regions are located, the no flow region where arching prevails, a flow region where no arching occurs and the silo discharges completely. In between is a region of uncertainty where unreliable or partial flow may occur. In all cases arching conditions refer to instantaneous conditions, e.g. the effects of extended periods of static storage have not been considered. The results obtained for 5 biomass materials were discussed in the section 5.2.1, 5.2.2, 5.2.3, 5.2.4, 5.2.5, 5.2.6, 5.2.7, 5.2.8, 5.2.9 and 5.2.10 below.

5.2.1 Chopped Miscanthus Behaviour at 41˚ wall angle

At the 41˚ hopper half angle both flow and no flow regions were measured. Six bed heads were looked at ranging from 50, 100, 200, 400, 600, 900 and 1250mm. The materials behave totally different at different bed heads. The research outcome shows that the outlet required for any biomass to flow (collapse) under gravity is a function of the materials bed head. In the flow region, the material flows reliably under gravity. The lower limit of the flow regions are 200, 250 and 300mm slot outlets. At 200mm outlet, the material only flowed at 50, 100, 210 420mm bed heads. At 250mm outlet, the material only flowed at 50, 100, 210 420 and 620mm bed heads. At 300mm outlet, the material flowed at all bed heads.

At no flow region, the material was dead inside the storage and formed an arch over the entire cross section of the outlet. The no flow region upper limits were 100, 200 and 250mm slot outlets. At 100mm outlet, the material was dead at all bed heads. At 200mm outlet, material started not to flow (collapse) at bed head above 620mm bed head. At 250mm outlet, material started not to flow at bed head above 900mm. This is reflected in the figure 74 below. The region where there are black arrows indicate variable behaviour region (i.e. region of uncertainty).

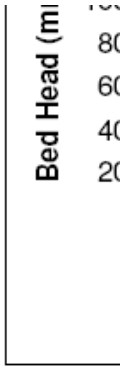

Figure 74: Silo discharge characteristics of chopped miscanthus at 41˚ hopper half angle.

5.2.2 Chopped Miscanthus Behaviour at 23˚ wall angle

The same approach employed at 41˚ hopper half angle was used here but the result was significantly different although the trend was qualitatively similar. The flow region lower limits here were 100, 200, 250 and 300mm slot outlets. At 100mm outlet, the material only flowed at 50mm bed head. At 200mm outlet, the material flowed at 50mm to 900mm bed heads. At 250mm and 300mm outlets, the material flowed at all bed heads employed (50mm to 1250mm bed heads). The no flow region upper limits were 100 and 200mm slot outlets. At the two outlets, the material was dead at 100mm and 1250mm bed heads. This is reflected in the figure 75 below. The region where there are black arrows indicate variable behaviour region (i.e. region of uncertainty).

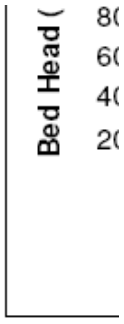

Figure 75: Silo discharge characteristics of chopped miscanthus at 23˚ hopper half angle.

5.2.3 Wood Shavings Behaviour at 41˚ wall angle

The flow region lower limits here were 200mm, 250mm and 300mm outlets. At 200mm outlet, the material flowed only at 50mm, 100mm, 210mm and 420mm bed heights. At the 250mm outlet, the material flowed at 50mm to 620mm bed heads. At 300mm outlet, the material flowed at all bed heads (50mm to 1250mm). The no flow region upper limits were 100mm, 200mm and 250mm outlets. At the three outlets, the materials were dead at 100mm, 620mm and 900mm bed heads respectively. This is reflected in the figure 76 below. The region where there are black arrows indicate variable behaviour region (i.e. region of uncertainty).

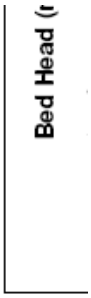

Figure 76: Silo discharge characteristics of wood shavings at 41˚wall angle

5.2.4 Wood Shavings Behaviour at 23˚ wall angle

The flow region lower limits here were; 100mm, 200mm, 250mm and 300mm outlets. At the 100mm outlet, material only flowed at a 50mm bed head. At the 200mm outlet, material flowed at bed heights from 50mm to 620mm. At the 250mm outlet, the material flowed at bed heights form 50mm to 900mm. Lastly, at 300mm outlet, material flowed at all the bed heights (50mm to 1250mm). The no-flow region upper limits were 100mm, 200mm and 250mm outlets. At the three outlets, the materials did not flow at bed heights 100mm, 900mm and 1250mm respectively. This is reflected in the figure 77 below. The region where there are black arrows indicate variable behaviour region (i.e. region of uncertainty).

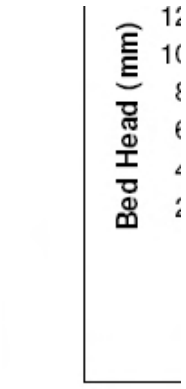

Figure 77: Silo discharge characteristics of wood shavings at 23˚wall angle

5.2.5 Straw Behaviour at 41˚ wall angle

The flow region lower limits were; 200mm, 250mm, 300mm, 400mm, and 500mm outlets. At the 200mm outlet, material only flowed at smallest bed height (50mm). At the 250mm outlet, material flowed at bed heights from 50mm and 100mm. At the 300mm outlet, material flowed at bed heights from 50mm, 100mm and 210mm. At the 400mm outlet, material flowed at bed heights from 50mm to 420mm. At 500mm outlet, material flowed at bed heights from 50mm to 620mm. The no flow region upper limits also took place at the same flow region lower limits but at different bed heads. There was no flow at bed heights of 100mm, 210mm, 420mm, 620mm and 900mm with respect to outlets of 200mm, 250mm, 300mm, 400mm and 500mm. This is reflected in the figure 78 below. The region where there are black arrows indicate variable behaviour region (i.e. region of uncertainty).

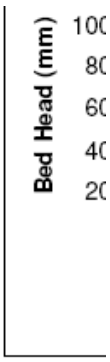

Figure 78: Silo discharge characteristics of straw at 41˚ wall angle

5.2.6 Straw Behaviour at 23˚ wall angle

The flow region lower limits were; 200mm, 250mm, 300mm, 400mm, and 500mm outlets. At the 200mm outlet, material flowed at bed heights of 50mm and 100mm. At the 250mm and 300mm outlets, material behaves very similar. There was flow at bed heights from 50mm to 420mm. At the 500mm outlet, there was flow at all bed heights (50mm to 1250mm). The no flow region upper limits were 200mm, 250, 300mm and 400mm outlets. Both 250mm and 300mm outlets have similar behaviour. There was no flow at all at the 620mm bed heights at both outlets. Also, there was no flow at the 210mm and 900mm bed heights in respect with 200mm and 400mm outlets. This is reflected in the figure 79 below. The region where there are black arrows indicate variable behaviour region (i.e. region of uncertainty).

Figure 79: Silo discharge characteristics of straw at 23˚ wall angle

5.2.7 Oat flakes Behaviour at 41˚ wall angle

Oat flakes is well-behaved and it could be termed as most free flowing material among all the materials tested in this project. Material flowed at all bed heads (50mm to 1250mm) at 50mm, 100mm, 200mm, 250mm and 300mm outlets. There was not flow only at 15mm and 25mm outlets. At 15mm outlet the gate was closed but at 25mm outlet there was no flow only at highest bed head (1250mm). This is reflected in the figure 80 below. The region where there are black arrows indicate the region where the outlet gate was closed and there was no movement (flow) of the particles.

Figure 80: Silo discharge characteristics of oat flakes at 41˚ wall angle

5.2.8 Oat flakes Behaviour at 23˚ wall angle

The discharge behaviour characteristics of oat flakes here is very similar to at 41° wall angle. The only difference here is that material flow reliably at 25mm outlet regardless of the bed head. This is reflected in the figure 81 below. The region where there are black arrows indicate the region where the outlet gate was closed and there was no movement (flow) of the particles.

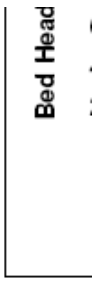

Figure 81: Silo discharge characteristics of oat flakes at 23˚wall angle

5.2.9 Reed Canary Grass Behaviour at 41˚ wall angle

This material has some similar discharge characteristics with wood shavings and miscanthus. Material flowed at 200mm, 250mm, 300mm and 400mm outlets but the flow only takes place at smaller bed heads at 200mm, 250mm and 300mm outlets. There was reliable discharge at 400mm outlet size regardless of the bed head. The no flow region upper limits takes place between 200mm and 300mm outlet sizes. The materials were stagnant at higher bed heads at this region. This is reflected in the figure 82 below. The region of uncertainty is displayed with black arrows on the graph (variable behaviour region).

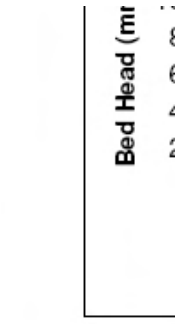

Figure 82: Silo discharge characteristics of reed canary grass at 41˚ wall angle

5.2.10 Reed Canary Grass Behaviour at 23˚ wall angle

At this wall angle (23˚) the material also has some similar discharge characteristics with wood shavings and miscanthus. The particles behave better here due to the steepness of the wall angle. Material flowed at 100mm, 200mm, 250mm and 300mm outlets but the flow only takes place at smaller bed heads at 100mm, 200mm and 250mm outlets. There was reliable discharge at 300mm outlet size regardless of the bed head. The no flow region upper limit takes place between 100mm and 250mm outlet sizes. The materials were stagnant at higher bed heads at this region. This is reflected in the figure 83 below. The region of uncertainty (variable behaviour region) is displayed with black arrows on the graph

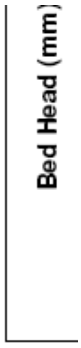

Figure 83: Silo discharge characteristics of reed canary grass at 23˚ wall angle

5.3 Conclusion

Based on the experimental investigations carried out on the novel silo the following conclusions were made:

- All the extreme shape materials were able to be discharged in mass flow provided the outlet dimension was large enough.
- The necessary size of outlet dimension increased with the height of material in the vessel. That is, the outlet required for a given material to be discharged reliably is a function of the bed height.
- The regions of uncertainty that is, variable behaviour regions in the graphs above varies slightly from each other. This region of uncertainty can help to identify the micromechanics source of resistance to flow further. It can also give an indication of mechanism of failure of the materials at these regions.
- Materials tend to flow better at the 23° hopper half angle (i.e. steeper converging angle) than at the 41° hopper half angle.
- Particles characteristics such as aspect ratio also have an impact on the flowability of the materials. Oat flakes which have very small aspect ratio discharge reliably at a very small outlet dimension while straw which has very large aspect ratio requires big outlet for the material to discharge reliably.

Chapter 6: Development and Evaluation of a Critical Arch Model

6.0 Introduction

This chapter presents the model for arch strength of extreme shape materials based on bulk tensile strength which has been evaluated against a range of biomass materials. It discusses the new predicted arching model versus actual arching dimension. The vertical stress profile for the different materials in the hopper was presented as a function of bed height. The stress profile was conducted on all the 8 materials employed in this project ranging from: oat flakes, woodchips, reed canary grass, wood shavings, straw, miscanthus, shredded paper and lawn grass.

Based on the results presented in figure 84 particularly on the aspect of arching dimension measurements, further analysis was done to obtain a more consistent prediction of arching dimensions. The actual arching dimension is the same here because it was the same test rig (wedge shape vessel) and the same materials were used. However, silo discharge test is elaborated more and flow/failure plots for the actual arching dimension are presented at two different wall angles (23^o and 41^o respectively) for oat flakes, wood shavings, straw, chopped miscanthus and reed canary grass showing flow and no flow regions as presented in chapter 5. Other materials like lawn grass and shredded paper were not shown because they were hindered due to the absence of sufficient materials to fill the second wedge hopper and therefore conduct a fair comparative test. Woodchips is not shown because it behaved consistently the same as miscanthus in all the tests undertaken in this project. They also have approximately equal particle size and shape characterisation (see table 1). As a result of this, chopped miscanthus was used as a representative sample for further test.

Furthermore, stress profile (stress distribution in wedge shape vessel) was modelled in order to see the impacts of stress on the flowability of the materials. The two equations presented in chapter 1 (section 1.5.2) were also utilised here but modified for the new modelling particularly equation 2. The tensile strength values presented in section 4.2.1 (figure 63) were extrapolated to generate new tensile stress values which were used for the stress profile analysis and predicted arching dimensions (see Appendix B). Also the actual bulk density which was presented in Table 1 is used as

part of key parameters in generating the new predicted bulk density values, new predicted normal stress that the materials experience inside the vessel and the new predicted arching dimensions (see Appendix B and C).

6.1 Arching Dimension Measurements

The critical arching dimension was measured for oat flakes, chopped miscanthus, wood shavings, reed canary grass and straw in a larger outlet (500mm max width) mass-flow silo for different fill heights. These actual arching dimensions have then been compared with predicted arching dimensions that have been determined from the tensile strength functions of the materials, to represent a tensile failure mechanism for the arch.

Taking the tensile strength as a function of normal stress, the tensile strength has been converted to an arching dimension by using equation 3 below, and the normal stress has been converted to a fill height using equation 4 below. The equation 4 below was adapted from hydrostatic equation because biomass materials tested so far in this project behave hydrostatically inside the vessel. The measured and predicted arching dimensions have then been compared at common fill heights for a range of test materials; oatflakes, chopped miscanthus, wood shavings and straw in sections 6.1.1, 6.1.2, 6.1.3, 6.1.4 and 6.1.5 respectively. Figure 61 below is used for the comparative analysis between actual and predicted arching dimensions for the 5 materials.

$$B = T/\rho_b g \qquad \text{Equation 3}$$

$$\sigma_1 = \rho_b g h \qquad \text{Equation 4}$$

Where: B = Arching Dimension (m)

T = Tensile strength (Pa)

ρ_b = Bulk Density (kg/m^3)

h = Particle Bed Head (m)

σ_1 = Normal Stress (Pa)

g = acceleration due to gravity (9.81m/s^2)

Tensile strength and bulk density were derived from tests using tensile tester and a cylindrical test cell (as explained in chapter 3: section 3.2). The bulk densities used for the calculations were taken at the highest normal stress (14KPa). This is because it simulates the actual condition the materials will experience inside the silo. The bulk density values are shown in table 1. The tensile strength values were taken from the failure plot between 0.02kPa to 0.24kPa. The tensile strength values correspond to the normal stress values which range from (2, 3, 4, 5, 6, 7kPa). This is reflected in figure 46 (section 4.2.1) in Chapter 4 for tensile measurements of extreme shape materials.

T = Force/Area

T = Tensile strength

Force = mg

Where m = mass of the material that is put inside the tensile tester

A = area of the plane failure in the tensile tester which are depth (D) and breadth (B) of the tensile tester (see figure 84)

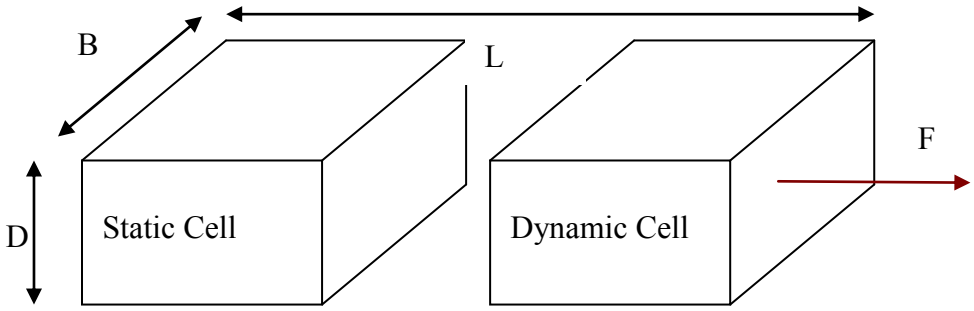

Figure 84: Tensile tester features

That is, A = B x D (m^2)

ρ_b = mass/Volume

Where m = mass of the material that is put inside the tensile tester

V = volume of the material inside the tensile tester which is length (L) times breadth (B) times depth (D) of the tensile tester (see figure 67 above)

That is, V= L x B x D (m^3)

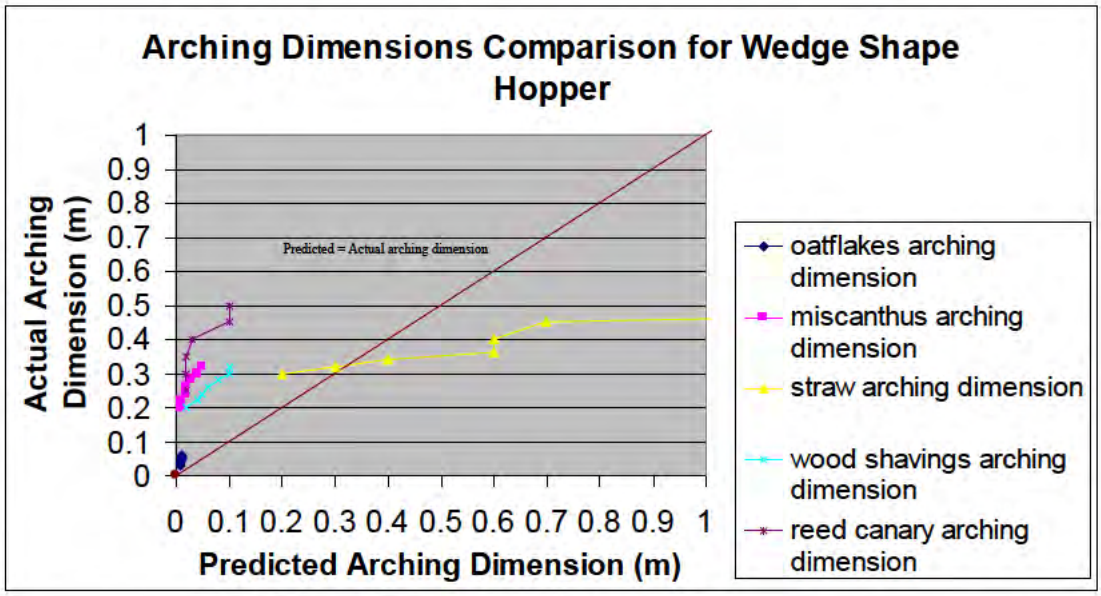

Figure 85: Arching Dimensions Comparison for Extreme Shape Materials (A)

6.1.1 Oat flakes: Predicted outlet dimensions are much lower than the measured outlets by a factor of between 3 and 6. However, both measured (actual) and predicted are very small in industrial terms. This is displayed in figure 85 above. The difficulty for this material was measuring the tensile strength. This was low and difficult to resolve against noise in the measurements.

6.1.2 Chopped Miscanthus: Results show that the tensile strength model significantly underestimates the strength of the actual arch. Key difference is that the tensile strength measurements are linear through the origin. Thus, predicted arching dimension is approximately zero for a low bed head. The actual arching dimension has a significant value at a very low bed head. This could be possibly due to the convergence of the hopper providing lateral compaction of the material. This is reflected in figure 85 above.

6.1.3 Wood Shavings: The material behaves consistently with chopped miscanthus during the silo discharge test (i.e. the actual arching dimension is the same). They

also have some level of similar traits in the predicted arching dimension values. This is reflected in the figure 85 above,

6.1.4 Straw: The material is the most troublesome one among the four materials. Both actual arching dimension and predicted arching dimension is very high compared to other materials. They require larger outlet for the material to discharge under gravity. This is reflected in the figure 85 above. The tensile strength approach accurately predicts the strength at low bed heads. At higher bed heads, the tensile strength significantly over estimates the strength of the material and the arching dimension. This could be due to large particle length of the straw particles i.e. length was approximately equal to that of tensile cell.

6.1.5 Reed Canary Grass: The material behaves consistently with chopped miscanthus and wood shavings during the silo discharge test (i.e. the actual arching dimension is the same) at lower bed heads. They also have some level of similar traits in the predicted arching dimension values at lower bed heads but at higher bed heads there is significant difference which was experienced in the silo discharge test and also in the predicted values but the predicted value of wood shavings is approximately equal with reed canary grass at higher bed heads. This is reflected in the figure 85 above.

6.1.6 Conclusion

Generally, there is no trend as yet, with both under and over prediction of the strength exhibited. However, there are significant limitations to the tensile tester used, which need to be overcome to generate more accurate measurements presented in figure 85 above.

Empirical data from the silo discharge test are consistent based on the material characteristics like bulk density and particle aspect ratio. Material with high bulk density and low aspect ratio behave very well. For example oat flakes is the most free-flowing material among the materials evaluated. This is because it has high bulk density and low aspect ratio. Both oat flakes predicted and actual values are approximately the same. Straw exhibits significantly different behaviour among the five materials. It is the most troublesome. Both predicted and actual arching dimensions are large in industrial terms. Regardless of the bed height it requires a

wide outlet size for reliable discharge. In the tensile strength measurement of the straw which is converted to the predicted arching dimension, straw exhibits high tensile strength property. All these attributes are due to low bulk density and high aspect ratio.

Other materials like reed canary grass, wood shavings and miscanthus behave consistently well at lower bed heights but at higher bed heights there is a significant difference. At some points they have similar traits in the predicted values. Their bulk density is quite low compared to oat flakes but higher than straw. Also, their aspect ratio is smaller compared to straw and higher compared to oat flakes.

Overall, the prediction greatly over estimates the arching dimension while the empirical approach gives a useful guide which can be employed in designing storage vessel required for discharge of biomass materials.

6.2 Improving the Arching Model

The model above (section 6.1) used a very much simplified approach in that the tensile strength was taken as a value at a fixed stress. But in reality, the tensile strength depends on the stress, which in turn depends on the head of material in the silo and its bulk density. So the obvious next step was to take account of stress in the outlet when selecting the value of tensile strength to use in the arching calculation.

The modelling was started with experimental calculation of bulk density as a function of normal stress. Both loose-fill and compacted bulk density were calculated for 8 biomass materials. The bulk density functions of the materials are given in the figure 86 below.

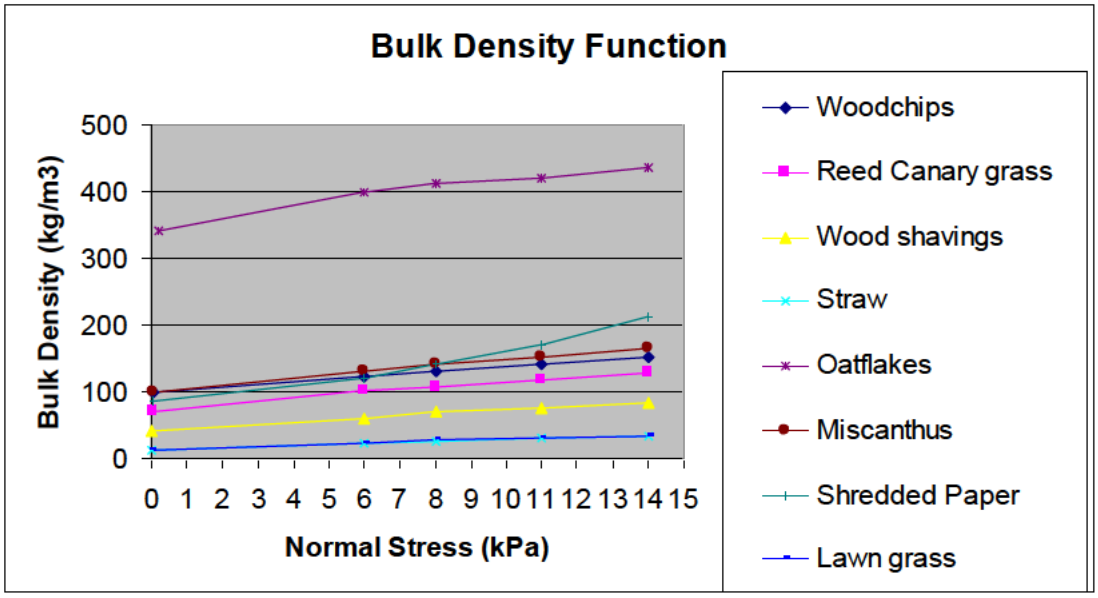

Figure 86: Bulk density functions for extreme shape materials

The highest compacted bulk densities are presented in Table 1 in chapter 3. The loose-fill bulk density is used as initial value in generating the new predicted values for normal stress, tensile stress and bulk density at corresponding materials bed head. As previously stated the maximum bed height for the new wedge vessel used in this project is 1250mm (1.25m). To predict bulk density and stress distribution, the vessel is sub-divided into 25 slices (elements) ranging from 0 to 1.25m. Each slice represents a bed height. These are taken in 0.05m steps. Meaning that after 0m bed head, the next bed head is 0.05m and subsequent ones are increased with 0.05 until the last bed height is reached which is 1.25m.

Two predicted normal stress values were calculated at each bed height. The first stress is calculated using the hydrostatic stress relationship shown in equation 4 in section 6.1 ($\sigma_1 = \rho_b gh$). The stress values were calculated for a constant bulk density assuming the loose-fill bulk density value. The second stress is also calculated using the hydrostatic stress relationship ($\sigma_2 = \rho_b gh$). In this case the values of stress were calculated from using a straight-line extrapolated of the bulk density function in the low stress region for all the materials as shown in the figure 86 above.

Predicted arching dimensions were calculated at two different wall angles. The first arching dimension was calculated at 23˚ wall angle and the second arching dimension was calculated at 41˚ wall angle. Both arching dimensions were calculated using the

modified Jenike arching dimension formula. It is modified because the Jenike formula addresses only traditional powders not biomass materials. The new formula (equation 3) which was presented in section 6.1 is $B = T/\rho_b g$. The modification made here is tensile stress (T) replaced the cohesive stress (C) which Jenike originally used (shown in section 1.5.2 Chapter 1). This is because biomass materials do not develop cohesive strength when compacted; they only develop tensile strength due to their entanglement/knitting potential. The tensile stress used in this calculation is generated from using a straight-line extrapolated of the tensile strength function as shown below in figure 87 and 88 for the extreme shape materials employed. The corresponding bulk density used for the calculation is the extrapolated bulk density generated from second stress described above.

The actual arching dimensions for both 23 and 41˚ wall angles were generated from the results obtained during the silo discharge tests presented in section 5.2

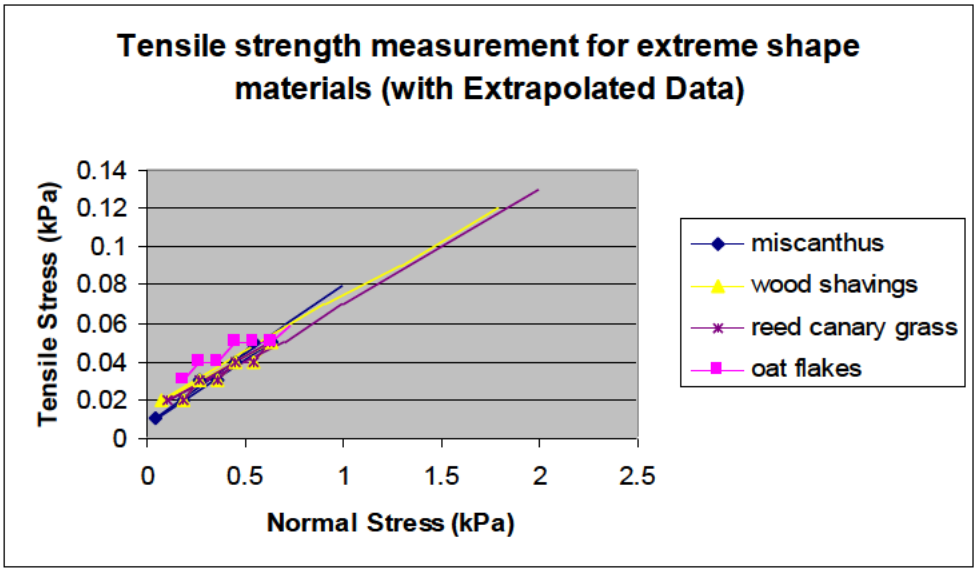

Figure 87: Tensile strength functions for extreme shape materials without straw

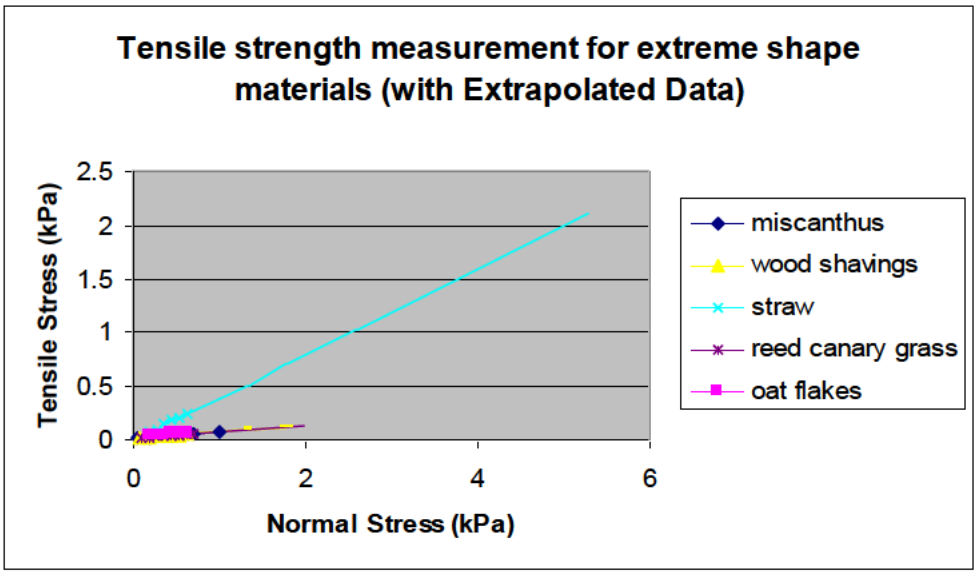

Figure 88: Tensile strength functions for extreme shape materials with straw included

6.3 Stress Distribution in Extreme Shape Materials Vessel

The calculated distribution of the vertical stress in plane flow silo with bed depth is shown in the figure 89 below and was generated from the theory described in the section 6.2 above. Both passive (σ_1) and active stress (σ_2) are presented. Passive stresses are calculated at the loose fill bulk density while the active stresses are calculated at compacted bulk density with corresponding bed heights.

This model assumes a hydrostatic stress, ignoring wall friction effects. The stress at the bottom of the vessel depends on the bed height. The higher the bed height, the higher the magnitude of the consolidation stresses. It is obvious from the plot below that bulk density is not constant over all the bed heights. Bulk density keeps on increasing as the bed height increases and consequently the vertical stress increases. Oat flakes has the highest value of the calculated vertical stress, highest bulk density with low particle aspect ratio and it is much less compressible compared to other biomass materials. In the silo discharge test, it is the only material that is relatively free flowing. Both woodchips and miscanthus behaved similarly and have intermediate vertical stress levels. Lawn grass has the smallest value of the vertical stress followed by straw. These two materials have very low bulk density with high particle aspect ratios. They are very difficult to discharge from the vessel particularly

straw which requires wide outlet size. Both predicted and actual arching dimensions have proved this estimation to be true though there is significant difference between the two values. Reed canary grass, wood shavings and shredded paper have similar values but they behave differently inside the silo particularly shredded paper. Wood shavings and reed canary grass have some silo discharge behaviour similarities especially at the lower bed heights.

Generally, from experience of the unconfined failure experiment with extreme shape materials the hydrostatic model that is used with extreme shape materials is justified due to the fact the material inter-particle forces are often vertical when they are compressed uni-axially (as discussed earlier in chapter 2, section 2.5.1.1). This replicates what is happening inside the silo. These extreme shape particles do not roll to the silo wall, so they exert a relatively small horizontal force on the silo wall, i.e. their lateral stress is always close to zero as a result they do not spread laterally therefore they do not flow often particularly at small outlet size and higher bed head.

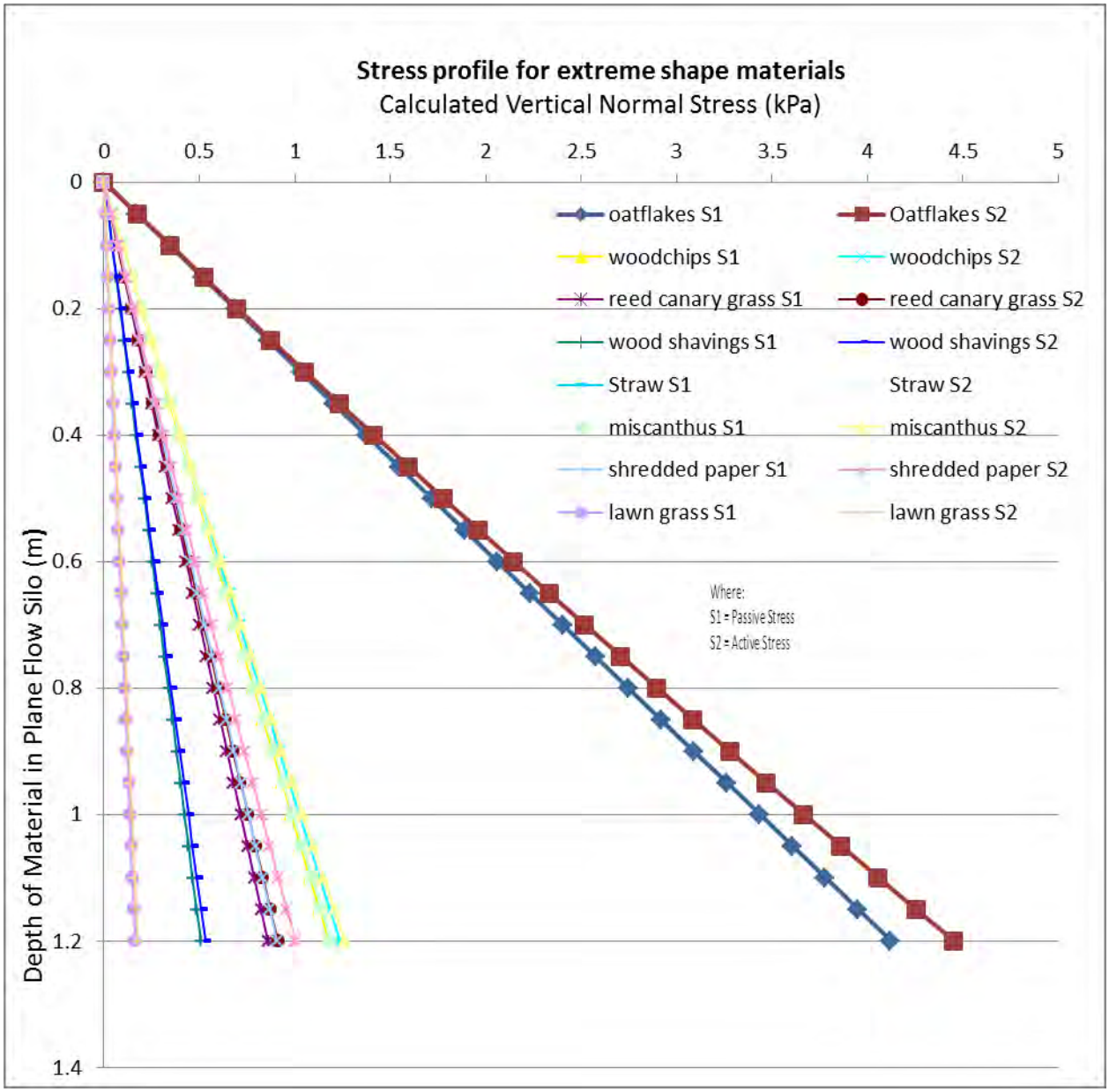

Figure 89: Assumed vertical stress distributions in the plane flow silo for various extreme shape materials (Where s1 refers to the passive stress state and s2 refers to the active stress state)

6.4 Arching Model

As previously described in section 6.2, the method used in calculating the results presented in this section is modified as compared to the results presented in section 6.1 particularly the predicted arching dimensions. The theory used includes purely analytical expressions for the distribution of active and passive stresses in the biomass

materials in the plane flow vessel as presented in the section 6.3. The new theory yields a reduction in the conservatism of the calculated arching dimensions presented previously in section 6.1. There is a trend in the data generated from the model (figure 90). That is, the data line for each extreme shape material at different angles falls approximately in the same region at both X and Y axis except straw which is presented in figure 91. The failure plots data are presented in Appendix C in tabular form.

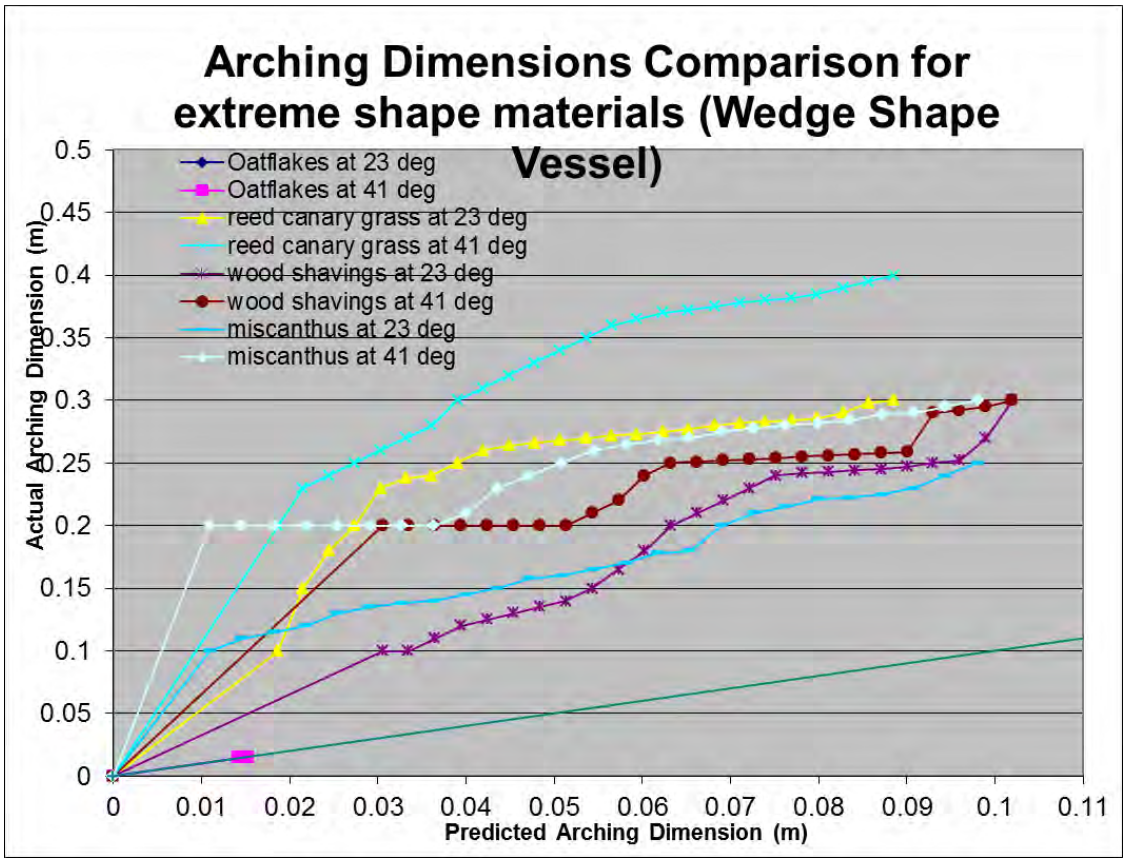

Figure 90: Arching Dimensions Comparison for Extreme Shape Materials without straw (B)

Two hopper half angles (23˚ and 41˚) were compared with each other for each material (Note that the total height of silo/ material head was the same in both tests despite the change in the half angles). At the steeper 23˚hopper half angle materials require smaller outlet dimension compared to the 41˚ angle. The predicted values consistently over-estimate the actual outlet dimension at both hopper half angles. Straw is the only material that required wide outlet dimension regardless of the wall angles. The oat flakes arching dimension estimation at the two wall angles is very small and they are the same for both actual and predicted data. Other materials

behave consistently well particularly at lower bed heights except reed canary grass which behaves totally different at 41° hopper half angle at the higher bed head for the actual dimension.

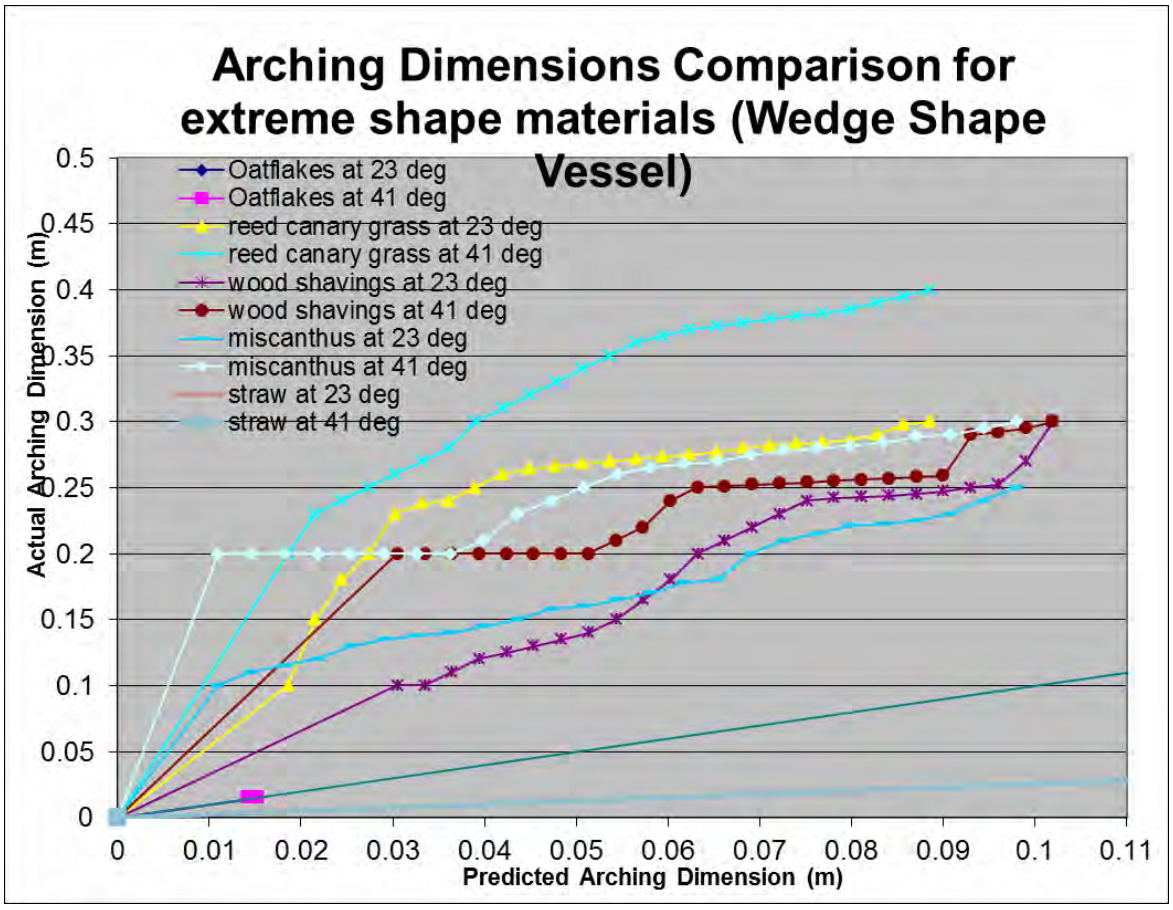

Figure 91: Arching Dimensions Comparison for Extreme Shape Materials with Straw included (B)

From the graph above, the difference between straw and others materials is due to the bulk density and particle size. The wide difference between straw and other materials in terms of bulk density is approximately 10:1 difference. The flakes are more free-flowing and have very small aspect ratio which is 2 while straw is pure long fibres without dust and the aspect ratio is 35. Other materials are short fibres with dust. All these attributes contribute to the wide difference in the behaviour of the materials particularly straw.

6.4.1 Arching Dimension versus Bed Head (Experimental and predicted results)

Experimental investigations carried out in this project particularly the silo discharge tests (Plane flow and cylindrical flat bottom silos): mass flow and core flow have shown that the outlet and wall angle required for extreme shape materials to discharge reliably depends on the bed height of the material.

The data used for the failure plots in this section are described in section 6.2. Also, the failure plots data are presented in Appendix C in tabular form. The comparative analysis is done at two wall angles (23˚ and 41˚) respectively. At both wall angles oat flakes behave consistently regardless of the bed height. The arching dimensions required for reed canary grass, wood shavings and miscanthus are significantly smaller at 23˚ wall angle compared to at 41˚ wall angle. This is reflected in the figures below. Wood shavings and miscanthus approximately behave equal at 41˚ wall angle and behave very similar at lower bed head at 23˚ wall angle. Reed canary grass behaves closely equal with wood shavings at higher bed height at 23˚ wall angle but behave totally different at 43˚ wall particularly at higher bed heights. As per straw, it requires large arching dimensions compare to other materials. It behaves the same at lower bed heads with reed canary grass at 23˚ wall angle. At 41˚ wall angle straw behaves more troublesome: at 0.62m bed head material requires largest arching dimension (0.5m) to discharge compare to 23˚ wall angle where material requires 0.4m arching dimension at 0.62 bed head to discharge from the vessel.

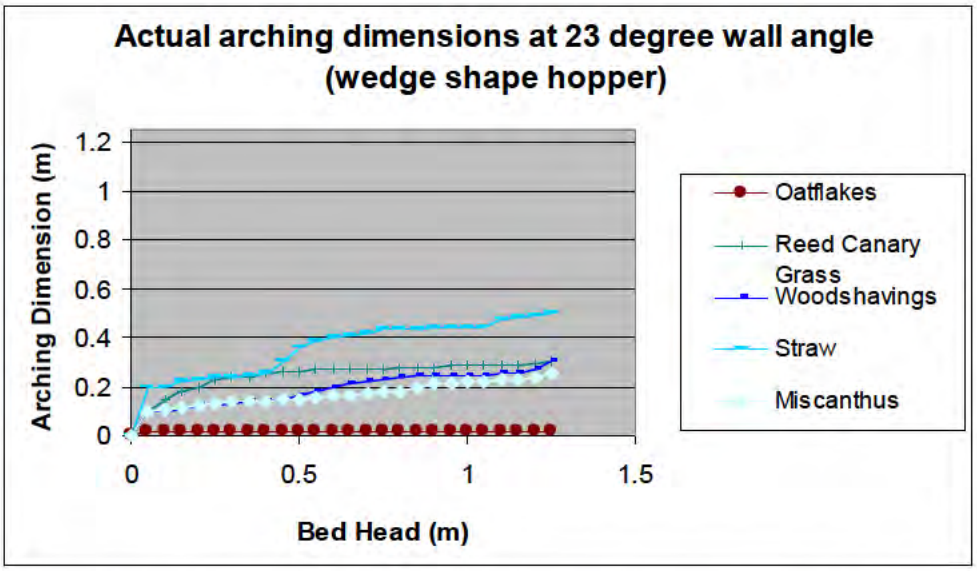

Figure 92: Actual arching dimensions versus bed head at 23 ° wall angle

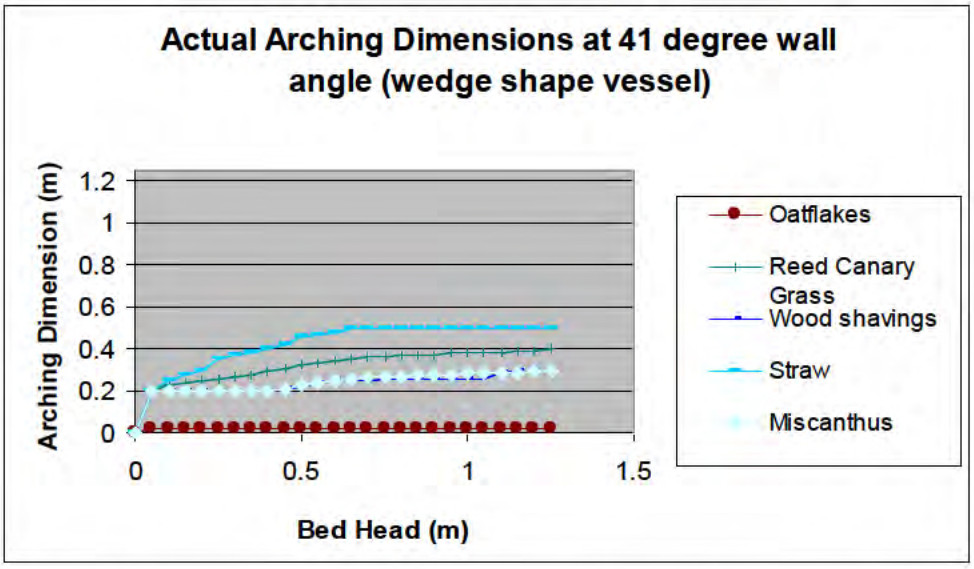

Figure 93: Actual arching dimensions versus bed head at 41 ° wall angle

Comparing the figures 92 & 93 above (actual measurements) with the figures 95 & 96 below (predicted data) it is obvious that oat flakes has similar trend with the actual data. Reed canary grass, wood shavings and miscanthus have some correlation with the actual data in terms of behavioural traits. They are significantly different in data comparison. They are under predicted. Straw is over predicted though it has some similarities with actual measurement in the sense that both data show that straw requires large arching dimension particularly at higher bed heights. Further correlation between particle size (both fibres and flakes) and the arching dimension is

that the shorter the particle size the lower the arching dimension required for the material to discharge reliably as in the case of oat flakes, reed canary grass, wood shavings, miscanthus while the longer the particle the higher the arching dimension required which is also a function of the particles bed height. This is clearly shown in the figure 94 below.

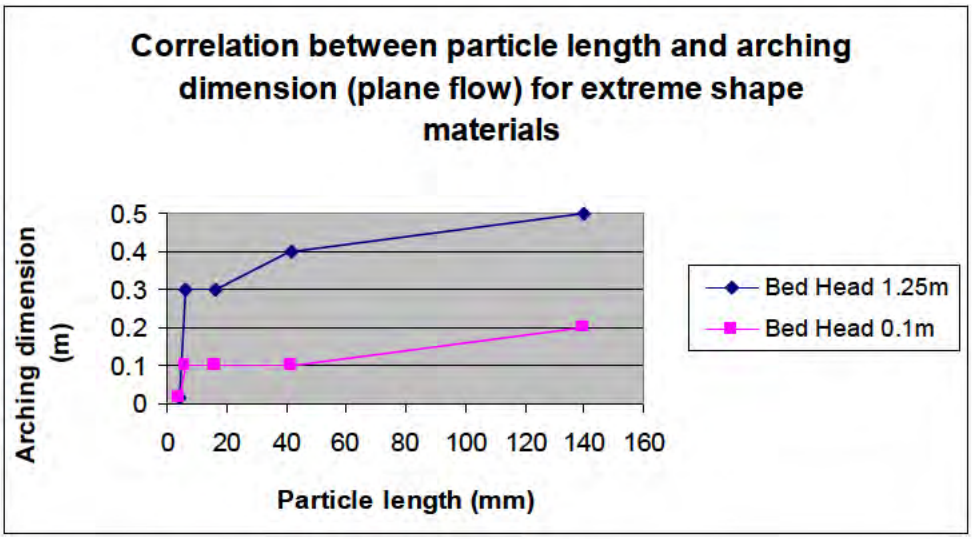

Figure 94: Correlation between particle length and actual arching dimension

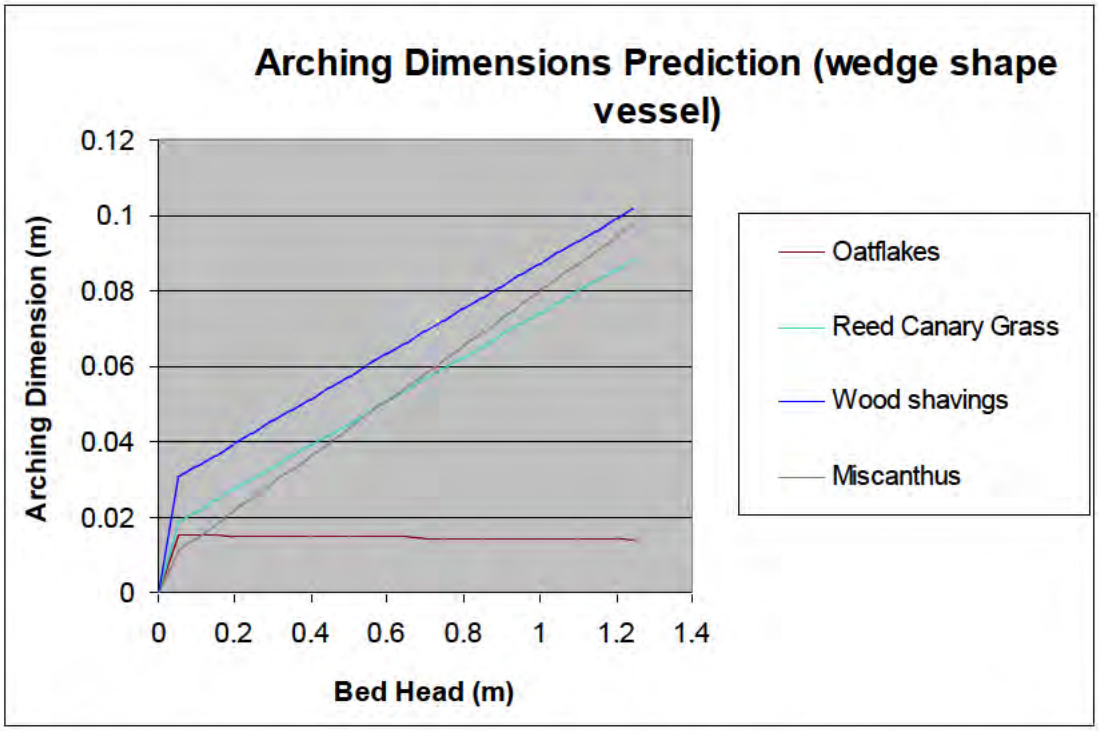

Figure 95: Predicted arching dimensions versus bed height without straw.

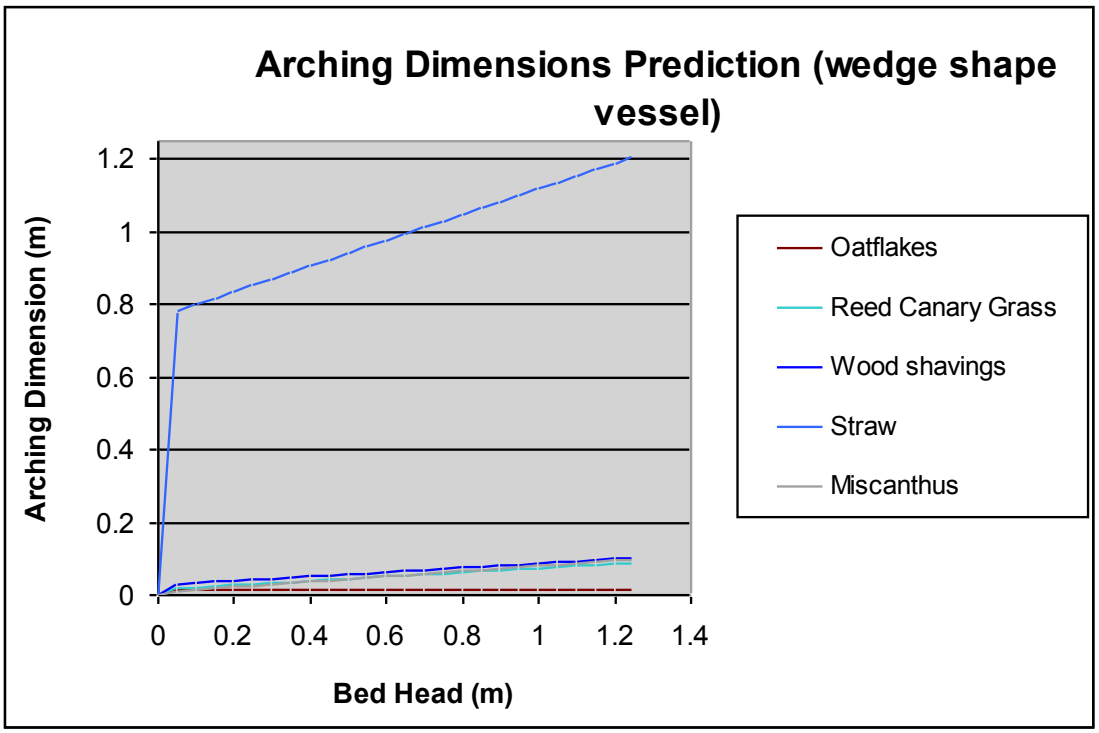

Figure 96: Predicted arching dimensions versus bed height with Straw included.

The point here is, the pattern of behaviour is similar between predicted and actual but the predicted value is over by a factor of about 5 except for straw.

6.5 Conclusion

Conclusively, based on the stress profile presented in this chapter: biomass materials that have the same particle characteristics presented in table 1 (Chapter 3) and micrographs in Chapter 3 will behave in the same way inside the plane flow vessel at the wall angles and outlet sizes used in this project. Biomass materials chosen for this project are industrial grades and they can serve as a benchmark for future biomass materials because biomass are seasonal and they come in different shape and size which is practically depend on the company's requirements and the granulator that does the size reduction in the forestry. Other intermediate treatments in the bio-refinery industry like biomass torrefaction and refuse derived fuels will have impacts on the flowability of the materials because it will affect the shape, size, texture, moisture content, aspect ratio, tensile strength and bulk density of the materials.

However, it is established in the experimental investigations that outlet size required for any given biomass materials to discharge reliably from the plane flow vessel depends on the materials bed head inside the vessel. Also, the aspect ratio or shape factor has significant impact on the flowability of the particles inside the vessel. This is an important guide to the bio-refinery industry.

Chapter 7: Conclusions and Recommendations for further work

7.0 Introduction

It is obvious that the work presented in this thesis requires continuation based on the bodies of literatures reviewed, experimental investigations carried out, industrial surveys carried out and constitutive mathematical models employed. The objectives of the project was completed particularly characterisation of extreme shape materials. Other two objectives require refinement for total completion. Knowledge has been added to the constitutive model but not totally completed. The model accuracy in this project is currently poor. It needs refinement in order to improve the trend in the result obtained especially the predicted results which were obtained from re-modification of Jenike Arching Theory. Based on this, the following conclusions and recommendations for further work are presented in the subsequent sections.

7.1 Silo Discharge Tests:

Silo discharge tests have been undertaken for extreme shape materials, using geometry that produces the two extremes of discharge patterns: core flow and mass flow.

- Core flow test have demonstrated that this flow pattern does not work for extreme shape materials as a result of this work does not need to be carried out further. Based on the test conducted outlet size approximately equal to bin size required, i.e. a full live bottom is required before material discharges in which case it is no longer core flow! Tests to investigate this have been undertaken on bins up to 0.7m diameter; the question is will this behaviour continue further as the bin diameter is increased? Clearly there are significant issues in verifying this experimentally due to the quantity of material and size of vessel required.
- Mass flow test have demonstrated that this can work for extreme shape materials provided the outlet is sufficiently large with an appropriate wall angle. Because of stress-phobic nature of extreme shape materials, outlet size required for reliable flow increases with the height of material in the silo and the stress. However, it is assumed that eventually the outlet size will become

independent of bed height (eventually stress will be supported by wall friction). Further work is required in this area because it can work for extreme shape materials and makes a much more economical solution than a full live bottom. I.e. storage vessels will require a smaller cross sectional area for the feeder and material will be stored vertically rather horizontally requiring less ground space per quantity of material.

- The correlation between the value of the lower limit of the flow region in the mass flow silo discharge test described in Chapter 5 and the tensile test result is that tensile strength often approach accurately predicts the strength at low bed heads. At higher bed heads, the tensile strength significantly over estimates the strength of the material and the arching dimension. This could be due to particle length or particle aspect ratio. For example straw particles length was approximately equal to that of tensile cell.

7.2 Characterisation Tests:

Characterisation tests were conducted on extreme shape materials and powders/granules with approximately rounded "equant" particles.

- A novel column test technique was developed at the initial stage of the research. This provides a qualitative screening test that can identify biomass or waste materials that exhibit nesting behaviour and will therefore be difficult to handle. If they are troublesome, then further testing is required to design a silo to handle them. If they do not form a column then the use of conventional technique like powder flow tester can be applied. The column test does not require further work because it cannot discriminate much among various extreme shape materials.

- The Wolfson tensile tester was adopted for further investigations of the behavioural traits of extreme shape materials. The tensile tester was employed to study the tensile strength of extreme shape materials. Results suggest that, if the materials had a tensile strength value it means such materials will be troublesome during handling; it requires mass flow hopper. To test this hypothesis further, a larger series of experiments (tensile strength and mass

flow arching), need to be undertaken to investigate a link between tensile strength and outlet span. Further work is required on tensile tester because experimental investigation has shown that it has the potential of discriminating various extreme shape materials. However, it requires re-engineering to make it more sophisticated such as a load cell to measure tensile force as a function of separation distance up to the point of failure, better control of the motion of the cell halves during separation (one fixed half, the other half mounted on a motorised machine slide) and rougher surfaces for the inside walls of the cell to prevent material slip.

- Wolfson-Brookfield Powder Flow Tester was employed for comparative testing between bulk solids with approximately spherical particle shape and extreme shape materials. The tests were conducted in order to ascertain why conventional shear testers give misleading results when used to measure the flow properties of extreme shape materials. Results show that extreme shape materials have very low bulk density and they don't slide (shear), so sample becomes redistributed in the cell, rather than shearing regardless of the size of the shear tester. No further work was undertaken in this area as it was considered outside the scope of this work.

- Uni-axial test technique was conducted to measure the unconfined yield strength of extreme shape materials. Results show that extreme shape materials are stress phobic. It means that they do not like stress/pressure. The more stress put behind them, the more it is difficult for them to discharge/flow from the storage irrespective of bulk density. However, when material is compacted to cause failure/flow, rather than expanding horizontally and flowing like a cohesive powder, material compresses vertically (and gets stronger) as fibres become orientated horizontally and move closer together. Further work is not required for this test because various tests have been conducted (based on literature review and experimental investigations) which has established the fact that extreme shape materials are stress phobic and that the uniaxial test does not discriminate between them.

- For non-extreme shape materials, the powder flow tester, other shear testers and uniaxial test technique can be used for the characterisation test. For extreme shape materials (biomass materials), tensile tester can be used for the characterisation. What is required now is a constitutive model relating the strength of the material to the strength of the mechanical arch, so that discharge behaviour from storage can be reliably predicted. This is where further work should be focused.

7.3 Modelling and Predicting Arching Dimension

Based on the flow data generated so far, a silo test rig was developed which was used in conjunction with the tensile tester for the characterisation and silo discharge tests of extreme shape materials in order to achieve mass flow pattern (first in, first out flow sequence) that is desired in the bioenergy industry and other process industries. The silo test rig has been used in conjunction with the tensile tester to do the new simulation (i.e. experimental investigation, modelling and prediction). The new simulation has been used to develop the new the failure criterion for extreme shape materials.

The novelty in this work has clearly come from the application of the tensile testing method in conjunction with a new failure criterion for extreme shape materials in mass flow hopper. The novel criterion has enabled further assessment of the shape impacts/effects on the flowability of biomass and waste materials. It has also help to determine the slot outlet where there is stress relief on the materials to enhance their discharge from storage. That is, the recommended outlet where materials tend to untangle and start discharging reliably under gravity. Other essential dimensions like wall slope and particle orientations inside the silo required to achieve mass flow have been measured and observed. However, it can also be employed to sub-classify "Class 3" materials which are extreme in shape because there is wide diversification in Class 3 materials based on the origin of the materials: treated/untreated biomass and waste materials vis-à-vis virgin biomass and waste materials, refuse derived fuel/solid derived fuel etc.

7.4 Further Work Suggestions

Due to the wide diversification of extreme shape materials and the continuous development of new biomass feedstocks further novel characterisation tests are required in order to produce holistic flow parameters (data) that will be useful to produce silo design guidelines for reliable flow (discharge) of extreme shape materials from storage irrespective of the origin of the materials and for the evaluation of the existing plants.

A key requirement is the determination of the particle mechanics that are responsible for the resistance to flow of the extreme shape materials. This could be investigated by developing a half model silo with a transparent end wall for visualising the extreme shape particle packing during arching and the relative particle movement during flow. Coloured particles in combination with video/photographic digital imaging could be used to visualise and measure this. The materials that can be used for these tests should be a material such as wood shavings as the fibres are relatively small 16mm length so, they can be tested in a relatively small model silo. Or any other extreme shape materials that fall into this particle size. Communition might be required for larger particles to achieve small length particles. Better still, it could be conducted in full scale using large particles like 250mm length by fitting a transparent end wall onto the plane flow silo delivered from this project.

This area of further work will enable further way to:

- Identify troublesome and well-behaved extreme shape materials
- Evaluate the impact of stress on the flowabilty of extreme shape materials
- Measure the nesting (entanglement) strength of extreme shape materials
- Measure the various phases of the process test vis-à-vis rathole, mechanical arch and various forms of hang-ups (cliffs) inside the vessel.

Further assessment and refinement of the proposed constitutive mathematical models used in this project to predict the arching dimension to setup gravity flow/no-flow criteria for extreme shape materials is required. This will help to determine minimum

outlet required to ensure the mechanical arch collapse. The two key parameters in the mathematical model are tensile strength and bulk density. The variations in these two values particularly tensile strength could be due to the filling method, particles bed height and accuracy of the distance the movable cell needs to travel before the material untangles require further assessment. This will help to resolve both under and over predictions in the values of actual (empirical data) and predicted arching dimension. The novel wedge shape hopper is robust to accommodate different extreme shape materials. Experience has shown that even the most troublesome of the materials tested on the rig which was straw discharge reliably at 23º wall angle and 500mm width of slot.

Furthermore, the use of discharge feeder to interface with the vessel to obtain discharge from the vessel might be relevant in order to observe the flow profile from top of the vessel but it has to be done with caution because most discharge feeders tend to draw preferentially from the vessel, e.g. screws draw from the back of the vessel and consolidate the material against the front vertical wall of the vessel. This occurs because the transport capacity of the feeder has not been matched to the outlet dimension of the vessel, so that the material draws from a single point. Often the material consolidation by the feeder results in severe material arching at the vessel outlet (Bundalli, 1986). This is one of the key reasons why the moving-hole feeder reviewed in chapter 2 was developed by Kamengo Technology in Canada. However, discharge feeders are often needed when the rate of flow that would occur from uncontrolled gravity discharge is higher than the rate at which downstream operations operate. Based on this it might be reasonable to focus on researching the failure criterion and anisotropic behaviour of extreme shape materials first because if the materials are not flowing inside the vessel the use of a discharge feeder will be useless. Experience has shown that extreme shape materials tangle rather than flowing when they are in a vessel. When they tangle inside the vessel, the use of discharge feeder will be useless because discharge feeder also needs a feeder as well which is the storage vessel. This needs to be researched further in order to determine the micromechanics at the source of their resistance to flow.

The remaining over prediction and under prediction in the predicted arching dimensions could probably originate from using straight-line extrapolation of the flow

properties particularly the bulk density function in the region of the low stresses. To overcome this uncertainty in the prediction data, the original course of the data must be measured down to very low stresses. Alternative method of measurement that can make this possible need to be looked at especially on the tensile strength measurements.

References

Berry R.J, Bradley M.S.A & McGregor R.J (2010), Development and Commercialisation of a new Powder Flow Tester for Powder Formulation Development, Quality Control and Equipment Design, Bulk Solids India 2010.

Bundalli Nazmir (1986): New developments in storage and handling of biomass. Proceedings from the Eight Annual Industrial Energy Technology Conference, Houston, TX, June 17-19.

Bundalli Nazmir (2000): Development of the "Moving Hole" Feeder. Kamengo Technology Incorporation. Canada.

Bundalli Nazmir (1989): Development of a simple flow test apparatus for biomass materials. Department of Energy, Mines and Resources, Canada.

Bates Lyn (2006) "Woodchip Bin Bridging" The Powder/Bulk Potter: (http://forum.bulk-online.com/showthread.php?7661-Wood-Chip-Bin-Bridging) Accessed on December 29, 2010.

Bates Lyn (2003) "Feeding Wood Chips" The Powder/Bulk Potter: (http://forum.bulk-online.com/showthread.php?1590-Wood-Chip-Handling). Accessed on 05/03/2012.

Bradley M.S.A and Farnish R.J (2004) "Discharging the Impossible: Understanding the Flow of Biomass and Waste Materials". Materials Handling Engineers' Association Annual Conference. Manchester Moat House Hotel, April 22-23, 2004.

Bradley M.S.A (2009) Waste Material Properties: How do you know what to expect, and how to hand it? Sustainable Waste Management Conference. Process Industries Division: Institution of Mechanical Engineers, London.

Bradley M.S.A (2010) Clean Tech, Clean Profits: Using effective innovation and sustainable business practices to win in the new low-carbon economy. Technology Strategy Board Handbook (Institute of Directors). Published by Kogan Page, United Kingdom.

Bradley M.S.A, Khan N.S, Berry R.J (2011) "Best Practice Guide Handling of Biomass Fuels and Coal-Biomass Mixes" A report prepared for the power industry. The Wolfson Centre for Bulk Solids Handling Technology. United Kingdom.
Eisentraut Anselm (2010) Sustainable Production of Second-Generation Biofuels: Potential and Perspectives in Major Economies and Developing Countries.

Basu Prabir (2010) Biomass Gasification and Pyrolysis: Practical Design and Theory. Elsevier. ISBN: 9780123749888.

Berry Rob (2004) "Review of the literature concerning powder failure properties, their measurement and the measuring devices".

Berry Rob (2003) "The Measurement of cohesive arches in silos using the technique of laser ranging" PhD Thesis. Wolfson Centre, University of Greenwich, United Kingdom.

Blott Simon J. and Pye Kenneth (2008) "Particle shape: a review and new methods of characterization and classification". Sedimentology 55. Page 31-63.

Bell T.A. (1999) "Industrial Needs in Solids Flow for the 21st Century" Powder Handling and Processing. Volume 11. No. 1. January/March 1999.

Bridgwater Tony 2002, "Current and future prospects for biomass and bioenergy"Bioenergy Research Group, Aston University, United Kingdom.

Chevanan Nehru, Woman Alvin R., Bitra Venkata S.P., Yoder Daniel C., Sokhansanj Shahab (2009) Flowability parameters for chopped switchgrass, wheat straw and corn stover. Powder Technology 193(2009) 78-86. Elsevier.

Charles Y.W and Essel B.H, (1996) Biomass Conversion and Technology.Unesco Energy Engineering Series. John Wiley and Sons, England.

Carson John W. and Wilms Harald (2006) Development of an international standard for shear testing. Powder Technology: Elsevier 167 (2006) 1-9.

Department of Energy and Climate Change, 2011 "UK Renewable Energy Road Map" (http://www.decc.gov.uk/assets/decc/11/meeting-energy-demand/renewable-energy/2167-uk-renewable-energy-roadmap.pdf) Accessed on November 18, 2011.

European Commission: Agricultural and Rural Development (source: http://ec.europa.eu/agriculture/bioenergy/biofuels/index_en.htm) Accessed on December 28, 2010.

Eckhoff, R.K. and Leversen, P.G. (1974) A further contribution to the evaluation of the Jenike method for design of mass flow hoppers. Powder Technology 10 (1974) 51-58.

Fasina Oladiran (2006) "Flowability of Biomass for Biorefinery". Power Point Presentation at the International Bioenergy Conference, Prince George, BC, Canada.

Faaij Andre, (2002) Modern Biomass Conversion Technologies, Utrecht University, Copernicus Institute, Department of Science, Technology and Society, The Netherlands.

Federation Europeenne De La Manutention Section ll: Continuous Handling (Properties of Bulk Materials); FEM 2581 and 2582. November 1991.

Goldemberg Jose (2000) World Energy Assessment. United Nations Development Programme and World Energy Council.

Grace John and Dai Jianjun (2011) Biomass granular screw feeding: An experimental investigation. Biomass and Bioenergy: Elsevier 35. Pp 942-955.

International Energy Agency: (http://www.iea.org/papers/2010/second_generation_biofuels.pdf). Accessed on December 28, 2010.

Idagbon Nicholas (2009) "Effect of strip length on flow of shredded sheet material" MSc Research Project at Wolfson Centre, University of Greenwich, United Kingdom.

Iowa Energy Centre Renewable Energy:
(http://www.energy.iastate.edu/renewable/biomass/) accessed on December 27 2010.

In situ Oil Sands Alliance, Alberta, Canada (source:
http://www.iosa.ca/the_issues/energy_supply/) Accessed on December 28, 2010.

Ileleji Klein (2010) "Energy wasted grinding switchgrass smaller to improve flowability". Purdue Newsroom. Purdue University, United States of America. (http://www.purdue.edu/newsroom/research/2010/100412IelejiMorphology.html) Accessed on December 29, 2010.

Jenike A.W. (1961) Gravity flow of bulk solids. Bulletin 108, University of Utah, USA.

Jenike A.W. (1964) Storage and flow of solids. Bulletin 123, University of Utah, USA.

Johanson Jerry R. (1989): Bin and Feeder Design for Woodchips and other Springy Bulk Solids. JR Johanson Inc. San Luis Obispo, CA 93401.

Khan Naushad Salim (2008) Handling characteristics of coal/biomass mixes: measurements and establishing benchmarks. PhD Thesis, Wolfson Centre, University of Greenwich, United Kingdom.

Mattsson, J.E (1990) Basic handling characteristics of wood fuels: Angle of repose, friction against surfaces and tendency to bridge for different assortments. Scandinavian Journal of Forest Research 5:583-597.

Mattsson, J.E. (1997) Tendency to bridge over openings for chopped phalaris and straw of triticum mixed in different proportions with woodchips. Pergamon Biomass and Bioenergy Journal. Volume 12, No.3, pp 199-210.

Mattsson J.E., Peter D.J., Kofman P.D., Klausner A. (2004) Tendency of wood fuels from whole trees, logging residues and roundwood to bridge over openings. Elsevier Biomass and Bioenergy Journal. Volume 26, pp 107-113.

Mattsson J.E. and Kofman P.D. (2002) Method and apparatus for measuring the tendency of solid biofuels to bridge over openings. Pergamon Biomass and Bioenergy Journal. Volume 22, pp 179-185.

McGee Eddie (2009) Keep Plugging Away! Sustainable Waste Management Conference. Process Industries Division: Institution of Mechanical Engineers, London.

Merrow Edward W. (1986) A Quantitative Assessment of R&D Requirements for Solids Processing Technology. Rand Report. The U.S. Department of Energy. The Private Sector Sponsors Program.

Marinelli Joseph (2000) "Testing Materials with Large Particles" Solids Handling Technologies.http://www.solidshandlingtech.com/ask_joe_articles/testing_materials_with_large_particles.htm (accessed on 08/09/09).

Marinelli Joseph (2011) "Mass flow design considerations" Solids Handling Technologies.
http://www.solidshandlingtech.com/ask_joe_articles/arching_part_one.htm (accessed on 25/11/2011)

Marinelli Joseph (2012) "All Hoppers are not created equal" Solids Handling Technologies.
(http://www.solidshandlingtech.com/ask_joe_articles/all_hoppers_are_not_created_equal.htm). Accessed on 05/03/2012.

Marinelli J and Carson J.W., 1992 “Solve Solids Flow Problems in Bins, Hoppers, Feeders” Jenike and Johanson Technical Paper. (http://www.jenike.com/TechPapers/solve-solids-flow-probs.pdf accessed on 07/09/09).

Owonikoko A., Bradley M.S.A and Berry R.J. (2010) “Characterisation of Extreme Shape Materials: Biomass and Waste Materials”. Bulk Solids Europe Conference, Glasgow, Scotland.

Schwedes Jorg (1999) Review on testers for measuring flow properties of bulk solids, Granular Matter 5, 1-43 (Based on an IFPRI-Report 1999). DOI 10.1007/s10035-002-0124-4.

Schulze D. (1996) Flowability and time consolidation measurements using a ring shear tester. Powder handling and processing, Vol. 8, No. 3, pp221-226.

Turkenburg Wim C., 2000 World Energy Assessment. United Nations Development Programme and World Energy Council.

The Roger, Couch Steven W., Bell Timothy A. (1994): Characterisation of flow properties of low bulk density materials. Delft University of Technology and E.I.du Pont de Nemours and Company.

United Nations Framework Convention on Climate Change: Clean Development Mechanism (CDM) (http://unfccc.int/kyoto_protocol/mechanisms/clean_development_mechanism/items/2718.php) Accessed on December 27, 2010.

Wolfson Centre: http://www.gre.ac.uk/wolfsoncentre/consultancy/hoppersandsilos . Accessed on July 23, 2011.

Wright H, 1970 Bunker Design for Iron Ores, PhD Thesis, University of Bradford, United Kingdom.

Appendix A

A.1 Results and Discussion of Biomass Characterisation Tests

A.1.1 Column Test

The biomass materials behave differently inside the tube as illustrated in chapter 3. The chopped miscanthus column height decreases downward and reaches a point where it increases (figure A1). This could be due to the particle shape and size as well the tube diameter. The wet woodchips/wet hammer milled wood has a higher column height inside the smaller tube diameter but decreases downward inside the large tube diameter. This is due to the moisture content of the particles. The particles are likely to be entangled a bit. The higher the column height inside the small diameter tube the likely the particles to be entangled inside the storage. The dry woodchip/dry hammer milled wood behaves very similar to the chopped miscanthus. It decreases down and later increases especially inside the long diameter tube. Overall, it can be inferred that the chopped miscanthus is less entangle among the three biomass particles employed in the experiment. The higher the column height of any material inside the tube, the likely the material will nest and entangle to each other and difficult to discharge inside the storage bin. The fourth biomass material which is ground palm kernel nut did not form any column at all. It only formed angle of repose. This kind of material can be characterised using shear cell. Also, shredded paper did not flow. No column protruded out of the tube because of the high aspect ratio of the materials. That is why both ground palm kernel nut and shredded paper are not reflecting in the graph below. Ground palm kernel nut biomass material could be tested inside the shear tester and give reliable design data.

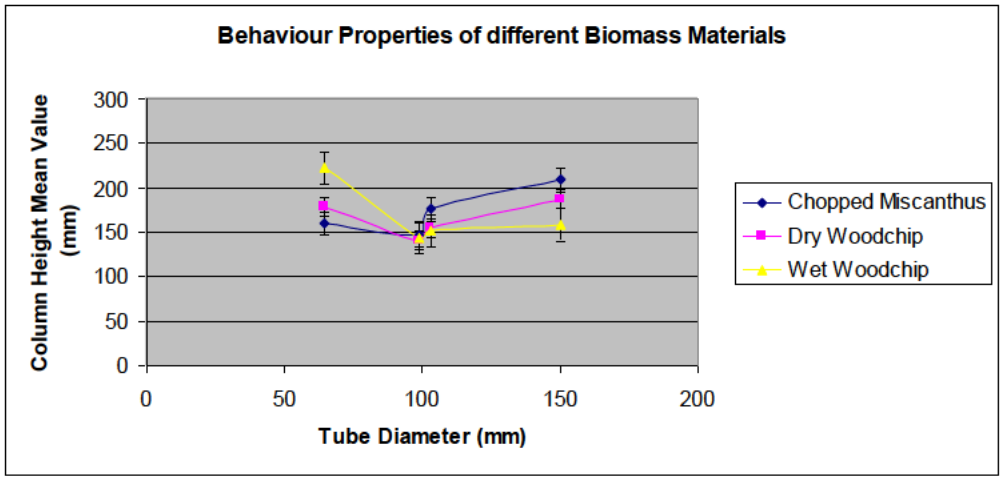

Figure A1: Flow characteristics of different biomass particles.

A.1.1.1 Conclusion

Characterising the flow and physical properties of biomass and waste materials particles is very pertinent in order to help solids handling equipment designer and for quality control in the process renewable energy industry. Therefore the need for the development of technique for quick biomass particles characterisation is very essential for the industry. Different bioenergy industries require different feedstock grades (e.g.Alstom's woodchips grade is totally different from Biojoule's woodchips grade). Alstom's woodchips was grounded/milled while Biojoule's woodchips was not grounded. This contributes to the extreme shape materials diversification. The column test technique has enabled quick characterisation of uniaxial failure mode of the extreme shape materials which is one of the main objectives of the project.

A.1.2 Tensile Tester

Mean value and standard deviation of the recorded data was employed to draw the bar chart for the results analysis. Tensile stress was calculated from relationship of S=F/A where F =mg, A= LB where g = 9.81m/s^2 (acceleration due to gravity), S = tensile stress (kPa), F= tensile force (N), M = tensile load (kg), A=area of the two cells (m^2), L = length of the two cells (m^2), B = breadth/width of the cell (m^2).

A1.2.1 Chopped Miscanthus, Dry Woodchips/Hammer Milled Wood and Wet Woodchips: The cells were dump-filled and levelled with hands. Tensile stress required to pull the dynamic cell for the 3 biomass materials was significantly

different. 0.1kPa was required to pull the dynamic cell for chopped miscanthus. There was no deviation in the parameters. 0.12kPa was required to pull the dynamic cell for dry woodchips. The standard deviation of the parameters was 0.04kPa. 0.14kPa was required to pull the dynamic cell for wet woodchips. The standard deviation of the parameters was 0.05kPa. This is reflected in the figure 36 below. There was reproducible/repeatable difference of 0.02kPa in the 3 tensile stress values with 0.01kPa difference in the standard deviation. This means that the 3 materials will behave differently inside the storage vessels. Also, the difference in their behavioural traits might be due to the inherent moisture content, bulk density and particle aspect ratios which account for their entanglement nature.

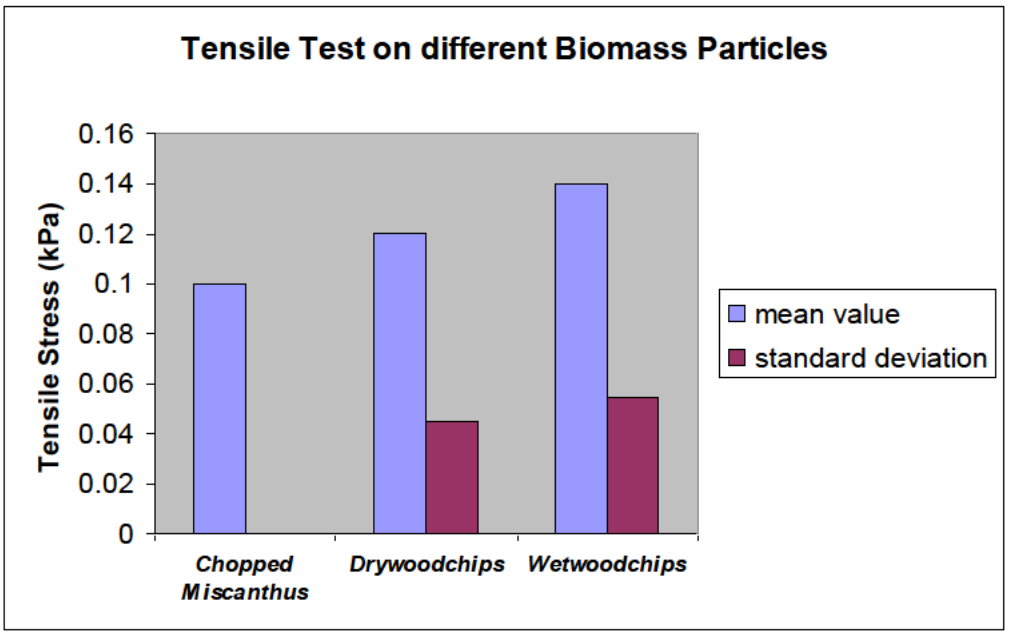

Figure A2: Tensile test results for biomass particles.

A1.2.2 Matchsticks: Five different lengths (5mm, 10mm, 20mm, 30mm, and 40mm) of matchsticks were tested on the tensile tester rig. Filling was done by random-spread approach. 0.02kPa was required to pull the dynamic cell for 5mm particle length. 0.022kPa was required to pull the dynamic cell for 10mm particle length. 0.03kPa was required to pull the dynamic cell for 20mm particle length. 0.034kPa was required to pull the dynamic cell for 30mm particle length and 0.042kPa was required to pull the dynamic cell for 40mm particle length. It can be inferred that, the longer the particle length, the higher the tensile stress required to pull the dynamic cell from static cell. This means that particles of long length will be resistant to flow inside the silo due to the entanglement of the particles. This agrees with column test results where particles

of longer length displayed high column height before failure. Particles of 5mm and 10mm lengths might behave exactly the same inside silo because of the insignificant difference in tensile stress parameters. The same thing goes to particles of 20mm and 30mm lengths. This is shown in the figure A3 below.

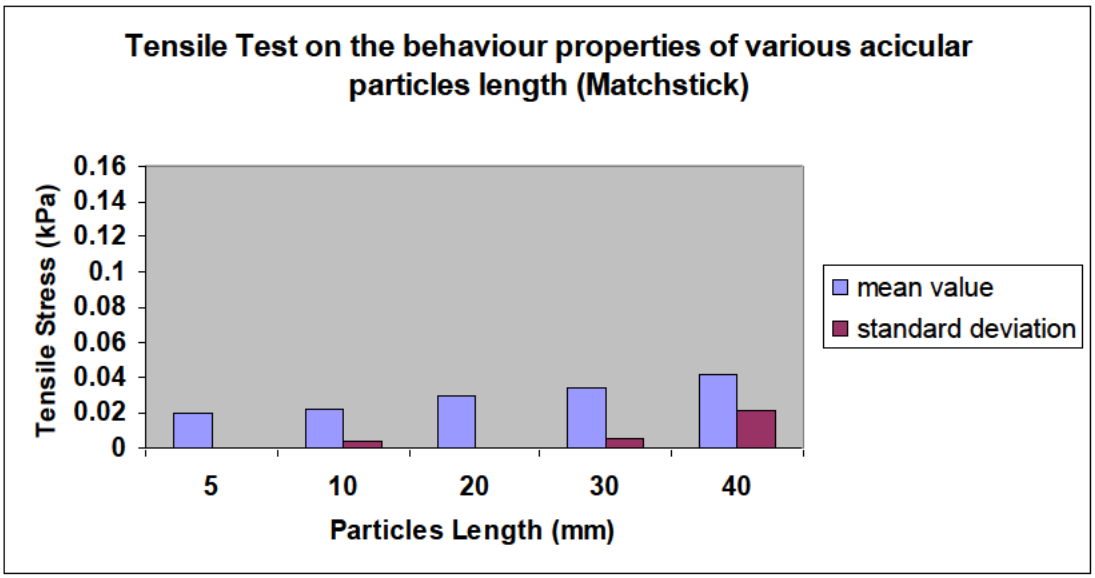

Figure A3: Tensile test results for acicular particles "matchstick".

A1.2.3 Lawn Grass and Shredded Papers: The lawn grass is succulent and soft in texture with a mixture of various particles lengths and breadth (width). Shredded paper is flexible and smooth on surface with a mixture of various strip lengths and breadth (width). Filling of the cells was done by dump filling and levelled. The amount of tensile stress required to pull the dynamic cell from static cell for shredded paper is more compare to lawn grass (figure 38 below). This is due to the aspect ratio of the two materials. Shredded paper has high aspect ratio while lawn grass has small aspect ratio. However, the aspect ratios of the materials are not even.

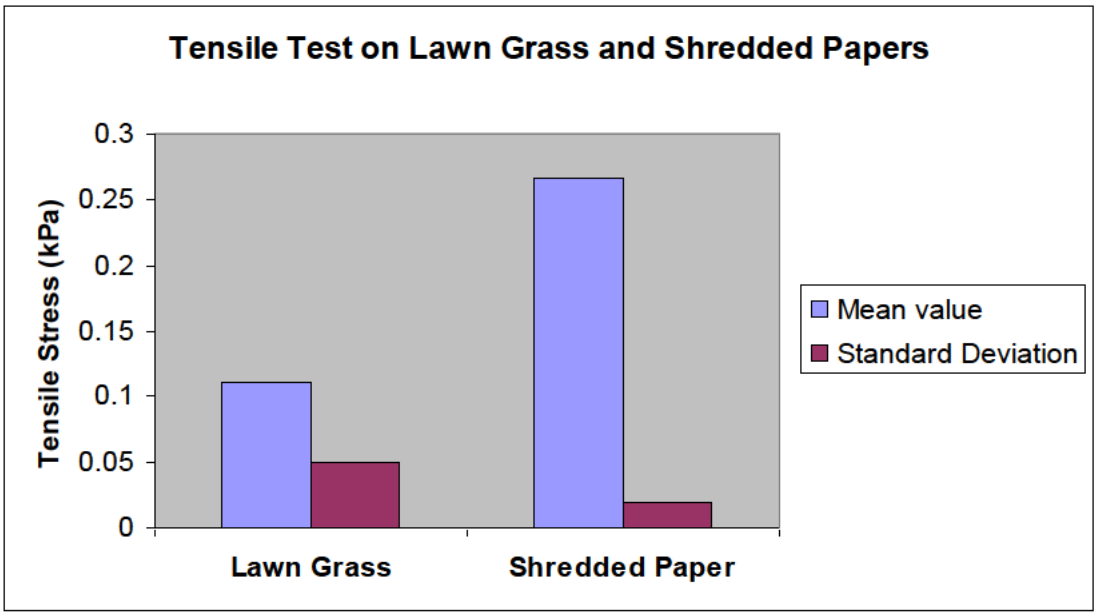

Figure A4: Tensile test results for biomass materials "lawn grass and shredded paper".

A.1.2.4 Conclusion

Extreme shape materials of high aspect ratio will give high tensile strength value because materials of high aspect ratio will interlock and entangle deeply. High tensile strength is a function of poor flowability and troublesome of the particles inside the bin. Other factors that could be attached to the high tensile strength are inherent moisture content and low bulk density. The tensile test technique has enabled quick characterisation of biaxial failure mode of the extreme shape materials which is one of the main objectives of the project.

A.2.0 Core Flow Silo Test

The results and discussion here will be divided into two based on the two types of rings employed, which are, first ring and second ring.

A.4.1 Effects of Bed Height (Head) on the Flowability of Woodchips and Chopped Miscanthus at Core Flow Test Rig A (First Ring).

A.4.1.1 On Woodchips/hammer milled wood

Generally, the particles tend to have high rathole parameters at smallest bed height. The higher the bed height, the more difficult for the particles to rathole and flow. Though, this does not hold all the time. The flow phase transition in the core flow discharge is: the particles start with arching and later transform to ratholing and later drain/discharge. The discharge is not always reliable (i.e. not under gravity).

After arching at bed height 800mm, the particles start ratholing at 250mm outlet diameter in the first test conducted and 300mm outlet diameter in the subsequent tests to 500mm outlet diameter which is the maximum outlet dimension used. Five tests were run on each outlet diameter. The particles did not rathole at all at 100mm, 150mm and 200mm outlet diameters, what it does was arching/bridging over the entire outlet area. Also, test 2 to test 5 did not rathole at 250mm and formed a big mass of interlocked particles over the outlet area. All ratholes formation at this bed head were generated after hammering the bin (i.e. after bashing the bin with rubber hammer). There was no flow at all whether with or without small/large hang-up on the obstruction. The only occurrence was arching and ratholing.

Figure A5: Rathole formation after bashing the bin with rubber hammer at Bed Height 810mm.

The behavioural traits of the particles at bed height 400mm is a little bit similar when the at bed height 800mm.The similarities is that, after arching/bridging, the particles start ratholing at 250mm outlet diameter but this time it was both first and second tests that ratholed at 250mm. Test 3 to test 5 did not rathole at 250mm. However, at 100mm, 150mm, and 200mm outlet diameters, the particles only formed mechanical arch (whereby the particles interlock) and no rathole was formed at all. The flow parameters obtained for the rathole measurements are significantly larger than what obtained at Bed Height 800mm. Also, there was discharge at 500mm outlet diameters for Test 1, 2 and 4 but the flow was with large hang-up on the obstruction. This could be effects of the bed height because the vertical stress (δv) acting on the outlet rings is less compare to vertical stress acting at Bed Height 800mm. Also the lateral stress acting on both sides of the cylinder ("silo") is less to "At Bed Height 800mm". It shows that the difference of 400mm between the two Bed Heights is enormous

enough to make significant effects. All ratholes formation were self-generated (i.e. without bin hammering).

The particles start ratholing at 200mm outlet diameter at bed height 200mm compared to other bed heights which start ratholing at 250mm outlet diameter. It was arched at 100mm and 150mm outlet diameters. No sign of ratholing during the investigation at these outlets. The flow behaviour of the particles at Bed Height 200mm is better than other bed heights (400 and 800mm). The flow parameters for the rathole are larger than other two bed heights. Interestingly, there was discharge at 500mm outlet diameter in all the five tests conducted but the flow was with small hang-up on the obstruction inside the bin. The reason for this could be attached to the difference in bed height value which is 200mm and 600mm respectively. It shows that the lateral stress in the bin and vertical stress (δv) acting on the outlet rings are very small. It enables the particles to fall on each other and particles flow centrally inside the cylinder. All ratholes formation were self-generated (i.e. without bin hammering).

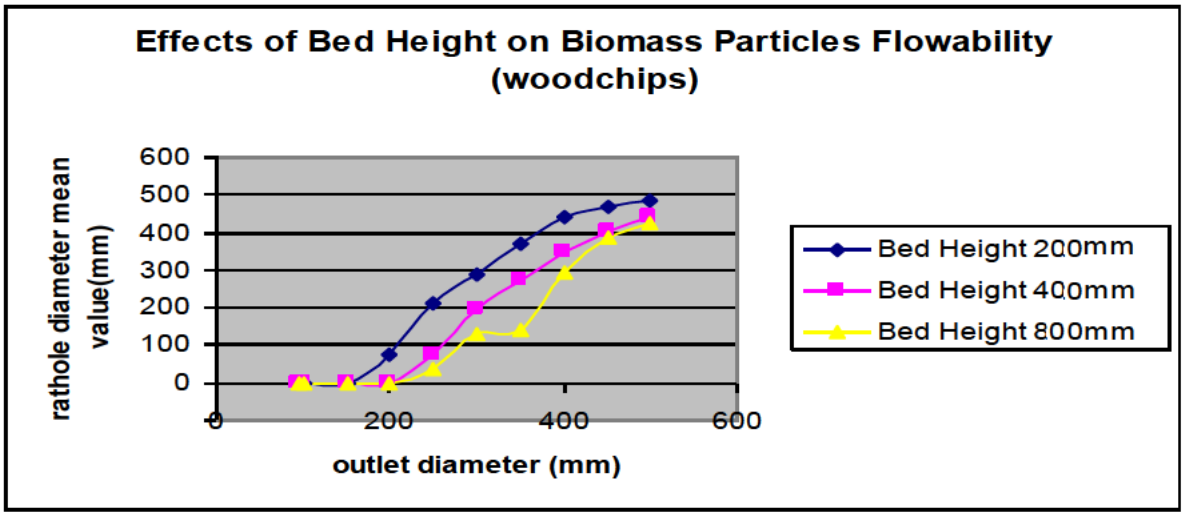

Figure A6: Effects of bed height on flowability of woodchips

A.4.1.2 On Chopped Miscanthus

There are similarities between woodchips and chopped miscanthus behaviour inside the bin. Both form arch, rathole and discharge (drain) but in different proportion. The following observations and results were made at different bed heights.

The five tests conducted when the bed height was at 800mm start ratholing at 350mm outlet diameter after arching. It was consistency throughout the tests but with different rathole data (figure A7). There was arch formation at 100mm, 150mm, 200mm, and

250mm outlet diameters. All ratholes formation at this bed head were generated after hammering the bin (i.e. after bashing the bin with rubber hammer) which is similar to what experienced in woodchips at the same bed head/height. No discharge (flow) at all except arching and ratholing formations. The key difference between the two particles is the distribution of rathole formation data. Woodchips starts ratholing at early stage (250mm outlet diameter) while chopped miscanthus starts ratholing at 350mm outlet diameter. These characteristics could be due to their various inherent moisture contents. The moisture content of chopped miscanthus is less than woodchip's moisture content. The amount of energy required to generate rathole during the hammering of the bin is enormous for chopped miscanthus.

When the particles were at bed height 400mm they behave differently. The formation of ratholes was a mixture of "after hammering" and "before hammering". The first rathole formed at 500mm outlet diameter after hammering the bin during the first test whereas in the second test, two ratholes were formed at 450mm and 500mm outlet diameters without hammering the bin (cylinder). Subsequent tests (3^{rd} and 4^{th} tests) formed rathole at 500mm after hammering the bin. The last test (5^{th} test) ratholed without hammering the bin. There was arch formation only at 100mm, 150mm, 200mm, 250mm, 300mm, 350mm, 400mm, 450mm outlet diameters except in the second test where arching and ratholing formed at 450mm and 500mm outlets respectively.

The particles exhibit three transitional behaviour: arching, ratholing and discharge at Bed Height 200mm. Though, the discharge (flow) was with small hang-up on the obstruction at 450mm and 500mm outlet diameters. This is similar to woodchips behaviour at the same bed height. In the first, second and third tests, the particles arch at 100mm, 150mm, 200mm, and 250mm outlet diameters and start ratholing at 300mm, 350mm, 400mm, 450mm, and 500mm outlet diameters. In the fourth test, particles start ratholing at 250mm outlet diameter and in the fifth test; ratholing starts at 350mm outlet diameter. All ratholes formation was self-generated (i.e. without bin hammering).

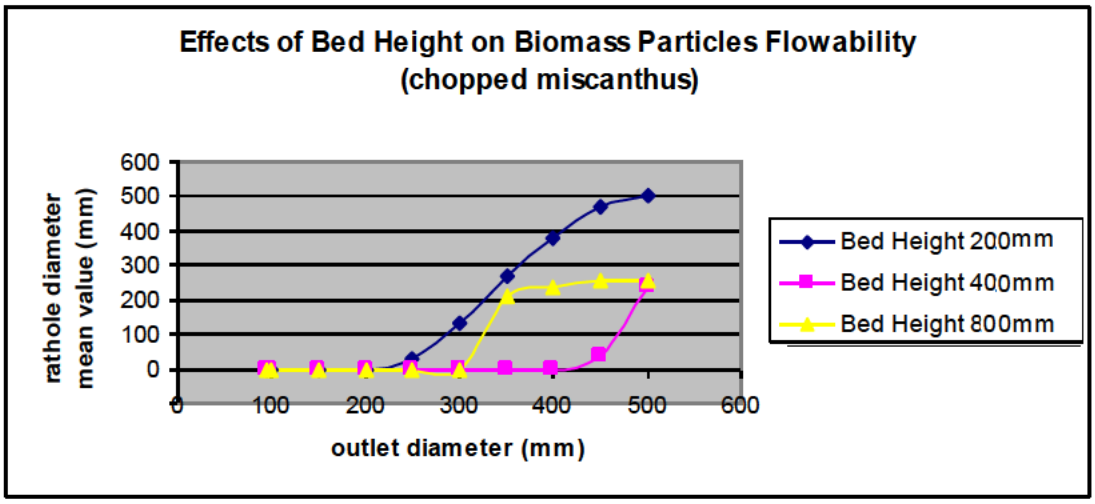

Figure A7: Effects of bed height on flowability of chopped miscanthus

A.4.2 Effects of Bed Height (Head) on the Flowability of Woodchips and Chopped Miscanthus at Core Flow Test Rig B (Second Ring).

A.4.2.1 On Woodchips/hammer milled wood

The filling method was critically looked at during the measurements. The filling methods employed was a mixture of "dump filling" and "dump-filled levelling" methods. Therefore, both bed head and filling effects were studied further. At each bed head, five tests were run. Filling method at each test is alternate to the subsequent tests. Thus, the following observations and results were made.

The first two tests behave in the same manner at bed height 800mm. They were filled with the same method (levelled after dump-filled). Both start ratholing at 500mm outlet diameter (figure A8). The rathole was generated after hammering the bin with rubber hammer. The discharge (flow) was achieved after continuous hammering but with small hang-up on the obstruction. At 400mm outlet diameters, the particles formed mechanical arch/bridge over the entire outlet area. The third test was dump-filled and starts ratholing at 400mm and 500mm outlet diameters. The rathole formation at 400mm outlet diameter was self-generated (i.e. without vibrating the bin with rubber hammer). At 500mm outlet diameter, the rathole was generated after hammering. At 500mm outlet diameter, there was discharge (flow) with small hang-up on the obstruction, which was achieved after continuous hammering the bin/cylinder. The fourth test behaves similar to the third test by ratholing at 400mm

and 500mm outlet diameters. The key difference is that, during the fourth test all the ratholes formed were self-generated (without hammering the bin). Also, there was discharge without hammering but with small hang-up on the obstruction at 400mm and 500mm outlet diameters. The fifth test behaves similar with the first two tests but with different filling method. The bin was dump-filled in the fifth test. It ratholes after hammering the bin at 500mm outlet diameter. There was discharge with small hang-up on the obstruction after continuous hammering the bin. Mechanical arch was formed at 400mm outlet diameters. The common link among the five tests is that all formed mechanical arch at 400mm outlet diameter, all rathole and discharge erratically at 500mm outlet diameter. Generally, "At Bed Height 800mm" it can be inferred that filling method has effect on the flowability of woodchips: when the bin was dump-filled in the third and fourth tests, rathole was formed at 400mm outlet diameters whereas it did not rathole at 400mm outlet diameter in the first two tests when the particles was levelled after dump-filled in the bin.

The first three tests were filled by "dump-filled levelling" method while the last two tests were filled by "dump-filled" method at bed height 400mm. All the five tests generate ratholes. At 400mm outlet diameter, all ratholes formed without hammering the bin. At 500mm outlet diameter, the ratholes formed after bin hammering. In the first test, there was no discharge (flow/failure) at 400mm outlet diameters. The particles only arch and later rathole without bin hammering. At 500mm outlet diameter, there was flow/discharge with small hang-up on the obstruction after continuous bin hammering. In the second test, at 400mm outlet diameter, it rathole and discharge (flow) with big hang-up on the obstruction without bin hammering. At 500mm outlet diameter, it ratholes and discharge with small hang-up on the obstruction after continuous bin hammering. In the third test, the particles behave similarly in the bin with the second test except rathole parameters differences. In the fourth and fifth tests, the particles behave exactly the same in the bin with second and third tests except filling methods and rathole parameters differences. Overall, the particles rathole and flow/discharge out of the bin with small hang-up on the obstruction after continuous bin hammering in all the five tests at 500mm outlet diameter. Filling methods variability at this bed head does not have significant effect on the flow behaviour of the particles.

Particles behave better at bed height 200mm. In all the five tests conducted, all ratholes were self-generated (without hammering the bin) except in the first test at 500mm outlet diameter where further ratholing was generated via bin hammering. There was mixture of discharge/flow with small and big hang-up on the obstruction in all the five tests. No mechanical arching formation in all the tests except ratholing and discharge. The first three tests was "dump-filled levelling" filling method. In the first test, there was flow with small hang-up on the obstruction after continuous bin hammering at 400mm and 500mm outlet diameters respectively. In the second test, the particles behave exactly in the same manner in the bin as in first test with the same rathole parameters (rathole data are repeatable at this stage). In the third test, there was flow with big hang-up on the obstruction without bin hammering at 400mm outlet diameters. At 500mm outlet diameter (third test), there was flow as well but with small hang-up on the obstruction after continuous bin hammering. The last two tests (i.e. 4^{th} and 5^{th} tests) were filled by "dump-filled" filling method. They flow/discharge similarly except rathole parameters which is slightly different. In both tests (4^{th} and 5^{th} tests), at 400mm and 500mm outlet diameters (4^{th} and 5^{th} tests), there was flow/discharge without bin hammering but with small hang-up on the obstruction. This kind of behavioural trait displayed here is better than what experienced in other bed heads and in the first ring. Filling method has significant effect at this bed head. In the last two tests (4^{th} and 5^{th} tests), when the bin was dump-filled, the flow displayed inside the bin was without bin hammering whereas in the first three tests (1^{st}, 2^{nd} and 3^{rd} tests), the flow displayed inside the bin was with a mixture of "before bin hammering and after bin hammering".

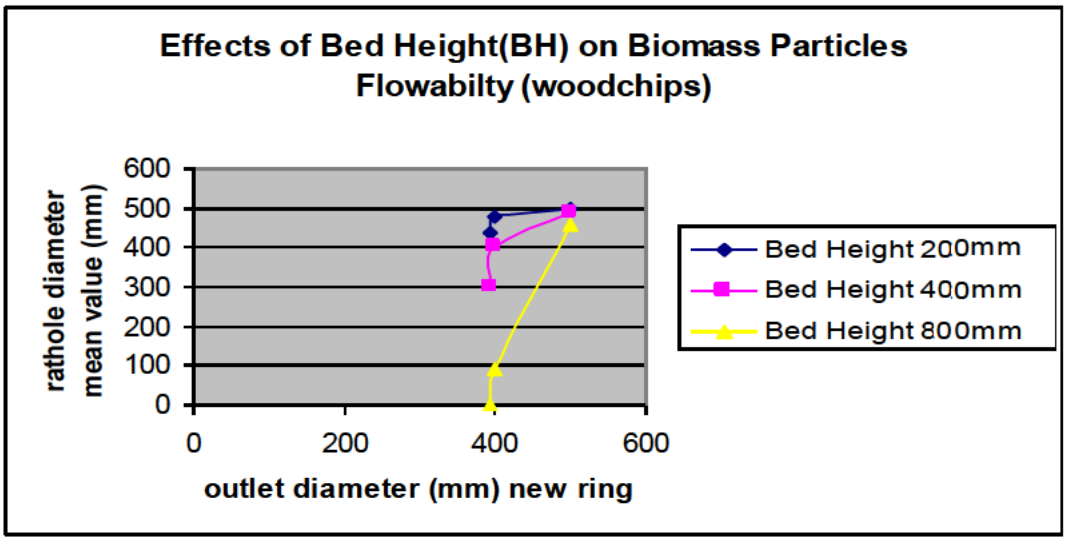

Figure A8: Effects of bed height on flowability of woodchips/hammer milled wood

A.4.2.2 On Chopped Miscanthus

Both bed head (height) and filling methods effects were critically examined as described earlier in woodchips. On the second ring, chopped miscanthus still seems to be more troublesome especially at highest bed head employed. The following observations and results were made at different bed heights with different filling approaches.

In all the five tests conducted at bed height 800mm, there was no rathole and no discharge/flow before bin hammering and after bin hammering. Particles are dead inside the bin. Filling method employed in all the five tests was "dump-filled levelling" method. The only flow phase formation was arching. The reason for this could be higher lateral pressure/stress acting beside particles column formation inside the bin and the higher vertical stress/pressure acting on the particles and the outlet rings.

The first three tests (1st, 2nd and 3rd tests) were filled by "dump-filled levelling" method and last two tests (4th and 5th tests) were filled by "dump-filled" method at bed height 400mm. In the first test, at 400mm and 500mm outlet diameters, the particles rathole in the bin without bin hammering with the same rathole parameters. There was flow with small hang-up on the obstruction between the bin and the outlet after continuous bin hammering. In the second test, the particles did not rathole inside the bin at 400mm outlet diameter. They (particles) only arch and flow with small

hang-up on the obstruction after continuous bin hammering. At 500mm outlet diameter (2nd test), the particles rathole inside the bin after bin hammering and flow with small hang-up on the obstruction after continuous bin hammering. In the third test, the particles behave in the bin exactly the same with the second test except rathole parameters difference at 500mm outlet diameter. Both fourth and fifth tests (4th and 5th tests) behave in the same manner except rathole parameters difference at 500mm outlet diameter. At 400mm outlet diameters (4th and 5th tests), particles only arch without rathole formation and flow with small hang-up on the obstruction after continuous bin hammering. There was rathole formation and flow with small hang-up on the obstruction after continuous bin hammering at 500mm outlet diameter. The effect of bed head is pronounced compared to the results gotten "At 800mm Bed Height". Particles are dead throughout the five tests conducted "At 800mm Bed Height" even after continuous bin hammering. At this bed head (i.e. 400mm Bed Height), particles behave better inside the bin. The three flow phases transition (arch, rathole and discharge) were experienced. Although, the discharge was erratic and unreliable. Variation in filling methods does not have significant effect on the flowability in the five tests. Particles behave similar in the bin when dump-filled and dump-filled levelled.

The particles seems to behave better at bed height 200mm inside the bin in all the five tests conducted because all the ratholes and flow generated were without bin hammering which is a good behavioural trait. Also, rathole data (parameters) are larger than what previously obtained from higher bed heads which is an indication to reliable discharge/flow. The first two tests (1st and 2nd Tests) were dump-filled levelled and behave very similar in the sense that: they rathole at 400mm and 500mm outlet diameters. At 400mm and 500mm outlet diameters (1st and 2nd Tests), the rathole parameters is repeatable and there was flow with small hang-up on the obstruction without bin hammering. In the last three tests (3rd, 4th and 5th tests), the filling method employed was "dump-filled" filling approach. At 400mm and 500mm outlet diameters (3rd, 4th and 5th tests), particles rathole inside the bin without bin hammering.

Also, there was flow with small hang-up on the obstruction without bin hammering.

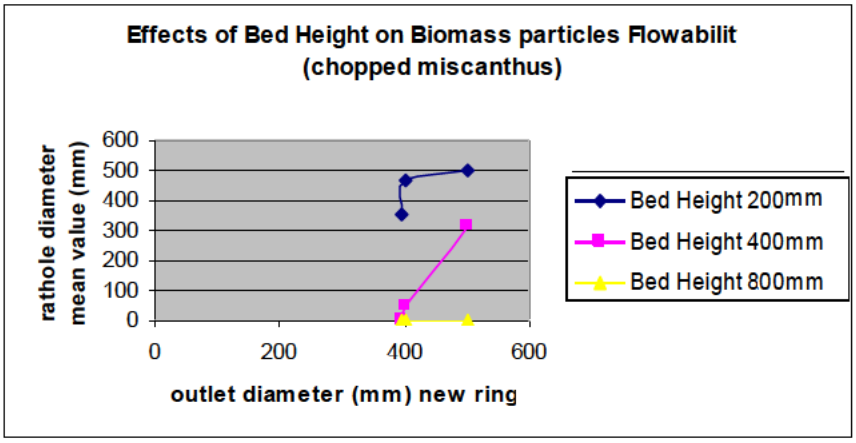

Figure A9: Effects of bed height on flowability of chopped miscanthus

A.4.3 Flow or No Flow Criteria on Core Flow Test Rig (First and Second Rings)

Part of the objectives of the project is to achieve a reliable flow (discharge). Reliable flow means: having all the particles out of the bin without small or big hang-up on the obstruction inside the bin/silo. Also, without bin hammering (i.e. without bashing the bin with hammer or poking the particle bed) before the particles will discharge.

The flow or no flow criteria was developed to assess and validate the experimental outputs. As a result of this, Percentage (%) Flow Weighting Analysis was employed to do the flow or no flow criteria on woodchips and chopped miscanthus. In both tests conducted on the first and second rings for the core flow test, it was observed that reliable flow has not been achieved on the two extreme shape materials. This is reflected in figure below. Percentage (%) Flow Weighting Analysis is done on the first and second rings for chopped miscanthus and woodchips was 0% Flow (figures below). It means that no reliable flow was achieved.

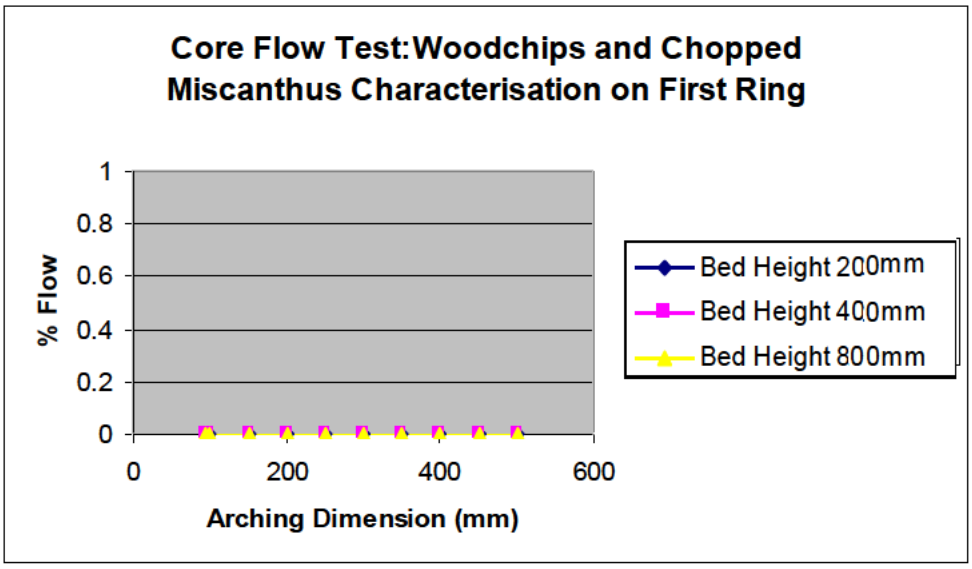

Figure A10: Flow/No Flow Criteria using Percentage (%) Flow Weighting Analysis on first ring

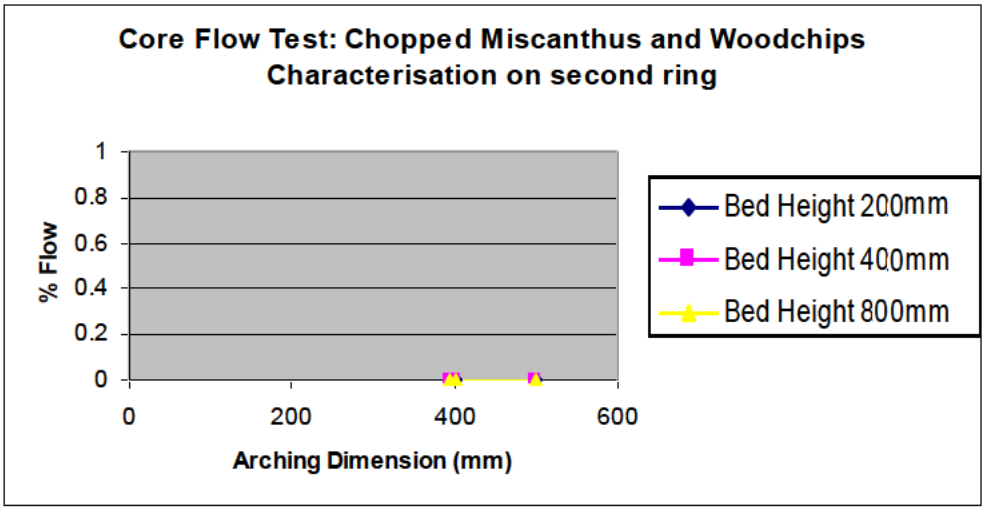

Figure A11: Flow/No Flow Criteria using Percentage (%) Flow Weighting Analysis on second ring

A.4.3.1 Conclusion

In both rings employed to characterise the extreme shape materials at the core flow test rig, it can be inferred that rathole formation with high parameters is an indication that the materials will flow/discharge. This agrees with the fact that: the lower the bed height, the higher the rathole parameters and the better the chance that the particles will flow reliably. This is clearly demonstrated by the figures below. In both rings, woodchips behaves better than chopped miscanthus. Physically, both extreme shape materials look alike but they behave differently inside the bin. This means that

extreme shape materials cannot be characterised based on physical characteristics alone. Both rings exhibit extreme shape materials flow phase transition which are arching, ratholing and discharge.

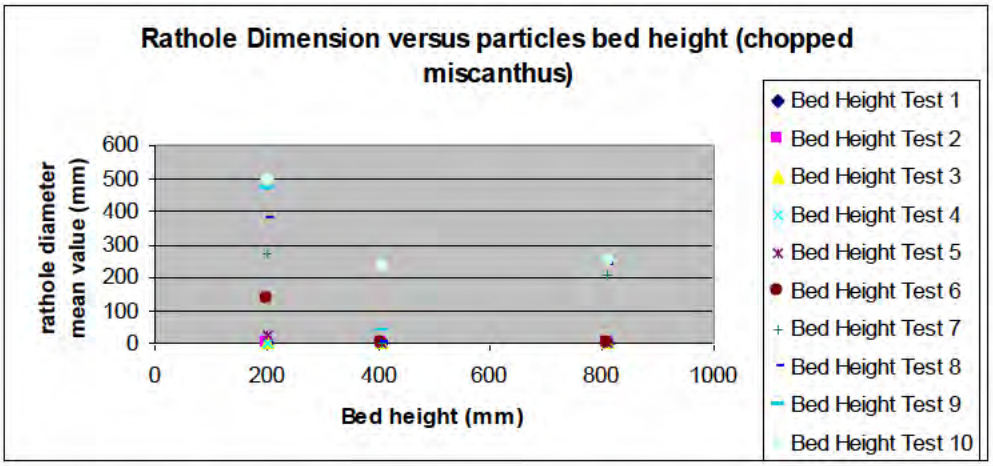

Figure A12: Effect of first ring on bed height and rathole parameters of chopped miscanthus at 200mm bed height, 400mm bed height and 800mm bed height.

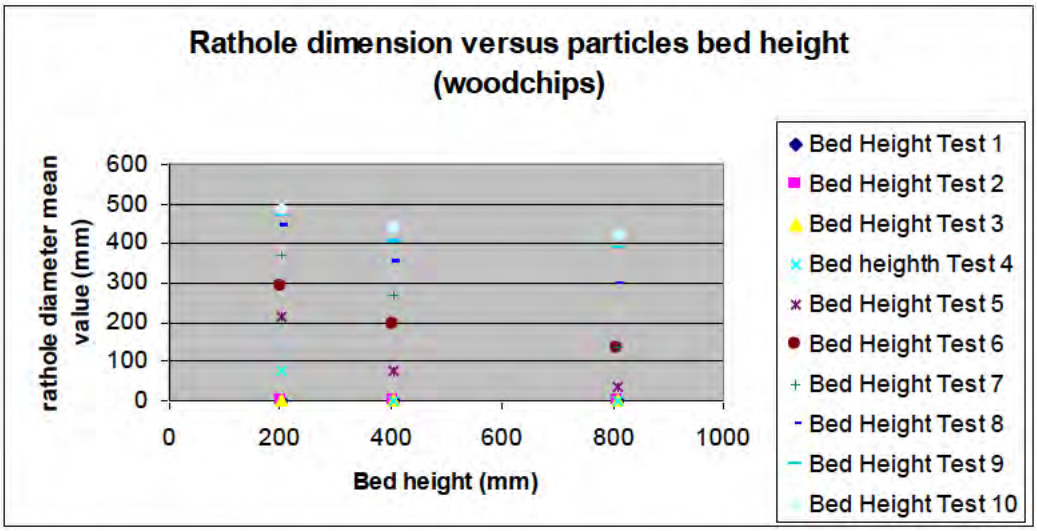

Figure A13: Effect of first ring on bed height and rathole parameters of woodchips/hammer milled wood at 200mm bed height, 400mm bed height and 800mm bed height.

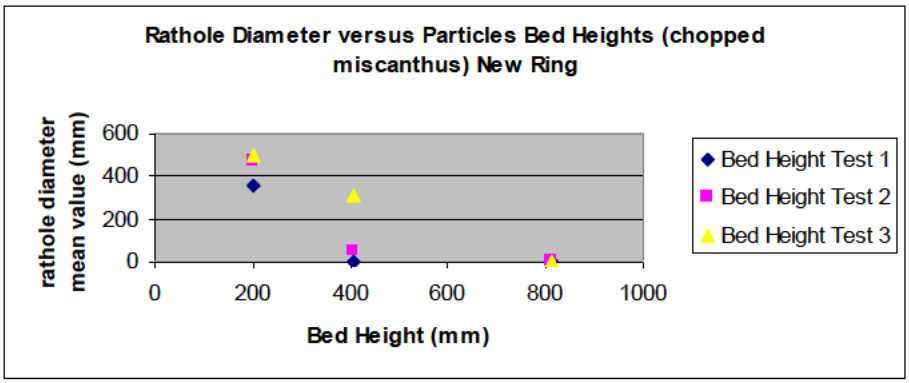

Figure A14: Effect of second ring on bed height and rathole parameters of chopped miscanthus at 200mm bed height, 400mm bed height and 800mm bed height.

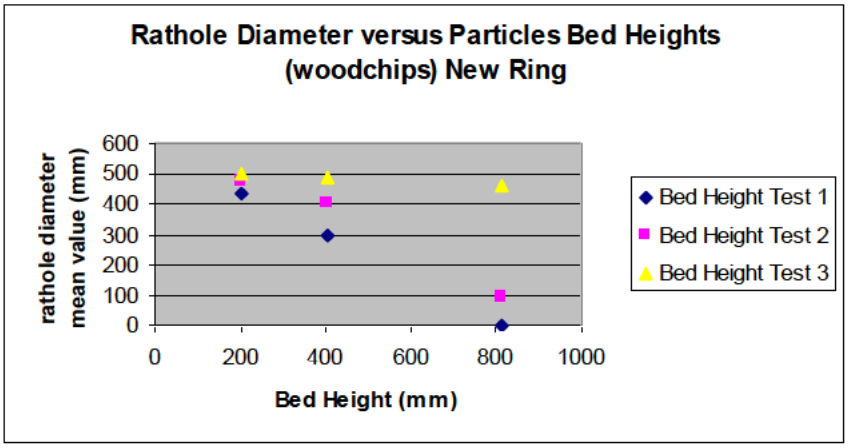

Figure A15: Effect of second ring on bed height and rathole parameters of woodchips/hammer milled wood at 200mm bed height, 400mm bed height and 800mm bed height.

A.4.4 Mass Flow Test

A.4.4.1 On Woodchips at Outlet Dimension100mmWidth:600mmLength

Woodchips seem to be less troublesome than chopped miscanthus at slot dimension 100mm width and 600mm length. There behavioural traits (woodchips and chopped miscanthus) are significantly different at different bed heads. The following observations and results were recorded at each bed heads. The steep/wall angle was 20º.

The test was conducted five times when the particles were at bed height 400mm. In the first and fifth tests, materials flow/discharge reliably without arching and ratholing

in the hopper. No hopper/bin hammering. This is the desired behaviour that the research project targeted at. In the second, third and fourth tests, materials flow without hopper hammering but with small hang-up in the hopper (figure A17). No rathole and arch formations in the bin. In the third test, the small hang-up was on the both sides of the hopper (figure A16).

Figure A16: Flow with small hang-ups on both sides of the hopper (Unreliable discharge)

Figure A17: Flow with hang-ups inside the hopper (Unreliable discharge)

The materials behave in the same manner in all the five tests conducted at bed height 600mm. No rathole and arch formations. The materials flow with small hang-up in the hopper. This type of flow is undesired.

In the first test, the particles flow/discharge reliably without arching and ratholing at bed height 800mm. In the second and fifth tests, the particles behave in the same manner: no arching and ratholing. They (particles) flow unreliably because there was small hang-up inside the hopper. In the third test, the particles formed long span mechanical arch without ratholing. There was flow after continuous hopper hammering. In the fourth test, the particles starting arching and later rathole without reliable discharge. The rathole generated without hopper hammering. There was

discharge/flow after continuous hopper hammering. This is undesired behavioural trait.

Figure A18: Flow with rathole inside the hopper (Unreliable discharge)

Figure A19: Flow with mechanical arch above hopper outlet (Unreliable discharge)

In the first test at bed height 1200mm, the particles flow/discharge with small hang-up inside the hopper without rathole and mechanical arch formation (figure A19). Both second and third tests behave exactly the same: particles flow after small hopper hammering. There was mechanical arch formation without rathole formation. In the fourth test, the particles arch and rathole inside the hopper without hopper hammering. The particles flow unreliably because there was flow/discharge after small hammering on the hopper. In the fifth test, the particles arch and rathole after hammering the hopper with rubber hammer. There was flow/discharge after small hammering on the hopper. Rathole parameters in fourth and fifth tests are 390mm and 240mm respectively and are significantly different.

A.4.4.2 <u>On Chopped Miscanthus at Outlet Dimension 100mmWidth:600Length.</u>

Chopped Miscanthus seems to be more troublesome because of the characteristics it displayed inside the hopper at 100mm width: 600mm length outlet dimension and various bed heads. The wall/steep angle was set up at 20º.

Particles behave exactly the same inside the hopper in all the five tests conducted at bed height 400mm. Before and after hammering the hopper with rubber hammer, long span mechanical arch was formed without particles ratholing and discharging. Hopper was emptied by continuous poking the particles bed head with "sweeper brush rod" and continuous hopper hammering. The particles were dead inside the hopper. At other bed heights (i.e.600, 800 and 1200mm) particles behave exactly the same as in bed height 400mm.

A.4.4.3 <u>On Woodchips at Outlet Dimension 150mmWidth:600mmLength.</u>

Woodchips behave more reliably at 150mmW:600mmL than at 100mmW:600mmL. The particles discharge reliably nearly in all the four bed heads except at 1220mm bed head where particles discharge reliably and unreliably. The steep/wall angle was 20º.
In all the five tests conducted at bed height 400mm, the particles discharge reliably. There was no arch and rathole formation. The particles discharge under gravity. The first, third, fourth and fifth tests behave exactly the same at bed height 600mm: the particles discharge reliably. No arch and rathole formation. In the second test, there was unreliable discharge because the discharge/flow was with small particles hang-up inside the hopper. No rathole and arch formation. At bed height 800mm, the particles behave exactly the same as in bed height 400mm. There was reliable discharge, no rathole and no arch in all the five tests conducted.

First, fourth and fifth tests at bed height 1200mm all behave in the same manner as in bed height 800mm. There was reliable discharge, no rathole and no arch. In the second test, the particles flow with small particles hang-up inside the hopper. No rathole and arch formation. In the third test, there was no flow, no rathole but there was large span mechanical arch. After continuous hopper hammering, there was erratic flow. It was erratic because the flow was with big sum of particles hang-up inside the hopper as shown in the figure A20 below.

Figure A20: Flow with hang-up inside the hopper (Unreliable discharge)

A.4.4.4 <u>On Chopped Miscanthus at Outlet Dimension 150mmWidth:600mmLength</u>

Chopped Miscanthus seems to be troublesome compared to results obtained for woodchips at the same outlet dimension. The following observations were made at different bed heads. The steep/wall angle was 20º.

In the first, second, third and fifth tests at bed height 400mm, the particles were dead inside the hopper; a large span mechanical arch was formed over the entire outlet. There was no rathole and no flow even after hopper hammering. The hopper was drained by poking the particles bed with "sweeper brush rod" continuously coupled with hopper hammering. In the fourth test, particles did not rathole but there was discharge/flow. The flow was with small particles hang-up inside the hopper which makes the flow to be erratic.

In the first three tests at bed height 600mm, the particles behave exactly inside the hopper: no rathole formation, there was flow with small particles hang-up inside the hopper. In the last two tests, the particles were dead inside the hopper; a large span mechanical arch was formed over the entire outlet. There was no rathole and no flow even after hopper hammering. The hopper was drained by poking the particles bed with "sweeper brush rod" continuously coupled with hopper hammering.

In all the five tests conducted at bed height 800mm and 1200mm, the particles were dead inside the hopper; a large span mechanical arch was formed over the entire outlet. There was no rathole and no flow even after hopper vibration. The hopper was drained by poking the particles bed with "sweeper brush rod" continuously coupled with hopper hammering. This kind of behavioural trait is undesired.

A.4.4.5 On Woodchips at Outlet Dimension 200mmWidth:600mmLength

Woodchips behave extremely better at this outlet dimension. There was reliable discharge in all the 20 tests conducted at different bed heads. The results are reproducible. No arch and rathole formations. Gravity flow was experienced.

A.4.4.6 On Chopped Miscanthus at Outlet Dimension 200mmWidth:600mmLength

Chopped Miscanthus displayed its consistent and repeatable behavioural trait at this outlet dimension which is troublesome. The following observations were made at different bed heads: There was reliable discharge in all the five tests conducted. No arch and rathole formations at bed height 400mm.

In the first test at bed height 600mm, the particles flow but with small hang-up at one side of the hopper. This is categorised as unreliable discharge. There were no arch and rathole formations. In the second test, particles flow reliably. There were no arch and rathole formations. In the third and fourth tests, particles flow unreliably because there was half discharge and half hang-up inside the hopper. There were no arch and rathole formations. In the last test, there was flow with small particles hang-up inside the hopper. The hang-up discharge after approximately 2 minutes. No arch and rathole formations. In the first two tests conducted at bed height 800mm, there was reliable discharge. No arch and rathole formations. In the third test, particles did not rathole and flow partially (i.e. flow with hang-up inside the hopper). In the fourth test, particles rathole after hopper hammering and later discharge/flow without any hang-up inside the hopper. In the last test ($5^{th\ test}$), particles discharge reliably. No arch and rathole formations.

All the five tests conducted at bed height 1200mm behave in the same manner: Particles were dead inside the hopper. Large span mechanical arch was formed over the entire outlet area. There were rathole formations without hopper hammering. Rathole parameters were not reproducible in all the five tests. It was only reproducible at 4^{th} and 5^{th} tests.Rathole parameters at each test are: 390mm, 300mm, 340mm and 320mm.

A.4.5 Flow or No Flow Criteria on Mass Flow Test Rig.

Flow or no flow criteria is established to categorise the reliability of particles discharge out of the bin. Based on this project, extreme shape materials are categorise as flow when all the particles discharge out of the bin without any particle retain inside the hopper and also without any bin hammering or particles bed poking. As a result of this, Percentage (%) Flow Weighting Analysis was developed to know the amount of reliable and unreliable discharge.

- **Percentage Flow Weighting Analysis on Woodchips**
    - **At Outlet Dimension 100Width:600Length**: When the test was conducted at Bed Height 400mm, it was 40% of the test (i.e.2 out of 5 tests) that flow reliably. Other 60% of the tests were unreliable. At Bed Height 600mm, there was 100% flow. No unreliable flow. At Bed Height 800mm, there was 20% flow and 80% unreliable flow. At Bed Height 1200mm, there was no reliable flow.
    - **At Outlet Dimension 150Width:600Length**: At Bed Height 400mm, there was 100% flow. No unreliable flow was experienced. At Bed Height 600mm, there was 80% flow and 20% unreliable flow. At Bed Height 800mm, there was 100% flow. No unreliable flow was experienced. At Bed Height 1200mm, there was 60% flow and 40% unreliable flow.
    - **At Outlet Dimension 200Width:600Length**: In all the 4 bed heads employed, there was 100% flow. All reflected in the figure A21 below.

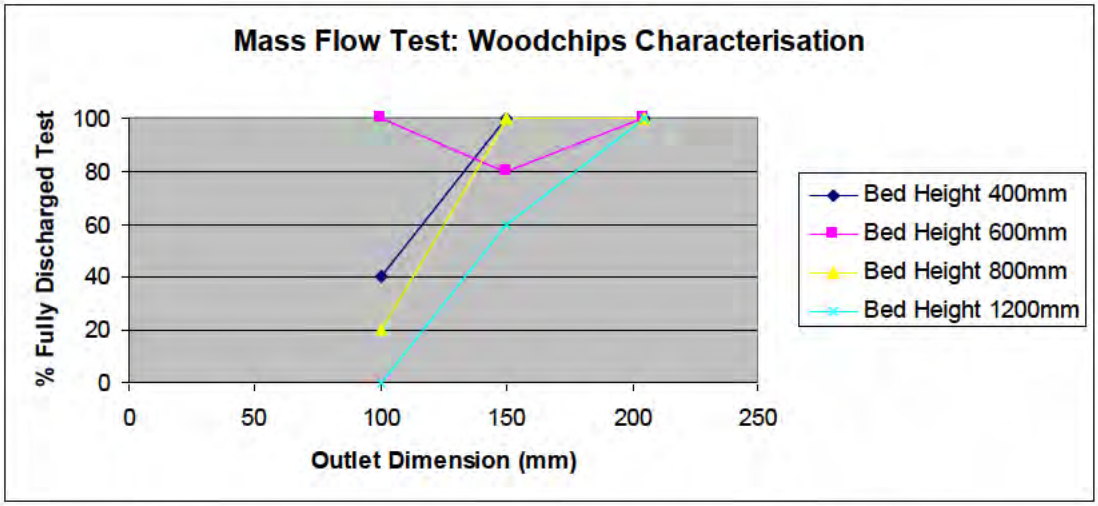

Figure A21: Flow/No Flow Criteria using Percentage Flow Weighting Analysis on Woodchips.

- **Percentage Flow Weighting Analysis on Chopped Miscanthus:**
    - **At Outlet Dimension 100Width:600Length**: In all the four bed heads employed (i.e. 400mm, 600mm, 800mm and 1200mm), there was no flow at all (i.e. 0%).
    - **At Outlet Dimension 150Width:600Length**: Ditto to "At Outlet Dimension 100Width:600Length".
    - **At Outlet Dimension 200Width:600Length**: At Bed Height 400mm, there was 100% flow. At Bed Height 600mm, there was 20% flow and 80% unreliable flow. At Bed Height 800mm, there was 40% flow and 60% unreliable flow. At Bed Height 1200mm, there was no flow at all. All reflected in the figure A22 below.

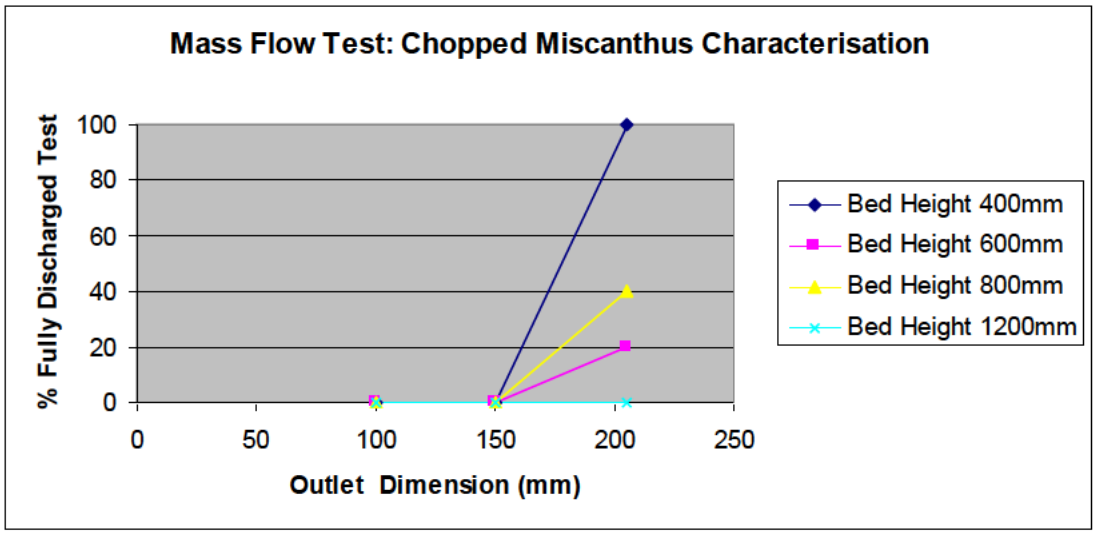

Figure A22: Flow/No Flow Criteria using Percentage Flow Weighting Analysis on Chopped Miscanthus.

A.4.5.1 Conclusions

Visual characterisation technique alone cannot give holistic flow data about extreme shape materials. Woodchips and chopped miscanthus look alike physically but they behave totally different inside the hopper. Bed head and filling have effect on the flowability of the two extreme shape materials employed but it is more significant at different bed heads and outlet dimensions. Both particles displayed the three flow phase transitions which are arching, ratholing and discharge. Overall, the lower the bed head, the higher the chance for reliable discharge.

A.4.6 Shear Tester

A.4.6.1 On Conventional Powders

The following 2 conventional powders were tested on the Powder Flow Tester: Granulated Sugar (VanGilse Holland) and Sodium Bicarbonate. The results show that granulated sugar is a free flowing particle while sodium carbonate is easy flowing inside conical hopper shape. At higher consolidation stress, granulated sugar developed insignificant failure strength while sodium carbonate failure strength increases with increase in consolidation stress. Thus, granulated sugar is more compressible than sodium carbonate. That is, the self-weight (bulk density) of granulated sugar is larger than the bulk density of sodium carbonate. The effective angle of internal friction of the two powders nearly level off and is quiet low to the values of the extreme shape materials employed for this test (woodchips and chopped

miscanthus). Based on this attributes that characterised with the powders, it shows that the two powders will flow reliably inside the conical hopper but granulated will likely behave better than sodium carbonate. This is illustrated in figures below.

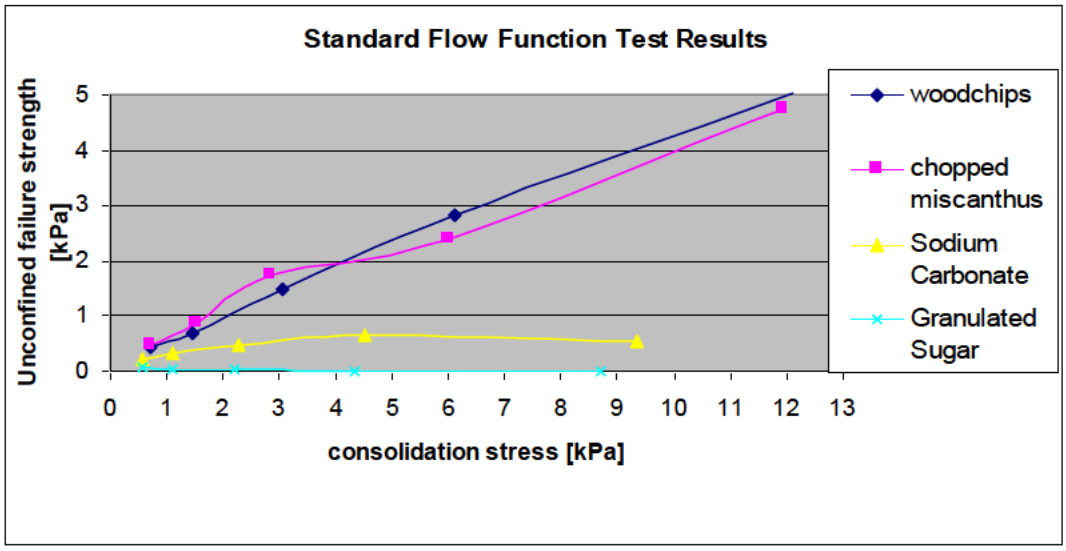

Figure A23: Comparative Test Analysis (Standard Flow Function Results)

A.4.6.2 On Extreme Shape Materials

The following 2 extreme shape materials were tested on the Powder Flow Tester: Woodchips and Chopped Miscanthus. Both extreme shape materials nearly behave in the same manner. Both particles have very low self-weight (bulk density). It means that they are less compressible. This is one of the factors that make them difficult to be transported over a long distance and difficult to be discharged from the silo (unreliable flow). Based on the results and Powder Flow Tester Flow criteria, the two particles are likely to be cohesive but woodchips is more cohesive. Their failure strengths increase with increase in consolidation stress but they did not shear properly because the particles are not spherical and also not even in shape. The more force (stress) put behind them (extreme shape materials), the more difficult for them to discharge reliably from the storage and the higher the internal friction. This was experienced during the mass and core flow tests especially when particles were dead inside the silo. Silo vibration with rubber hammer makes them to be more troublesome. Most of the times, particles bed need to be poked several times with wooden rod to drain the silo. They (materials) are needle-like, flat and springy which account for their entanglement and high effective angle of internal friction as compared to conventional powders. This could be correlated to the column test

technique and tensile test technique, where column height failure and tensile strength are function of particle aspect ratio and shape.

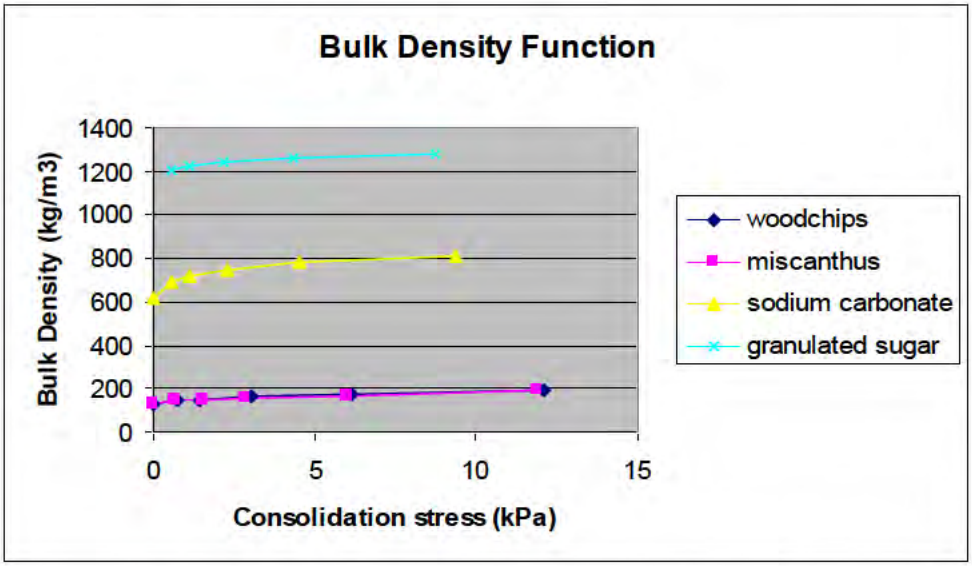

Figure A24: Comparative Test Analysis (Standard Flow Function Results: Bulk Density Curve)

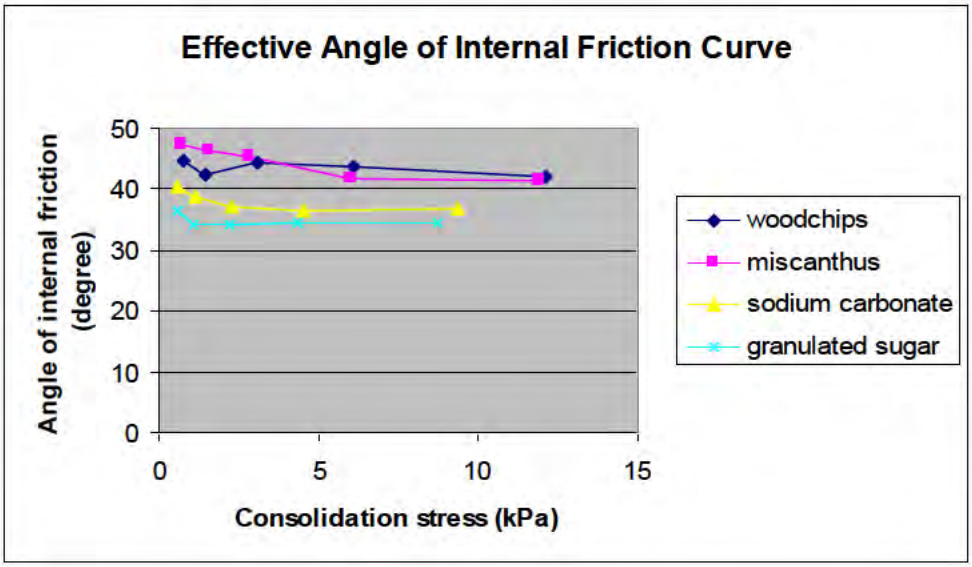

Figure A25: Comparative Test Analysis (Standard Flow Function Results: Effective Angle of Internal Friction Curve)

A.4.6.3 Conclusion

Wolfson-Brookfield Powder flow tester is versatile on particulate materials especially with particles of many fines (powder). It (Powder flow tester) can also be employed for the standard flow function test of Wolfson Class 1 (free flowing without extreme particle shape e.g. Wheatfeed pellets, a cereal coproduct*)* and Class 2 (cohesive without extreme particle shape e.g. milled nuts*)* of biomass and waste materials but the pitfall is with Wolfson Class 3 (materials with extreme particle shape e.g. woodchips, chopped miscanthus, saw dust*)* materials because of their entanglement (interlocking) character (Bradley et al, 2004). The pitfall of Powder flow tester with Wolfson Class 3 materials had been established with the comparative test conducted on the tester. Further research on Wolfson Class 3 materials has delivered promising various flow/failure techniques like: Column Tester, Core Flow Test, Tensile Test Technique, Uniaxial tester and Mass Flow Test.

Table Appendix (A) for Core Flow Test

Core Flow Test: Effects of particles bed height on the flowability of biomass particles.

Experiment Title: Core Flow Test: Biomass Particles Bed Height Variation and Filling (levelling with hands after dumping the particles inside the cylinder)…….....

Test Date: 20-01-2010……

Test Material: Dry…Woodchips/hammer milled wood …….

Bed Height: 200mm…….

OD(mm)	95	100	150	200	250	300	350	400	450	500
RHD(mm)	No	No	No	150	250	300	380	430	440	470
F/NF	NF	NF	NF	NF	NF	NF	NF	NF	NF	Flow but with small hang-up on the obstruction

OD(mm)	95	100	150	200	250	300	350	400	450	500
RHD(mm)	No	No	No	50	200	240	370	440	470	490
F/NF	NF	NF	NF	NF	NF	NF	NF	NF	NF	Flow but with small hang-up on the obstruction

OD(mm)	95	100	150	200	250	300	350	400	450	500
RHD(mm)	No	No	No	80	140	330	330	440	480	490
F/NF	NF	NF	NF	NF	NF	NF	NF	NF	NF	Flow but with small hang-up on the obstruction

OD(mm)	95	100	150	200	250	300	350	400	450	500
RHD(mm)	No	No	No	15	250	260	360	450	470	480
F/NF	NF	NF	NF	NF	NF	NF	NF	NF	NF	Flow but with small hang-up on the obstruction

OD(mm)	95	100	150	200	250	300	350	400	450	500
RHD(mm)	No	No	No	80	230	310	410	440	490	500
F/NF	NF	NF	NF	NF	NF	NF	NF	NF	NF	Flow but with small hang-up on the obstruction

Note:
OD = Outlet Diameter
RHD = Rathole Diameter
F/NF = Flow or No Flow Criteria

Experiment Title:…… Core Flow Test: Biomass Particles Bed Height Variation and Filling (Levelling with hands after dumping the particles inside the cylinder)……....

Test Date: 20-01-2010……

Test Material: Dry Woodchips/hammer milled wood…….

Bed Height: 400mm…….

OD(mm)	95	100	150	200	250	300	350	400	450	500
RHD(mm)	No	No	No	No	200	230	280	350	400	500
F/NF	NF	NF	NF	NF	NF	NF	NF	NF	NF	Flow but with large hang-up on the obstruction

OD(mm)	95	100	150	200	250	300	350	400	450	500
RHD(mm)	No	No	No	No	180	200	290	380	470	500
F/NF	NF	NF	NF	NF	NF	NF	NF	NF	NF	Flow but with large hang-up on the obstruction

OD(mm)	95	100	150	200	250	300	350	400	450	500
RHD(mm)	No	No	No	No	No	200	240	300	320	340
F/NF	NF	NF	NF	NF	NF	NF	NF	NF	NF	NF

OD(mm)	95	100	150	200	250	300	350	400	450	500
RHD(mm)	No	No	No	No	No	230	340	390	440	480
F/NF	NF	NF	NF	NF	NF	NF	NF	NF	NF	Flow but with large hang-up on the obstruction

OD(mm)	95	100	150	200	250	300	350	400	450	500
RHD(mm)	No	No	No	No	No	105	210	330	380	390
F/NF	NF	NF	NF	NF	NF	NF	NF	NF	NF	NF

Note:
OD = Outlet Diameter
RHD = Rathole Diameter
F/NF = Flow or No Flow Criteria

NOTE:
Core Flow Test: All ratholes generated without bin hammering (i.e. without bashing the cylinder/hopper) except at bed height 810mm.

Experiment Title: Core Flow Test @ Bed Height 810mm with Dump Filling method…….....

Test Date: 21-01-2010……

Test Material: Dry woodchips/hammer milled wood…….

Bed Height: 800mm…….

OD(mm)	95	100	150	200	250	300	350	400	450	500
RHD(mm)	0	0	0	0	170	175	200	355	360	380
F/NF	NF	NF	NF	NF	NF	NF	NF	NF	NF	NF

OD(mm)	95	100	150	200	250	300	350	400	450	500
RHD(mm)	0	0	0	0	0	115	120	125	300	350
F/NF	NF	NF	NF	NF	NF	NF	NF	NF	NF	NF

OD(mm)	95	100	150	200	250	300	350	400	450	500
RHD(mm)	0	0	0	0	0	120	125	330	380	450
F/NF	NF	NF	NF	NF	NF	NF	NF	NF	NF	NF

OD(mm)	95	100	150	200	250	300	350	400	450	500
RHD(mm)	0	0	0	0	0	120	125	330	440	470
F/NF	NF	NF	NF	NF	NF	NF	NF	NF	NF	NF

OD(mm)	95	100	150	200	250	300	350	400	450	500
RHD(mm)	0	0	0	0	0	120	125	330	440	470
F/NF	NF	NF	NF	NF	NF	NF	NF	NF	NF	NF

Note:
OD = Outlet Diameter
RHD = Rathole Diameter
F/NF = Flow or No Flow Criteria

NOTE:
All ratholes were generated after bin hammering (i.e. after bashing the cylinder/silo/barrel)

Experiment Title: Core Flow Test: Bed Height Variation and filling (levelling with hands after dumping the particles inside the cylinder)…….....

Test Date: 21 -01- 2010……

Test Material: Chopped Miscanthus…….

Bed Height: 200mm…….

OD(mm)	95	100	150	200	250	300	350	400	450	500
RHD(mm)	0	0	0	0	0	160	180	310	460	500
F/NF	NF	NF	NF	NF	NF	NF	NF	NF	Flow with small hang-up on the obstruction	Flow with small hang-up on the obstruction

OD(mm)	95	100	150	200	250	300	350	400	450	500
RHD(mm)	0	0	0	0	0	230	330	390	460	500
F/NF	NF	NF	NF	NF	NF	NF	NF	NF	Flow with small hang-up on the obstruction	Flow with small hang-up on the obstruction

OD(mm)	95	100	150	200	250	300	350	400	450	500
RHD(mm)	0	0	0	0	0	70	330	380	460	500
F/NF	NF	NF	NF	NF	NF	NF	NF	NF	Flow with small hang-up on the obstruction	Flow with small hang-up on the obstruction

OD(mm)	95	100	150	200	250	300	350	400	450	500
RHD(mm)	0	0	0	0	135	200	240	380	480	500
F/NF	NF	NF	NF	NF	NF	NF	NF	NF	Flow with small hang-up on the obstruction	Flow with small hang-up on the obstruction

OD(mm)	95	100	150	200	250	300	350	400	450	500
RHD(mm)	0	0	0	0	0	0	280	430	480	500
F/NF	NF	NF	NF	NF	NF	NF	NF	NF	Flow with small hang-up on the obstruction	Flow with small hang-up on the obstruction

Note:
OD = Outlet Diameter
RHD = Rathole Diameter
F/NF = Flow or No Flow Criteria

NOTE:
Core Flow Test: All ratholes generated without bashing the storage vessel with hammer.

Experiment Title: Core Flow Test: Bed Height variation and filling (levelling with hands after dumping the particles inside the cylinder)…….....

Test Date: 21-01-2010……

Test Material: Chopped Miscanthus…….

Bed Height: 400mm…….

OD(mm)	95	100	150	200	250	300	350	400	450	500
RHD(mm)	0	0	0	0	0	0	0	0	0	250: after bin hammering
F/NF	NF	NF	NF	NF	NF	NF	NF	NF	NF	NF

OD(mm)	95	100	150	200	250	300	350	400	450	500
RHD(mm)	0	0	0	0	0	0	0	0	190: without bin hammering	200: without bin hammering
F/NF	NF	NF	NF	NF	NF	NF	NF	NF	NF	NF

OD(mm)	95	100	150	200	250	300	350	400	450	500
RHD(mm)	0	0	0	0	0	0	0	0	0	240: after bin hammering
F/NF	NF	NF	NF	NF	NF	NF	NF	NF	NF	NF

OD(mm)	95	100	150	200	250	300	350	400	450	500
RHD(mm)	0	0	0	0	0	0	0	0	0	260: after bin hammering
F/NF	NF	NF	NF	NF	NF	NF	NF	NF	NF	NF

OD(mm)	95	100	150	200	250	300	350	400	450	500
RHD(mm)	0	0	0	0	0	0	0	0	0	220: without bin hammering
F/NF	NF	NF	NF	NF	NF	NF	NF	NF	NF	NF

Note:
OD = Outlet Diameter
RHD = Rathole Diameter
F/NF = Flow or No Flow Criteria

Experiment Title: Core Flow Test @ Bed Height 810mm with dump filling method…….....

Test Material: Chopped Miscanthus…….

Bed Height: 800mm…….

OD(mm)	95	100	150	200	250	300	350	400	450	500
RHD(mm)	0	0	0	0	0	0	210	240	260	260
F/NF	NF	NF	NF	NF	NF	NF	NF	NF	NF	NF

OD(mm)	95	100	150	200	250	300	350	400	450	500
RHD(mm)	0	0	0	0	0	0	200	230	240	240
F/NF	NF	NF	NF	NF	NF	NF	NF	NF	NF	NF

OD(mm)	95	100	150	200	250	300	350	400	450	500
RHD(mm)	0	0	0	0	0	0	200	230	240	24
F/NF	NF	NF	NF	NF	NF	NF	NF	NF	NF	NF

OD(mm)	95	100	150	200	250	300	350	400	450	500
RHD(mm)	0	0	0	0	0	0	220	240	270	270
F/NF	NF	NF	NF	NF	NF	NF	NF	NF	NF	NF

OD(mm)	95	100	150	200	250	300	350	400	450	500
RHD(mm)	0	0	0	0	0	0	210	230	270	270
F/NF	NF	NF	NF	NF	NF	NF	NF	NF	NF	NF

Note:
OD = Outlet Diameter
RHD = Rathole Diameter
F/NF = Flow or No Flow Criteria

NOTE:
All ratholes were generated after bashing the storage vessel with hammer.

Experiment Title: Core flow test with New Rings (Height Variations on Flowability)
Test Material: Chopped Miscanthus
Bed Height: 200mm
Test Date: 04/02/2010

OD (mm)	394	400	500
RHD (mm)	370 WH	470 WH	500 WH
F/NF	NF	FWC	FWC

Filling method: Levelled after dump-filled

OD (mm)	394	400	500
RHD (mm)	250 WH	470 WH	500 WH
F/NF	NF	FWC	FWC

Filling method: Levelled after dump-filled

OD (mm)	394	400	500
RHD (mm)	390 WH	470 WH	500 WH
F/NF	NF	FWC	FWC

Filling method: Dump-filled

OD (mm)	394	400	500
RHD (mm)	360 WH	470 WH	500 WH
F/NF	NF	FWC	FWC

Filling method: Dump-filled

OD (mm)	394	400	500
RHD (mm)	390 WH	470 WH	500 WH
F/NF	NF	FWC	FWC

Filling method: Dump-filled

Note:
OD = Outlet Diameter
RHD = Rathole Diameter
F/NF = Flow or No Flow Criteria
FWC = Flow with Cliffs
WH = without hammering the storage vessel

Experiment Title: Core flow test with New Rings (Height Variations on Flowability)
Test Material: Chopped Miscanthus
Bed Height: 400mm
Test Date: 03/02/2010

OD (mm)	394	400	500
RHD (mm)	0	250 WH	250 WH
F/NF	NF	NF	NF

Filling method: Levelled after dump-filled

OD (mm)	394	400	500
RHD (mm)	0	0	300 AH
F/NF	NF	NF	NF

Filling method: Levelled after dump-filled

OD (mm)	394	400	500
RHD (mm)	0	0	270 AH
F/NF	NF	NF	NF

Filling method: Levelled after dump-filled

OD (mm)	394	400	500
RHD (mm)	0	0	350 WH
F/NF	NF	NF	NF

Filling method: Dump-filled

OD (mm)	394	400	500
RHD (mm)	0	0	400 WH
F/NF	NF	NF	NF

Filling method: Dump-filled

Note:
OD = Outlet Diameter
RHD = Rathole Diameter
F/NF = Flow or No Flow Criteria
WH = without hammering the storage vessel
AH = after hammering the storage vessel
NF = No flow

Experiment Title: Core flow test with New Rings (Height Variations on Flowability)
Test Material: Chopped Miscanthus
Bed Height: 800mm
Test Date: 03/02/2010

OD (mm)	394	400	500
RHD (mm)	0	0	0
F/NF	NF	NF	NF

Filling method: Levelled after dump-filled

OD (mm)	394	400	500
RHD (mm)	0	0	0
F/NF	NF	NF	NF

Filling method: Levelled after dump-filled

OD (mm)	394	400	500
RHD (mm)	0	0	0
F/NF	NF	NF	NF

Filling method: Levelled after dump-filled

OD (mm)	394	400	500
RHD (mm)	0	0	0
F/NF	NF	NF	NF

Filling method: Levelled after dump-filled

OD (mm)	394	400	500
RHD (mm)	0	0	0
F/NF	NF	NF	NF

Filling method: Levelled after dump-filled

Note:

OD = Outlet Diameter
RHD = Rathole Diameter
F/NF = Flow or No Flow Criteria
NF = No flow

Experiment Title: Core flow test with New Rings (Height Variations on Flowability)
Test Material: Woodchip/ hammer milled wood
Bed Height: 200mm
Test Date: 05-02-2010

OD (mm)	394	400	500
RHD (mm)	450 WH	470 WH	500 AH
F/NF	NF	NF	NF

Filling method: Levelled after dump-filled

OD (mm)	394	400	500
RHD (mm)	450 WH	470 WH	500 WH
F/NF	NF	NF	NF

Filling method: Levelled after dump-filled

OD (mm)	394	400	500
RHD (mm)	440 WH	490 WH	500 WH
F/NF	NF	NF	NF

Filling method: Levelled after dump-filled

OD (mm)	394	400	500
RHD (mm)	440 WH	490 WH	500 WH
F/NF	NF	NF	NF

Filling method: Dump-filled

OD (mm)	394	400	500
RHD (mm)	410 WH	490 WH	500 WH
F/NF	NF	NF	NF

Filling method: Dump-filled

Note:
OD = Outlet Diameter
RHD = Rathole Diameter
F/NF = Flow or No Flow Criteria
WH = without hammering the storage vessel
AH = after hammering the storage vessel
NF = No flow

Experiment Title: Core flow test with New Rings (Height Variations on Flowability)
Test Material: Woodchip/ hammer milled wood
Bed Height: 400mm
Test Date: 04/02/2010

OD (mm)	394	400	500
RHD (mm)	260 WH	340 WH	470 AH
F/NF	NF	NF	NF

Filling method: Levelled after dump-filled

OD (mm)	394	400	500
RHD (mm)	260 WH	400 WH	470 AH
F/NF	NF	NF	NF

Filling method: Levelled after dump-filled

OD (mm)	394	400	500
RHD (mm)	360 WH	420 WH	500 AH
F/NF	NF	NF	NF

Filling method: Levelled after dump-filled

OD (mm)	394	400	500
RHD (mm)	360 WH	420 WH	500 AH
F/NF	NF	NF	NF

Filling method: Dump-filled

OD (mm)	394	400	500
RHD (mm)	250 WH	420 WH	500 AH
F/NF	NF	NF	NF

Filling method: Dump-filled

Note:
OD = Outlet Diameter
RHD = Rathole Diameter
F/NF = Flow or No Flow Criteria
WH = without hammering the storage vessel
AH = after hammering the storage vessel
NF = No flow

Experiment Title: Core flow test with New Rings (Height Variations on Flowability)
Test Material: Woodchip/ hammer milled wood
Bed Height: 800mm
Test Date: 04/02/2010

OD (mm)	394	400	500
RHD (mm)	0	0	420 AH
F/NF	NF	NF	NF

Filling method: Levelled after dump-filled

OD (mm)	394	400	500
RHD (mm)	0	0	470 AH
F/NF	NF	NF	NF

Filling method: Levelled after dump-filled

OD (mm)	394	400	500
RHD (mm)	0	70 WH	470 AH
F/NF	NF	NF	NF

Filling method: Dump-filled

OD (mm)	394	400	500
RHD (mm)	0	380 WH	470 WH
F/NF	NF	NF	NF

Filling method: Dump-filled

OD (mm)	394	400	500
RHD (mm)	0	0	470 AH
F/NF	NF	NF	NF

Filling method: Dump-filled

Note:
OD = Outlet Diameter
RHD = Rathole Diameter
F/NF = Flow or No Flow Criteria
WH = without hammering the storage vessel
AH = after hammering the storage vessel

Result Analysis using percentage weighting approach: Core Flow Test (Woodchips) (1st Ring)

Material	Outlet Diameter (mm)	Bed Height (mm)	% RH (Rathole Formation)	% F (Flow)	%NF (No-flow)
Woodchips	95	200	0	0	100
Woodchips	100	200	0	0	100
Woodchips	150	200	0	0	100
Woodchips	200	200	100	0	100
Woodchips	250	200	100	0	100
Woodchips	300	200	100	0	100
Woodchips	350	200	100	0	100
Woodchips	400	200	100	0	100
Woodchips	450	200	100	0	100
Woodchips	500	200	100	0	100

Material	Outlet Diameter (mm)	Bed Height (mm)	% RH (Rathole Formation)	% F (Flow)	%NF (No-flow)
Woodchips	95	400	0	0	100
Woodchips	100	400	0	0	100
Woodchips	150	400	0	0	100
Woodchips	200	400	0	0	100
Woodchips	250	400	40	0	100
Woodchips	300	400	100	0	100
Woodchips	350	400	100	0	100
Woodchips	400	400	100	0	100
Woodchips	450	400	100	0	100
Woodchips	500	400	100	0	100

Material	Outlet Diameter (mm)	Bed Height (mm)	% RH (Rathole Formation)	% F (Flow)	%NF (No-flow)
Woodchips	95	800	0	0	100
Woodchips	100	800	0	0	100
Woodchips	150	800	0	0	100
Woodchips	200	800	0	0	100
Woodchips	250	800	20	0	100
Woodchips	300	800	100	0	100
Woodchips	350	800	100	0	100
Woodchips	400	800	100	0	100
Woodchips	450	800	100	0	100
Woodchips	500	800	100	0	100

Result Analysis using percentage weighting approach: Core Flow Test (Chopped Miscanthus) (1st Ring)

Material	Outlet Diameter (mm)	Bed Height (mm)	% RH (Rathole Formation)	% F (Flow)	%NF (No-flow)
Chopped Miscanthus	95	200	100	0	100
Chopped Miscanthus	100	200	100	0	100
Chopped Miscanthus	150	200	100	0	100
Chopped Miscanthus	200	200	100	0	100
Chopped Miscanthus	250	200	20	0	100
Chopped Miscanthus	300	200	80	0	100
Chopped Miscanthus	350	200	100	0	100
Chopped Miscanthus	400	200	100	0	100
Chopped Miscanthus	450	200	100	0	100
Chopped Miscanthus	500	200	100	0	100

Material	Outlet Diameter (mm)	Bed Height (mm)	% RH (Rathole Formation)	% F (Flow)	%NF (No-flow)
Chopped Miscanthus	95	400	0	0	100
Chopped Miscanthus	100	400	0	0	100
Chopped Miscanthus	150	400	0	0	100
Chopped Miscanthus	200	400	0	0	100
Chopped Miscanthus	250	400	0	0	100
Chopped Miscanthus	300	400	0	0	100
Chopped Miscanthus	350	400	0	0	100
Chopped Miscanthus	400	400	0	0	100
Chopped Miscanthus	450	400	20	0	100
Chopped Miscanthus	500	400	100	0	100

Material	Outlet Diameter (mm)	Bed Height (mm)	% RH (Rathole Formation)	% F (Flow)	%NF (No-flow)
Chopped Miscanthus	95	800	0	0	100
Chopped Miscanthus	100	800	0	0	100
Chopped Miscanthus	150	800	0	0	100
Chopped Miscanthus	200	800	0	0	100
Chopped Miscanthus	250	800	0	0	100
Chopped Miscanthus	300	800	0	0	100
Chopped Miscanthus	350	800	100	0	100
Chopped Miscanthus	400	800	100	0	100
Chopped Miscanthus	450	800	100	0	100
Chopped Miscanthus	500	800	100	0	100

Result Analysis using percentage weighting approach: Core Flow Test (Chopped Miscanthus) (2nd Ring)

Material	Outlet Diameter (mm)	Bed Height (mm)	% RH (Rathole Formation)	% F (Flow)	%NF (No-flow)
Chopped Miscanthus	394	200	100	0	100
Chopped Miscanthus	400	200	100	0	100
Chopped Miscanthus	500	200	100	0	100
Chopped Miscanthus	394	400	0	0	100
Chopped Miscanthus	400	400	20	0	100
Chopped Miscanthus	500	400	100	0	100
Chopped Miscanthus	394	800	0	0	100
Chopped Miscanthus	400	800	0	0	100
Chopped Miscanthus	500	800	0	0	100

Result Analysis using percentage weighting approach: Core Flow Test (Woodchips/ hammer milled wood) (2nd Ring)

Material	Outlet Diameter (mm)	Bed Height (mm)	% RH (Rathole Formation)	% F (Flow)	%NF (No-flow)
Woodchips	394	200	100	0	100
Woodchips	400	200	100	0	100
Woodchips	500	200	100	0	100
Woodchips	394	400	100	0	100
Woodchips	400	400	100	0	100
Woodchips	500	400	100	0	100
Woodchips	394	800	0	0	100
Woodchips	400	800	40	0	100
Woodchips	500	800	100	0	100

Table Appendix (B) for Mass Flow Test

Mass Flow Test: Effects of bed height (BH) on flowability @ 150mmW:600mmL
Test Material: Woodchips/ hammer milled wood
Test Date: 15022010 & 16022010

Test Run	Bed Height (mm)	Outlet Dimension (mm) (slot)	Rathole Diameter (mm)	Flow/No Flow Criteria
1	400	150W: 600L	0	Flow
2	400	150W: 600L	0	Flow
3	400	150W: 600L	0	Flow
4	400	150W: 600L	0	Flow
5	400	150W: 600L	0	Flow

Table 1: Mass flow test data for woodchips at BH 400mm

Test Run	Bed Height (mm)	Outlet Dimension (mm) (slot)	Rathole Diameter (mm)	Flow/No Flow Criteria
1	600	150W: 600L	0	Flow
2	600	150W: 600L	0	Flow with Cliff
3	600	150W: 600L	0	Flow
4	600	150W: 600L	0	Flow
5	600	150W: 600L	0	Flow

Table 2: Mass flow test data for woodchips at BH 600mm

Test Run	Bed Height (mm)	Outlet Dimension (mm) (slot)	Rathole Diameter (mm)	Flow/No Flow Criteria
1	800	150W: 600L	0	Flow
2	800	150W: 600L	0	Flow
3	800	150W: 600L	0	Flow
4	800	150W: 600L	0	Flow
5	800	150W: 600L	0	Flow

Table 3: Mass flow test data for woodchips at BH 800mm

Test Run	Bed Height (mm)	Outlet Dimension (mm) (slot)	Rathole Diameter (mm)	Flow/No Flow Criteria
1	1200	150W: 600L	0	Flow
2	1200	150W: 600L	0	Flow with Cliff
3	1200	150W: 600L	0	No Flow
4	1200	150W: 600L	0	Flow
5	1200	150W: 600L	0	Flow

Table 4: Mass flow test data for woodchips at BH 1200mm

Mass Flow Test: Effects of bed height (BH) on flowability @ 150mmW:600mmL
Test Material: Chopped Miscanthus
Test Date: 16022010 & 18022010

Test Run	Bed Height (mm)	Outlet Dimension (mm) (slot)	Rathole Diameter (mm)	Flow/No Flow Criteria
1	400	150W: 600L	0	No Flow
2	400	150W: 600L	0	No Flow
3	400	150W: 600L	0	No Flow
4	400	150W: 600L	0	Flow with Cliff
5	400	150W: 600L	0	No Flow

Table 1: Mass flow test data for Chopped Miscanthus at BH 400mm

Test Run	Bed Height (mm)	Outlet Dimension (mm) (slot)	Rathole Diameter (mm)	Flow/No Flow Criteria
1	600	150W: 600L	0	Flow with Cliff
2	600	150W: 600L	0	Flow with Cliff
3	600	150W: 600L	0	Flow with Cliff
4	600	150W: 600L	0	Flow with Cliff
5	600	150W: 600L	0	No Flow

Table 2: Mass flow test data for Chopped Miscanthus at BH 600mm

Test Run	Bed Height (mm)	Outlet Dimension (mm) (slot)	Rathole Diameter (mm)	Flow/No Flow Criteria
1	800	150W: 600L	0	No Flow
2	800	150W: 600L	0	No Flow
3	800	150W: 600L	0	No Flow
4	800	150W: 600L	0	No Flow
5	800	150W: 600L	0	No Flow

Table 3: Mass flow test data for Chopped Miscanthus at BH 800mm

Test Run	Bed Height (mm)	Outlet Dimension (mm) (slot)	Rathole Diameter (mm)	Flow/No Flow Criteria
1	1200	150W: 600L	0	No Flow
2	1200	150W: 600L	0	No Flow
3	1200	150W: 600L	0	No Flow
4	1200	150W: 600L	0	No Flow
5	1200	150W: 600L	0	No Flow

Table 4: Mass flow test data for Chopped Miscanthus at BH 1200mm

Mass Flow Test: Effects of particles bed height on flowability
Test Material: Woodchips/Hammer milled wood
Test Date: 11/01/2010, 01/02/2010 & 02/02/2010

Test Run	Bed Height (mm)	Outlet Dimension (mm) (slot)	Rathole Diameter (mm)	Flow/No Flow Criteria
1	400	Width:200 Length:600	0	Flow
2	400	Width:200 Length:600	0	Flow
3	400	Width:200 Length:600	0	Flow
4	400	Width:200 Length:600	0	Flow
5	400	Width:200 Length:600	0	Flow

Table 1: Mass Flow Data for woodchips at bed height 400mm

Test Run	Bed Height (mm)	Outlet Dimension (mm) (slot)	Rathole Diameter (mm)	Flow/No Flow Criteria
1	600	Width:200 Length:600	0	Flow
2	600	Width:200 Length:600	0	Flow
3	600	Width:200 Length:600	0	Flow
4	600	Width:200 Length:600	0	Flow
5	600	Width:200 Length:600	0	Flow

Table 2: Mass Flow Data for woodchips at bed height 600mm

Test Run	Bed Height (mm)	Outlet Dimension (mm) (slot)	Rathole Diameter (mm)	Flow/No Flow Criteria
1	800	Width:200 Length:600	0	Flow
2	800	Width:200 Length:600	0	Flow
3	800	Width:200 Length:600	0	Flow
4	800	Width:200 Length:600	0	Flow
5	800	Width:200 Length:600	0	Flow

Table 3: Mass Flow Data for woodchips at bed height 800 mm

Test Run	Bed Height (mm)	Outlet Dimension (mm) (slot)	Rathole Diameter (mm)	Flow/No Flow Criteria
1	1200	Width:200 Length:600	0	Flow
2	1200	Width:200 Length:600	0	Flow
3	1200	Width:200 Length:600	0	Flow
4	1200	Width:200 Length:600	0	Flow
5	1200	Width:200 Length:600	0	Flow

Table 4: Mass Flow Data for woodchips at bed height 1200mm

Mass Flow Test: Effects of particles bed height on the flowability of biomass particles. (Filling: levelling with brush after dumping the particles inside the hopper)
Test Material: Chopped Miscanthus
Test Date: 12/01/2010

Test Run	Bed Height (mm)	Outlet Dimension (mm) (slot)	Rathole Diameter (mm)	Flow/No Flow Criteria
1	400	Width: 200, Length: 600	No Rathole	Flow
2	400	Width: 200, Length: 600	No Rathole	Flow
3	400	Width: 200, Length: 600	No Rathole	Flow
4	400	Width: 200, Length: 600	No Rathole	Flow
5	400	Width: 200, Length: 600	No Rathole	Flow

Table 1: Mass Flow data for chopped miscanthus at bed height 400mm

Test Run	Bed Height (mm)	Outlet Dimension (mm) (slot)	Rathole Diameter (mm)	Flow/No Flow Criteria
1	600	Width: 200, Length: 600	No Rathole	Flow but with small hang-up at one side of the hopper
2	600	Width: 200, Length: 600	No Rathole	Flow
3	600	Width: 200, Length: 600	No Rathole	Partial Flow: half discharge: half hang-up
4	600	Width: 200, Length: 600	No Rathole	Partial Flow: half discharge: half hang-up
5	600	Width: 200, Length: 600	No Rathole	Flow but small hang-up and discharge after 2 minutes (approximately)

Table 2: Mass Flow data for chopped miscanthus at bed height 600mm

Test Run	Bed Height (mm)	Outlet Dimension (mm) (slot)	Rathole Diameter (mm)	Flow/No Flow Criteria
1	800	Width: 200, Length: 600	No Rathole	Flow
2	800	Width: 200, Length: 600	No Rathole	Flow
3	800	Width: 200, Length: 600	No Rathole	Partial Flow
4	800	Width: 200, Length: 600	230 : After vibration	Flow but rathole
5	800	Width: 200, Length: 600	No Rathole	No flow

Table 3: Mass Flow data for chopped miscanthus at bed height 800mm

Test Run	Bed Height (mm)	Outlet Dimension (mm) (slot)	Rathole Diameter (mm)	Flow/No Flow Criteria
1	1200	Width:200 Length:600	390	No Flow
2	1200	Width:200 Length:600	300	No Flow
3	1200	Width:200 Length:600	340	No Flow
4	1200	Width:200 Length:600	320	No Flow
5	1200	Width:200 Length:600	320	No Flow

Table 4: Mass Flow Data for chopped miscanthus at bed height 1200mm

NOTE:

Mass Flow Test: All ratholes generated without vibration (i.e. without bashing the cylinder/hopper) except at bed height (1200mm).

Mass Flow Test: Effects of particles Bed Height on Flowability
Test Material: Chopped Miscanthus
Test Date: 09/02/2010

Test Run	Bed Height (BH) (mm)	Outlet Dimension (mm) (slot)	Rathole Diameter (mm)	Flow/No Flow Criteria
1	400	100mm width; 600mm length	0	No Flow
2	400	100mm width; 600mm length	0	No Flow
3	400	100mm width; 600mm length	0	No Flow
4	400	100mm width; 600mm length	0	No Flow
5	400	100mm width; 600mm length	0	No Flow

Table 1: Mass flow test data for chopped miscanthus at BH 400mm

Test Run	Bed Height (BH) (mm)	Outlet Dimension (mm) (slot)	Rathole Diameter (mm)	Flow/No Flow Criteria
1	600	100mm width; 600mm length	0	No Flow
2	600	100mm width; 600mm length	0	No Flow
3	600	100mm width; 600mm length	0	No Flow
4	600	100mm width; 600mm length	0	No Flow
5	600	100mm width; 600mm length	0	No Flow

Table 2: Mass flow test data for chopped miscanthus at BH 600mm

Test Run	Bed Height (BH) (mm)	Outlet Dimension (mm) (slot)	Rathole Diameter (mm)	Flow/No Flow Criteria
1	800	100mm width; 600mm length	0	No Flow
2	800	100mm width; 600mm length	0	No Flow
3	800	100mm width; 600mm length	0	No Flow
4	800	100mm width; 600mm length	0	No Flow
5	800	100mm width; 600mm length	0	No Flow

Table 3: Mass flow test data for chopped miscanthus at BH 800mm

Test Run	Bed Height (BH) (mm)	Outlet Dimension (mm) (slot)	Rathole Diameter (mm)	Flow/No Flow Criteria
1	1200	100mm width; 600mm length	0	No Flow
2	1200	100mm width; 600mm length	0	No Flow
3	1200	100mm width; 600mm length	0	No Flow
4	1200	100mm width; 600mm length	0	No Flow
5	1200	100mm width; 600mm length	0	No Flow

Table 4: Mass flow test data for chopped miscanthus at BH 1200mm

Mass Flow Test: Effects of particles Bed Height on Flowability
Test Material: Woodchips/Hammer milled wood
Test Date: 10/02/2010

Test Run	Bed Height (BH) (mm)	Outlet Dimension (mm) (slot)	Rathole Diameter (mm)	Flow/No Flow Criteria
1	400	100mm width; 600mm length	0	Flow
2	400	100mm width; 600mm length	0	Flow with Cliff
3	400	100mm width; 600mm length	0	Flow with Cliff
4	400	100mm width; 600mm length	0	Flow with Cliff
5	400	100mm width; 600mm length	0	Flow

Table 1: Mass flow test data for woodchips at BH 400mm

Test Run	Bed Height (BH) (mm)	Outlet Dimension (mm) (slot)	Rathole Diameter (mm)	Flow/No Flow Criteria
1	600	100mm width; 600mm length	0	Flow with Cliff
2	600	100mm width; 600mm length	0	Flow with Cliff
3	600	100mm width; 600mm length	0	Flow with Cliff
4	600	100mm width; 600mm length	0	Flow with Cliff
5	600	100mm width; 600mm length	0	Flow with Cliff

Table 2: Mass flow test data for woodchips at 600mm

Test Run	Bed Height (BH) (mm)	Outlet Dimension (mm) (slot)	Rathole Diameter (mm)	Flow/No Flow Criteria
1	800	100mm width; 600mm length	0	Flow
2	800	100mm width; 600mm length	0	Flow with Cliff
3	800	100mm width; 600mm length	0	No Flow
4	800	100mm width; 600mm length	300	No Flow
5	800	100mm width; 600mm length	0	Flow with Cliff

Table 3: Mass flow test data for woodchips at 800mm

Test Run	Bed Height (BH) (mm)	Outlet Dimension (mm) (slot)	Rathole Diameter (mm)	Flow/No Flow Criteria
1	1200	100mm width; 600mm length	0	Flow with Cliff
2	1200	100mm width; 600mm length	0	No Flow
3	1200	100mm width; 600mm length	0	No Flow
4	1200	100mm width; 600mm length	390 (WV)	No Flow
5	1200	100mm width; 600mm length	240 (AV)	No Flow

Table 4: Mass flow test data for woodchips at BH 1200mm

Note:
FWC = flow with cliffs
AV = after hammering the storage vessel
WV = without hammering the storage vessel

Result Analysis using percentage weighting approach: Mass Flow Test (Woodchips/Hammer milled wood)

Material	Outlet Dimension (mm)	Bed Height (mm)	Wall Angle (degree)	% RH (Rathole Formation)	% F (Flow)	% NF (No-flow)
Woodchips	100W:600L	400	65	0	40	60
Woodchips	100W:600L	600	65	0	100	0
Woodchips	100W:600L	800	65	20	20	80
Woodchips	100W:600L	1200	65	40	0	100

Material	Outlet Dimension (mm)	Bed Height (mm)	Wall Angle (degree)	% RH (Rathole Formation)	% F (Flow)	% NF (No-flow)
Woodchips	150W:600L	400	65	0	100	0
Woodchips	150W:600L	600	65	0	80	20
Woodchips	150W:600L	800	65	0	100	0
Woodchips	150W:600L	1200	65	0	60	40

Material	Outlet Dimension (mm)	Bed Height (mm)	Wall Angle (degree)	% RH (Rathole Formation)	% F (Flow)	% NF (No-flow)
Woodchips	200W:600L	400	65	0	100	0
Woodchips	200W:600L	600	65	0	100	0
Woodchips	200W:600L	800	65	0	100	0
Woodchips	200W:600L	1200	65	0	100	0

Result Analysis using percentage weighting approach: Mass Flow Test (Chopped Miscanthus)

Material	Outlet Dimension (mm)	Bed Height (mm)	Wall Angle (degree)	% RH (Rathole Formation)	% F (Flow)	% NF (No-flow)
Chopped Miscanthus	100W:600L	400	65	0	0	100
Chopped Miscanthus	100W:600L	600	65	0	0	100
Chopped Miscanthus	100W:600L	800	65	0	0	100
Chopped Miscanthus	100W:600L	1200	65	0	0	100

Material	Outlet Dimension (mm)	Bed Height (mm)	Wall Angle (degree)	% RH (Rathole Formation)	% F (Flow)	% NF (No-flow)
Chopped Miscanthus	150W:600L	400	65	0	0	100
Chopped Miscanthus	150W:600L	600	65	0	0	100
Chopped Miscanthus	150W:600L	800	65	0	0	100
Chopped Miscanthus	150W:600L	1200	65	0	0	100

Material	Outlet Dimension (mm)	Bed Height (mm)	Wall Angle (degree)	% RH (Rathole Formation)	% F (Flow)	% NF (No-flow)
Chopped Miscanthus	200W:600L	400	65	0	100	0
Chopped Miscanthus	200W:600L	600	65	0	20	80
Chopped Miscanthus	200W:600L	800	65	80	40	60
Chopped Miscanthus	200W:600L	1200	65	100	0	100

Photographic Appendix (A) for Core Flow Test

Figure P1: Core Flow Test Rig Development Stages (First and Second Rings)

Figure P2: Different filling methods (dump-filled and dump-levelled) at Core Flow Test Rig

Figure P3: Mechanical arching formations at different outlet dimensions with different extreme shape materials on Core Flow Rig

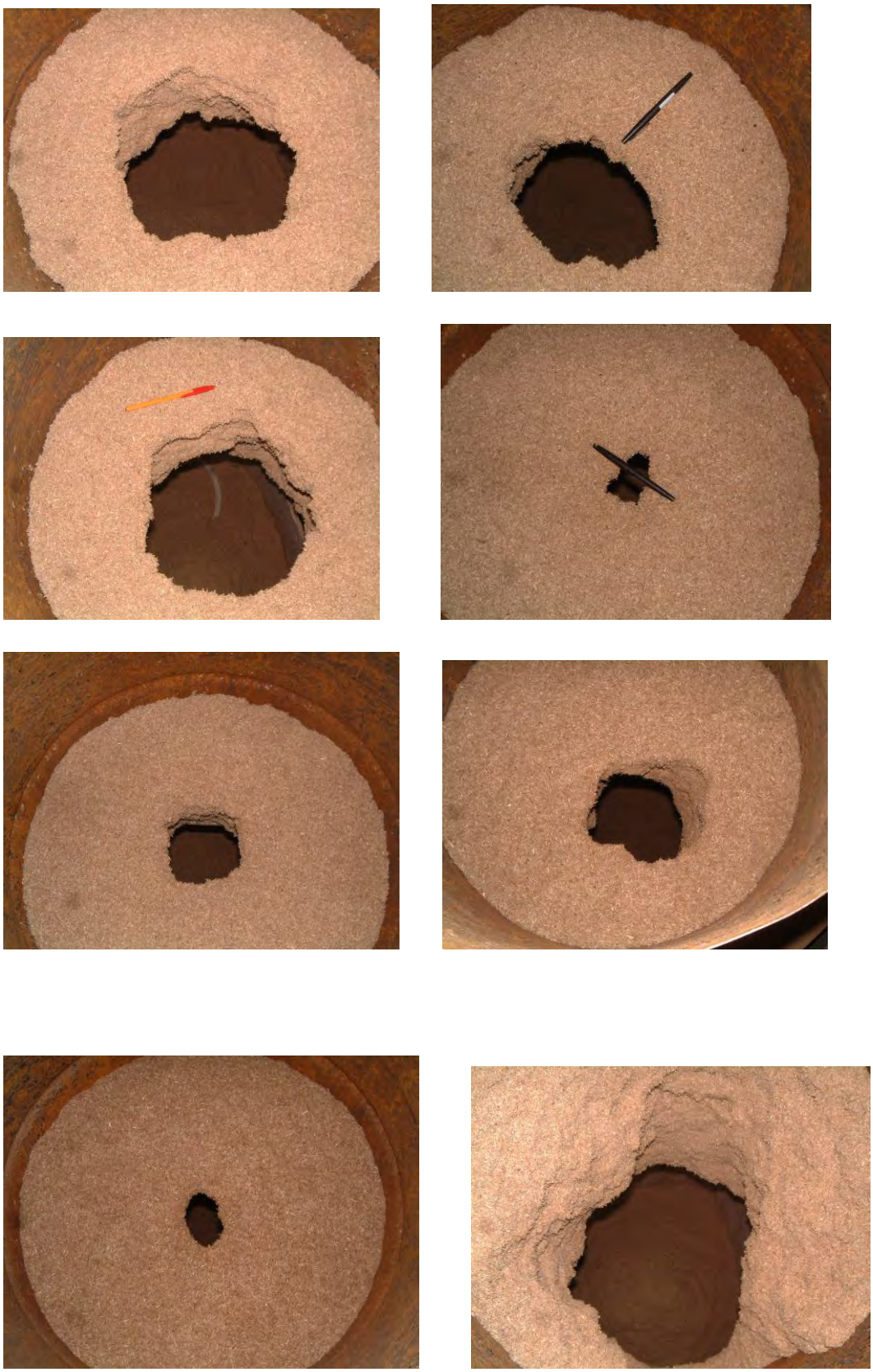

Figure P4: Rathole formations at different outlet dimensions with different extreme shape materials on Core Flow Rig

Photographic Appendix (B) for Mass Flow Test

Figure B1: Mass Flow Test Rig showing different bed heads and materials.

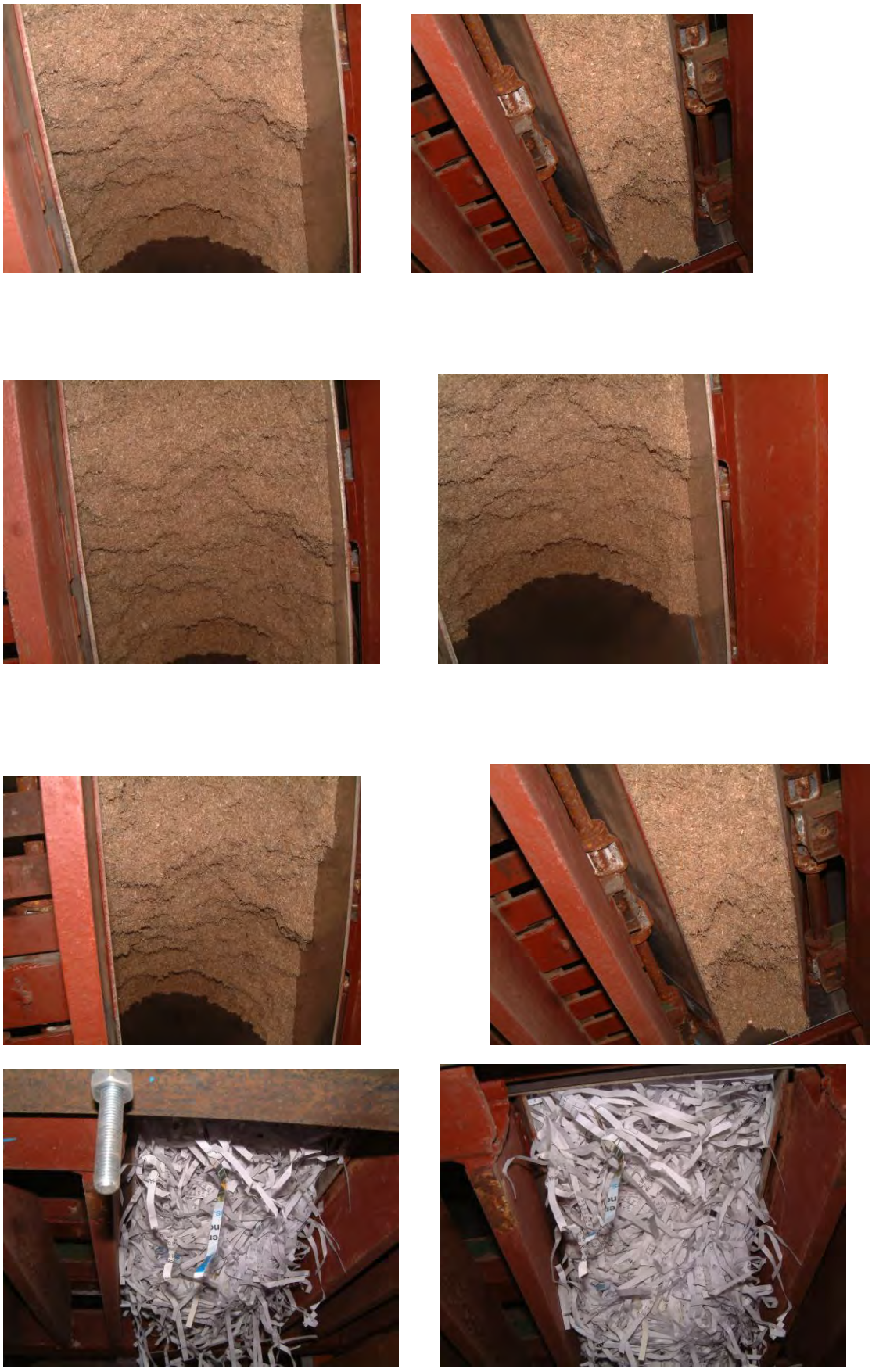

Figure B2: Different Mechanical arch formations at mass flow test rig.

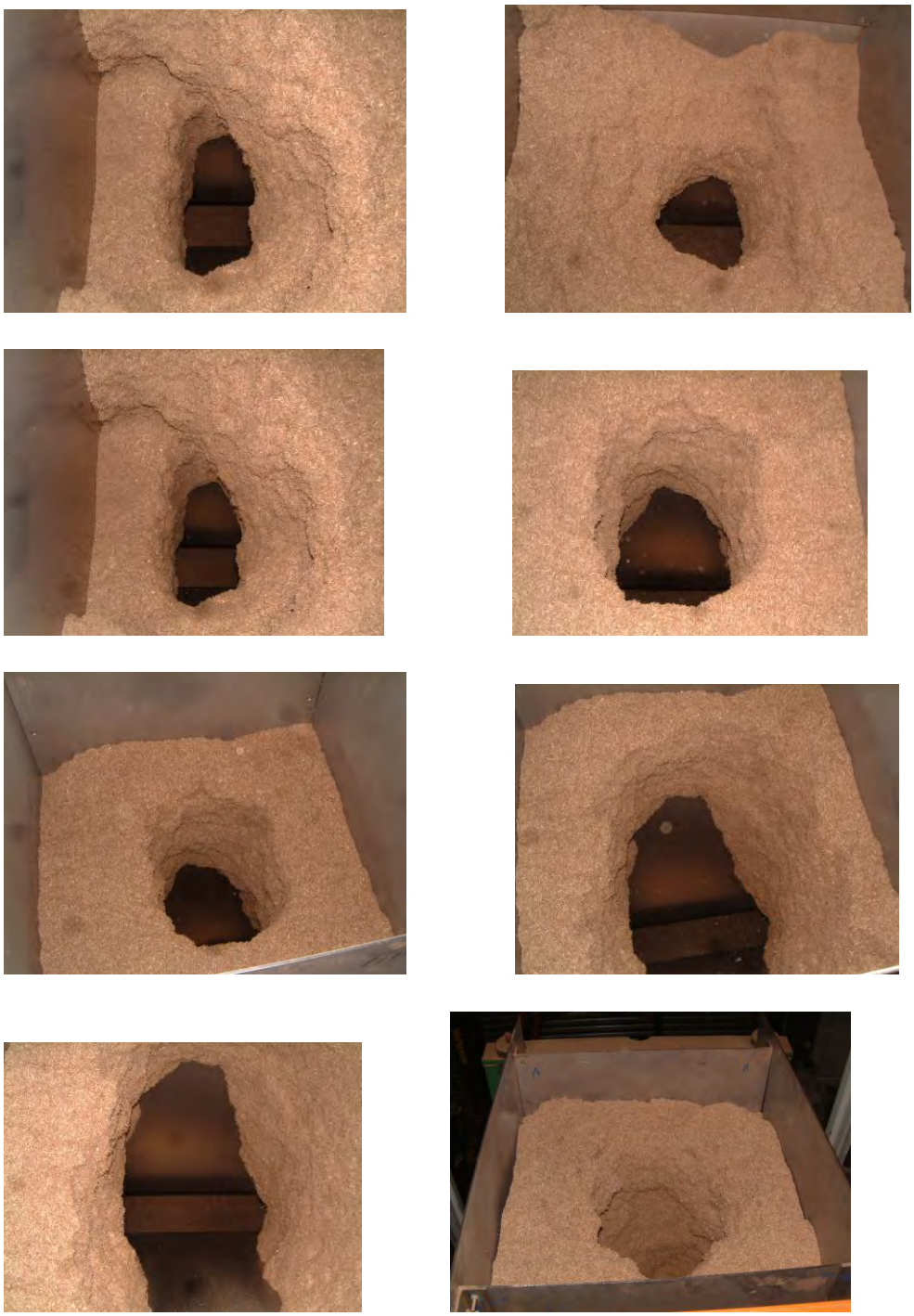

Figure B3: Different rathole formations at mass flow test rig.

Figure B4: Different hang-up (cliffs) formations at mass flow test rig.

Photographic Appendix (C) for Column Test

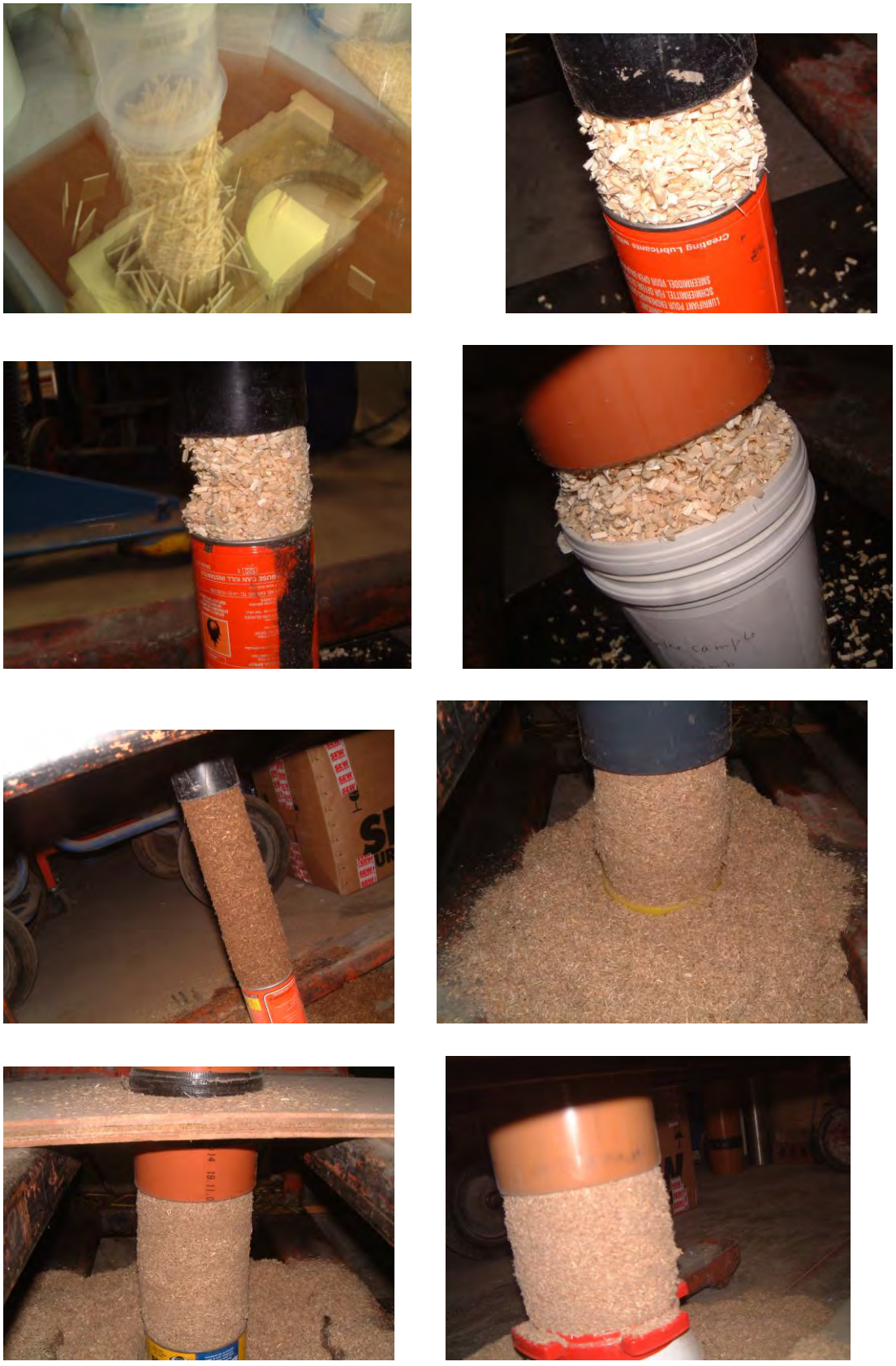

Figure C1: Column Characterisation Technique (Extreme Shape Materials)

Figure C2: Column Characterisation Technique (Extreme Shape Materials)

Photographic Appendix (D) for Core and Mass Flow Test at the Initial Stage

Figure D1: Mass and Core Flow Characterisation Techniques

Figure D2: Core Flow Characterisation Techniques (Extreme Shape Materials)

Photographic Appendix (E) for Uniaxial Failure Test on Extreme Shape Materials (ESM)

Figure E: Uniaxial Unconfined Failure Test on Extreme Shape Materials

Appendix B

B(i) : Bulk Density Measurements Results

The bulk densities of the eight extreme shape biomass materials were measured in the large 300mm diameter cell of 100mm height, with a match lid. The extreme shape material was carefully poured into the cell and strickled level to the top of the ring. A consolidation load is applied to extreme shape materials by fitting the lid and then placing 10kg dead weights on top. The reduction is lid height was measured for each consolidation load. After the sample had been compacted to all the required loads, the cell was dis-assembled taking care to retrieve all the extreme shape material so that the sample weight could be determined. These are presented below in the figure B 1, which compares all the materials on a single chart.

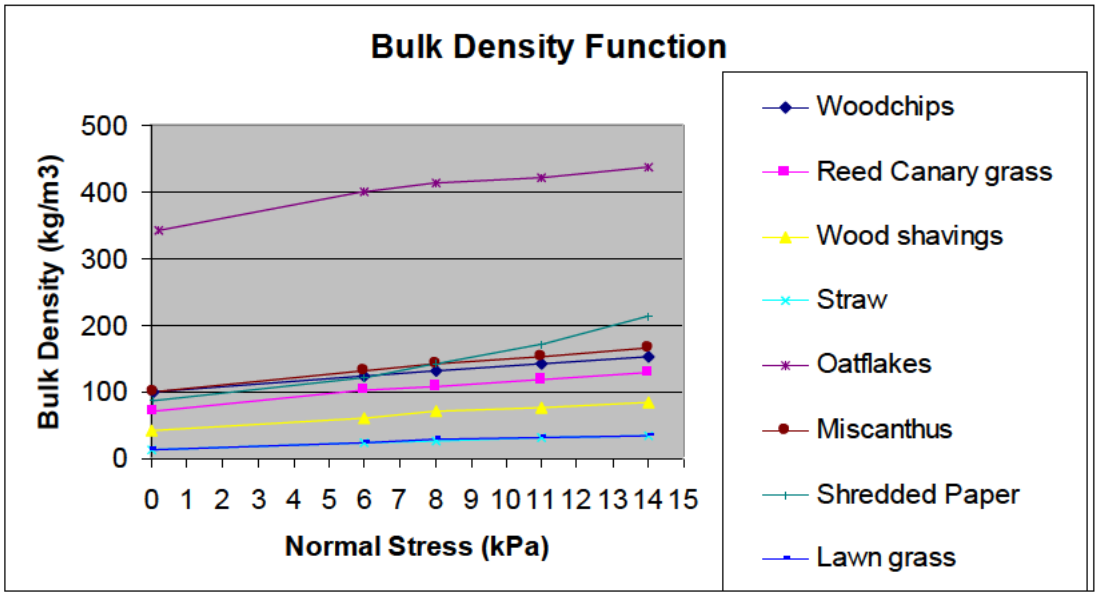

Fig B1: Comparison of the bulk density curves for the eight extreme shape biomass materials

Individual charts for the bulk density curves of the eight extreme shape materials are presented in figs B2 to B9 below. In these figures best fit straight lines have been used to describe the bulk density as a function of stress. The linear fit gives a reasonable approximation as the material is extremely elastic/ compressible over the range of relatively low consolidation stresses tested.

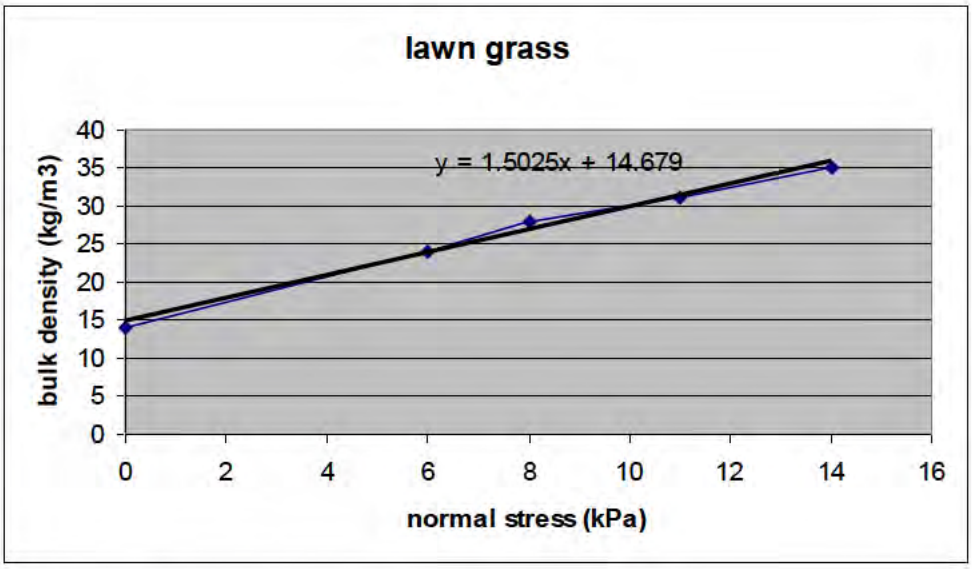

Fig B2: Bulk density curves for lawn grass

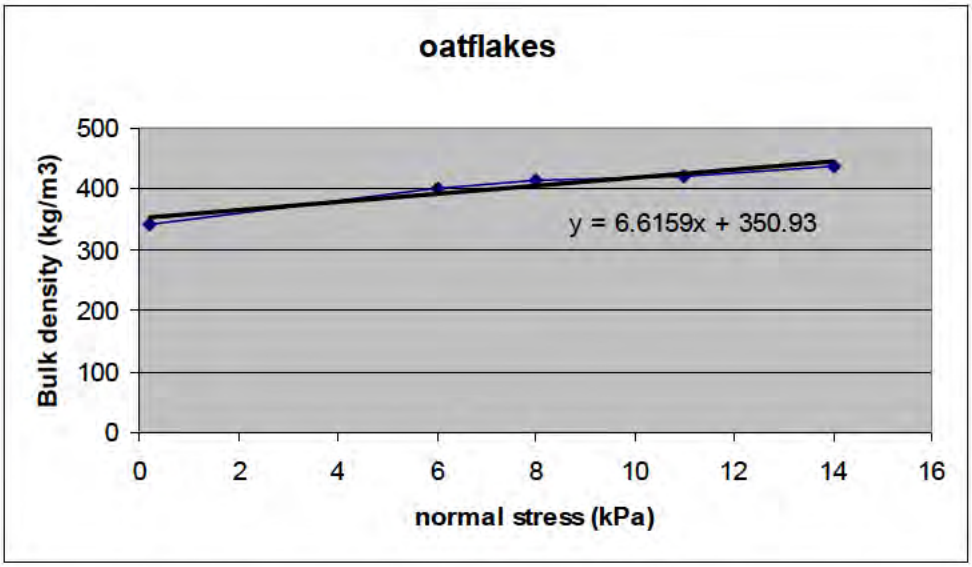

Fig B3: Bulk density curves for oat flakes

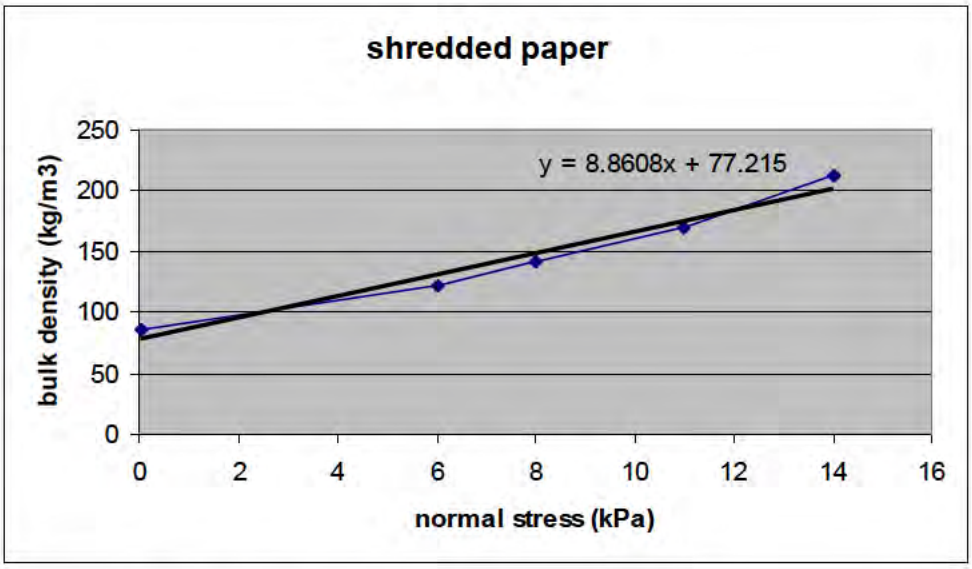

Fig B4: Bulk density curves for shredded paper

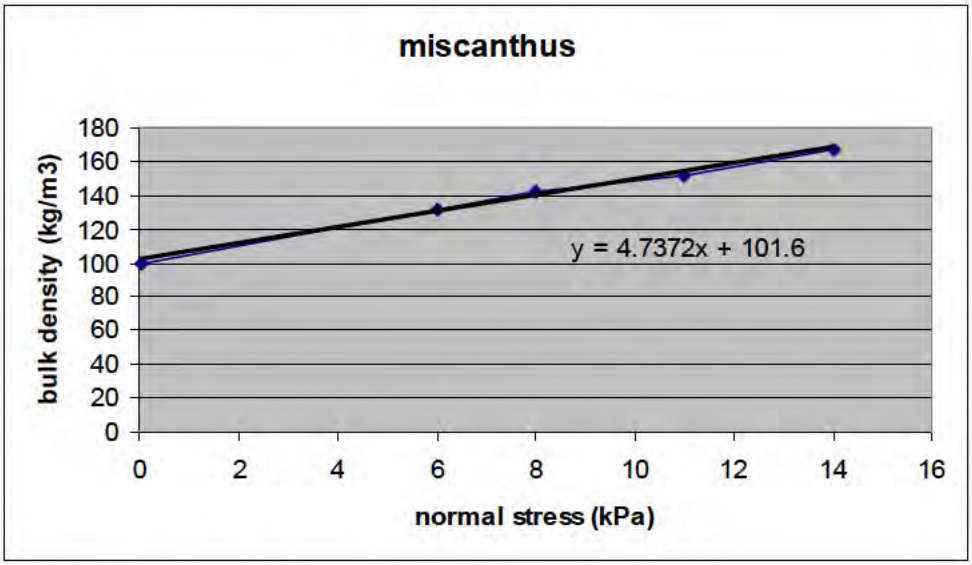

Fig B5: Bulk density curves for miscanthus

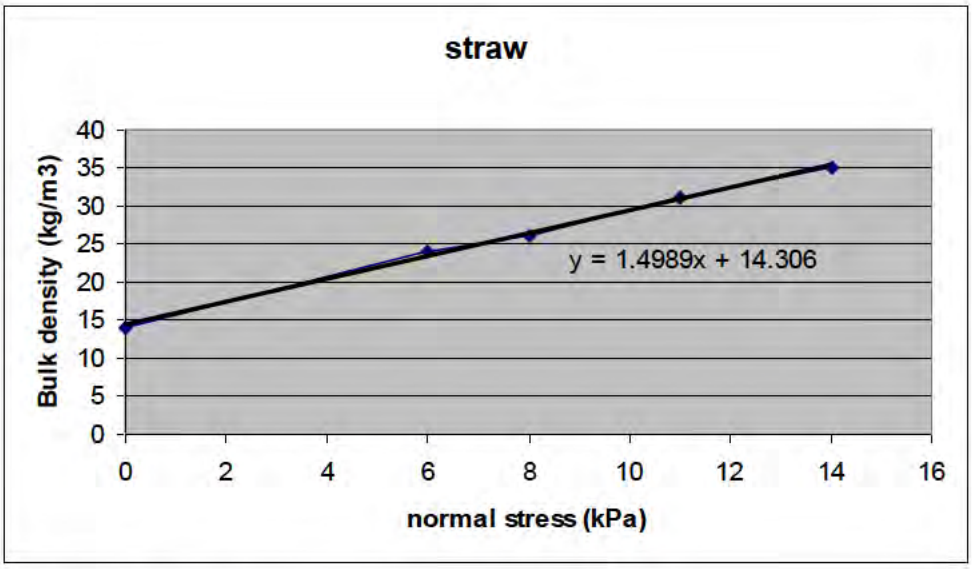

Fig B6: Bulk density curves for straw

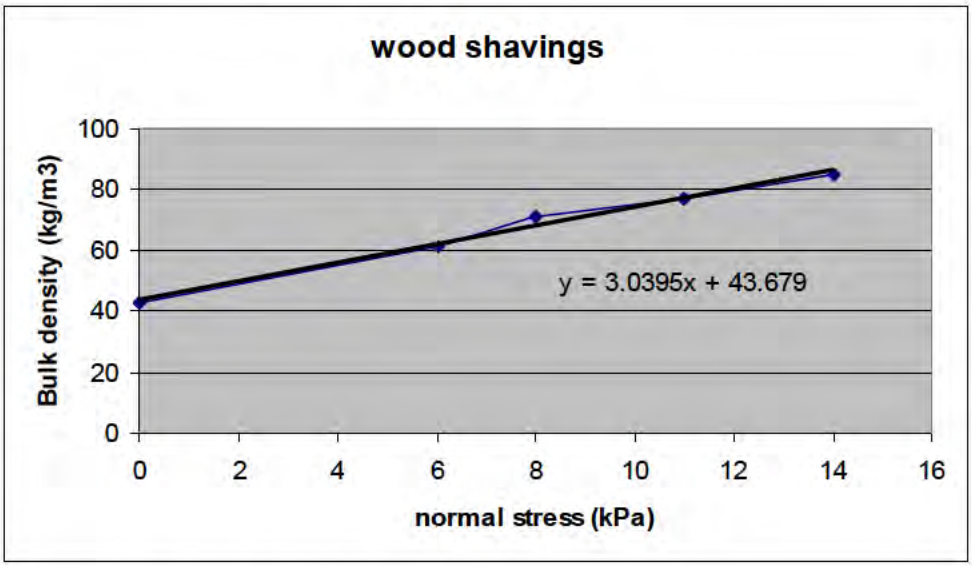

Fig B7: Bulk density curves for wood shavings

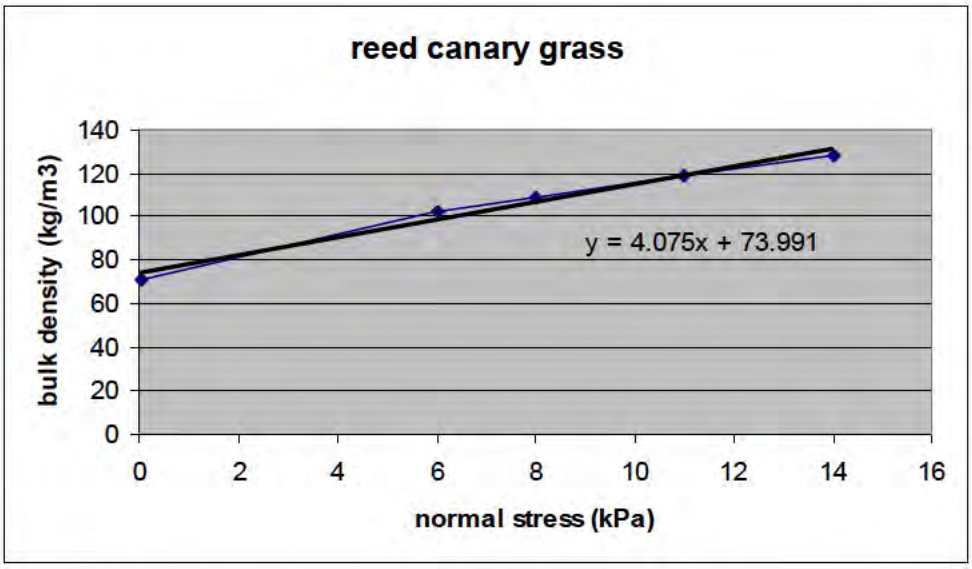

Fig B8: Bulk density curves for reed canary grass

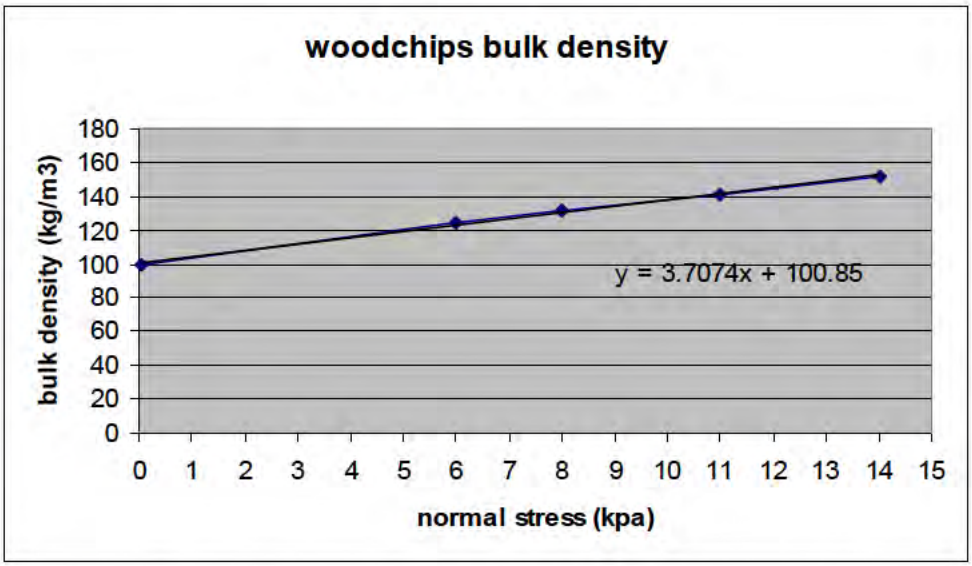

Fig B9: Bulk density curves for woodchips/hammer milled wood

B (ii): Tensile Strength Measurements with Extrapolated Data

The results of the tensile strength measurements undertaken for five extreme shape materials are presented below. A best fit straight line has been drawn through the measured data and used to extrapolate the strength into the low normal stress region assumed to be occurring during arching experiments.

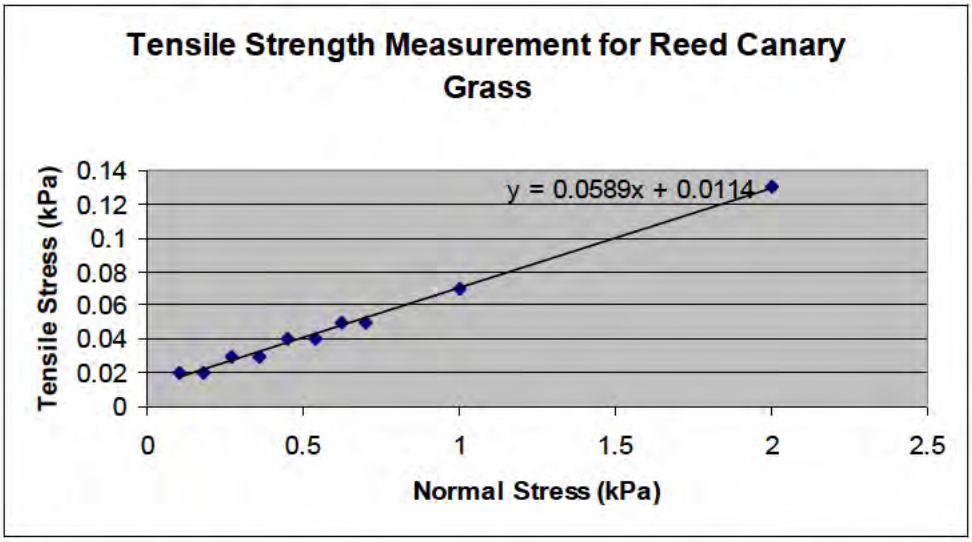

Fig B10: Tensile strength measurements for reed canary grass

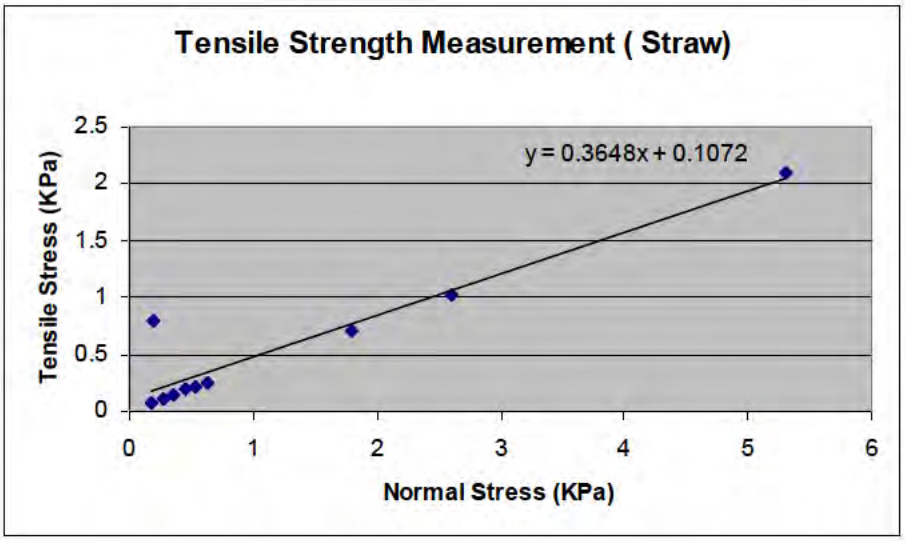

Fig B11: Tensile strength measurements for straw

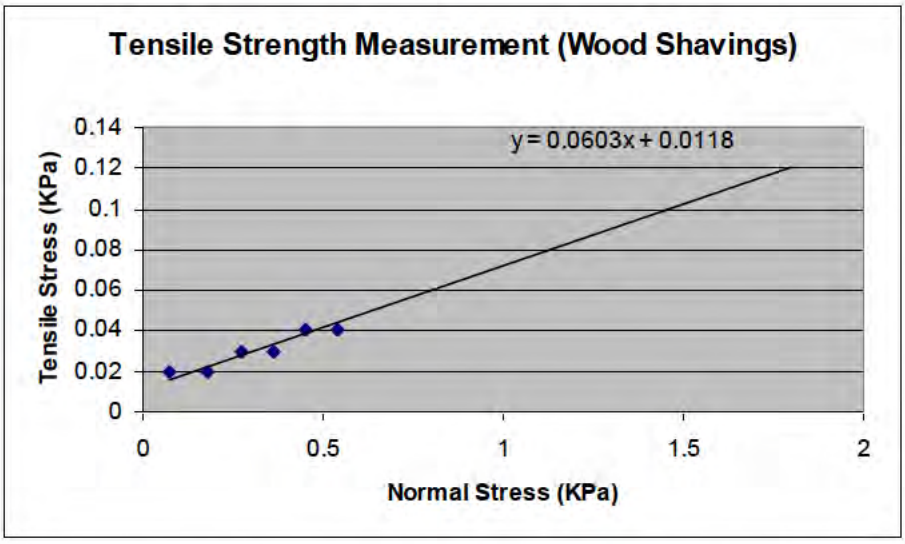

Fig B12: Tensile strength measurements for wood shavings

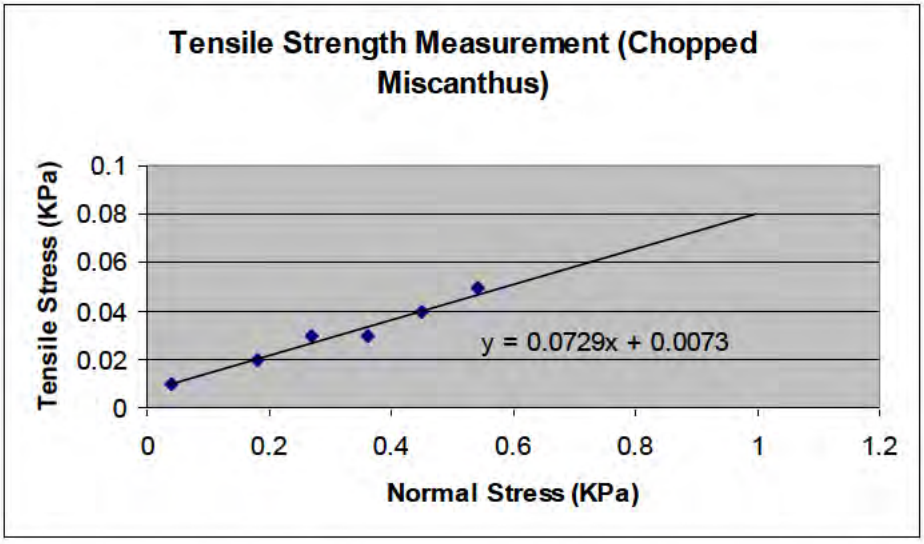

Fig B13: Tensile strength measurements for chopped miscanthus

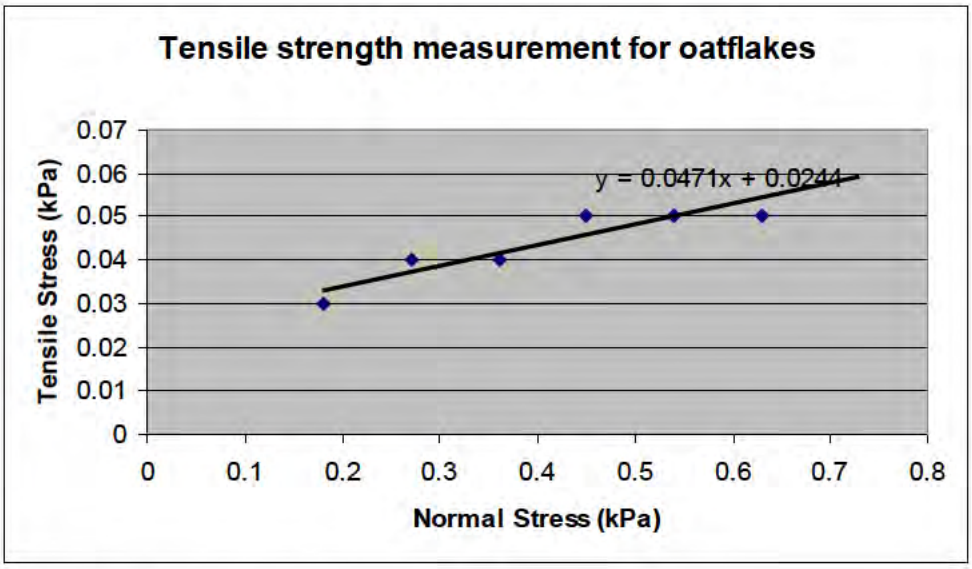

Fig B14: Tensile strength measurements for oat flakes

Appendix C

Calculated Stress Distribution and Arching Dimensions

Table C1: Oat flakes Stress Distribution Data and Arching Dimensions (Predicted and Actual)

Note: Passive stresses (S1) are calculated at the loose fill bulk density while the Active stresses (S2) are calculated at compacted bulk density with corresponding bed heights.

Bed head (m)	Stress 1 (kPa)	Bulk density (kg/m3)	Stress 2 (kPa)	Tensile stress (Pa)	Predicted Arching Data (m)	Actual Arching Data(m) at 23 degree wall angle	Actual Arching Data (m) at 41 degree wall angle
0	0	350.94	0	52.7	0	0	0
0.05	0.171675	352.0758	0.172693	52.7	0.015258	0.015	0.015
0.1	0.34335	353.2116	0.346501	52.7	0.015209	0.015	0.015
0.15	0.515025	354.3474	0.521422	52.7	0.01516	0.015	0.015
0.2	0.6867	355.4831	0.697458	52.7	0.015112	0.015	0.015
0.25	0.858375	356.6189	0.874608	52.7	0.015064	0.015	0.015
0.3	1.03005	357.7547	1.052872	52.7	0.015016	0.015	0.015
0.35	1.201725	358.8905	1.232251	52.7	0.014969	0.015	0.015
0.4	1.3734	360.0263	1.412743	52.7	0.014921	0.015	0.015
0.45	1.545075	361.1621	1.59435	52.7	0.014874	0.015	0.015
0.5	1.71675	362.2978	1.777071	52.7	0.014828	0.015	0.015
0.55	1.888425	363.4336	1.960906	52.7	0.014781	0.015	0.015
0.6	2.0601	364.5694	2.145856	52.7	0.014735	0.015	0.015
0.65	2.231775	365.7052	2.331919	52.7	0.01469	0.015	0.015
0.7	2.40345	366.841	2.519097	52.7	0.014644	0.015	0.015
0.75	2.575125	367.9768	2.707389	52.7	0.014599	0.015	0.015
0.8	2.7468	369.1126	2.896795	52.7	0.014554	0.015	0.015
0.85	2.918475	370.2483	3.087316	52.7	0.014509	0.015	0.015
0.9	3.09015	371.3841	3.27895	52.7	0.014465	0.015	0.015
0.95	3.261825	372.5199	3.471699	52.7	0.014421	0.015	0.015
1	3.4335	373.6557	3.665562	52.7	0.014377	0.015	0.015
1.05	3.605175	374.7915	3.86054	52.7	0.014333	0.015	0.015
1.1	3.77685	375.9273	4.056631	52.7	0.01429	0.015	0.015
1.15	3.948525	377.063	4.253837	52.7	0.014247	0.015	0.015
1.2	4.1202	378.1988	4.452157	52.7	0.014204	0.015	0.015
1.25	4.291875	379.3346	4.651591	52.7	0.014162	0.015	0.015

Table C2: Reed Canary Grass Stress Distribution Data and Arching Dimensions (Predicted and Actual)

Bed head (m)	stress1 (kPa)	Bulk density (kg/m3)	Stress 2 (kPa)	Tensile stress (Pa)	Predicted arching data (m)	Actual arching data (m) at 23 degree wall angle	Actual arching data (m) at 41 degree wall angle
0	0	73.991	0	11.4	0	0	0
0.05	0.035807	74.13691	0.036364	13.54185	0.01862	0.1	0.2
0.1	0.071613	74.28282	0.072871	15.69213	0.021534	0.15	0.23
0.15	0.10742	74.42873	0.109522	17.85084	0.024448	0.18	0.24
0.2	0.143226	74.57465	0.146315	20.01798	0.027363	0.2	0.25
0.25	0.179033	74.72056	0.183252	22.19355	0.030277	0.23	0.26
0.3	0.214839	74.86647	0.220332	24.37756	0.033192	0.238	0.27
0.35	0.250646	75.01238	0.257555	26.56999	0.036107	0.24	0.28
0.4	0.286452	75.15829	0.294921	28.77085	0.039022	0.25	0.3
0.45	0.322259	75.3042	0.33243	30.98015	0.041937	0.26	0.31
0.5	0.358065	75.45011	0.370083	33.19788	0.044852	0.264	0.32
0.55	0.393872	75.59603	0.407878	35.42404	0.047767	0.266	0.33
0.6	0.429678	75.74194	0.445817	37.65862	0.050683	0.268	0.34
0.65	0.465485	75.88785	0.483899	39.90164	0.053598	0.27	0.35
0.7	0.501291	76.03376	0.522124	42.15309	0.056514	0.272	0.36
0.75	0.537098	76.17967	0.560492	44.41298	0.059429	0.273	0.365
0.8	0.572904	76.32558	0.599003	46.68129	0.062345	0.275	0.37
0.85	0.608711	76.4715	0.637658	48.95803	0.065261	0.277	0.372
0.9	0.644517	76.61741	0.676455	51.2432	0.068177	0.28	0.375
0.95	0.680324	76.76332	0.715396	53.53681	0.071093	0.282	0.378
1	0.71613	76.90923	0.75448	55.83885	0.07401	0.283	0.38
1.05	0.751937	77.05514	0.793706	58.14931	0.076926	0.284	0.382
1.1	0.787743	77.20105	0.833077	60.46821	0.079843	0.286	0.385
1.15	0.82355	77.34696	0.87259	62.79554	0.082759	0.29	0.39
1.2	0.859356	77.49288	0.912246	65.1313	0.085676	0.298	0.395
1.25	0.895163	77.63879	0.952046	67.47549	0.088593	0.3	0.4

Table C3: Wood Shavings Stress Distribution Data and Arching Dimensions (Predicted and Actual)

Bed head (m)	Stress 1 (kPa)	Bulk density (kg/m3)	Stress 2 (kPa)	Tensile stress (Pa)	Predicted arching data (m)	Actual arching data (m) at 23 degree wall angle	Actual arching data (m) at 41 degree wall angle
0	0	43.679	0	11.8	0	0	0
0.05	0.021092	43.74311	0.021456	13.0938	0.030513	0.1	0.2
0.1	0.042183	43.80722	0.042975	14.39139	0.033488	0.1	0.2
0.15	0.063275	43.87132	0.064557	15.69277	0.036463	0.11	0.2
0.2	0.084366	43.93543	0.086201	16.99794	0.039438	0.12	0.2
0.25	0.105458	43.99954	0.107909	18.3069	0.042413	0.125	0.2
0.3	0.126549	44.06365	0.129679	19.61966	0.045388	0.13	0.2
0.35	0.147641	44.12775	0.151513	20.93621	0.048363	0.135	0.2
0.4	0.168732	44.19186	0.173409	22.25655	0.051339	0.14	0.2
0.45	0.189824	44.25597	0.195368	23.58069	0.054314	0.15	0.21
0.5	0.210915	44.32008	0.21739	24.90862	0.05729	0.165	0.22
0.55	0.232007	44.38418	0.239475	26.24033	0.060266	0.18	0.24
0.6	0.253098	44.44829	0.261623	27.57585	0.063242	0.2	0.25
0.65	0.27419	44.5124	0.283833	28.91515	0.066218	0.21	0.251
0.7	0.295281	44.57651	0.306107	30.25824	0.069194	0.22	0.252
0.75	0.316373	44.64061	0.328443	31.60513	0.07217	0.23	0.253
0.8	0.337464	44.70472	0.350843	32.95581	0.075147	0.24	0.254
0.85	0.358556	44.76883	0.373305	34.31028	0.078123	0.242	0.255
0.9	0.379647	44.83294	0.39583	35.66855	0.0811	0.243	0.256
0.95	0.400739	44.89704	0.418418	37.03061	0.084076	0.244	0.257
1	0.42183	44.96115	0.441069	38.39645	0.087053	0.245	0.258
1.05	0.442922	45.02526	0.463783	39.7661	0.09003	0.247	0.259
1.1	0.464013	45.08937	0.486559	41.13953	0.093007	0.25	0.29
1.15	0.485105	45.15348	0.509399	42.51676	0.095984	0.252	0.292
1.2	0.506196	45.21758	0.532301	43.89777	0.098961	0.27	0.295
1.25	0.527288	45.28169	0.555267	45.28258	0.101939	0.3	0.3

Table C4: Straw Stress Distribution Data and Arching Dimensions (Predicted and Actual)

Bed head (m)	Stress 1 (kPa)	Bulk density (kg/m3)	Stress 2 (kPa)	Tensile stress (Pa)	Predicted arching data (m)	Actual arching data (m) at 23 degree wall angle	Actual arching data (m) at 41 degree wall angle
0	0	14.306	0	107.2	0	0	0
0.05	0.006867	14.31629	0.007022	109.7617	0.78154	0.2	0.2
0.1	0.013734	14.32659	0.014054	112.327	0.799231	0.2	0.25
0.15	0.020601	14.33688	0.021097	114.8961	0.816924	0.22	0.28
0.2	0.027468	14.34717	0.028149	117.4688	0.834617	0.23	0.3
0.25	0.034335	14.35746	0.035212	120.0452	0.852311	0.235	0.35
0.3	0.041202	14.36776	0.042284	122.6253	0.870006	0.24	0.37
0.35	0.048069	14.37805	0.049367	125.2091	0.887701	0.245	0.38
0.4	0.054936	14.38834	0.05646	127.7966	0.905398	0.25	0.4
0.45	0.061803	14.39864	0.063563	130.3877	0.923095	0.3	0.42
0.5	0.06867	14.40893	0.070676	132.9825	0.940793	0.36	0.46
0.55	0.075537	14.41922	0.077799	135.581	0.958491	0.38	0.47
0.6	0.082404	14.42952	0.084932	138.1832	0.976191	0.4	0.48
0.65	0.089271	14.43981	0.092075	140.7891	0.993891	0.41	0.5
0.7	0.096138	14.4501	0.099229	143.3987	1.011592	0.42	0.5
0.75	0.103005	14.46039	0.106392	146.0119	1.029293	0.43	0.5
0.8	0.109872	14.47069	0.113566	148.6289	1.046996	0.431	0.5
0.85	0.116739	14.48098	0.12075	151.2495	1.064699	0.435	0.5
0.9	0.123606	14.49127	0.127943	153.8738	1.082403	0.44	0.5
0.95	0.130473	14.50157	0.135147	156.5018	1.100108	0.442	0.5
1	0.13734	14.51186	0.142361	159.1334	1.117813	0.443	0.5
1.05	0.144207	14.52215	0.149585	161.7688	1.13552	0.445	0.5
1.1	0.151074	14.53244	0.15682	164.4078	1.153227	0.47	0.5
1.15	0.157941	14.54274	0.164064	167.0505	1.170935	0.48	0.5
1.2	0.164808	14.55303	0.171318	169.6969	1.188643	0.49	0.5
1.25	0.171675	14.56332	0.178583	172.347	1.206352	0.5	0.5

Table C5: Miscanthus Stress Distribution Data and Arching Dimensions (Predicted and Actual)

Bed head (m)	Stress 1 (kPa)	Bulk density (kg/m3)	Stress 2 (kPa)	Tensile stress (Pa)	Predicted arching data (m)	Actual arching data (m) at 23 degree wall angle	Actual arching data (m) at 41 degree wall angle
0	0	101.6	0	7.3	0	0	0
0.05	0.049541	101.8347	0.04995	10.94135	0.010952	0.1	0.2
0.1	0.099081	102.0694	0.10013	14.59948	0.014581	0.11	0.2
0.15	0.148622	102.304	0.15054	18.2744	0.018209	0.115	0.2
0.2	0.198162	102.5387	0.201181	21.96609	0.021837	0.12	0.2
0.25	0.247703	102.7734	0.252052	25.67458	0.025466	0.13	0.2
0.3	0.297243	103.0081	0.303153	29.39984	0.029094	0.135	0.2
0.35	0.346784	103.2428	0.354484	33.14189	0.032723	0.138	0.2
0.4	0.396324	103.4775	0.406046	36.90072	0.036351	0.14	0.2
0.45	0.445865	103.7121	0.457837	40.67634	0.03998	0.145	0.21
0.5	0.495405	103.9468	0.509859	44.46874	0.043609	0.15	0.23
0.55	0.544946	104.1815	0.562111	48.27792	0.047238	0.158	0.24
0.6	0.594486	104.4162	0.614594	52.10388	0.050867	0.16	0.25
0.65	0.644027	104.6509	0.667306	55.94663	0.054496	0.165	0.26
0.7	0.693567	104.8856	0.720249	59.80617	0.058125	0.17	0.265
0.75	0.743108	105.1202	0.773422	63.68248	0.061754	0.178	0.268
0.8	0.792648	105.3549	0.826826	67.57558	0.065383	0.18	0.27
0.85	0.842189	105.5896	0.880459	71.48546	0.069012	0.2	0.275
0.9	0.891729	105.8243	0.934323	75.41213	0.072642	0.21	0.278
0.95	0.94127	106.059	0.988417	79.35558	0.076271	0.215	0.28
1	0.99081	106.2937	1.042741	83.31581	0.079901	0.221	0.282
1.05	1.040351	106.5283	1.097295	87.29282	0.08353	0.2225	0.284
1.1	1.089891	106.763	1.15208	91.28662	0.08716	0.225	0.289
1.15	1.139432	106.9977	1.207095	95.29721	0.09079	0.23	0.29
1.2	1.188972	107.2324	1.26234	99.32457	0.094419	0.24	0.295
1.25	1.238513	107.4671	1.317815	103.3687	0.098049	0.25	0.3

Table C6: Shredded Paper Stress Distribution Data

Note: Arching dimension data are not given here based on the reason given in Chapter 6 (Section 6.0).

Bed head (m)	Stress 1 (kPa)	Bulk density (kg/m3)	Stress 2 (kPa)
0	0	77.215	0
0.05	0.037769	77.54966	0.038038
0.1	0.075537	77.88432	0.076405
0.15	0.113306	78.21898	0.115099
0.2	0.151074	78.55364	0.154122
0.25	0.188843	78.8883	0.193474
0.3	0.226611	79.22295	0.233153
0.35	0.26438	79.55761	0.273161
0.4	0.302148	79.89227	0.313497
0.45	0.339917	80.22693	0.354162
0.5	0.377685	80.56159	0.395155
0.55	0.415454	80.89625	0.436476
0.6	0.453222	81.23091	0.478125
0.65	0.490991	81.56557	0.520103
0.7	0.528759	81.90023	0.562409
0.75	0.566528	82.23489	0.605043
0.8	0.604296	82.56955	0.648006
0.85	0.642065	82.90421	0.691297
0.9	0.679833	83.23886	0.734916
0.95	0.717602	83.57352	0.778863
1	0.75537	83.90818	0.823139
1.05	0.793139	84.24284	0.867743
1.1	0.830907	84.5775	0.912676
1.15	0.868676	84.91216	0.957937
1.2	0.906444	85.24682	1.003526
1.25	0.944213	85.58148	1.049443

Table C7: Lawn grass Stress Distribution Data

Note: Arching dimension data are not given here based on the reason given in Chapter 6 (Section 6.0).

Bed head (m)	Stress 1 (kPa)	Bulk density (kg/m3)	Stress 2 (kPa)
0	0	14.679	0
0.05	0.006867	14.68932	0.007205
0.1	0.013734	14.69964	0.01442
0.15	0.020601	14.70995	0.021646
0.2	0.027468	14.72027	0.028881
0.25	0.034335	14.73059	0.036127
0.3	0.041202	14.74091	0.043382
0.35	0.048069	14.75122	0.050648
0.4	0.054936	14.76154	0.057924
0.45	0.061803	14.77186	0.06521
0.5	0.06867	14.78218	0.072507
0.55	0.075537	14.79249	0.079813
0.6	0.082404	14.80281	0.087129
0.65	0.089271	14.81313	0.094456
0.7	0.096138	14.82345	0.101793
0.75	0.103005	14.83377	0.109139
0.8	0.109872	14.84408	0.116496
0.85	0.116739	14.8544	0.123863
0.9	0.123606	14.86472	0.131241
0.95	0.130473	14.87504	0.138628
1	0.13734	14.88535	0.146025
1.05	0.144207	14.89567	0.153433
1.1	0.151074	14.90599	0.160851
1.15	0.157941	14.91631	0.168278
1.2	0.164808	14.92662	0.175716
1.25	0.171675	14.93694	0.183164

Table C8: Woodchips/Hammer milled wood Stress Distribution Data

Note: Arching dimension data are not given here based on the reason given in Chapter 6 (Section 6.0).

Bed head (m)	Stress 1 (kPa)	Bulk density (kg/m3)	Stress 2 (kPa)
0	0	100.85	0
0.05	0.04905	101.0318	0.049556
0.1	0.0981	101.2137	0.099291
0.15	0.14715	101.3955	0.149204
0.2	0.1962	101.5774	0.199295
0.25	0.24525	101.7592	0.249565
0.3	0.2943	101.9411	0.300013
0.35	0.34335	102.1229	0.350639
0.4	0.3924	102.3048	0.401444
0.45	0.44145	102.4866	0.452427
0.5	0.4905	102.6685	0.503589
0.55	0.53955	102.8503	0.554929
0.6	0.5886	103.0322	0.606447
0.65	0.63765	103.214	0.658144
0.7	0.6867	103.3959	0.710019
0.75	0.73575	103.5777	0.762073
0.8	0.7848	103.7596	0.814305
0.85	0.83385	103.9414	0.866715
0.9	0.8829	104.1233	0.919304
0.95	0.93195	104.3051	0.972071
1	0.981	104.487	1.025017
1.05	1.03005	104.6688	1.078141
1.1	1.0791	104.8507	1.131443
1.15	1.12815	105.0325	1.184924
1.2	1.1772	105.2144	1.238583
1.25	1.22625	105.3962	1.292421

Standard Deviation Values for Particle Dimensions

Material	Long Length	Intermediate Length	Short Length
Woodchips/Hammer milled wood	0.063766	0.055621	0.004472
Miscanthus	0.063766	0.055621	0.004472
Wood shavings	4.973898	2.688746	0.332177
Oat flakes	0.615466	0.226614	0.131873
Straw	25.27316	0.429216	0.119587
Reed canary grass	2.132573	0.283869	0.082468
Grass A	9.894571	-	-
Grass B	7.994595	-	-
Paper	-	-	-
Matchsticks	-	-	-